1974

The Measurement And Effect Of Dissolved Oxygen On Candida Lipolytica

Robert Kok

THE MEASUREMENT AND EFFECT OF DISSOLVED OXYGEN ON *CANDIDA LIPOLYTICA*

by

Robert Kok

Faculty of Engineering Science

Submitted in partial fulfillment
of the requirements for the degree of
Doctor of Philosophy

Faculty of Graduate Studies
The University of Western Ontario
London, Ontario

August, 1974

ABSTRACT

It has been reported in the literature for several microorganisms that the quantities of cytochromes and other respiratory enzymes present in the cells are dependent on the conditions under which they are grown.

The effect of the dilution rate and the dissolved oxygen tension during continuous culture on the respiratory system content of *Candida lipolytica* was investigated. No direct measurements of the enzyme content were performed. Instead, the maximum rate of respiration and the oxygen tension at which the respiration rate was at one-half its maximum level were used as indicators of the respiratory system content of *Candida lipolytica*. These were measured simultaneously with a dropping mercury polarograph (DMP) and a membrane-covered oxygen probe.

A galvanic and a polarographic membrane-covered oxygen probe were investigated to define their dynamic behavior and suitability for the measurement of the parameters. A model for the polarographic membrane-covered probe was found which was used to correct for its dynamic lag.

Good agreement was found between the maximum respiration rates of *Candida lipolytica* obtained with the DMP and the polarographic membrane-covered probe. Agreement between

values of the oxygen tension at one-half the maximum respiration rate was poor. This was ascribed to improper functioning of the DMP.

An inverse relationship was obtained between the oxygen tension during growth and the respiratory system activity; a direct relationship was obtained between the dilution rate and the respiratory system activity of *Candida lipolytica*.

These results were in agreement with the findings of others for various microorganisms. The values obtained for the oxygen tensions at one-half the maximum respiration rates were of the same magnitude as those reported in the literature.

ACKNOWLEDGEMENT

Foremost amongst all those who have during the past four years shared and contributed to my joy and pain in completing this work stands J.E. Zajic.

His constant encouragement and enthusiasm, his never-failing open-mindedness and the ability to allow independence in others have been a constant source of inspiration for me. I hope I shall be able to follow his example and live up to the academic ideals he has taught me.

The generosity of Shell Canada Limited in their support of both myself and my research was greatly appreciated and has allowed me during the pursuit of my education a degree of freedom which could hardly have been rivalled.

My first teacher was my father. I thank him for all he has taught me. It was his influence, his stimulating curiosity and love of learning that took me past the first mileposts on the road that I find myself on now.

To all my colleagues and friends I express a sincere gratitude for the support and help they have given me.

Tanya Wellon, who typed this manuscript, deserves special praise for the conscientious and excellent manner in which she has completed her task.

TABLE OF CONTENTS

Page

Page

Page

NOMENCLATURE

a	electrolyte layer thickness : cm
a^*	distance from membrane to reservoir-cathode coupling point : cm
A	duration of probe exposure : sec
A^*	surface area for both membrane and electrolyte layers perpendicular to the oxygen flux : cm^2
b	membrane thickness : cm
B	response characteristic for a diffusion layer : $sec^{1/2}$
B_e	response characteristic for the electrolyte layer : $sec^{1/2}$
B_m	response characteristic for the membrane : $sec^{1/2}$
B_r	response characteristic for the central well : $sec^{1/2}$
C	ratio of electrolyte layer to membrane thickness
C^*	C/k_2 : dimensionless
C_2	size of step input : atm
C_c	chain capacitance in polarographic apparatus : microfarad
C_i	fraction of probe current due to oxygen transfer from the reservoir at the time a downstep occurs
C_p	probe constant : microamp/atm O_2

C_r proportionality constant between oxygen tension at a^* and the resultant current : microamp/atm O_2

D diffusion coefficient of oxygen: cm^2/sec

D_e diffusion coefficient of oxygen in electrolyte : cm^2/sec

D_m diffusion coefficient of oxygen in membrane material : cm^2/sec

E average percentage deviation of the mathematical model from the observed downstep response : %

f oxygen flux : micromoles/sec

F 96,496 coulomb/equivalent

$F_1(\lambda)$ time-variant function of oxygen activity at the cathode : atm

$F_2(\lambda)$ time-variant function of oxygen activity at the probe face : atm

i probe current : microamp

i_∞ probe current at steady-state : microamp

i_A probe current after A seconds of exposure : microamp

i_L current due to oxygen diffusion through the membrane-electrolyte layer system : microamp

i_R current due to oxygen flux from the central well : microamp

k mass transfer coefficient of membrane and electrolyte layer system : gm/sec/cm^2/atm

k_1 ratio of oxygen solubilities in membrane material and external phase

k_2	ratio of oxygen solubilities in membrane material and electrolyte
K_1	Michaelis-Menten constant for substrate 1 : gm/l
K_2	Michaelis-Menten constant for substrate 2 : gm/l
K_m	Michaelis-Menten constant of organism for oxygen : atm O_2
K_v	volumetric mass transfer coefficient : kg-mole/hr/m^3/atm O_2
ℓ	layer thickness : cm
L_e	electrolyte layer thickness : cm
L_m	membrane thickness : cm
n	number of electrons transferred per molecule of oxygen reduced
n_1	number of observations obtained during a downstep response
P	power input per unit volume : horse power/m^3
P_0	initial oxygen tension : atm
P_1	step increase in oxygen tension : atm
P_{0_2}	oxygen tension : atm
$P_{0_{2i}}$	initial oxygen tension : atm
Q	solubility of oxygen in culture medium : gm/l/atm
R	electrolyte resistance factor : $microamp^{-1}$
R_c	chain resistance in polarographic apparatus : ohm
s	Laplace transform variable
S	solubility of oxygen in water : mg/l @ 1 atm O_2
S_1	concentration of substrate 1 : gm/l

S_2	concentration of substrate 2 : gm/l
S_{1i}	initial concentration of substrate 1 : gm/l
S_e	solubility of oxygen in electrolyte : $gm/cm^3/atm$
S_m	solubility of oxygen in membrane material : $gm/cm^3/atm$
t	time : sec
t^*	dimensionless time
T	temperature : °C
V_s	superficial gas velocity : m/hr
x	distance : cm
x^*	dimensionless distance
Y	ratio of glucose to oxygen consumption : gm/gm
α	proportionality constant for the Nernst equation
λ	time variable : sec
μ	organism growth rate : hr^{-1}
μ_{max}	maximum organism growth rate : hr^{-1}

CHAPTER 1

INTRODUCTION

Oxygen is an important factor in both aerobic and anaerobic fermentations, acting as a metabolite in the former and as an inhibitor in the latter. In aerobic fermentations it can be regarded as an ordinary nutrient. Since the concentrations of ordinary nutrients influence the metabolism in a manner commonly expressed by a Michaelis-Menten type relationship, oxygen concentration might be expected to be similarly related to metabolic performance. Oxygen differs however from other nutrients by its very limited solubility in aqueous media (approximately 8 ppm at 25°C and 1 atm.) thus requiring constant replenishment during submerged aerobic fermentations. Usually it is the designer's concern to keep the dissolved oxygen level above a certain accepted minimum, a commonly accepted level for activated sludge being 1-2 ppm.

A frequently-used parameter, the critical oxygen tension, relates the organism's metabolic performance to the oxygen concentration in the aqueous medium in which the microbe is growing. The critical oxygen tension is defined as that oxygen concentration (or its equivalent, pressure or tension in atm.) above which the cell's metabolism is not influenced by any further increase. Historically this has been regarded as a constant for a given organism. If however a Michaelis-Menten type relationship exists between metabolism and oxygen concentration the definition of critical oxygen tension would render the concept useless due to the hyperbolic nature of the Michaelis-Menten equation.

A much more convenient constant would be the Michaelis-Menten half-rate constant K_m. The value of K_m (the oxygen concentration at which the metabolic rate would be one half its maximum) would however quite likely be influenced by the metabolic state of the cell (growth phase etc.) as well as its degree of adaptation to a given environment. In the past very often other growth conditions were not reported together with the critical oxygen tensions or values of K_m. This has frequently led to disputes and confusion when very widely divergent values were reported by different authors for the same organisms.

The necessity of generating K_m data for organisms grown under strictly controlled conditions therefore becomes apparent when the following are considered:

a) Supplying oxygen by sparging is one of the main operating costs of submerged fermentations so that it is economically advantageous to control dissolved oxygen at the lowest possible concentration thus maximizing the mass transfer driving force.

b) The dissolved oxygen concentration which is maintained can considerably influence the metabolic products formed.

Critical oxygen tension and K_m values have historically been obtained with the Warburg respirometer and the dropping mercury polarograph. The Warburg respirometer has the disadvantages of being cumbersome to operate and being inaccurate. The dropping mercury polarograph, although simple to operate, produces a large and unpredictable residual current when operated in a fermentation broth. This is caused by the presence of mineral salts and organic molecules in solution.

A third method of obtaining these data was therefore employed. This approach utilized a membrane-covered oxygen probe. Although such probes have been successfully used for the measurement of very low oxygen pressures in both aqueous and gaseous phases, this was usually done under equilibrium conditions. Since K_m values are however obtained under dynamic conditions (the oxygen tension decreases continuously) it is necessary that the probe's dynamic lag caused by oxygen diffusion through a membrane and electrolyte layer be known in detail in order to make a proper correction for it. The residual current (the signal given off at zero oxygen tension) would however be expected to be considerably smaller than that of the polarograph since the membrane is impermeable to dissolved solids and large organic molecules.

The problem of obtaining critical oxygen tensions and K_m values can therefore be broken down into several sections as has been done in the thesis:

Chapter 2 - Dissolved Oxygen Measurement With the Membrane-Covered Probe.

The static and dynamic characteristics of several types of probes were determined. Probe behavior was mathematically modelled. The model was then used to investigate probe dynamic behavior when subjected to simulated decreases in oxygen tension similar to those expected in experiments to determine the K_m of microorganisms.

Chapter 3 - Dissolved Oxygen Measurement With the Dropping Mercury Polarograph.

Optimal operating conditions were determined.

Chapter 4 - Dissolved Oxygen Control.

The limitations placed on allowable controlled oxygen tensions by the oxygen consumption rate, fermentor conformation and control equipment response were investigated.

Chapter 5 - Determination of K_m data for *Candida lipolytica*.

The membrane-covered probe and the dropping mercury polarograph were used simultaneously, thus yielding at the same time data and an evaluation of the new method to measure K_m.

Since the variable K_m through definition by many past authors has acquired the repute of being a constant for a given organism, it is referred to as the 'oxygen tension at half-maximal slope' throughout the experimental part of Chapter 5.

CHAPTER 2

DISSOLVED OXYGEN MEASUREMENT WITH THE MEMBRANE-COVERED PROBE

2.1 Introduction

A membrane-covered dissolved oxygen probe is an electrochemical cell containing a pair of electrodes and an electrolyte phase. The electrodes and electrolyte are separated by the membrane from the medium in which the oxygen activity is measured. The membrane is usually constructed of Teflon or polyethylene. It is readily permeable only to small gas molecules such as oxygen and nitrogen so that probe operation is largely independent of the chemical composition of the external phase. Both the electrodes are usually metallic, the cathode always being located close to the membrane. The cell can either be galvanic or polarographic. In the former, in the presence of oxygen at the cathode, the electrochemical potential causes a current to flow between the electrodes through an external link, whereas in the latter oxygen is reduced at the cathode by a voltage applied externally to the cell. In both, the current through the cell is directly proportional to the quantity of oxygen entering through the membrane.

During operation a turbulent bulk flow is directed across the probe's face. Diffusional resistance to oxygen transport from the bulk to the cathode surface is divided between a stagnant fluid layer outside the probe, the membrane and the electrolyte layer between the membrane and the cathode surface. The probe can be designed to make the membrane mass-transport controlling, thus rendering the probe largely independent of bulk hydrodynamics as well as bulk chemical composition.

The membrane-covered dissolved oxygen probe has however also some inherent disadvantages. The membranes tend to become fouled when used in submerged fermentations and exhibit 'aging', thus affecting system calibration. They are difficult to steam sterilize and have a considerable dynamic lag. The latter factor limits their usefulness for dissolved oxygen control and other dynamic applications. The membrane is also an obvious mechanical weak point, especially in an intensely-stirred fermentor.

In this chapter the various types of probes and the mechanism of their operation are reviewed, a galvanic and a polarographic probe are studied in detail and a method to compensate for the dynamic lag of the polarographic probe is developed.

2.2 Literature Review of the Membrane-Covered Probe

2.2.1 Galvanic Probes

Johnson and Borkowski [38,12] have described a steam-sterilizable oxygen probe with a silver cathode, a lead anode, acetate buffer electrolyte and a Teflon membrane. They used an acidic buffer rather than a basic one since alkaline buffers often react with the high carbon dioxide concentrations frequently encountered in fermentations. A small glass wool filter installed between the cathode and the anode to catch falling lead particles allowed trouble-free operation for a year. The probe is illustrated in Figure 2.1.

Van Hemert *et al.* [68] also used a silver-lead system with a very large cathodic surface area to increase the current output. The electrolyte used was basic $KHCO_3$ solution which was added after the probe had been sterilized to prevent degradation during the heating period. It is shown in Figure 2.2.

Mackereth [43] designed a probe which has subsequently strongly influenced probe design by others by employing a silver cathode and a lead anode. It is however not steam sterilizable. The Mackereth probe is illustrated in Figure 2.3.

FIGURE 2.1

The Galvanic Probe Described By

Johnson and Borkowski [12,38]

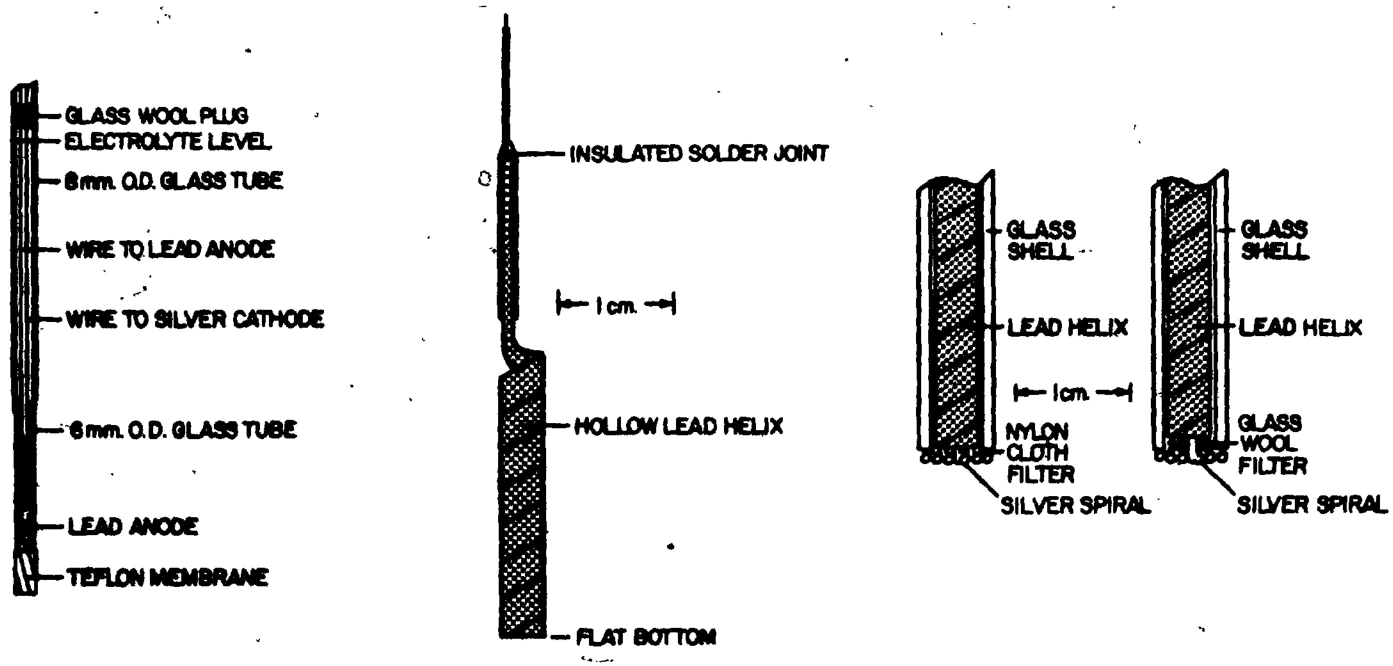
GLASS WOOL PLUG
ELECTROLYTE LEVEL
8mm. O.D. GLASS TUBE
WIRE TO LEAD ANODE
WIRE TO SILVER CATHODE
6mm. O.D. GLASS TUBE
LEAD ANODE
TEFLON MEMBRANE
INSULATED SOLDER JOINT
1 cm.
HOLLOW LEAD HELIX
FLAT BOTTOM
GLASS SHELL
LEAD HELIX
1cm.
NYLON CLOTH FILTER
SILVER SPIRAL
GLASS SHELL
LEAD HELIX
GLASS WOOL FILTER
SILVER SPIRAL

FIGURE 2.2

The Galvanic Probe Described By

Van Hemert *et al.*[68]

1. electrolyte addition tube (Teflon)
2. fitting
3. electrolyte reservoir (Nylon)
4. reservoir holding ring (Stainless Steel)

4a O-ring

5. O-ring
6. ring (Stainless Steel)
7. Insulating disc (porous PVC)
8. Teflon membrane
9. silver cathode
10. O-ring
11. lead anode
12. fastening bolt
13. probe housing
14. sealing fitting
15. copper wire (Teflon Insulated)

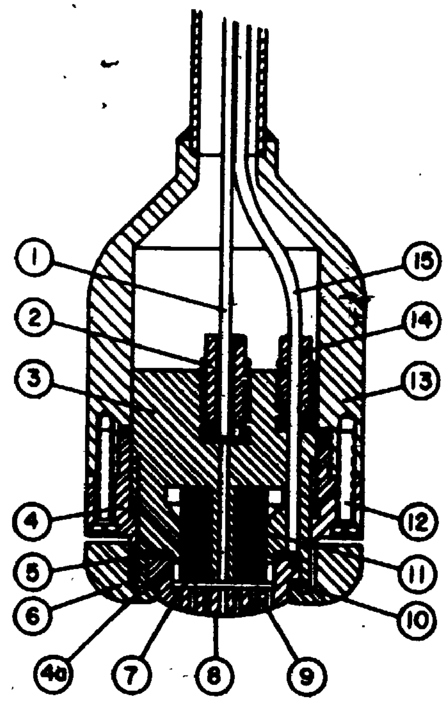
1
2
3
4
5
6
4a
7
8
9
10
11
12
13
14
15

FIGURE 2.3

Mackereth's [43] Galvanic
Dissolved Oxygen Probe

A) side view of probe
B) section of probe

1, Perspex body; 2, silver electrode; 3, porous lead electrode; 4, Perspex end cap; 5, threaded Perspex spigot; 6, annular space between electrodes; 7, silver contact cylinder; 8, lead contact cylinder; 9, 10, counter-bores in Perspex body; 11, 12, 16, 17, 19, 22, 32, 33, 35, neoprene O-rings of appropriate size; 13, 14, brass studs; 15, tubular Polythene membrane; 18, filler aperture; 20, stainless-steel screw; 21, brass cap sealing cable connections; 23, four-core cable; 24, rubber washer; 25, 26, Tufnol washers; 27, brass screw cap for cable gland; 28, 29, push-on connectors; 30, brass securing nuts; 31, thermistor; 34, drilled brass screw compressing 33.

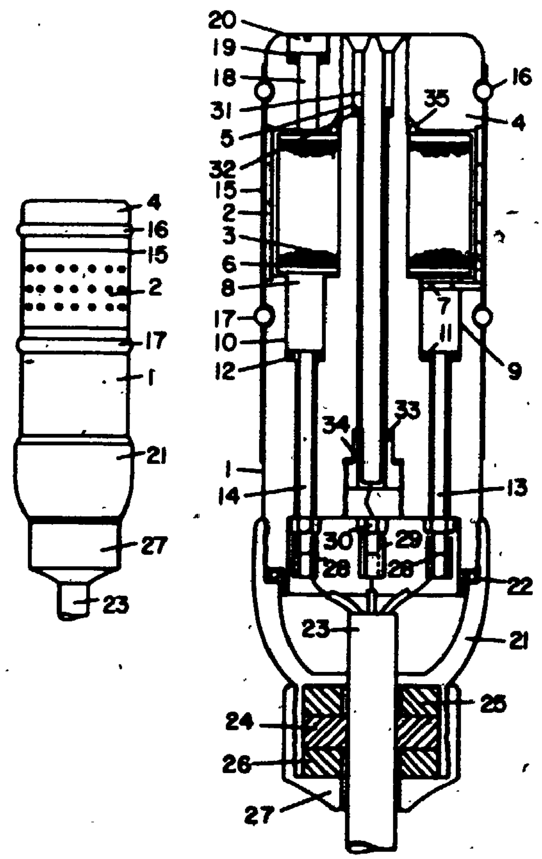
4
16
15
2
17
1
21
27
23
20
19
18
31
5
32
15
2
3
6
8
17
10
12
1
14
16
35
4
7
11
9
34
33
13
30
29
28
28
22
23
21
24
25
26
27

(A) (B)

2.2.2 Polarographic Probes

Phillips and Johnson [52] used a system of two silver wires and an aqueous potassium chloride solution (0.75M) as electrolyte for their polarographic probe. It is shown in Figure 2.4.

Aiba *et al.* [4] have described a polarographic oxygen probe with a platinum cathode and a silver anode which was used to determine the diffusion coefficients of gases in various polymeric membranes. It is illustrated in Figure 2.5.

Benedek and Heideger [10] employed a polarographic probe (also used in this research) produced by the Yellow Springs Instrument Company (Ohio, U.S.A.). It is shown in Figure 2.6.

Saito [59] has reported a sputtered platinum film on glass electrode. Estabrook [22] has used a platinum wire as cathode and calomel electrode as reference. Enoch and Falkenflug [21] devised a method to make the membrane of the probe mass-transfer limiting under unfavourable hydrodynamic conditions by adding a second membrane as shown in Figure 2.7.

2.3 Mechanism of Probe Operation and Probe Design Features

2.3.1 Mechanism at the Cathode

In all dissolved oxygen probes, oxygen is reduced at a noble metal cathode (e.g. Ag, Au, Pt) according to Equation 2.1:

FIGURE 2.4

The Polarographic Probe of

Phillips and Johnson [52]

FIGURE 2.5

The Polarographic Probe of

Aiba *et al.* [4]

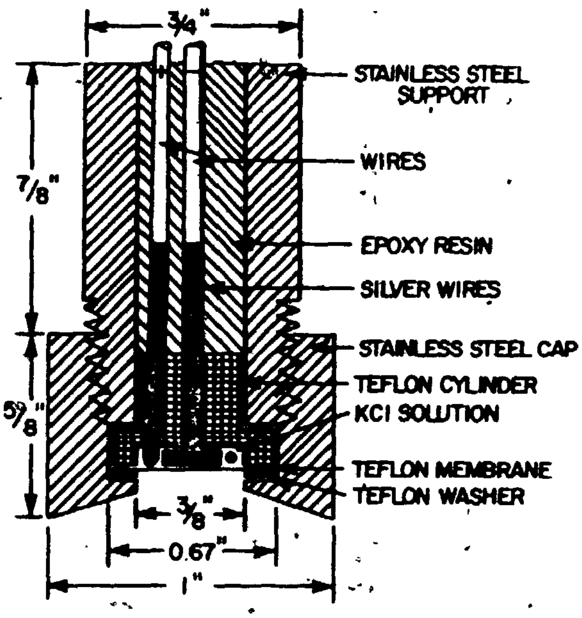
3/4"
STAINLESS STEEL SUPPORT
WIRES
7/8"
EPOXY RESIN
SILVER WIRES
STAINLESS STEEL CAP
TEFLON CYLINDER
5/8"
KCl SOLUTION
TEFLON MEMBRANE
TEFLON WASHER
3/8"
0.67"
1"

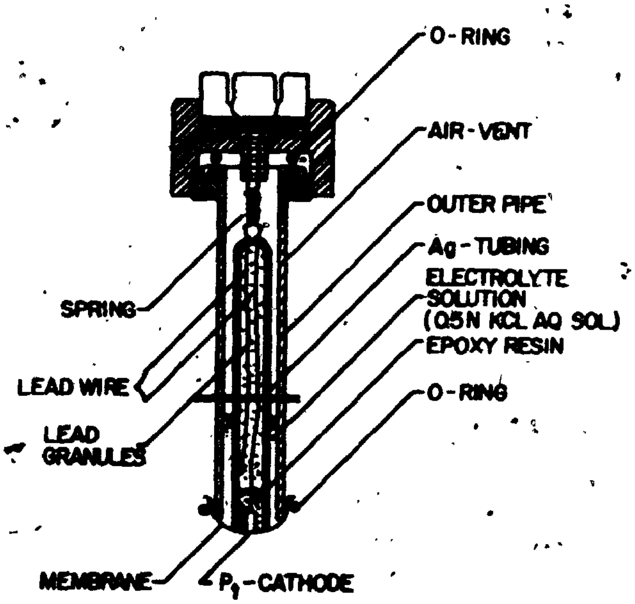
O-RING
AIR-VENT
OUTER PIPE
Ag-TUBING
ELECTROLYTE SOLUTION (0.5N KCL AQ SOL)
EPOXY RESIN
O-RING
SPRING
LEAD WIRE
LEAD GRANULES
MEMBRANE
Pt-CATHODE

FIGURE 2.6

The YSI Polarographic Probe

(Yellowstone Instrument Co.)

FIGURE 2.7

Enoch's and Falkenflug's [21]

Probe

(Modified Beckman Probe)

1. cathode
2. anode
3. insulator
4. electrode housing

5. and 6. O-rings

7. electrolyte
8. outer membrane
9. inner membrane
10. porous nylon spacer

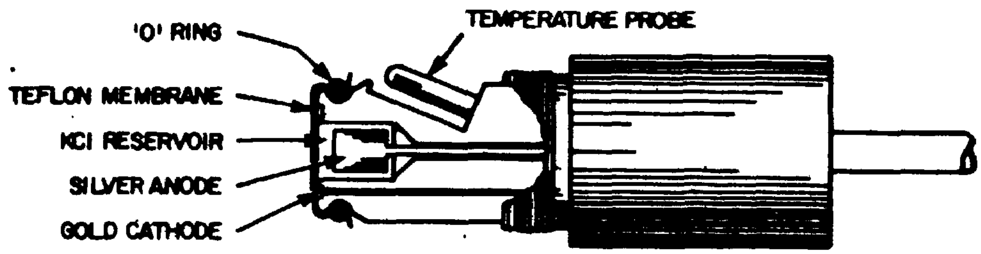
TEMPERATURE PROBE
'O' RING
TEFLON MEMBRANE
KCl RESERVOIR
SILVER ANODE
GOLD CATHODE

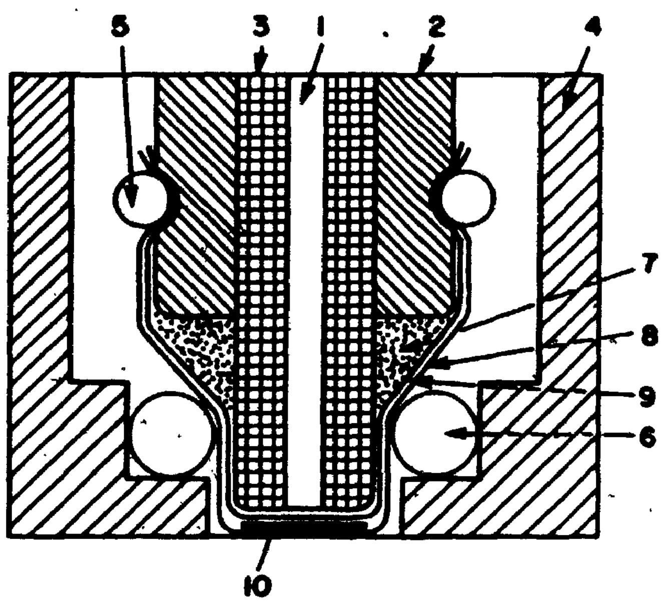
5
3
1
2
4
7
8
9
6
10

$$1/2\ O_2 + H_2O + 2e^- \rightarrow 2OH^- \quad (2.1)$$

During such a reduction process one charge layer exists near the electrode and another on the electrode surface with a potential gradient between them [39]. To measure the potential of this electrode a second electrode, i.e. the reference electrode, must be utilized to complete the circuit.

If a current is allowed to flow in either the spontaneous (galvanic) or non-spontaneous (electrolytic) direction through the cell, the electrical response of the cell is controlled by two rate processes:

- The rate of the electron-transfer reaction at the cathode surface.

- The rate of mass-transfer of reactant and product to and from the electrode surface.

If a voltage equal to but opposite in sign to that of the cell's is applied, no current flows and the cell is in equilibrium. If however any other voltage is applied which is either slightly larger (causing electrolysis) or slightly smaller (allowing a galvanic reaction), the current flowing through the cell is a function of the rates of the mass transport and the electron transport processes. As the voltage difference is increased the electron-transfer process rate is also increased so that the current increases. At the maximum attainable current all the material reaching the electrode is used up immediately so that the concentration of reactant at the electrode surface becomes essentially zero. At voltage differences greater than this critical difference the mass transport process is rate limiting and the resulting current is directly proportional to the bulk concentration of the reactant.

In order for a dissolved oxygen probe to have a linear relationship between the bulk oxygen activity and the output current, the oxygen activity at the cathode surface must be kept negligible by manipulation of the external potential for a polarographic probe and by adjustment of the external load resistance for a galvanic probe.

Phillips and Johnson's [52] results as shown in Figure 2.8 illustrate the effect of a voltage increase on the electrolytic current obtained with their dissolved oxygen probe.

2.3.2 Activity Gradients Between the Bulk Phase and the Cathode Surface

The resistance to mass transport of oxygen from the bulk to the cathode surface can be broken down into three parts [2]:

- the fluid layer between the bulk phase and the probe membrane

FIGURE 2.8

The Effect of Voltage on the Polarographic Current in Air-Saturated Water and In Sodium Sulfite Solution. From Phillips and Johnson [52]

FIGURE 2.9

The Relationship Between the Film Mass Transfer Coefficient of Oxygen at the Probe Face, the Stream Velocity Past the Probe Face and the Bulk Phase Viscosity. From Aiba and Huang [2]

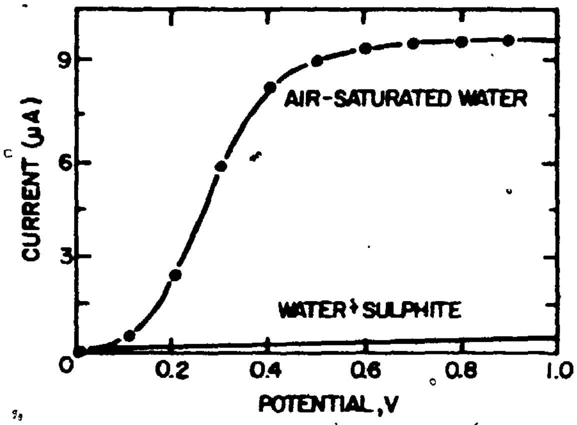

CURRENT (μA)
9
6
3
0
0.2
0.4
0.6
0.8
1.0
POTENTIAL, V
AIR-SATURATED WATER
WATER + SULPHITE

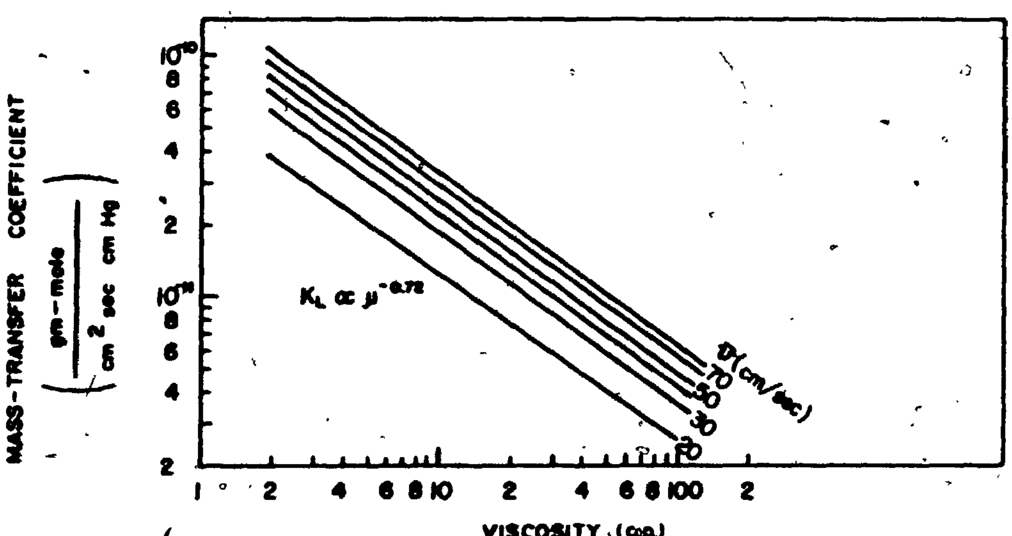

MASS-TRANSFER COEFFICIENT
(gm-mole / cm² sec cm Hg)
VISCOSITY (cp.)
$K_L \propto \mu^{-0.72}$
D (cm/sec)
70
50
30
20

- the membrane
- the electrolyte layer between the membrane and the cathode surface.

To make the output current directly proportional to the bulk oxygen activity, the mass transfer coefficient of the fluid layer should be kept much larger than the combined mass transfer coefficient of the membrane and the electrolyte layer. Decreasing the latter can be accomplished quite readily by increasing the membrane thickness although this decreases the current output of the probe and slows its response considerably. Enoch and Falkenflug [21] have devised a method whereby the influence of the external environment on the probe output current is completely eliminated by using two spaced membranes forming a diffusion chamber. Aiba and Huang [2] have presented data on the mass-transfer coefficient of the fluid layer as a function of fluid viscosity and velocity past the probe face. The graphical correlation is shown in Figure 2.9.

2.3.3 Oxygen Pressure, Tension, Activity and Concentration

At steady state the dissolved oxygen probe's output current is directly proportional to the oxygen flux through the membrane and electrolyte layer. The oxygen flux is in turn directly proportional to the oxygen activity in the bulk phase and the mass transfer coefficient of the membrane and electrolyte layer system. Although the solubility of oxygen in water is strongly influenced by ionic strength [53], a probe's output current would not be affected by variations in ionic strength of a solution in equilibrium with a gas phase of a given oxygen partial pressure [69, 58]. Most commonly a probe's output current is interpreted in terms of oxygen 'tension' which is equivalent to oxygen activity.

Robinson and Cooper [58] have pointed out that errors as high as 25% can be introduced into experimental results if it is assumed that polarography measures oxygen concentration rather than oxygen tension.

Although the solubility of oxygen is almost independent of the total pressure and the absence of other gases, it is a function of temperature according to equation 2.2 [3].

$$S = 14.16 - 0.3943T + 0.007714T^2 - 0.0000646T^3 \quad (2.2)$$

Again, this should not influence the oxygen activity of a solution in equilibrium with a gas phase of a given oxygen partial pressure. Since however gases permeate plastics by a diffusional process due to their molecular vibrations and motion between the plastic molecules, temperature effects follows an Arrhenius-type relationship [5]. It is therefore advisable to calibrate probes at the temperature at which use is anticipated. Aiba and Huang [2] have determined that membrane permeability remains unaffected by immersion in water. This allows the probe to be calibrated in a gas phase and then to be used in aqueous solutions for oxygen tension measurement.

2.3.4 Operational Characteristics at Steady-State

Johnson and Borkowski [38] have reported that the steady-state current of the galvanic probe shown in Figure 2.1 was a linear function of oxygen tension in the ranges 10^{-4} to 10^{-2} atm. of oxygen and from 0 to 0.20 atm. oxygen. Several other workers [42, 43, 68] have reported similar steady-state behavior for galvanic probes. Steady-state behavior of such probes is well understood although due to practical difficulties in the control and measurement of electrolyte layer and membrane thicknesses, output current cannot be readily predicted. Benedek and Heideger [10] have found that membrane tautness greatly influences these factors.

2.3.5 Operational Characteristics Under Unsteady-State Conditions

Several workers have reported on response times of dissolved oxygen probes. Van Hemert *et al.* [68], MacLennan and Pirt [42] and Mackereth [43] have reported 90% response in 15 seconds after an upstep of 0.21 atm. oxygen. Benedek and Heideger [10] also obtained 90% response in 15 seconds with the polarographic YSI probe. Johnson and Borkowski [38] obtained 90% response after 1 minute and 99% response after 3 minutes. If the probe were operated in air for a few hours it took however about three hours to return to its normal value of residual current after a downstep to zero oxygen tension.

2.3.6 Deviations From Theoretical Behavior and Probe Design Features

Although dissolved oxygen probe operation can be adequately discussed theoretically, several problems have arisen in practice. One such problem is the disintegration of the anode. In the polarographic probes containing silver anodes and potassium chloride electrolyte, the anodic reaction is as shown in Equation 2.3:

$$Cl^- + Ag^0 \rightarrow AgCl + e^- \qquad (2.3)$$

When the electrolyte becomes exhausted of chloride ion an alternative reaction occurs as in Equation 2.4 [52]:

$$OH^- + Ag^0 \rightarrow AgOH + e^- \qquad (2.4)$$

The disadvantage of the latter reaction over the former is that AgOH does not adhere strongly to the anode and is much more soluble than AgCl. It thus causes ion migration to the cathode and 'thread-formation' between anode and cathode, thus producing a large and unsteady residual current. Probe life is therefore limited by the supply of chloride ion in the electrolyte and silver in the anode.

Phillips and Johnson [52] have pointed out that in the presence of high concentrations of potassium chloride, silver chloride forms a complex ion which readily migrates to the cathode. An optimal chloride ion concentration of 0.75 M was advocated.

To increase the effective supply of anodic silver, Yellow Springs Instrument Co. uses a porous sintered silver anode.

Molloy's invention [45] of machining an annular groove in the probe's face to prevent metallic thread formation is also employed by this company to prolong the life of their probes. Anodic disintegration in polarographic probes causes therefore a residual current which is controlled by the availability of silver ions to the cathode.

Disintegration of Johnson and Borkowski's [12] lead anode has caused "shorting problems" in their galvanic probe. The life of the probe was prolonged by inserting a glasswool plug between the cathode and the anode to catch falling debris.

A second problem which has occurred is non-linear steady-state response. Van Hemert *et al.* have shown that insufficient cathodic surface roughness causes non-linear behavior. A non-linear relationship between oxygen tension and output current can also be observed for galvanic probes if the voltage drop across the external link is excessive. Johnson and Borkowski [38] have cautioned that the voltage drop should always be less than 10 millivolt. They did not however discuss the effect of output voltage on dynamic response. MacLennan and Pirt [42] kept the output voltage of their Mackereth-type probe below 1 millivolt to optimize probe response and successfully measured and controlled dissolved oxygen tension at 0.26 mm Hg. If oxygen tension measurement over a wide range is desired, it is therefore necessary to vary the load resistance in such a manner that the output signal can be readily measured without adversely affecting either linearity of operation or dynamic response.

Although in the discussion of probe operation it has been assumed that oxygen diffusion occurs only perpendicularly to the cathode surface, in reality dynamic response is considerably influenced by oxygen diffusion to the cathode from reservoirs where oxygen is unintentionally stored. Such reservoirs occur for example in the grooves of spiral-wound cathodes (Figure 2.1) and in the anodic compartments of probes with annular cathodes (Figure 2.6). Thus an essential design feature of a probe having a fast dynamic response is that its oxygen reservoir volume should be reduced to a minimum.

The effects of external load on the steady and unsteady-state response of a galvanic probe will be discussed in sections 2.6 to 2.8; the non-ideal behavior of a polarographic probe is dealt with in sections 2.9 to 2.14.

Throughout the following sections use is made of the cupric ion-catalysed reaction of sodium sulfite with oxygen to provide oxygen-free environments. In Appendix 2.1 an appraisal of this method is presented.

2.4 The Galvanic Probe

To study the steady and unsteady-state behavior of a galvanic probe a lead-silver type probe was constructed. A schematic representation of it is given in Figure 2.10. The probe body was machined from acrylic resin. The lead anode was cut from 0.008" lead foil (Fisher Scientific), flattened between two steel plates, dipped in 1N nitric acid, rinsed with distilled water and dried between two paper towels. Any skin contact with the lead was carefully avoided following the cleaning steps. The layer separating the cathode and anode was a disc cut from no. 4 Whatman filter paper. The silver cathode consisted of a spiral constructed from 0.032" diameter pure silver wire. The silver wire was cleaned with emery cloth and washed with distilled water before being wound into a spiral shape. Both the cathode and anode had contact wires which were extensions of their main parts and which passed through two 1/8" holes in the

FIGURE 2.10

Cross Sectional View of the Galvanic Probe

1. epoxy
2. probe body
3. neoprene ring
4. membrane
5. electrolyte
6. lead anode
7. insulating disc
8. silver cathode

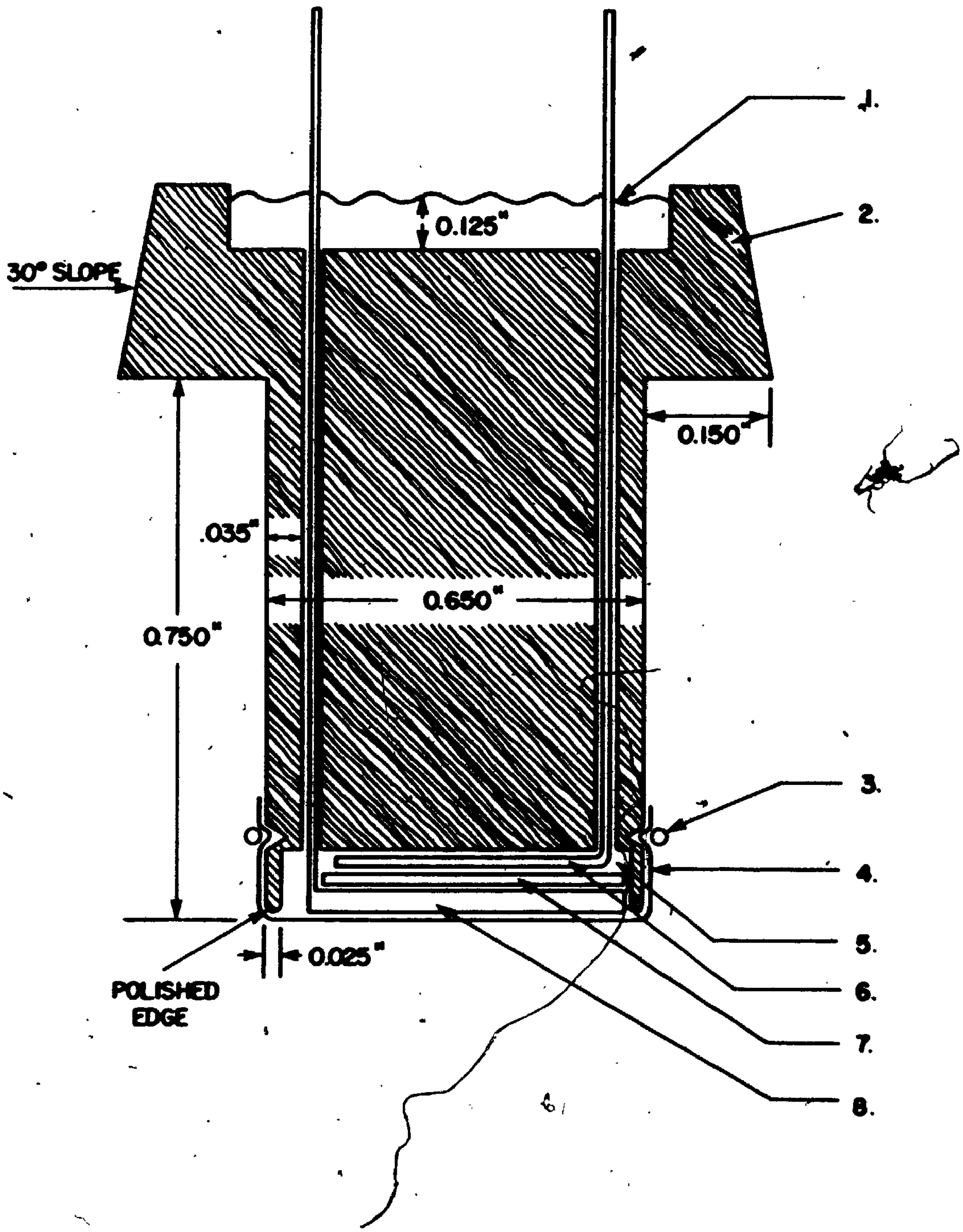
0.125"
30° SLOPE
0.150"
.035"
0.650"
0.750"
0.025"
POLISHED EDGE
1.
2.
3.
4.
5.
6.
7.
8.

body to the top of the probe. The outside surface of the cathode spiral extended a few thousandths of an inch beyond the polished edge of the body to enhance intimate contact between the membrane and the cathode face. The electrodes were cemented in place by filling the cavity in the top of the body with epoxy (Hysol # 309).

The probe was filled with electrolyte of the following composition:

CH_3COOH	5 M
CH_3COONa	0.5 M
$(CH_3COO)_2Pb$	0.08 M
Glycerol	3.3 M

Care was taken to prevent any bubbles from being included under the membrane. The membrane (1 mil Teflon, YSI) was held in place by a neoprene ring which fitted tightly in the groove.

To eliminate wiring resistance and thermal effects the probe was mounted directly underneath an external load switch so that only 2 inches of wiring was in series with it. Resistors of 0, 10, 24, 120, 620 and 3.00K ohm could be switched into the circuit. The switch was enclosed in an acrylic container. The assembly is shown in Photograph 2.1. The circuitry is depicted in Figure 2.11. The voltage signal across the load was fed to a microvoltmeter (HP 419A - accuracy 2% of scale + 1 microvolt). Meter input impedance

PHOTOGRAPH 2.1

The Galvanic Probe and the
Resistance-Switching Assembly

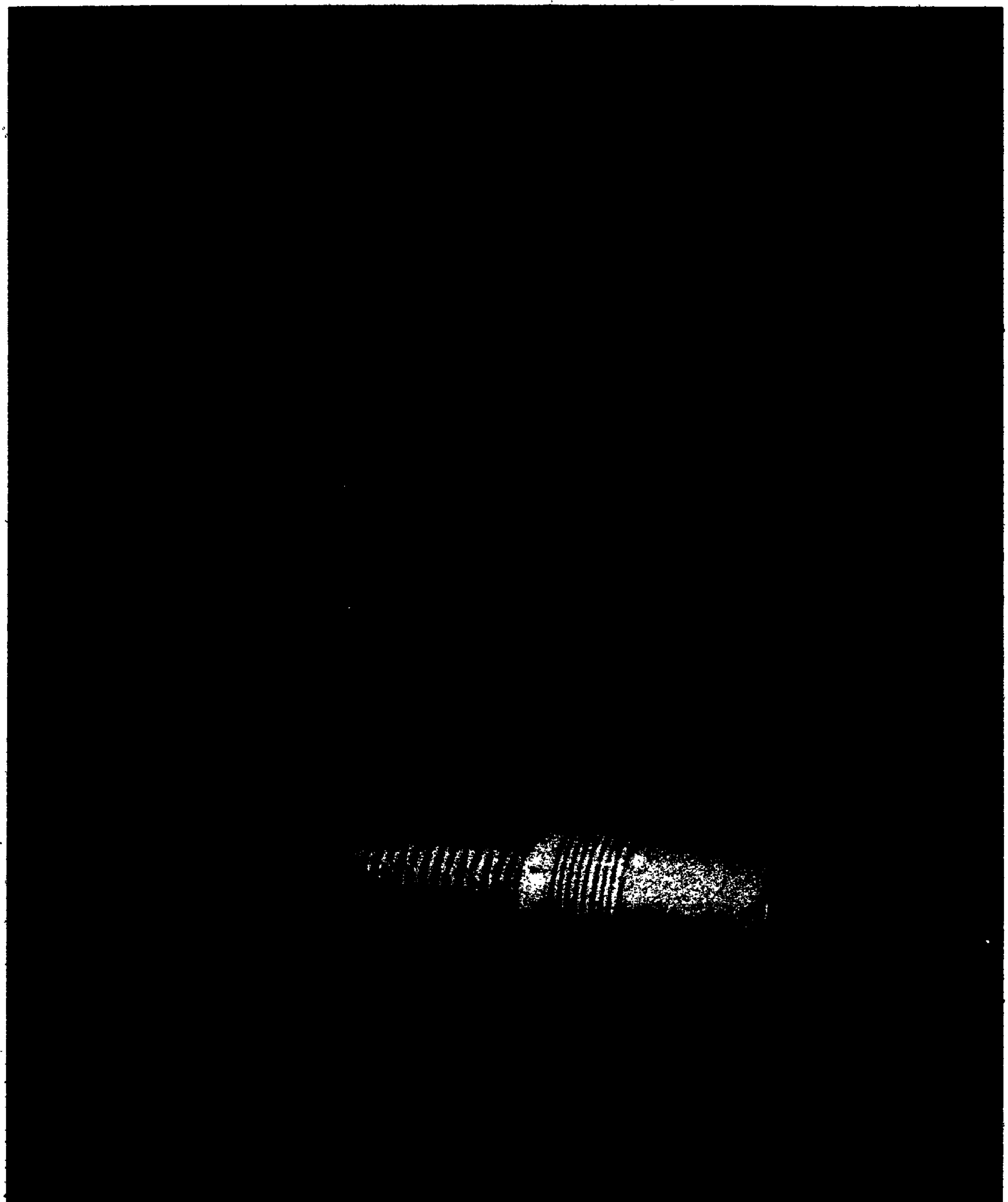

FIGURE 2.11

Schematic of the Circuitry Used With the Galvanic Probe. P-probe; V-voltmeter; R-recorder

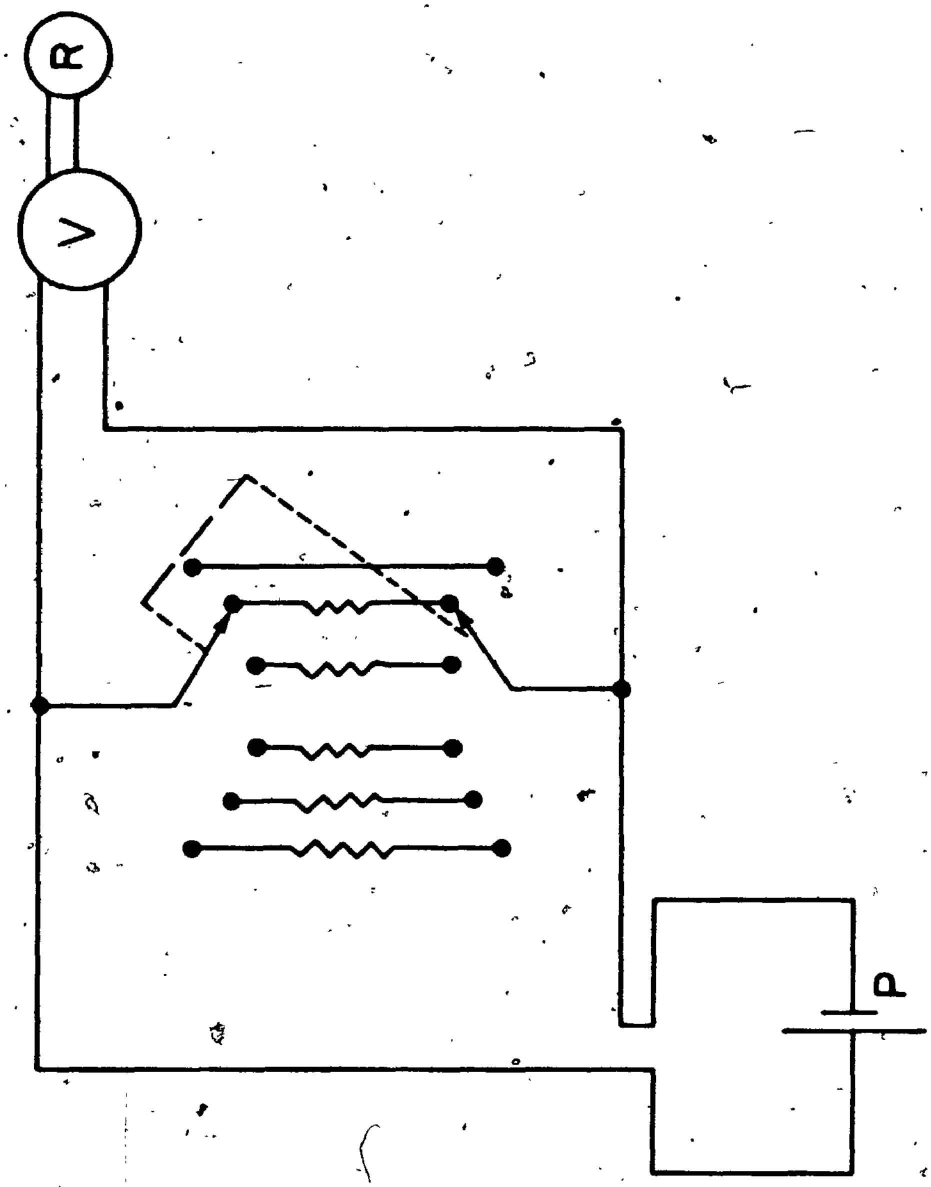
R
V
P

on the lower voltage ranges slightly decreased the effective external load. For voltage ranges lower than 3 mv the effective input impedances of the 620 and 3K ohm resistors were 616 and 2.91K ohm respectively. A 0-1 volt signal from the meter was used as input for a Clevite 'Brush' recorder. Before each experiment the probe was submerged in sodium sulfite solution and the zero resistance was switched in and the meter zeroed. After each experiment this was repeated to check for instrument drift. Only on very few occasions was any drift noticed. Results from these experiments were discarded and the experiments repeated.

2.5 Experimental Methods for the Galvanic Probe Characterization

Experiments were performed to yield information on:

a) The effects of temperature and load resistance on the steady-state current output of the galvanic probe when exposed to air-saturated water.

b) Probe dynamic response to downsteps of 0.21 atm. and 9.26×10^{-4} atm. oxygen under various conditions of load resistance.

The determination of downstep response was regarded as more relevant than upstep response since the ultimate use of the probe was envisaged to be to follow a decrease of oxygen tension during the determination of K_m values for micro-organisms.

The following experiments were performed:

i) Steady-State Output Current

The probe-switch assembly was mounted on a water-filled chamber in which the temperature could be controlled by means of a heating-cooling coil and which was sparged with air. The complete unit is shown in Photograph 2.2. The chamber was constantly agitated by a magnetic stirrer to such an intensity that any further increase in stirring speed would not increase probe current when the chamber contents were saturated with air. Mass transfer resistance from the bulk to the membrane surface was therefore constant. The probe constant (current/oxygen tension) was thus obtained under closely controlled conditions. The chamber could also be sparged with gases of other oxygen content.

ii) Dynamic Response to 0.21 atm. Oxygen Downstep

During these experiments the probe was suspended in air for one, two or three minutes and then quickly submerged in a 5% sodium sulfite solution containing a cupric ion concentration greater than 10^{-6} M. Mass transfer resistance from the gas phase to the membrane surface is generally considered to be negligible [2]. Load resistance was either kept constant or switched in such a fashion as to keep the

PHOTOGRAPH 2.2

The Probe-Switch Assembly Mounted on the Sparging Chamber

output voltage below a threshold value throughout the response.

iii) Dynamic Response to 9.26×10^{-4} atm. oxygen

The probe-switch assembly was mounted at an angle on top of a chamber partly filled with sodium sulfite solution containing cupric ion at a concentration greater than 10^{-6} M. The space above the liquid was constantly flushed with the calibration gas (926 ppm oxygen in nitrogen, Liquid Carbonic Corporation). The liquid level could be adjusted to either submerge the probe face or leave it exposed to the gas phase by manipulating a reservoir connected to the chamber. The probe was mounted at an angle to prevent bubble formation on the probe face during submergence. The gas exit flow was exhausted to atmosphere through ten feet of 1/4 inch I.D. tubing to prevent air from being sucked into the head space during the lowering of the liquid level. Submergence of the probe face took always less than two seconds. This was regarded as an adequate approximation to a step function. The experimental arrangement is depicted in Figure 2.12.

2.6 Results for the Galvanic Probe

2.6.1 Steady-State Current

Detailed results for the steady-state current experiments are presented in Appendix 2.2. The least-square lines of the results are graphed in Figure 2.13. The probe constant

FIGURE 2.12

Experimental Apparatus Used For the Determination of the Galvanic Probe Responses to Downsteps of 9.26×10^{-4} atm. O_2

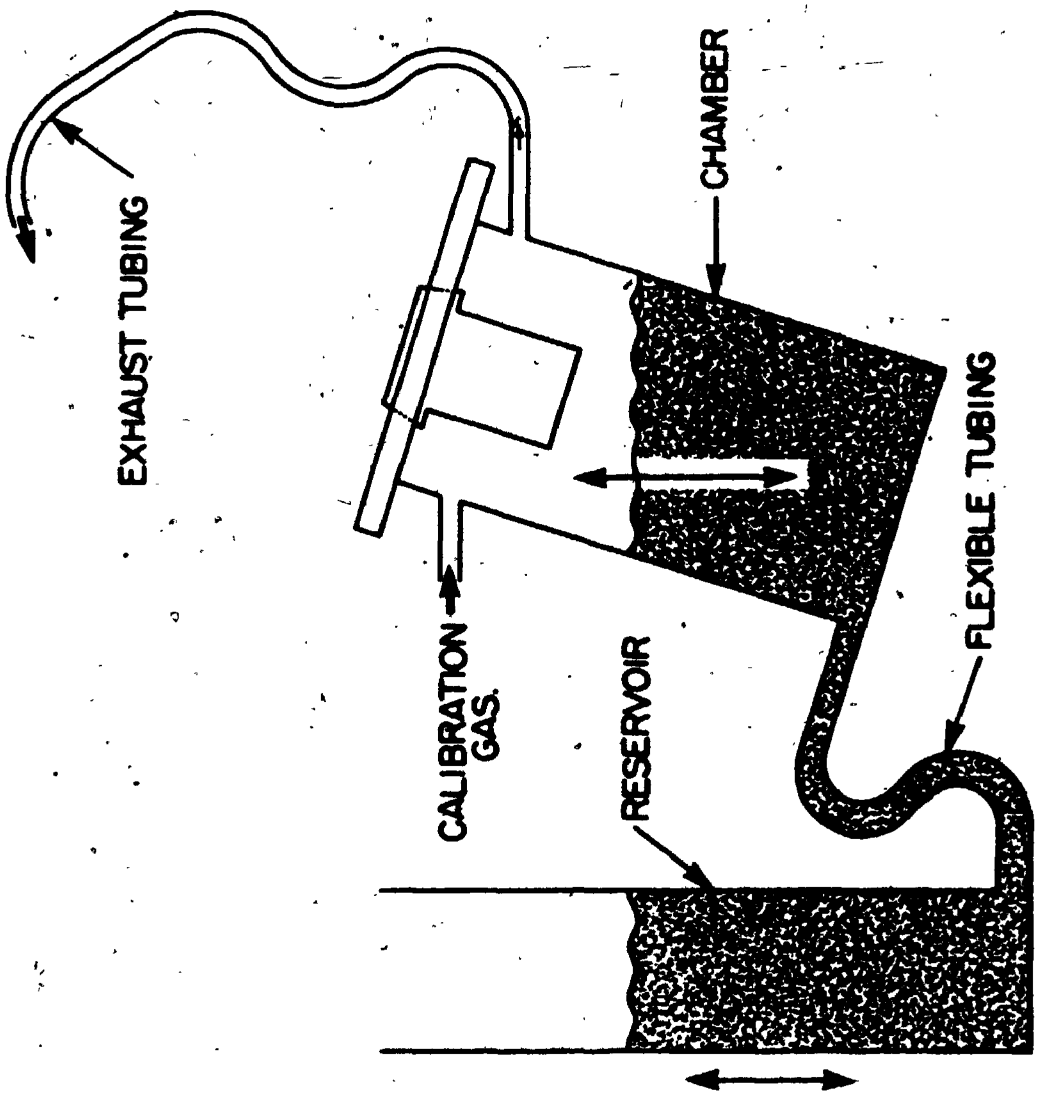
EXHAUST TUBING
CHAMBER
CALIBRATION GAS
RESERVOIR
FLEXIBLE TUBING

FIGURE 2.13

Relationship Between the Probe Constant of the Galvanic Probe and the Temperature

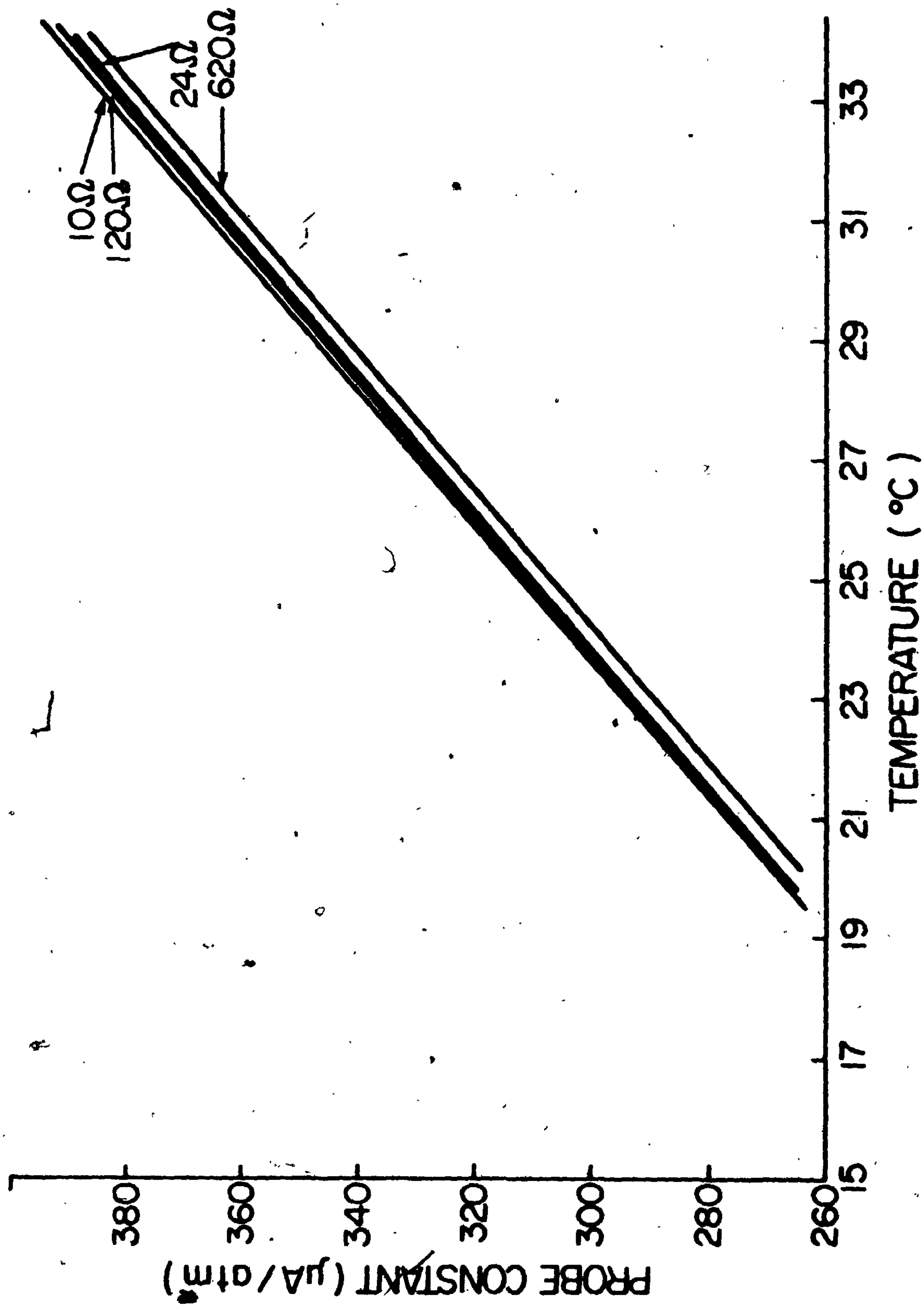

PROBE CONSTANT (μA/atm)
380
360
340
320
300
280
260
15
17
19
21
23
25
27
29
31
33
TEMPERATURE (°C)
10Ω
120Ω
24Ω
620Ω

changed 3%/°C at 25°C. It had a value of 320 microamp/atm. O_2 when the external load was 120 ohm at 26°C. When the water in the chamber was saturated with 926 ppm oxygen in nitrogen gas (at 26°C) a probe constant of 308 microamp/atm. O_2 was obtained. For a similar probe, values of 255 and 261 microamp/atm. O_2 were obtained at 0.21 and 9.26×10^{-4} atm. O_2 respectively. The latter probe was used for subsequent experiments on the dynamic response.

2.6.2 Dynamic Response to 0.21 atm. Oxygen Downstep

The results for the downstep responses at constant external load after one, two or three minutes exposure to air are graphed in Figures 2.14 to 2.18. The same results are graphed again in Figures 2.19 to 2.21 with all the response curves grouped according to their exposure times.

2.6.3 Dynamic Response to 0.21 atm. Oxygen Downstep With Output Voltage Kept Below a Limit

On Figure 2.22 responses to downsteps of 0.21 atm. oxygen after two minutes exposure are compared for the following situations:

- load resistor kept constant at 10 ohm
- load resistor varied so that the voltage output was always smaller than 1 mv

FIGURE 2.14

Comparison of the Downstep Responses of the Galvanic Probe After 1, 2 and 3 Minutes Exposure to 0.21 atm. O_2 With a Load Resistance of 10 ohms

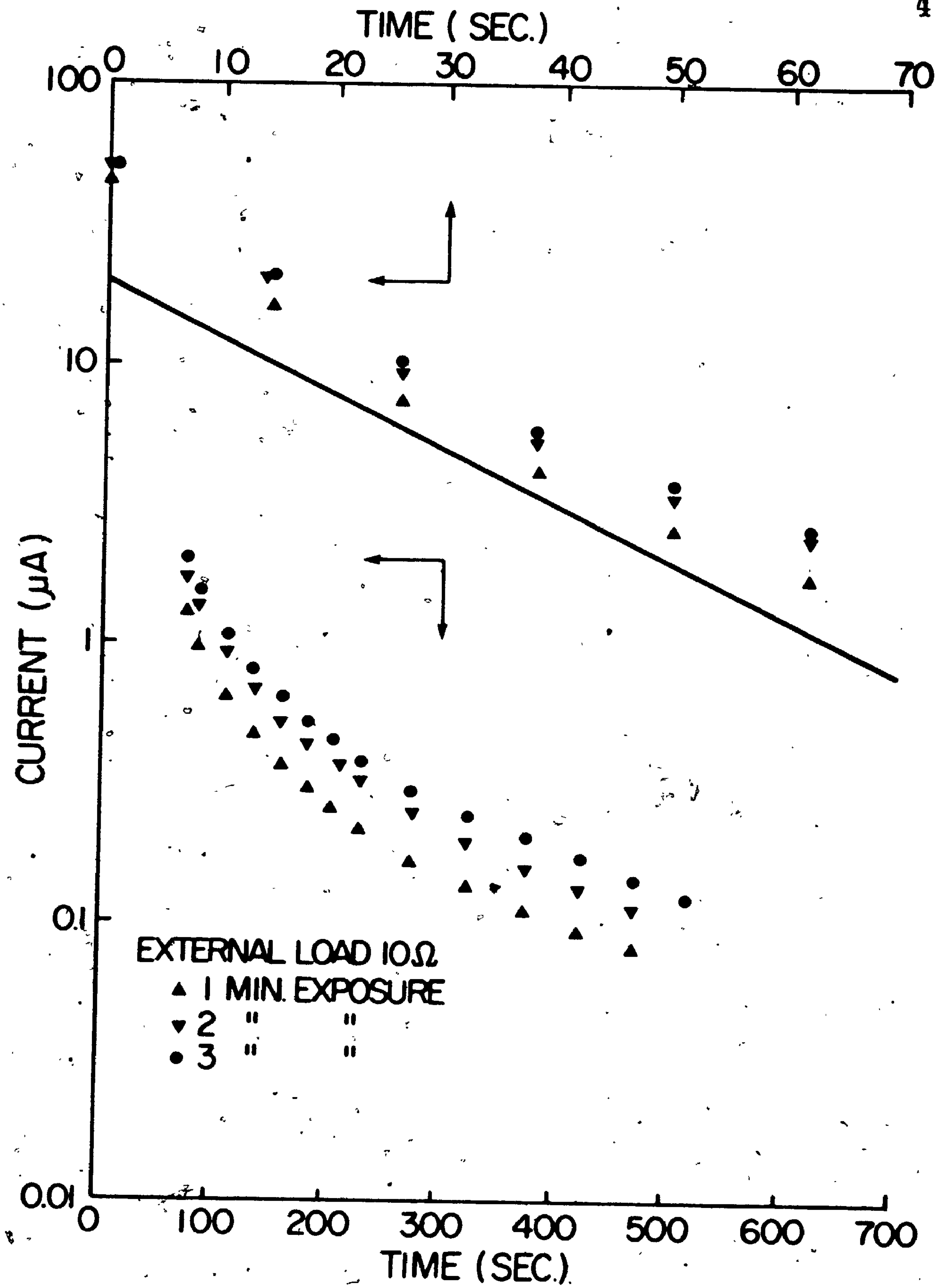
TIME (SEC.)
0
10
20
30
40
50
60
70
100
10
1
0.1
0.01
CURRENT (μA)
EXTERNAL LOAD 10Ω
▲ 1 MIN. EXPOSURE
▼ 2 " "
● 3 " "
0
100
200
300
400
500
600
700
TIME (SEC.)

FIGURE 2.15

Comparison of the Downstep Responses of the Galvanic Probe After 1, 2 and 3 Minutes Exposure to 0.21 atm. O_2 With a Load Resistance of 24 Ohms

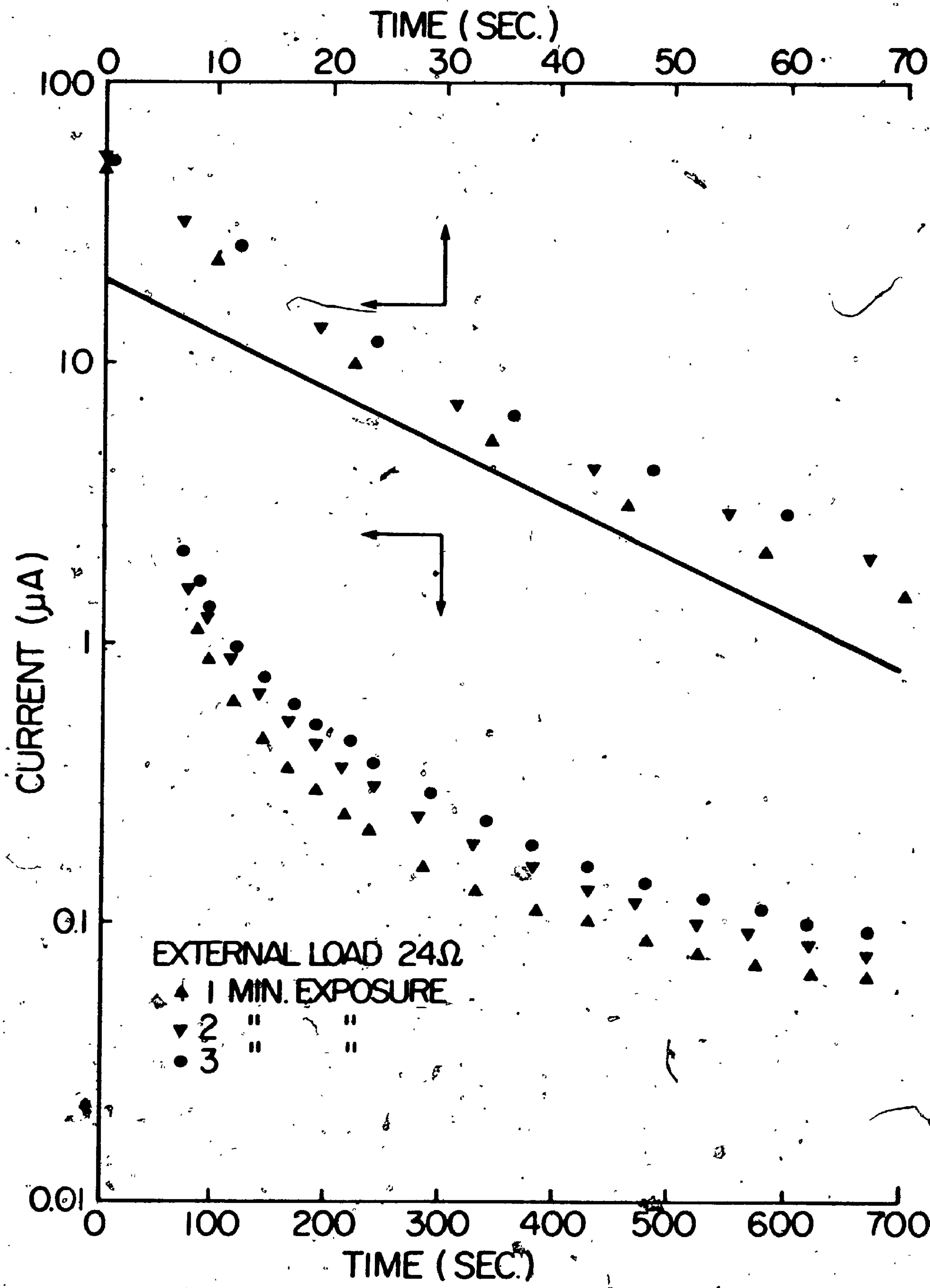
TIME (SEC.)
0
10
20
30
40
50
60
70
100
10
1
0.1
0.01
CURRENT (μA)
EXTERNAL LOAD 24Ω
▲ 1 MIN. EXPOSURE
▼ 2 " "
● 3 " "
0
100
200
300
400
500
600
700
TIME (SEC.)

FIGURE 2.16

Comparison of the Downstep Responses of the Galvanic Probe After 1, 2 and 3 Minutes Exposure to 0.21 atm. O_2 With a Load Resistance of 120 Ohms

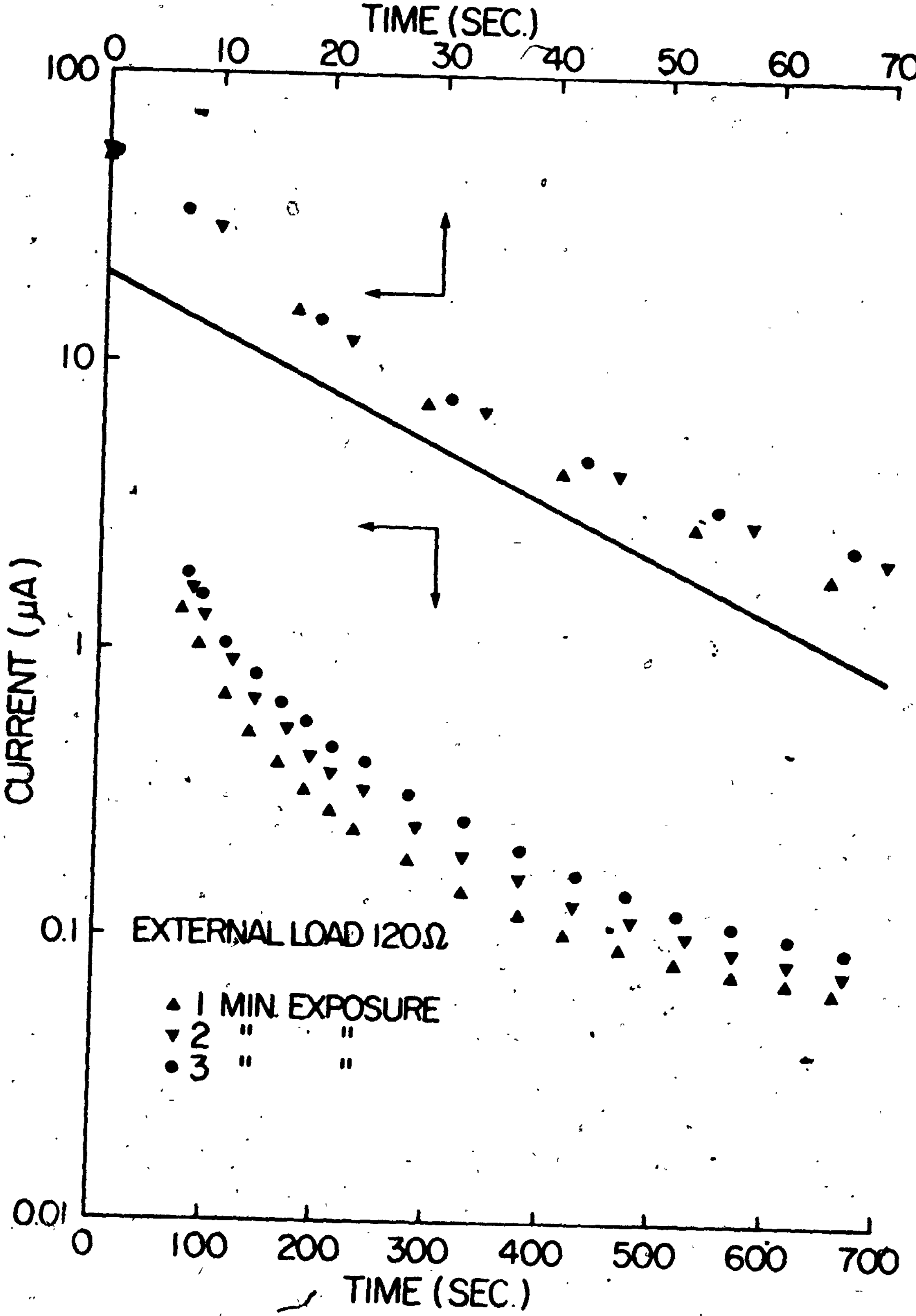
TIME (SEC.)
0 10 20 30 40 50 60 70
100
10
1
0.1
0.01
CURRENT (μA)
EXTERNAL LOAD 120Ω
▲ 1 MIN. EXPOSURE
▼ 2 " "
● 3 " "
0 100 200 300 400 500 600 700
TIME (SEC.)

FIGURE 2.17

Comparison of the Downstep Responses of the Galvanic Probe After 1, 2 and 3 Minutes Exposure to 0.21 atm. O_2 With a Load Resistance of 620 Ohms

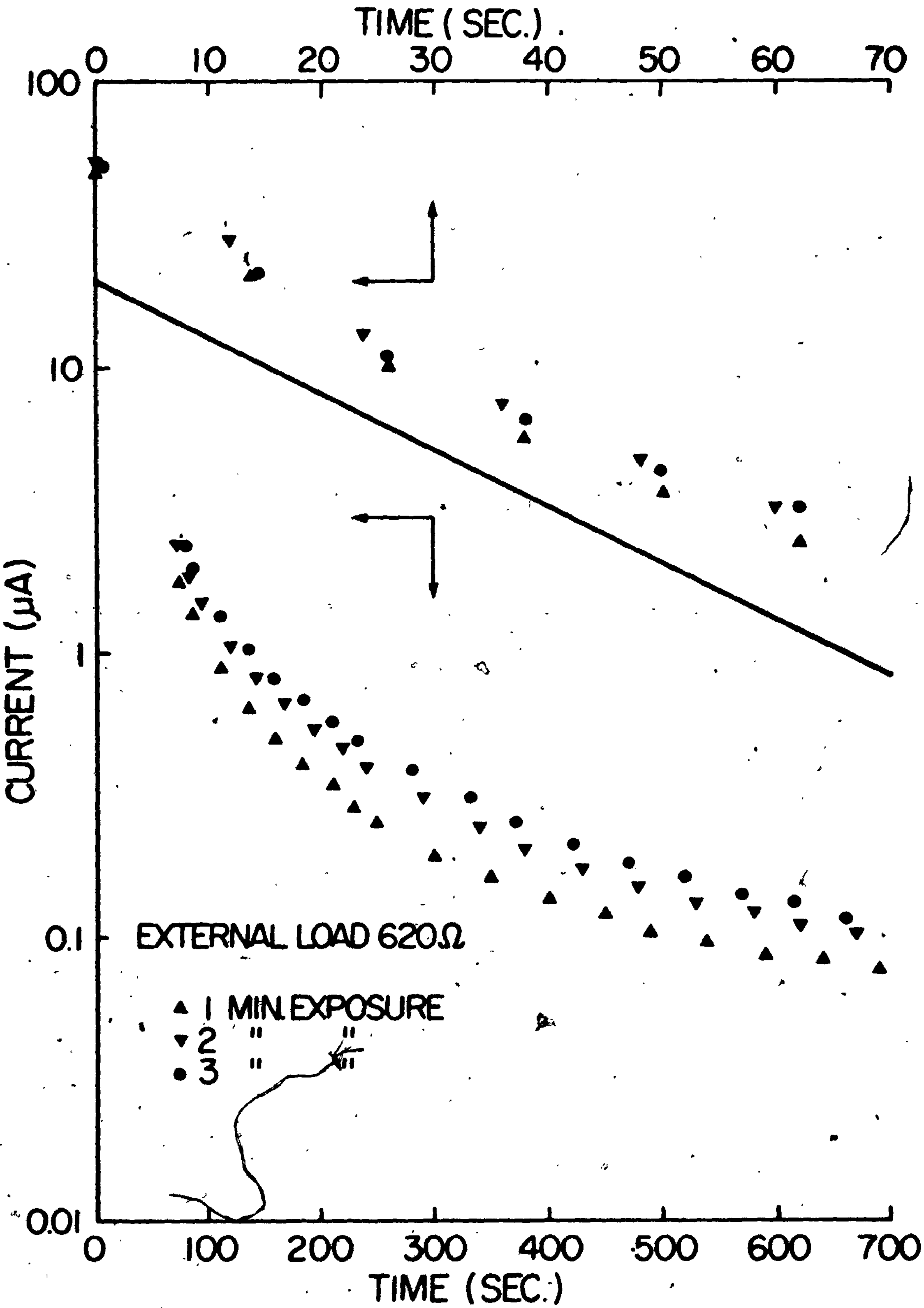
TIME (SEC.)
0
10
20
30
40
50
60
70
100
10
1
0.1
0.01
CURRENT (μA)
EXTERNAL LOAD 620Ω
▲ 1 MIN. EXPOSURE
▼ 2 " "
● 3 " "
0
100
200
300
400
500
600
700
TIME (SEC.)

FIGURE 2.18

Comparison of the Downstep Responses of the Galvanic Probe After 1, 2 and 3 Minutes Exposure to 0.21 atm. O_2 With a Load Resistance of 3K Ohms

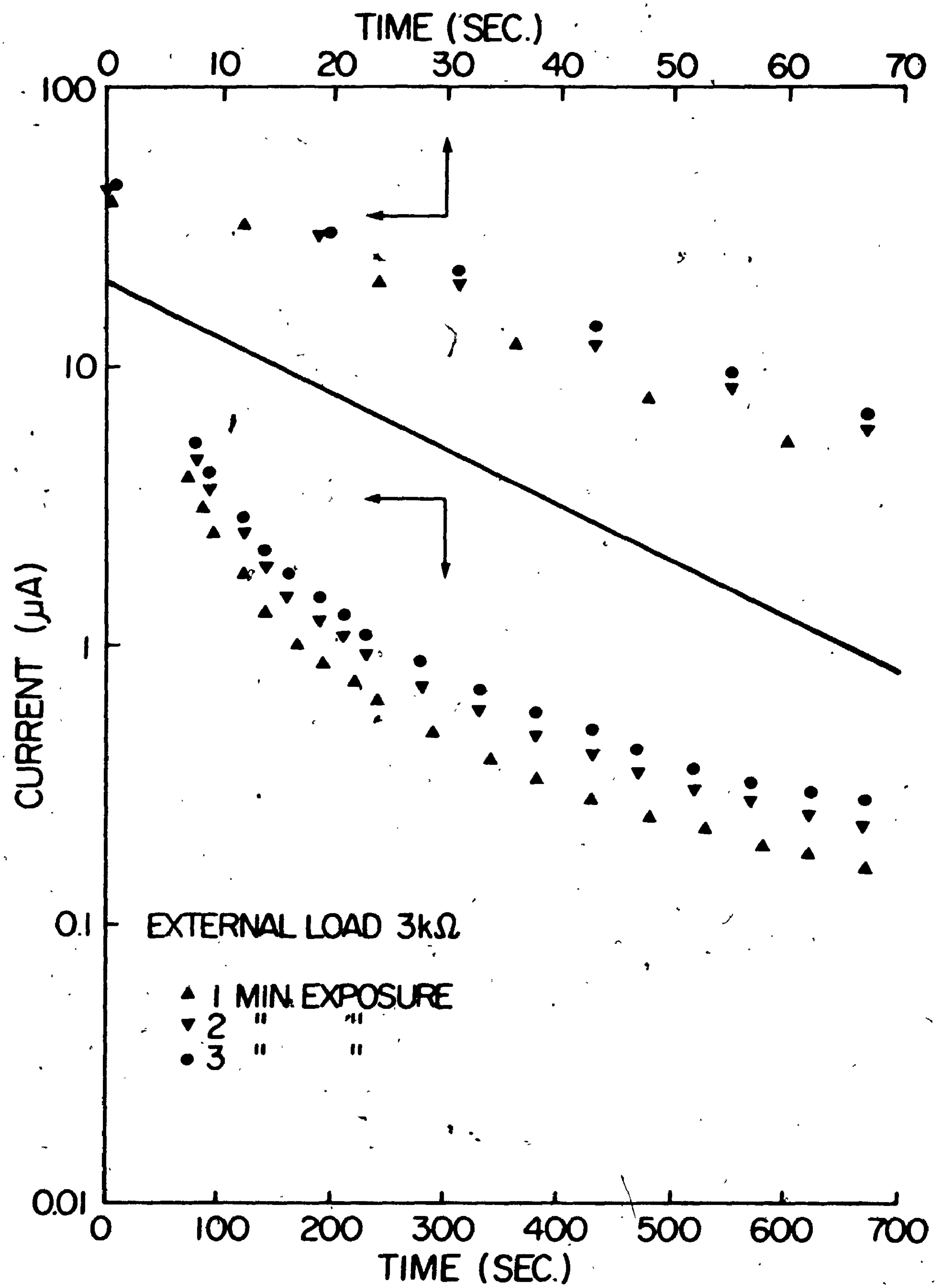

TIME (SEC.)
0 10 20 30 40 50 60 70
100
10
1
0.1
0.01
CURRENT (μA)
EXTERNAL LOAD 3kΩ
▲ 1 MIN. EXPOSURE
▼ 2 " "
● 3 " "
0 100 200 300 400 500 600 700
TIME (SEC.)

FIGURE 2.19

Comparison of the Downstep Responses of the Galyanic Probe After 1 Minute Exposure To 0.21 atm. O_2 With Various Load Resistances

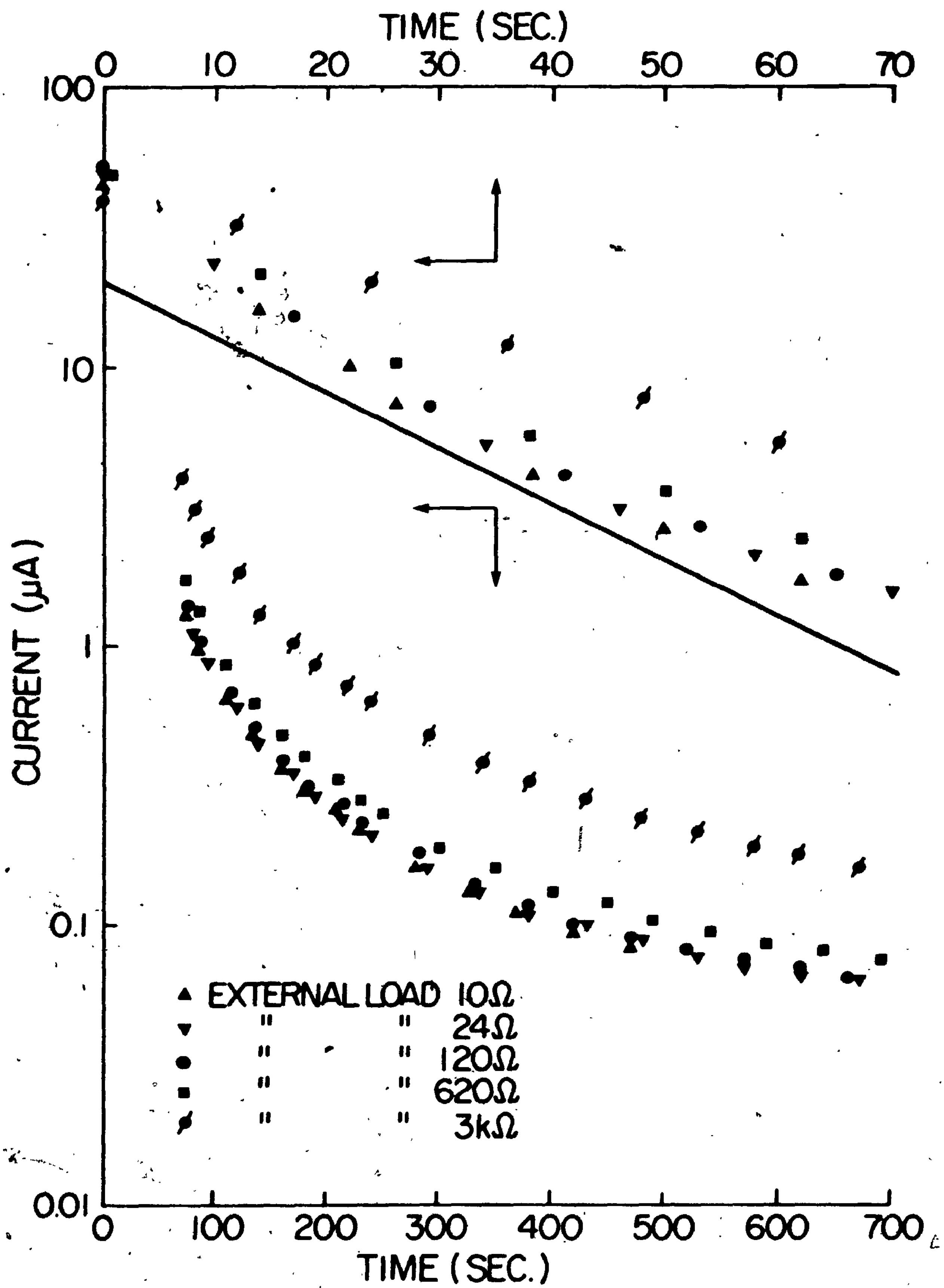
TIME (SEC.)
0 10 20 30 40 50 60 70
100
10
1
0.1
0.01
CURRENT (μA)
EXTERNAL LOAD 10Ω
" " 24Ω
" " 120Ω
" " 620Ω
" " 3kΩ
0 100 200 300 400 500 600 700
TIME (SEC.)

FIGURE 2.20

Comparison of the Downstep Responses of the Galvanic Probe After 2 Minutes Exposure To 0.21 atm. O_2 With Various Load Resistances

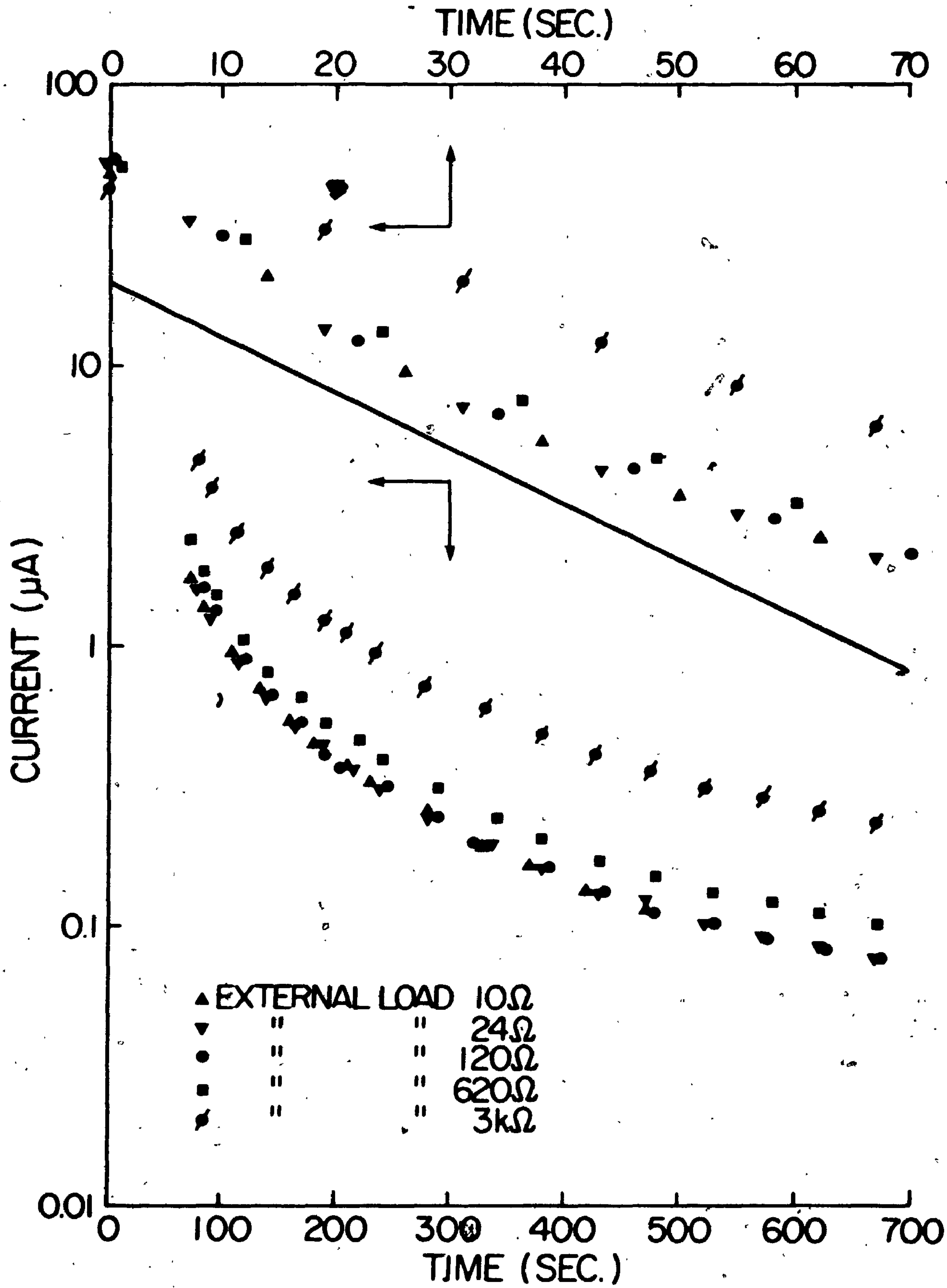

TIME (SEC.)
0
10
20
30
40
50
60
70
100
10
1
0.1
0.01
CURRENT (μA)
▲ EXTERNAL LOAD 10Ω
▼ " " 24Ω
● " " 120Ω
■ " " 620Ω
ø " " 3kΩ
0
100
200
300
400
500
600
700
TIME (SEC.)

FIGURE 2.21

Comparison of the Downstep Responses of the Galvanic Probe After 3 Minutes Exposure To 0.21 atm. O_2 With Various Load Resistances

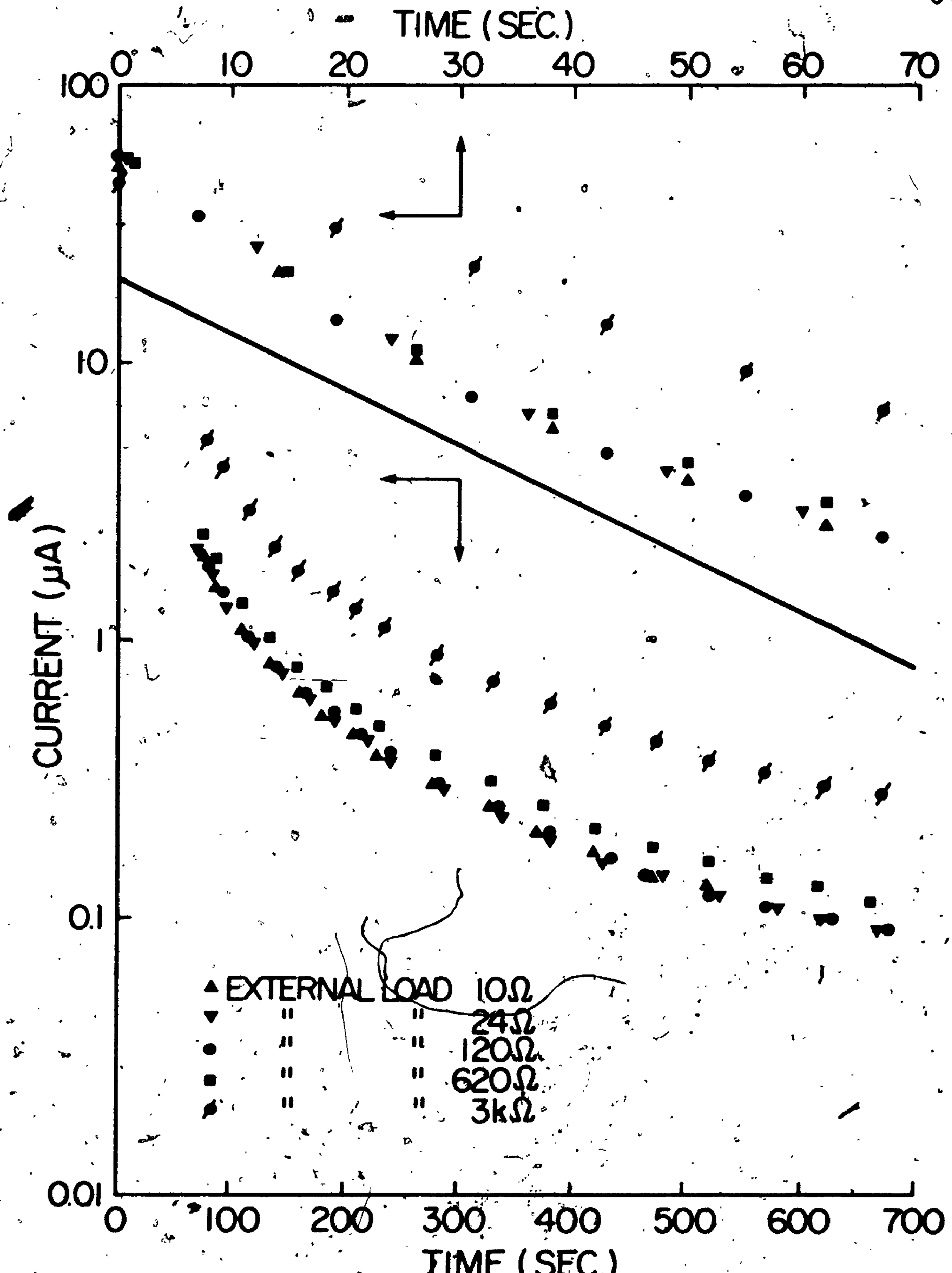
TIME (SEC.)
0
10
20
30
40
50
60
70
100
10
1
0.1
0.01
CURRENT (μA)
EXTERNAL LOAD 10Ω
" " 24Ω
" " 120Ω
" " 620Ω
" " 3kΩ
0
100
200
300
400
500
600
700
TIME (SEC.)

FIGURE 2.22

Comparison of the Downstep Responses of the Galvanic Probe After 1 Minute Exposure To 0.21 atm. O_2 and Various Load Resistance Switching Sequences

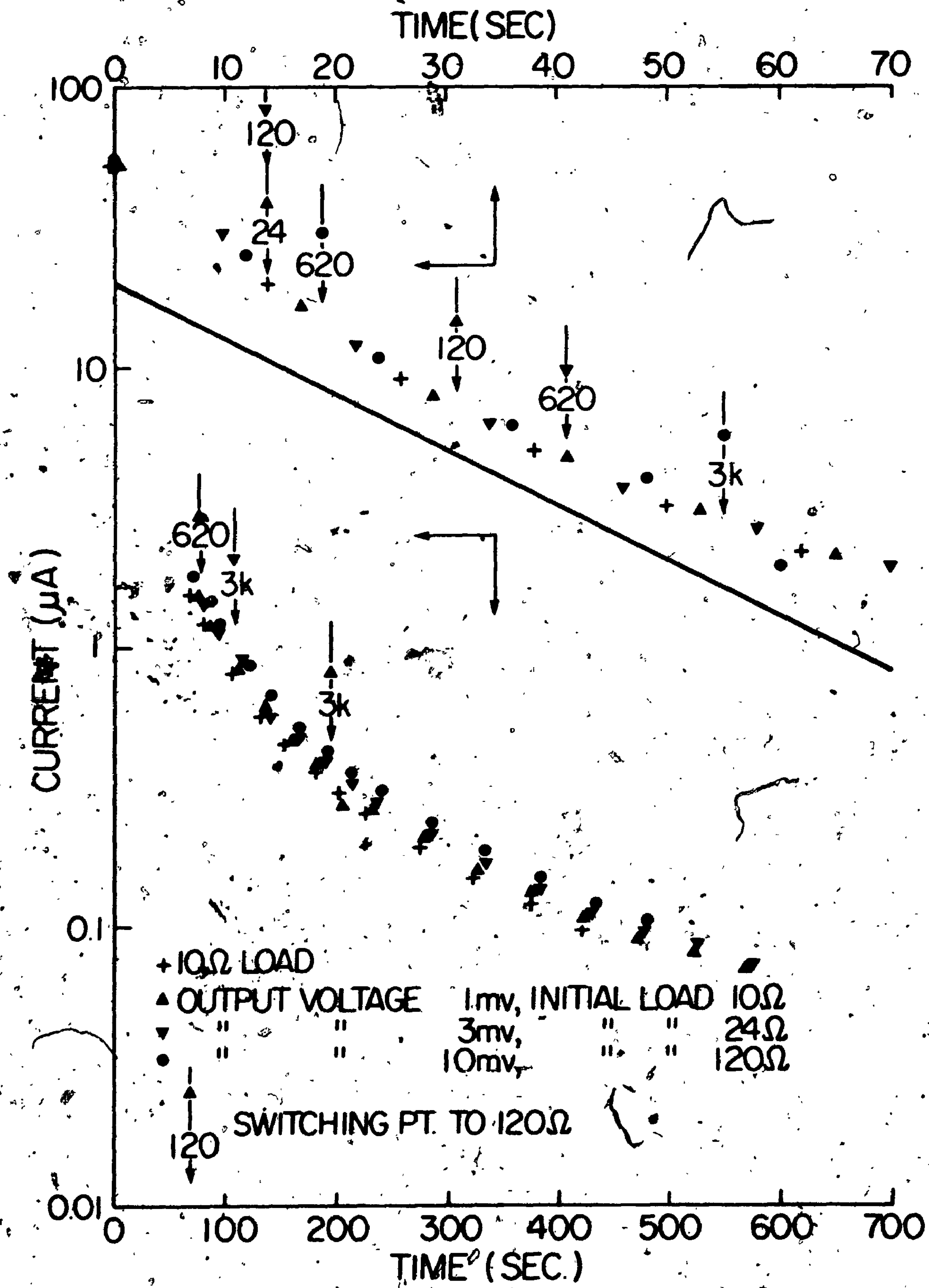
TIME (SEC)
0 10 20 30 40 50 60 70
100
10
1
0.1
0.01
CURRENT (μA)
120
24
620
120
620
3k
620
3k
3k
+ 10Ω LOAD
▲ OUTPUT VOLTAGE 1mv, INITIAL LOAD 10Ω
▼ " " 3mv, " " 24Ω
● " " 10mv, " " 120Ω
120 SWITCHING PT. TO 120Ω
0 100 200 300 400 500 600 700
TIME (SEC.)

- load resistor varied so that the voltage output was always smaller than 3 mv
- load resistor varied so that the probe output voltage was always smaller than 10 mv.

2.6.4 Dynamic Response to 9.26×10^{-4} atm. Oxygen Downstep

Responses to downsteps of 9.26×10^{-4} atm. oxygen after two and three minutes exposure for external loads of 24, 120, 616 and 2.91K ohm are recorded in Figures 2.23 and 2.24.

2.7 Discussion of Galvanic Probe Behavior

2.7.1 Steady-State Current

In Figure 2.13 the steady-state response of the probe is shown as a function of temperature and external load. The probe constant changed 3%/°C at 25°C. Johnson and Borkowski [38] found a value of 2%/°C at this temperature. The 620 ohm external load line lies considerably below the other three. This indicates that at an oxygen tension of 0.21 atm. the 620 ohm resistor caused an excessive voltage drop. The voltage drop varied from 33.0 to 44.5 mv, depending on the temperature. With an external load of 120 ohm the values of the probe constant obtained at 0.21 atm. and 9.26×10^{-4} atm. oxygen differed by 4% and 2% for two different probes.

FIGURE 2.23

Comparison of the Downstep Responses of the Galvanic Probe After 2 Minutes Exposure To 9.26×10^{-4} atm. O_2 With Various Load Resistances

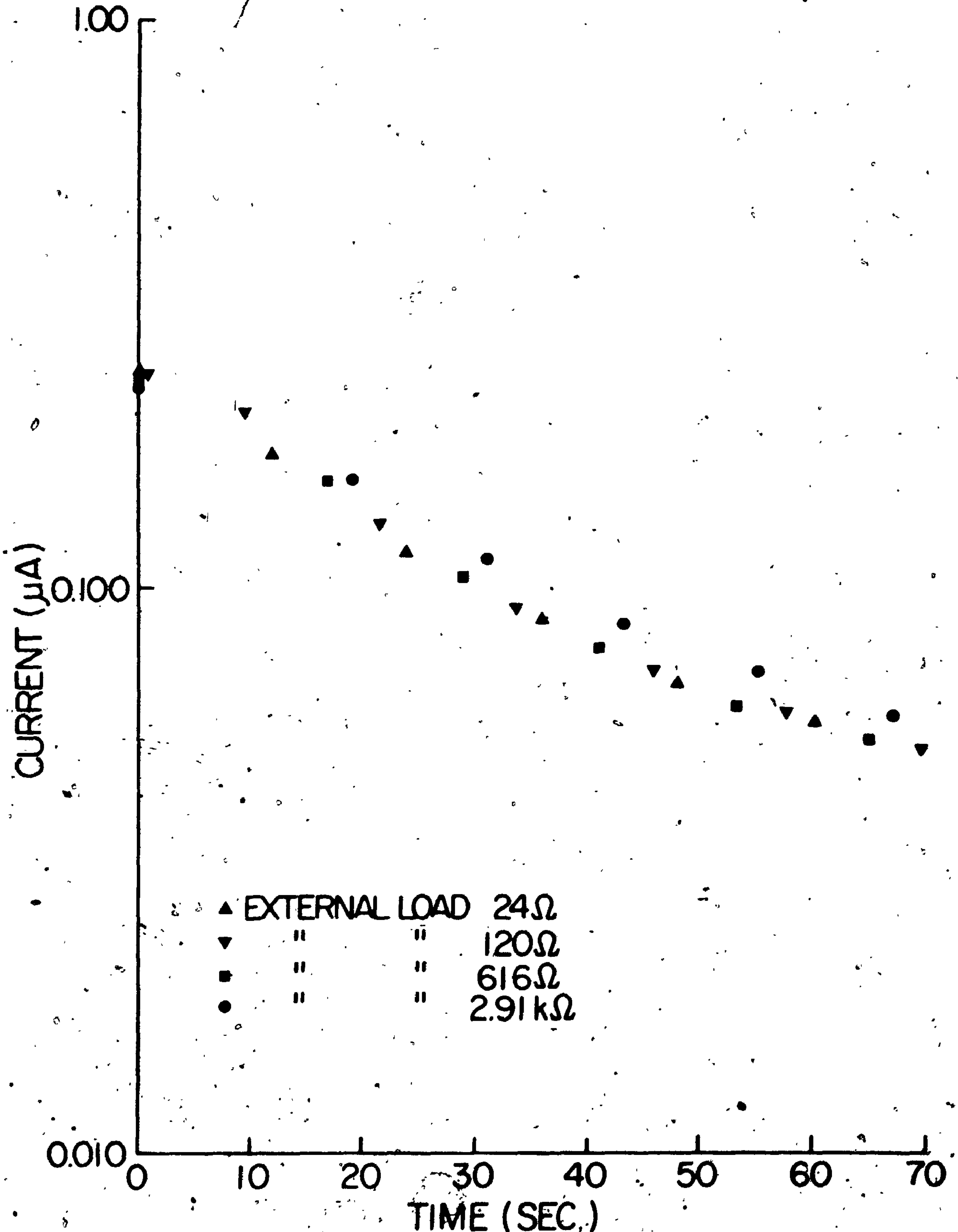
1.00
0.100
0.010
CURRENT (μA)
0
10
20
30
40
50
60
70
TIME (SEC.)
▲ EXTERNAL LOAD 24Ω
▼ " " 120Ω
■ " " 616Ω
● " " 2.91 kΩ

FIGURE 2.24

Comparison of the Downstep Responses of the Galvanic Probe After 3 Minutes Exposure To 9.26×10^{-4} atm. O_2 With Various Load Resistances

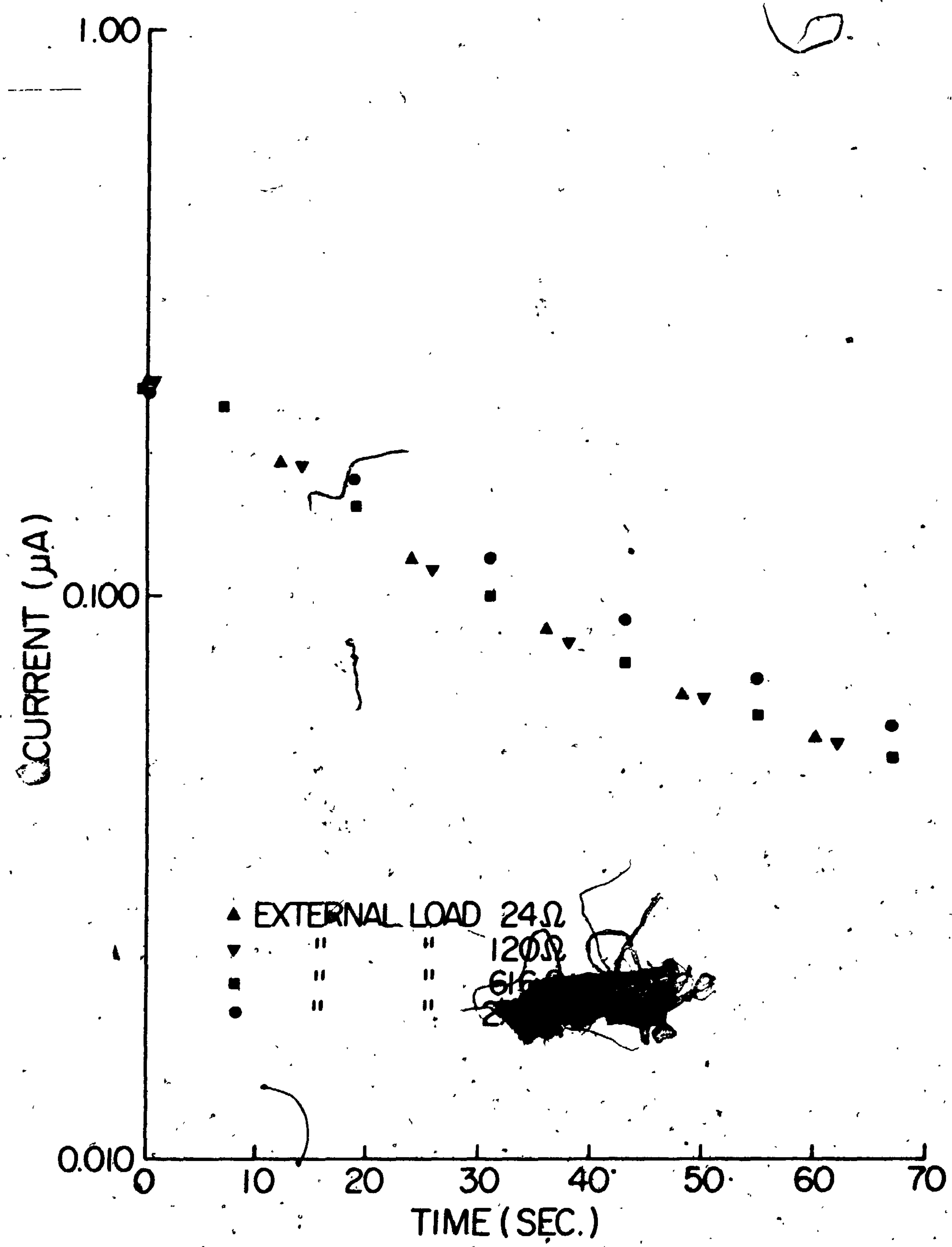
1.00
0.100
0.010
CURRENT (μA)
0
10
20
30
40
50
60
70
TIME (SEC.)
EXTERNAL LOAD 24Ω
" " 120Ω

2.7.2 Dynamic Response to 0.21 atm. Oxygen Downstep

As is evident from Figures 2.14 to 2.18, the duration of exposure significantly influenced the dynamic response for all magnitudes of external load. Dynamic response was adversely affected by the external load when the 620 ohm resistor was switched in and much more significantly during use of the 3K ohm resistor. This is illustrated in Figures 2.19 to 2.21. That the load resistors with higher values can be used to advantage by increasing the output voltage at low currents without causing significant deterioration of the downstep response, can be deduced from the comparison of the four similar results from different switching patterns as shown in Figure 2.22. During these experiments the output voltage was kept below 10 mv at all times. It was observed earlier that the probe's steady-state output current when exposed to 0.21 atm. oxygen was noticeably smaller when the external load was 620 ohm and its output voltage 35 mv than when either the 10, 24 or 120 ohm loads were used. The probe's dynamic response was also somewhat slower at this value of external resistance than at any of the lower values. This therefore justifies at least in part Johnson and Borkowski's [38] statement that the output voltage should never exceed 10 mv. However, it is justified in so far as that it is true when the downstep starts at 0.21 atm. oxygen.

2.7.3 Dynamic Response to 9.26×10^{-4} atm. Oxygen Downstep

As shown in Figures 2.23 and 2.24, probe responses to a downstep of 9.26×10^{-4} atm. oxygen were very similar for external loads of 24, 120 and 616 ohm but were slightly slower for a load of 2.91K ohm. Output voltages at 9.26×10^{-4} atm. oxygen were 0.147 mv and 0.675 mv at loads of 616 and 2.91K ohm respectively. This suggests that at an oxygen tension of 9.26×10^{-4} atm., insertion of an external load causing a voltage drop of 0.675 mv would adversely affect the dynamic response to a downstep. The allowable voltage output of the galvanic probe therefore decreases with decreasing oxygen tension if linearity of steady-state response and optimality of dynamic response is to be retained.

2.7.4 Comparison of Responses to 0.21 atm. and 9.26×10^{-4} atm. Oxygen Downsteps

In Figure 2.25 dynamic responses as percentages of maximum current are plotted for 9.26×10^{-4} atm. and 0.21 atm. oxygen downsteps. Response to the smaller downstep was considerably slower.

2.8 Conclusions for the Galvanic Probe

In the foregoing it was noticed that probe steady-state response to a given oxygen tension was a function of external load and temperature and that the dynamic response

FIGURE 2.25

Comparison of the Downstep Responses of the Galvanic Probe After 2 Minutes Exposure To 0.21 atm. O_2 and 9.26×10^{-4} atm. O_2. Load Resistances Were 24 and 120 Ohms Respectively

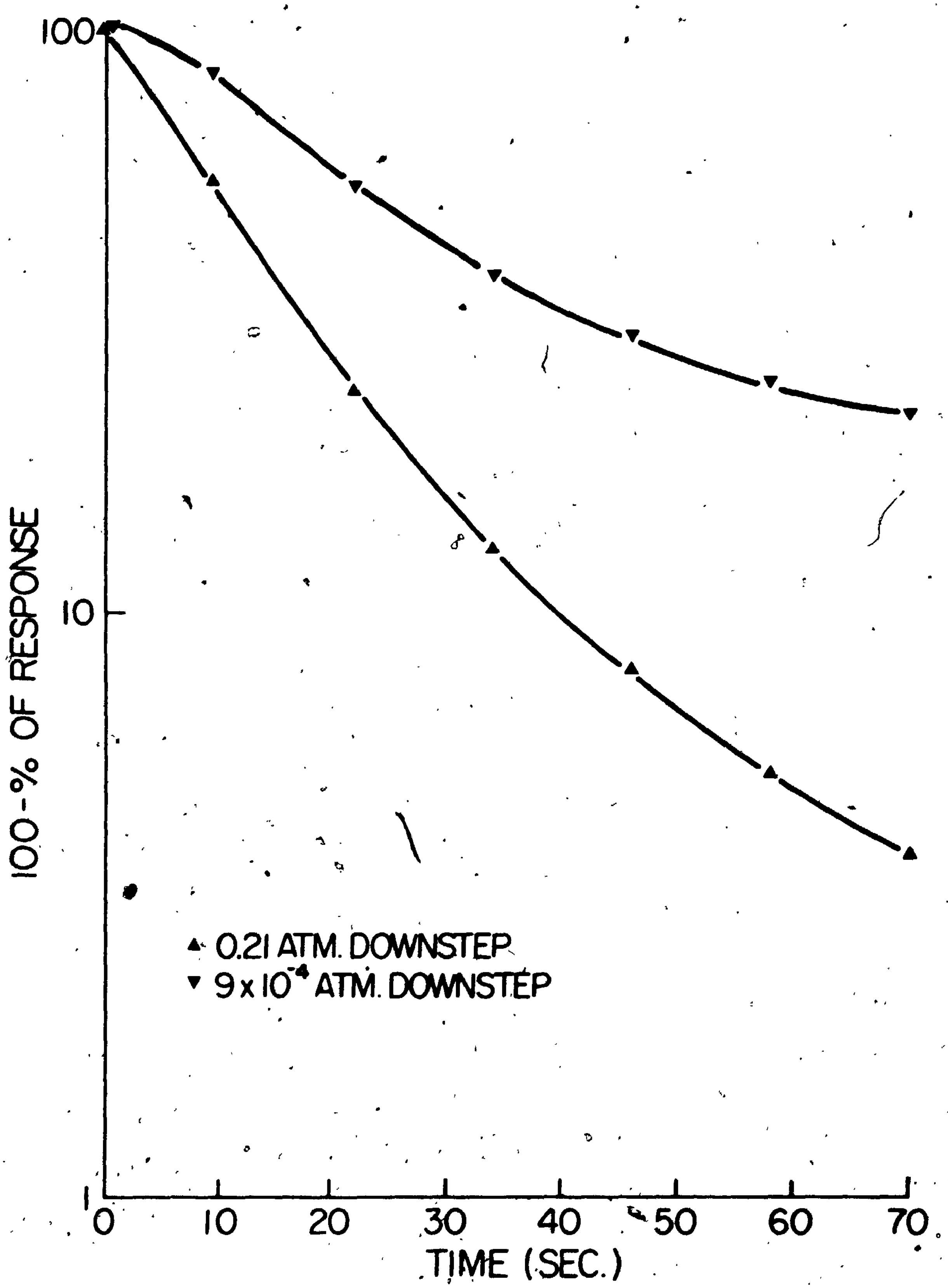

100
10
1
100-% OF RESPONSE
0
10
20
30
40
50
60
70
TIME (SEC.)
▲ 0.21 ATM. DOWNSTEP
▼ 9 x 10^{-4} ATM. DOWNSTEP

was influenced by external load, duration of exposure prior to the downstep and the oxygen tension to which the probe was exposed. To obtain optimal response and yet have an adequately large voltage output throughout a wide range of oxygen tensions it is necessary to increase the external load as the oxygen tension decreases. This should be done in such a manner that the voltage output never exceeds the critical value at a given oxygen tension. This critical voltage is approximately 10 mv at 0.21 atm. oxygen and considerably below 1 mv at 9.26 x 10^{-4} atm. oxygen tension for the system studied.

The above mentioned effects are thought to be due to the necessary presence of a very low oxygen tension at the cathode surface in order to generate the output voltage. The higher this output voltage is required to be, the higher the oxygen tension at the cathode must be. An unduly high cathodic oxygen tension would decrease the mass-transfer driving force, thus decreasing the steady-state current output. It would also constitute an oxygen reservoir, affecting the dynamic response.

The dynamic response obtained herein of 90% in approximately 45 seconds after 1 minute exposure to 0.21 atm. oxygen was very similar to data reported by Johnson and Borkowski [38]. MacLennan and Pirt [42], Mackereth [43] and Van Hemert *et al.* [68] all obtained 90% response in 15 seconds under similar conditions. In both this study and the work of Johnson and Borkowski [38] a spiral-form cathode was used, whereas all the others used a solid cathode with a roughened surface. It seems therefore that the spiral form of cathode enhances the formation of oxygen storage reservoirs. Although the type of probe investigated had a slower response characteristic than some of the others described in the literature, it is suggested that the conclusions reached are also applicable to other, faster galvanic probes since they operate on the same principle.

2.9 Apparatus For the Polarographic Probe

Use of the polarographic probe is much more cumbersome than of a galvanic one since the latter generates its own voltage so that output measuring equipment consists of an appropriate output impedance and a meter, whereas the former requires an external polarizing source of constant potential and a means of measuring the current in the polarizing circuit.

2.9.1 The YSI Probe

The polarographic probe used was supplied by the Yellow Spring Instrument Company (Ohio, U.S.A.), model G-1678-5. It is illustrated in Figure 2.6 and photograph 2.3. Its specifications as given by the manufacturer are listed in Appendix 2.3. The probe has an annular gold cathode, a sintered silver anode and contains 2.5 M KCl solution as its internal electrolyte phase. A small amount of 'Kodak Photo-

PHOTOGRAPH 2.3

The YSI Polarographic Probe

2 OF/DE 6

'Flo' is added to the electrolyte to ensure electrolyte penetration of the anode. Throughout this work membranes of nominal 1/2 mil thickness (YSI) were employed. During the mounting of the membrane, thickness can be influenced considerably by stretching. Benedek and Heideger [10] have pointed out the importance of membrane tautness.

2.9.2 Electronics Design Concept

Residual current of the probe when submerged in cupric ion-catalysed sodium sulfite solution or when flushed with pure nitrogen gas was approximately 0.010 microamp. When exposed to air, current was of the order of 35 microamp. At an applied voltage of 0.800 volt the equivalent resistance of the probe was therefore 80M ohm and 23K ohm respectively for these situations. To measure and control the polarizing voltage of the probe within close tolerances, the measuring and feedback circuits had to have extremely high input impedances so as not to constitute current paths parallel to the probe. In Figure 2.26 the basic circuit concept used is illustrated. The Impedance Matching Circuit (IMC) is in effect parallel to the probe. It reproduced exactly the voltage at its output at low impedance as it received on its input at very high impedance. The variable power supply adjusted its output voltage so that the voltage on its feedback circuit always remained at a pre-set value. The current through R_c was therefore almost exactly the same as

FIGURE 2.26

Basic Circuit Concept For the Measurement of the Polarographic Probe Current. V_1, V_2 - Voltmeters; R_c - Chain Resistance

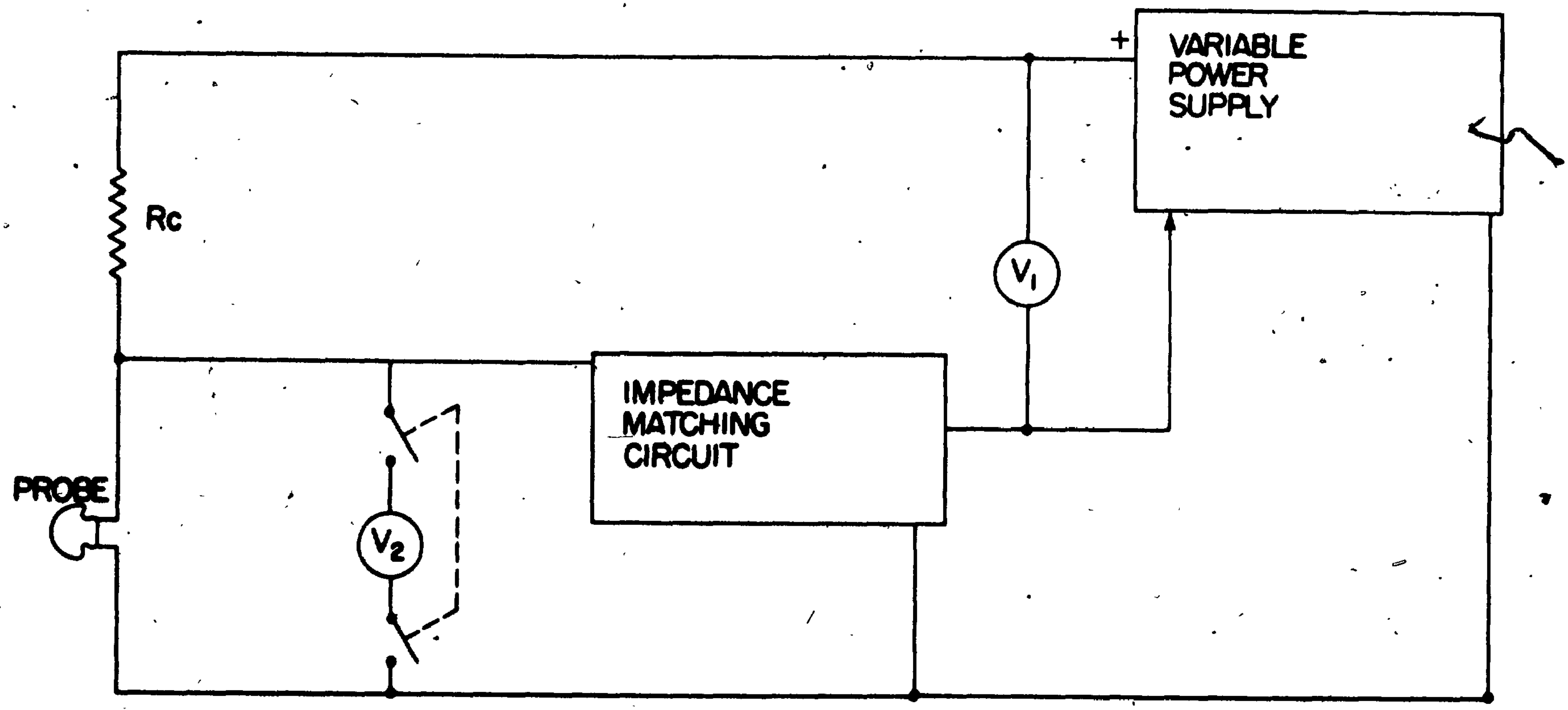
VARIABLE
POWER
SUPPLY
+
V1
Rc
IMPEDANCE
MATCHING
CIRCUIT
V2
PROBE

through the probe so that the voltage drop across R_c was proportional to the oxygen tension to which the probe was exposed. V_1 was placed behind the IMC so that its input impedance would not affect the value of R_c. To monitor the polarizing voltage directly without interfering with the probe current measurement, a high-impedance meter V_2 (10M ohm) could be switched into the circuit temporarily.

2.9.3 The Circuit

The schematics for the IMC and its associated power supply are shown in Figures 2.27 and 2.28. High input impedance was provided by a reverse-biased field effect transistor. The theoretical input impedance of this transistor is listed as 7.5×10^9 ohm. The input circuit has a gain of slightly less than one. The output circuit therefore has a variable gain of slightly larger than one to compensate for this. The middle circuit compensates for initial bias current. The two controls enable the IMC to be properly calibrated.

The circuit also contained three other independent power supplies. Their configuration is shown in Figure 2.29.

The interconnecting circuitry and switching arrangement are shown in Figure 2.30. The apparatus together with measuring and recording equipment is shown in Photograph 2.4. Meters used were a Philips Digital Multimeter model PM 2422 in parallel with the probe and a Hewlett Packard D.C.

FIGURE 2.27

Circuit Diagram For the Impedance Matching Device

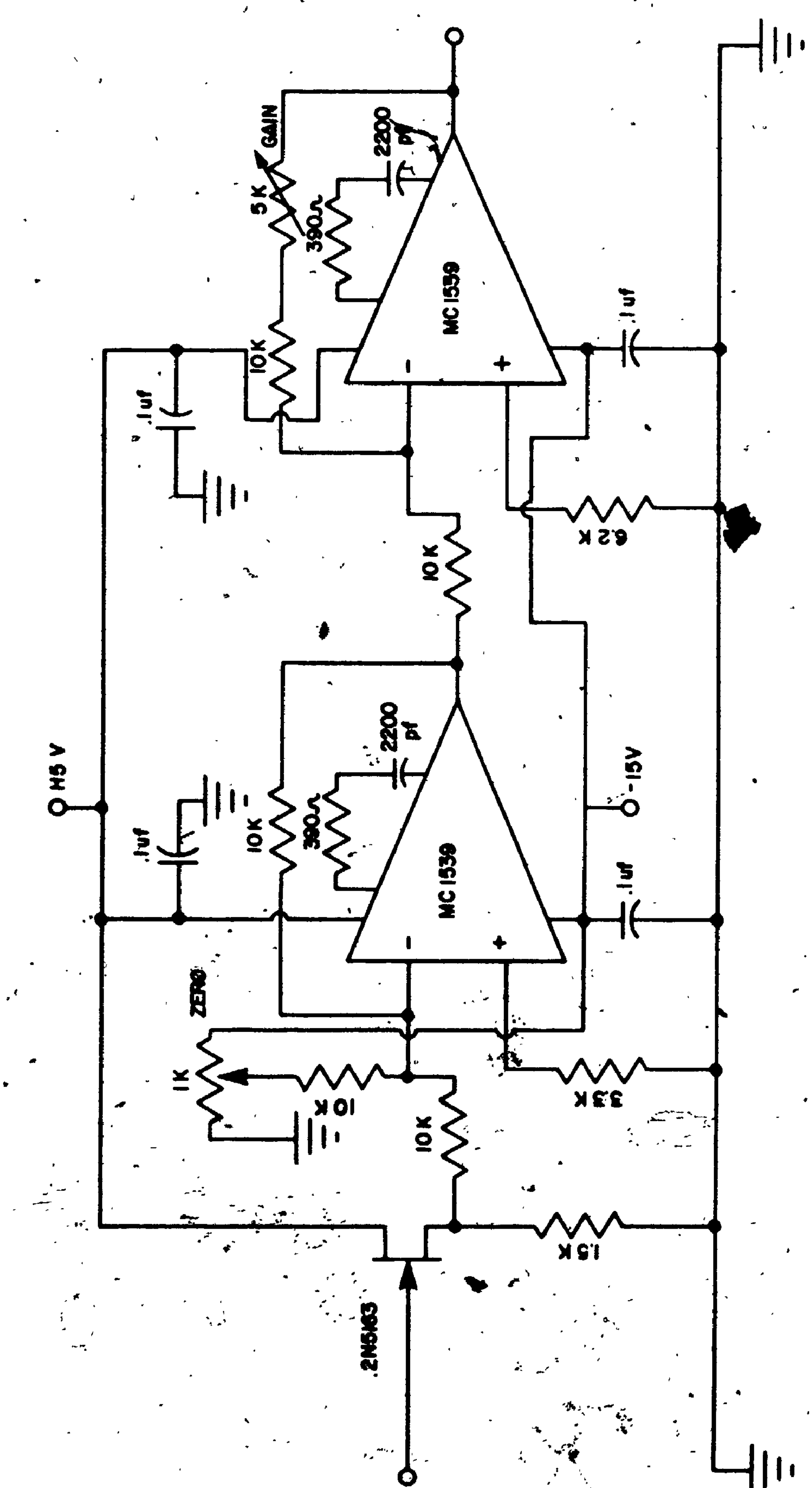
MC1539
MC1539
GAIN
5 K
390Ω
2200 pf
10K
10 K
.1uf
6.2 K
+15 V
-15V
ZERO
1K
3.3 K
1.5 K
2N5163

FIGURE 2.28

Circuit Diagram For the Power Supply of the Impedance Matching Device (*The Microelectronics data book*, Motorola Semiconductor Product, Inc., Dec. 1969)

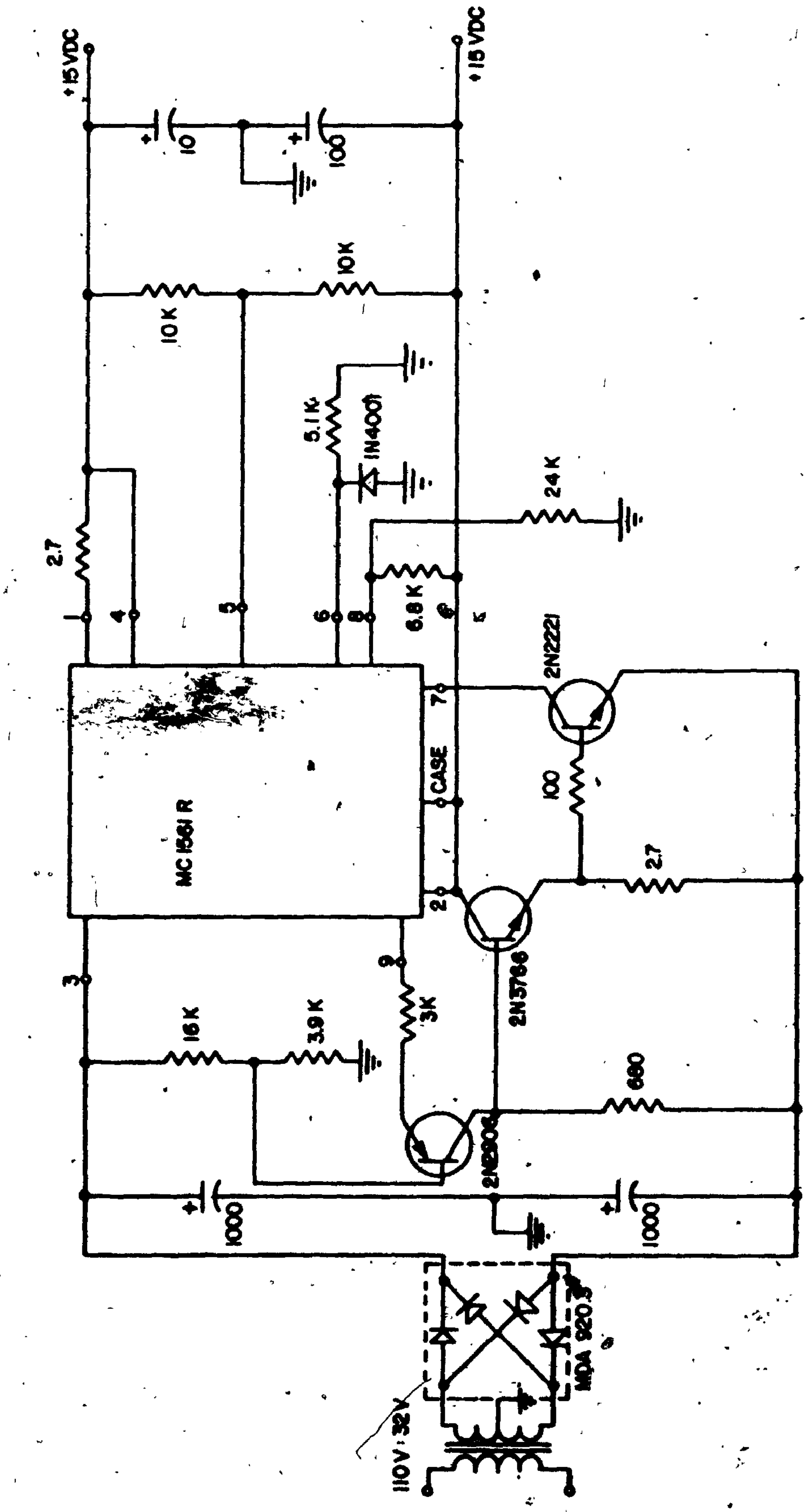
+15 VDC
+15 VDC
10
100
10 K
10 K
5.1 K
1N4001
24 K
2.7
6.8 K
MC 1561 R
CASE
2N2221
100
2.7
2N5766
16 K
3.9 K
3K
680
2N2905
1000
1000
MDA 920.3
110V : 32V

FIGURE 2.29

Circuit Diagram For the Power Supplies

Producing V_A, V_B and V_C

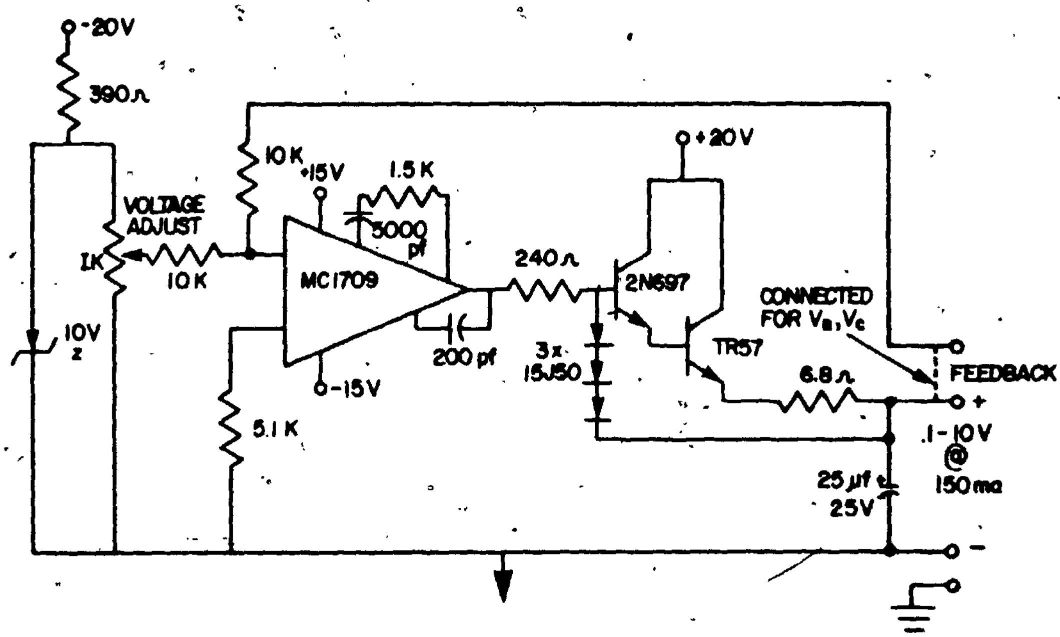
-20V
390Ω
10 K
+15V
1.5 K
5000 pf
VOLTAGE ADJUST
1K
10 K
MC1709
240Ω
+20V
2N697
TR57
CONNECTED FOR V_B, V_C
FEEDBACK
10V z
200 pf
3x 1SJ50
-15V
6.8Ω
+
.1-10V @ 150ma
5.1 K
25 µf 25V
−

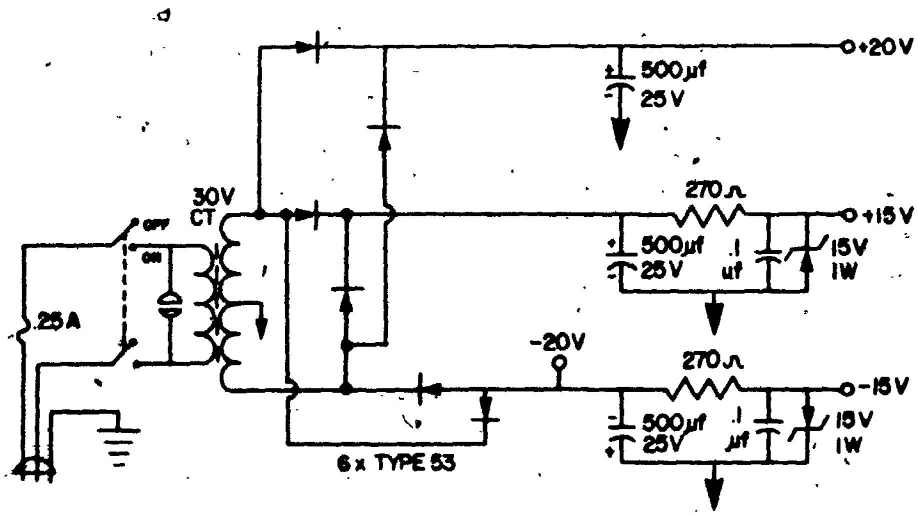
+20V
500µf 25V
30V CT
OFF
ON
270Ω
+15V
500µf 25V
.1 µf
15V 1W
.25A
-20V
270Ω
-15V
500µf 25V
.1 µf
15V 1W
6 x TYPE 53

FIGURE 2.30

Circuit Diagram For the Interconnecting Circuitry and Switching Arrangement For the YSI Polarographic Probe

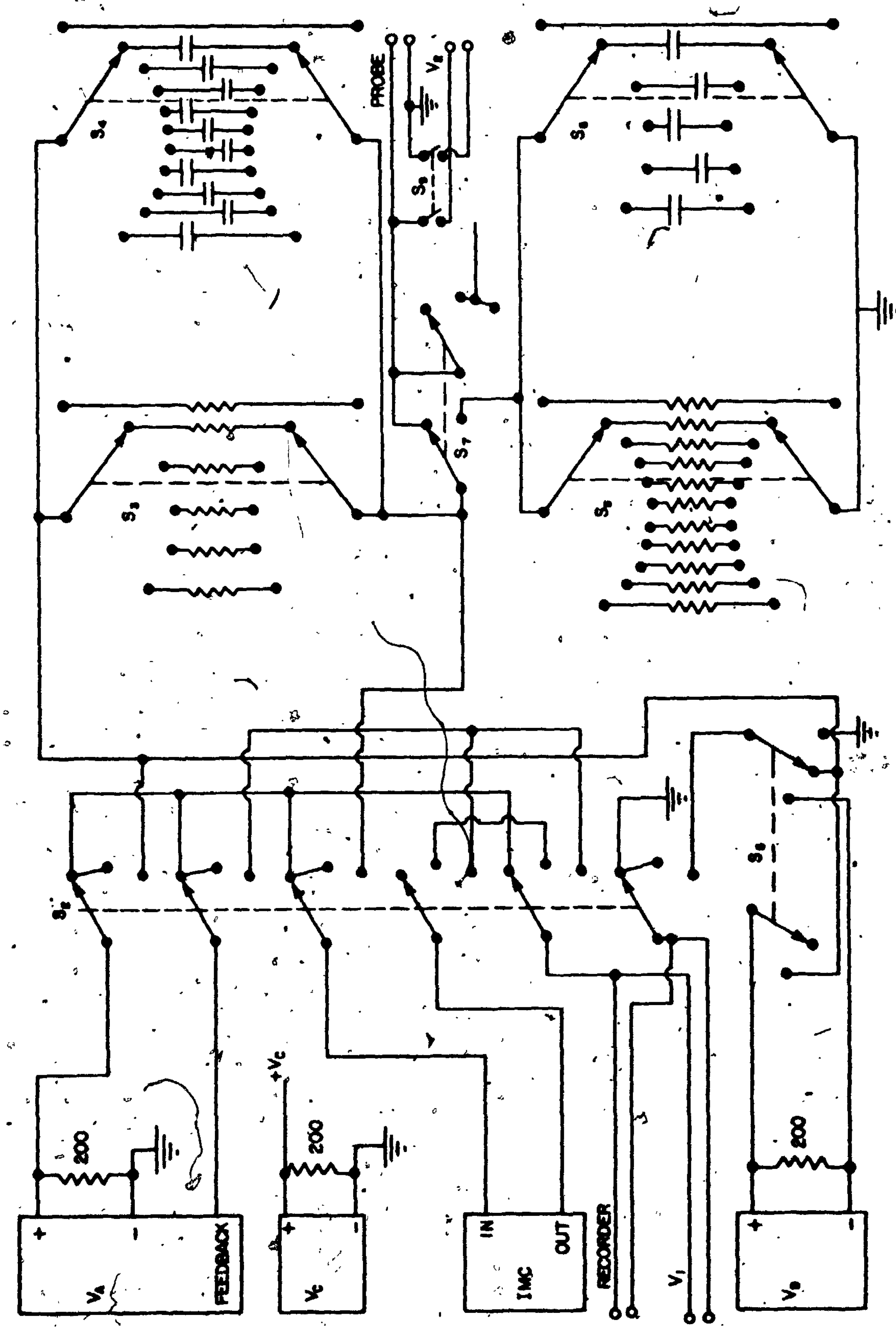
PROBE
S4
S5
S6
S7
S8
S2
200
200
200
+Vc
+
-
FEEDBACK
VA
Vc
IN
OUT
IMC
RECORDER
V1
VB

PHOTOGRAPH 2.4

The Measuring and Recording Equipment

For the Polarographic Probe

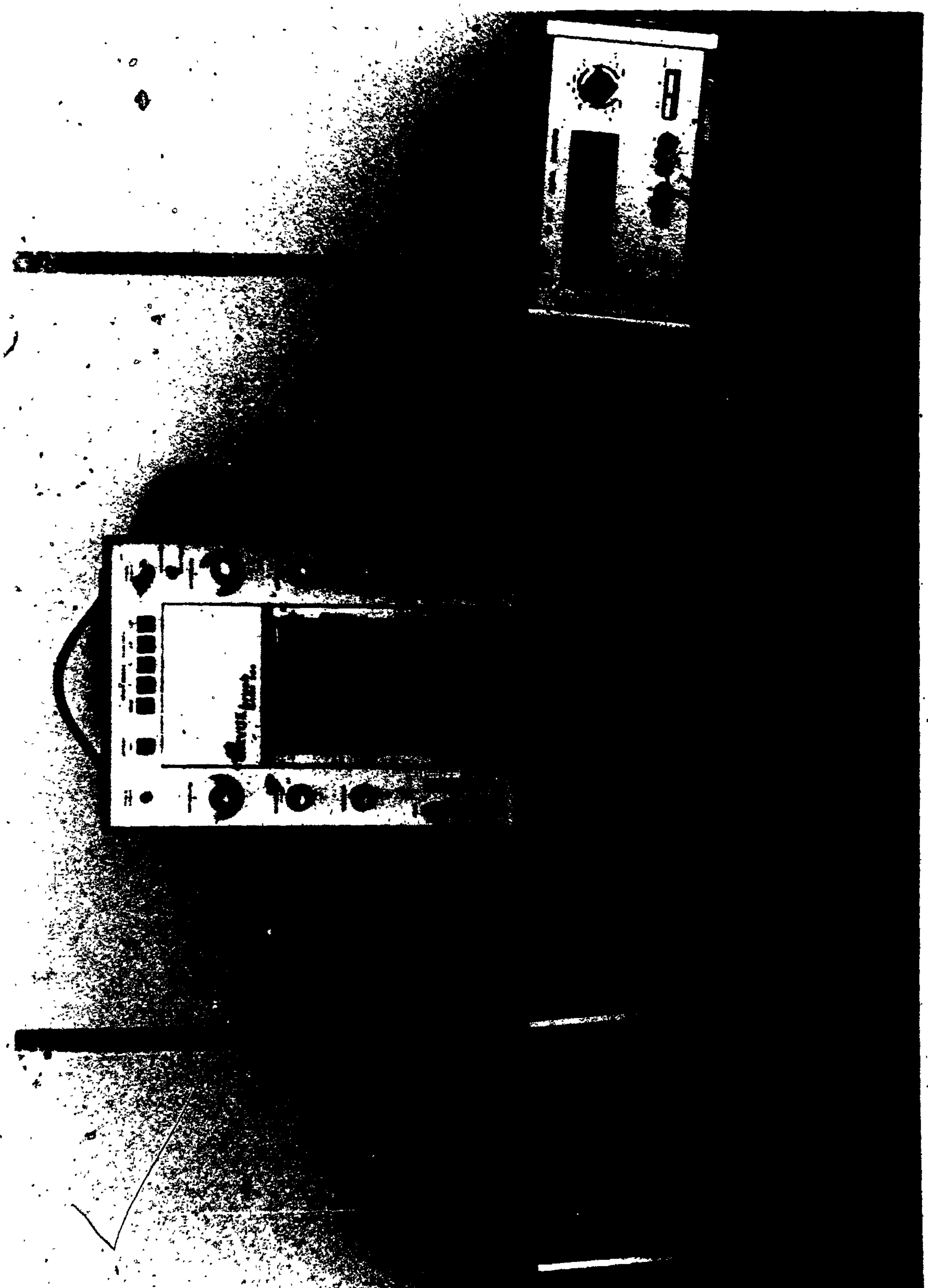

voltmeter model 419A as the output device. A Clevite 'Brush' recorder model Mark 220 was employed in parallel with the D.C. voltmeter to obtain a permanent record of the output.

The three positions of S2 provide the capability of displaying either the polarizing voltage, the IMC output without the probe being connected or the voltage drop across R_c on the D.C. voltmeter. The latter is its normal position; the two former positions are used only during the calibration procedure. S3 allows choice of R_c values of 3.3K, 10K, 33K, 100K, 270K, or 1M ohm (±0.5%). S4 allows capacitors of 0, 0.05, 0.1, 0.22, 0.5, 1.0, 2.2, 5, 10, 25, or 50 microfarad to be switched in parallel with R_c for noise suppression or system stabilization. S5 is the dummy load resistance switch. Dummy loads of 20K, 47K, 68K, 100K, 200K, 270K, 1M, 3.9M, 6.8M, 9.1M or 18M ohm (± 1%) can be switched into the circuit. Capacitances of 0, 5, 10, 25, 50 or 100 microfarad can be switched in parallel with the dummy load by S6. S7 can be used to switch the polarizing voltage onto either the probe, a dummy load resistance bank or an infinitely large impedance open-circuit. Whenever the polarizing voltage from power supply V_A is not connected to the probe, the auxiliary polarizing power supply V_C preset at 0.800 volt is connected so that at no time during the calibration procedure the probe is without a polarizing source. S8 allows either the probe polarizing voltage, the voltage across R_c or the latter voltage minus a suppressor voltage V_B to be displayed on the D.C. voltmeter. The digital voltmeter, used to monitor the probe polarizing voltage can be switched into or out of the circuit by S9. Some of the apparent redundancy of meter and switching functions was found to be necessary to allow complete calibration of all system components in a minimum of time and was very useful during testing of the apparatus and repair work.

2.9.4 Electronics Operating Characteristics

Steady-State Operation

The electronic apparatus was sensitive to temperature changes. When room temperature was held constant the polarizing voltage varied less than 1 mv over 24 hours. It was attempted to estimate the IMC input impedance by disconnecting the dissolved oxygen probe from the apparatus during normal operating conditions and measuring the current through R_c. No current could be observed. Precision resistors connected to the apparatus instead of the probe always caused currents well within expected limits as calculated from their tolerances. Internal dummy load resistors being switched in had the same effect.

Dynamic Response

All permanent records were obtained with the 'Brush' recorder. Response time to a full chart-width step input is less than 25 msec. Dynamic response of the electronics was governed by the time constant of the R_c-C_c network and was found to be independent of the value of the dummy load resistance at all available values of the latter. The time constant of the electronic circuit to a step increase or decrease in either the chain resistance or dummy load resistance was practically identical to the theoretical time constant of the R_c-C_c network. The expected minimum probe time constant was 5 seconds. Since the maximum available R_c value was 1M ohm the 0.5 microfarad capacitor C_c could be safely used at all times without appreciably affecting the measurement of probe response. In practice the largest capacitance used was 0.1 microfarad except during the dynamic response measurement to a downstep of 1.76 x 10^{-4} atm. oxygen which is described later.

2.10 Experimental Methods for Polarographic Probe Characterization

During all experiments with the polarographic probe the polarizing voltage was controlled at the manufacturer's recommended voltage of 0.800 volt. At this voltage the current is limited by the mass-transfer rate instead of electron-transfer rate. Difficulties were experienced several times with excessive residual currents which were caused by ground loops. Similar problems were later also noticed with commercially-acquired equipment mounted on a pilot plant fermentor. All baths, sparging chambers and other vessels containing liquids in which the probe was submerged were therefore insulated from ground to such an extent that no leakage current could be detected. Experiments performed to characterize the polarographic probe are described in the following sections.

2.10.1 Temperature Dependence of Probe Output Current

The polarographic probe was mounted in the side of the same water-filled controlled temperature chamber as was used for the galvanic probe. The assembly is shown in Photograph 2.5. The temperature was controlled by a polypropylene heating/cooling coil supplied by a constant temperature bath. The polypropylene provided sufficient electrical insulation between the bath and the circulating water so as to prevent any ground loop currents from affecting probe residual current. The chamber was constantly sparged with air through a fritted bubble sparger. The probe was fitted with a 1 mil Teflon (YSI) membrane. Temperature in the chamber was measured by a thermometer submerged in the chamber contents.

2.10.2 Steady-State Response

The polarographic probe was mounted in a chamber which was flushed with calibration gas in a manner identical to the method described for the galvanic probe in section 2.5 and depicted in Figure 2.12. For these tests the liquid was

PHOTOGRAPH 2.5

The YSI Probe Mounted in the Controlled Temperature Sparging Chamber

completely withdrawn from the chamber when it was flushed with calibration gas. The calibration gases used were: 176 ppm, 926 ppm, 0.30%, 1.01%, 3.02%, 9.96% and 21% oxygen in nitrogen (Liquid Carbonic).

2.10.3 Unsteady-State Response

The polarographic probe was mounted in a chamber in a manner identical to the procedure described in section 2.5. Probe downstep responses were recorded for each of the calibration gases after exposures of one, two or three minutes duration in the order described in Table 2.1.

After each downstep response was obtained the probe was allowed to return to its residual current before the next exposure-downstep cycle was started. Downstep responses for the 9.96×10^{-2} and 0.21 atm. oxygen gases were obtained a day after the others were completed. During all downstep experiments the probe was fitted with a 1/2 mil. Teflon (YSI) membrane.

TABLE 2.1

Order of Calibration Gas Utilization and Probe Exposures

Gas Oxygen Tension (atm.)	Order and Duration of Exposures (min.)	Comments
3.0×10^{-3}	1,1,1,2,1,2,1,3,1,3,1,1	
1.01×10^{-2}	1,1,1,2,1,2,1,3,1,3,1,1	
9.26×10^{-4}	1,1,1,2,1,2,1,3,1,3,1,1	
1.76×10^{-4}	1,1,1,2,1,2,1,3,1,3,1,1	← C_o was 1 microfarad except for 2nd exposure
3.02×10^{-2}	1,1,1,2,1,2,1,3,1,3,1,1	
9.96×10^{-2}	1,1,1,2,3,1,1	
0.21	1,1,1,2,1,3,1	

2.11 Experimental Results From the Polarographic Probe Characterization

2.11.1 Temperature Dependence of Probe Output Current

Data obtained during this experiment are graphed together with their least-square line in Figure 2.31. The probe constant at 25°C was 77.1 microamp/atm. oxygen and varied at a rate of 2.1 microamp/atm. O_2/°C or 3%/°C at 25°C.

2.11.2 Steady-State Response

Steady-state data obtained are listed in Appendix 2.4. Average currents and probe constants for three trials at each oxygen tension are listed in Table 2.2. The average probe constant was 137 microamp/atm. oxygen at 22°C with a standard deviation of 3.7%.

2.11.3 Unsteady-State Response

Numerical records of downstep responses were printed by the processing program KOK1 listed in Appendix 2.5. All recorded currents were calculated from the observed currents by subtracting the residual current for the particular downstep. Downstep data are listed in Appendix 2.6. A typical record of a downstep response is shown in Figure 2.32. Fifth-order least-square polynomials were fitted through the time vs ln(current) data by program KOK2. Program KOK2 is listed in Appendix 2.7, together with the user-supplied

FIGURE 2.31

Relationship Between the Output Current of the YSI Probe and the Temperature. The Membrane Thickness Was Nominally 1 mil. Shown Are the Data Points and the Least-Square Line

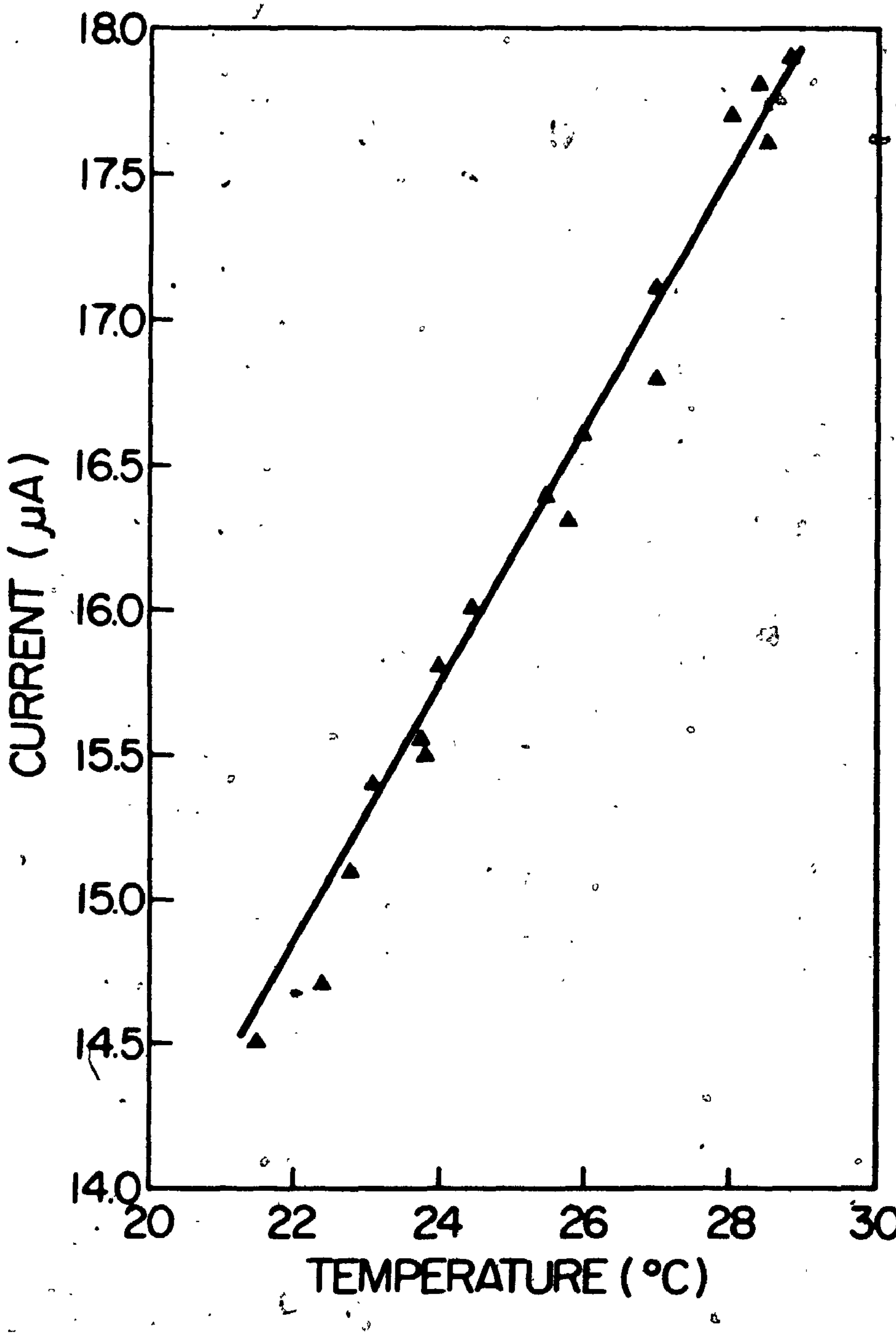

18.0
17.5
17.0
16.5
16.0
15.5
15.0
14.5
14.0
CURRENT (μA)
20
22
24
26
28
30
TEMPERATURE (°C)

FIGURE 2.32

A Typical Recorded Trace of an Exposure-Downstep Response Cycle. Chart Speed Was 125 mm/min. The Oxygen Tension Was Calculated From the Signal By Multiplying With the Appropriate Amplifier and Recorder Gains and Subtracting the Residual Signal

a) initial residual current at high amplifier gain
b) initial residual current at low amplifier gain
c) exposure to oxygen-containing gas
d) submersion of the probe in sodium sulfite solution
e), f) amplifier gain switching during downstep
g) post-exposure residual current

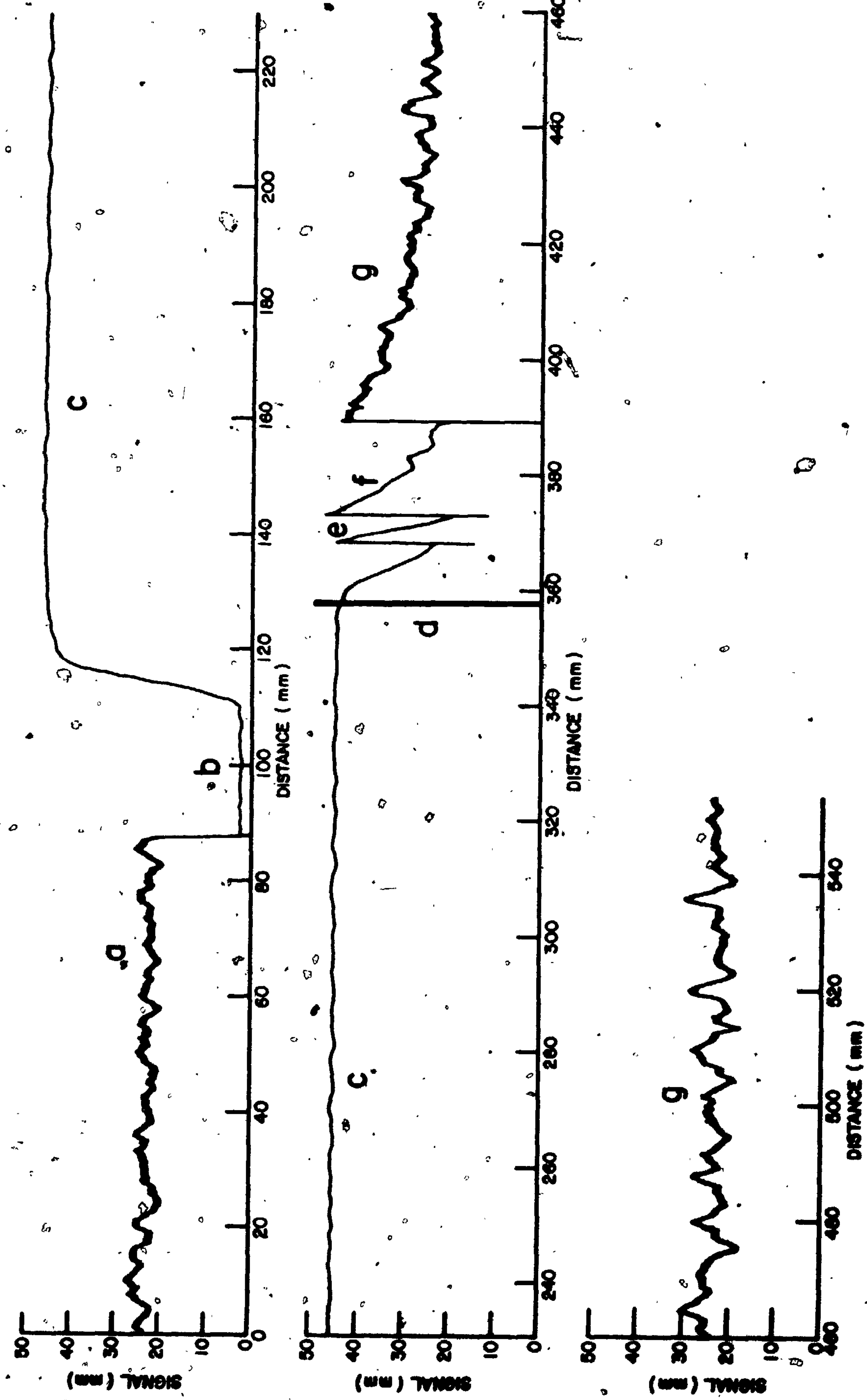
SIGNAL (mm)
DISTANCE (mm)
a
b
c
d
e
f
g

TABLE 2.2

Steady-State Results

Test #	Oxygen Tension (atm.)	Average Current of Three Samples (microamp)	Probe Constant (microamp/atm. O_2)
I	1.76×10^{-4}	0.025	142
II	9.26×10^{-4}	0.129	139
III	3.0×10^{-3}	0.386	129
IV	1.01×10^{-2}	1.423	141
V	3.02×10^{-2}	4.186	139
VI	9.96×10^{-2}	12.947	130
VII	2.1×10^{-1}	29.407	140

subroutine POLY. Output from program KOK2 is listed in Appendix 2.8. Average maximum currents and probe constants together with their confidence intervals are listed in Table 2.3. A sample calculation illustrating the method whereby the confidence intervals were obtained is presented in Appendix 2.9. The polynomials fitted through the downstep response data at the various oxygen concentrations and exposure durations are compared in Figures 2.33 to 2.39. Probe performance as modelled with the fitting polynomials is evaluated for the different oxygen tensions after one, two and three minutes exposures in Figures 2.40 to 2.42.

2.12 Discussion of Polarographic Probe Behavior

Before proceeding with the discussion of the data presented in the previous section several difficulties encountered in working with the dissolved oxygen probe should be discussed. The most serious of these were the lack of absolute reproducibility of the experimental situation and fouling of the cathode. What is meant by 'lack of absolute reproducibility' is that although the experimental procedure could be repeated easily the results would differ numerically between experiments although the character of the results would be similar. This was attributed to the lack of control over the thicknesses of the membrane and the electrolyte layer.

TABLE 2.3

Average Maximum Currents and Probe Constants For the YSI Polarographic Probe

Downstep Set No.	Oxygen Concentration	Duration of Probe Exposure (Min.)	No. of Downsteps Recorded	Average Maximum Current For Downsteps of The Same Exposure Duration (μA)	Average Maximum Current At This Oxygen Concentration (μA)	C_p (μA/atm.) (γ = 0.95)
I	0.30%	1	8	0.437	0.436	145 ± 8
		2	2	0.437		
		3	2	0.432		
II	1.01%	1	8	1.425	1.423	141 ± 13
		2	2	1.422		
		3	2	1.415		
III	926 ppm	1	8	0.122	0.122	132 ± 7
		2	2	0.122		
		3	2	0.123		
IV	176 ppm	1	8	0.123	0.025	142 ± 9
		2	2	0.024		
		3	2	0.024		
V	3.02%	1	8	4.084	4.082	135 ± 7
		2	2	4.102		
		3	2	4.055		
VI	9.96%	1	4	12.824	12.751	128 ± 8
		2	1	12.606		
		3	1	12.606		
VII	21%	1	5	25.663	25.577	122 ± 8
		2	1	25.363		
		3	1	25.361		

FIGURE 2.33

Least-Square Fifth-Order Polynomials Calculated From the YSI Probe Downstep Response Data By Program KOK2. The Oxygen Tension During Exposure Was 3.0×10^{-3} atm. O_2. The Exposure Durations were: Curve 1 - 1 Minute; Curve 2 - 2 Minutes; Curve 3 - 3 Minutes Chart Speed Was 125 mm/min.

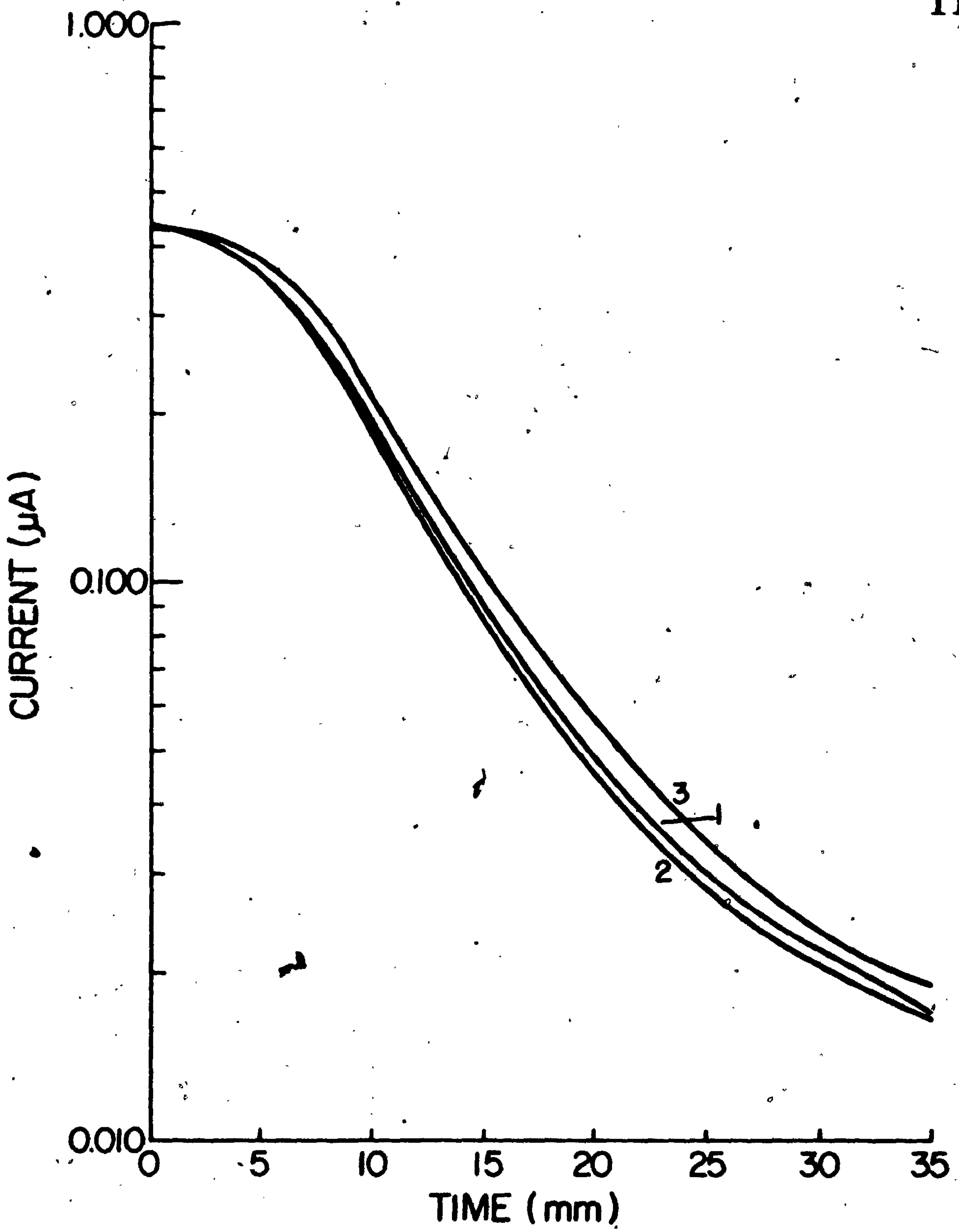
1.000
0.100
0.010
CURRENT (μA)
0
5
10
15
20
25
30
35
TIME (mm)
3
2

FIGURE 2.34

Least-Square Fifth-Order Polynomials Calculated From the YSI Probe Downstep Response Data By Program KOK2. The Oxygen Tension During Exposure Was 1.01×10^{-2} atm. O_2. The Exposure Durations Were: Curve 1 - 1 Minute; Curve 2 - 2 Minutes; Curve 3 - 3 Minutes Chart Speed Was 125 mm/min.

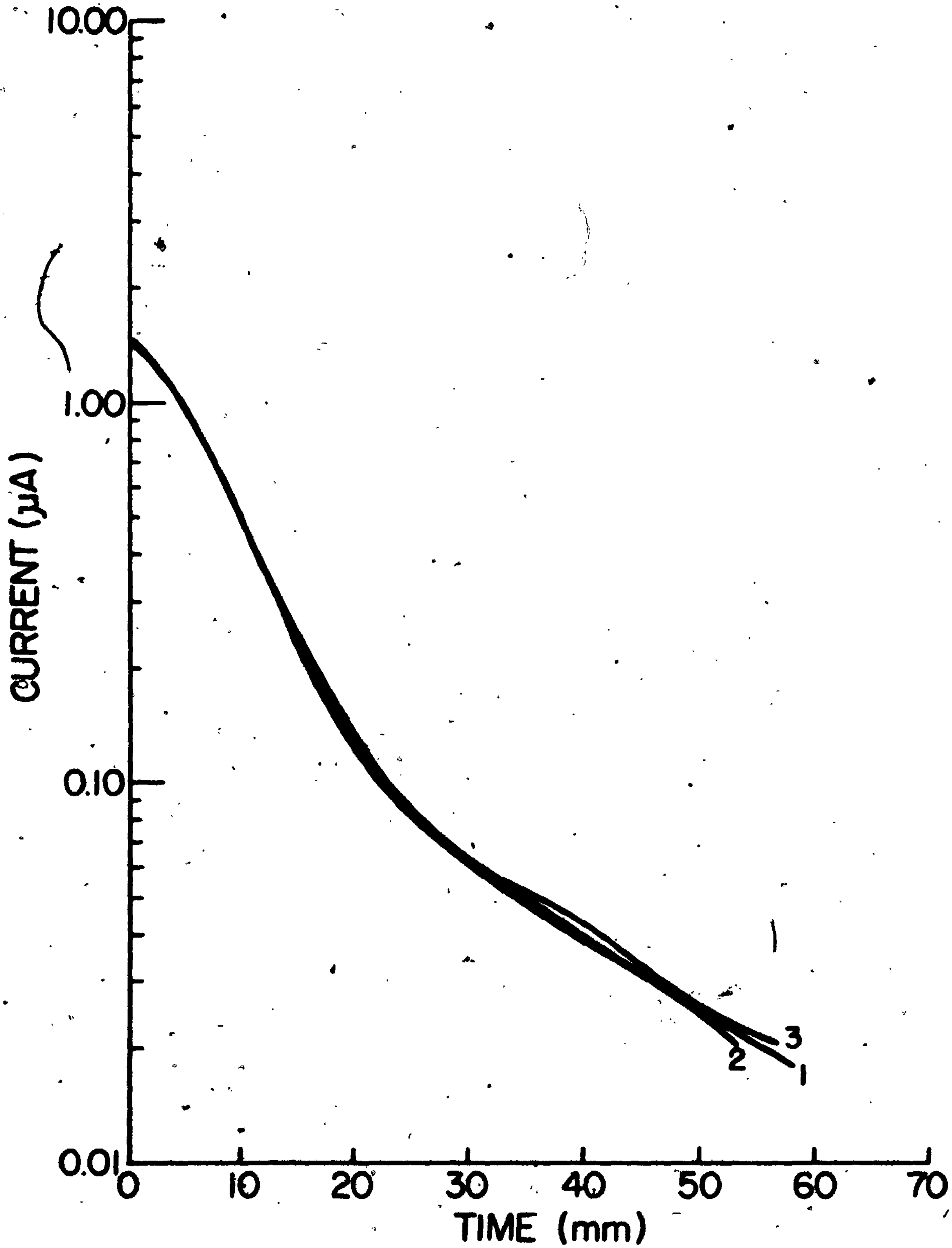
CURRENT (μA)
10.00
1.00
0.10
0.01
0
10
20
30
40
50
60
70
TIME (mm)
1
2
3

FIGURE 2.35

Least-Square Fifth-Order Polynomials Calculated From the YSI Probe Downstep Response Data By Program KOK2. The Oxygen Tension During Exposure Was 9.26×10^{-4} atm. O_2. The Exposure Durations Were: Curve 1 - 1 Minute; Curve 2 - 2 Minutes; Curve 3 - 3 Minutes Chart Speed Was 125 mm/min.

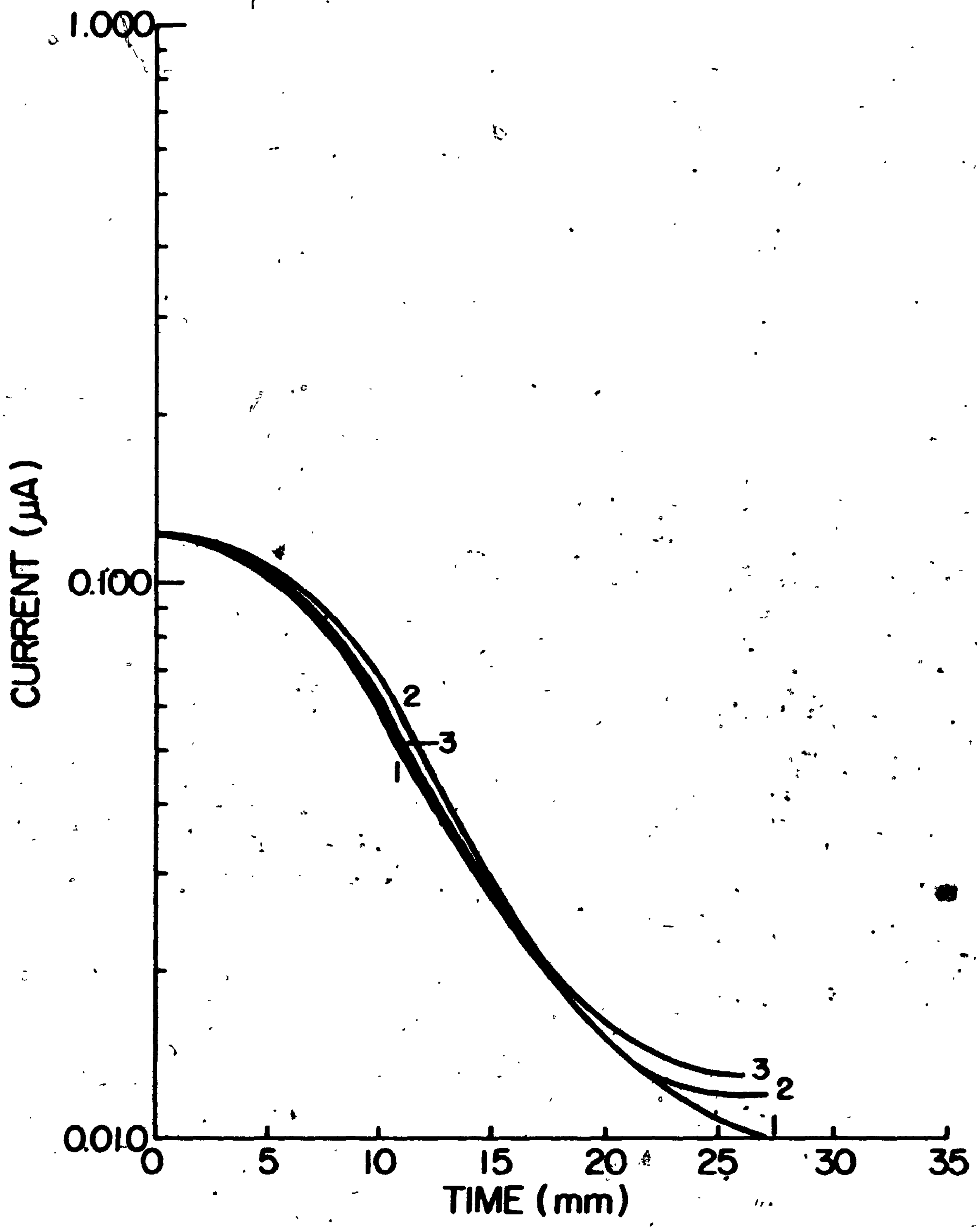
1.000
0.100
0.010
CURRENT (μA)
0
5
10
15
20
25
30
35
TIME (mm)
1
2
3
3
2

FIGURE 2.36

Least-Square Fifth-Order Polynomials Calculated From the YSI Probe Downstep Response Data By Program KOK2. The Oxygen Tension During Exposure Was 1.76×10^{-4} atm. O_2. The Exposure Durations Were: Curve 1 - 1 Minute; Curve 2 - 2 Minutes; Curve 3 - 3 Minutes Chart Speed Was 125 mm/min.

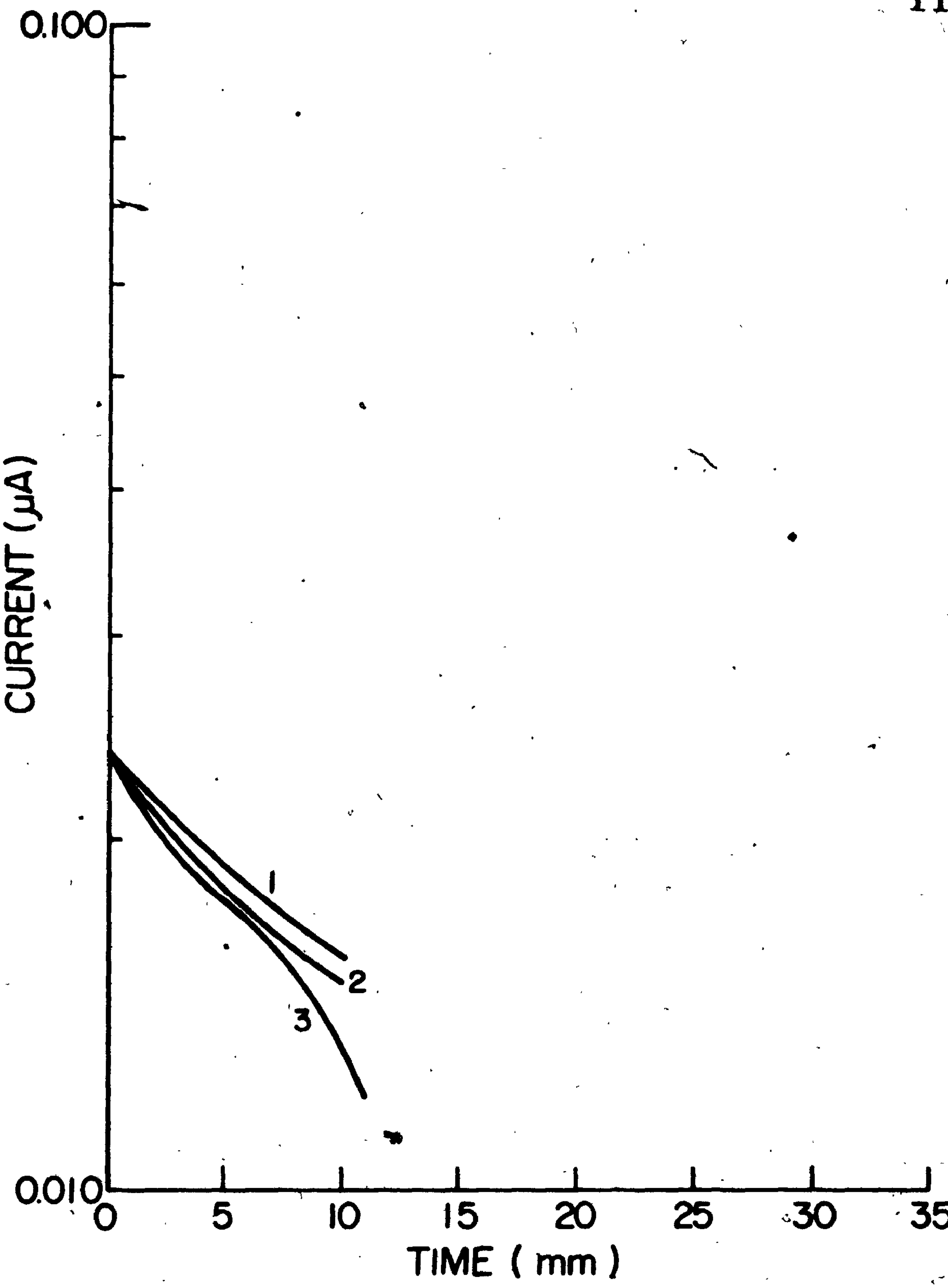
0.100
0.010
CURRENT (μA)
1
2
3
0
5
10
15
20
25
30
35
TIME (mm)

FIGURE 2.37

Least-Square Fifth-Order Polynomials Calculated From the YSI Probe Downstep Response Data by Program KOK2. The Oxygen Tension During Exposure Was 3.02×10^{-2} atm. O_2. The Exposure Durations Were: Curve 1 - 1 Minute; Curve 2 - 2 Minutes; Curve 3 - 3 Minutes Chart Speed Was 125 mm/min.

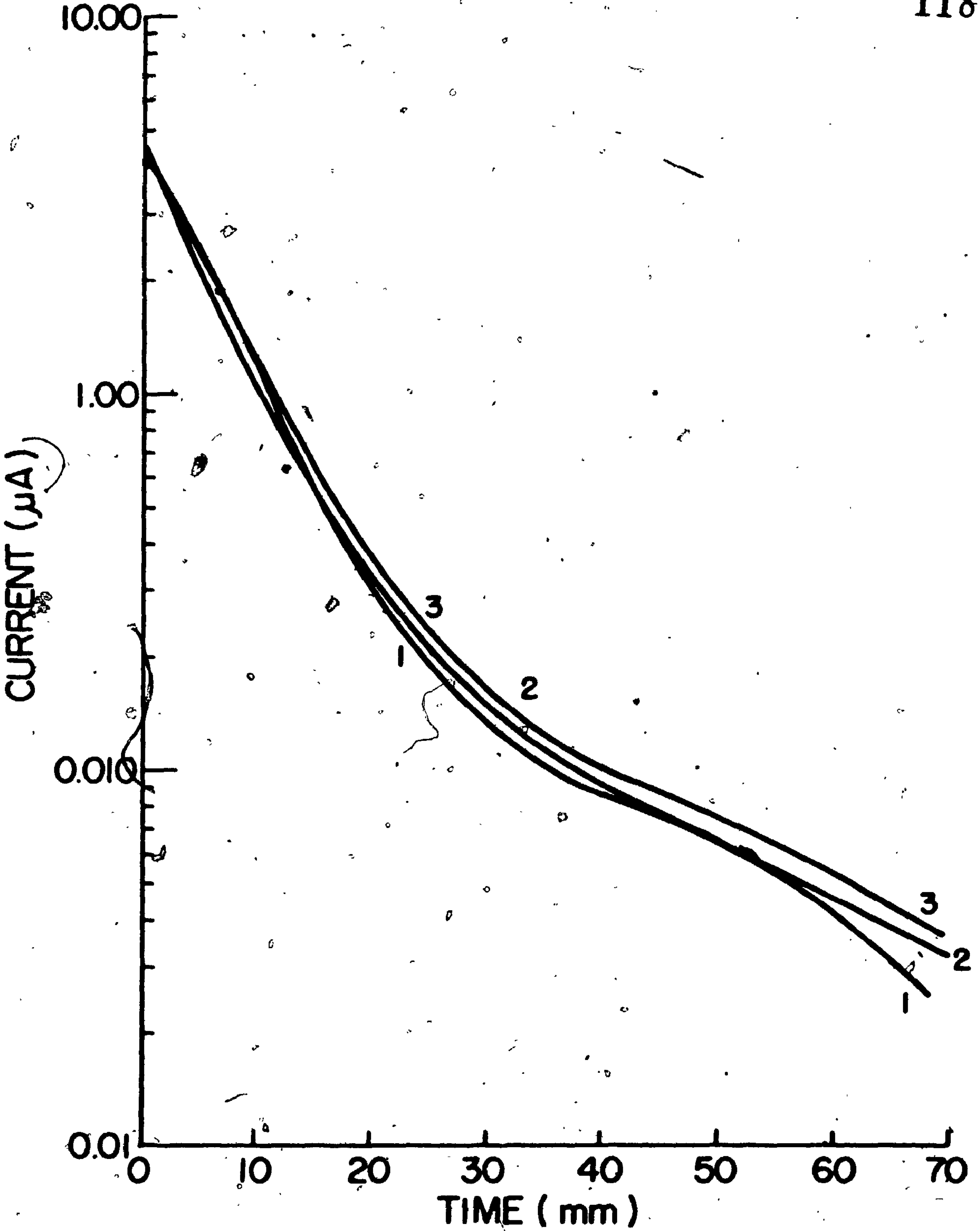
10.00
1.00
0.010
0.01
CURRENT (μA)
0
10
20
30
40
50
60
70
TIME (mm)
1
2
3
3
2
1

FIGURE 2.38

Least-Square Fifth-Order Polynomials Calculated From the YSI Probe Downstep Response Data By Program KOK2. The Oxygen Tension During Exposure Was 9.96×10^{-2} atm. O_2. The Exposure Durations Were: Curve 1 - 1 Minute; Curve 2 - 2 Minutes; Curve 3 - 3 Minutes Chart Speed Was 125 mm/min.

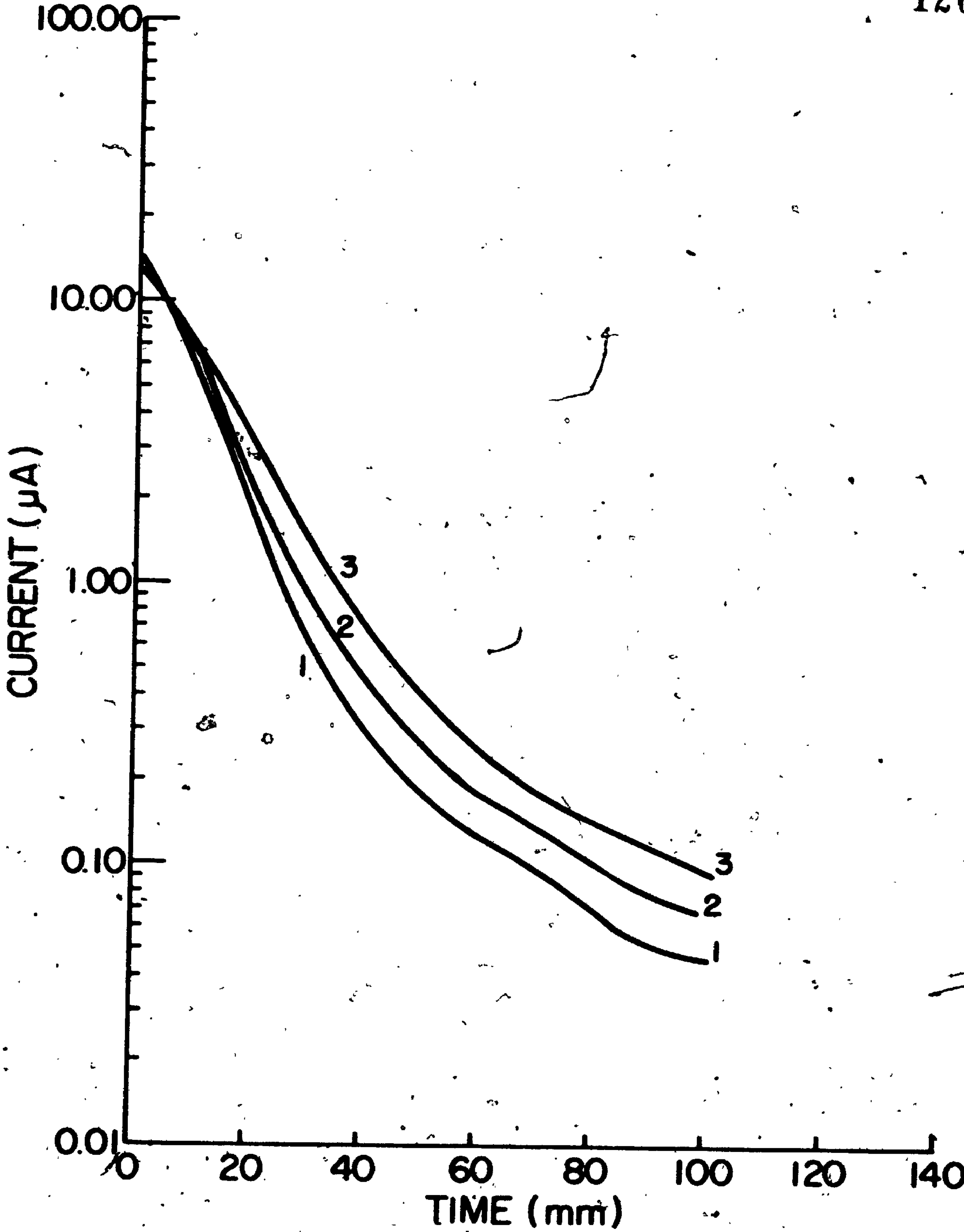
100.00
10.00
1.00
0.10
0.01
CURRENT (μA)
3
2
1
3
2
1
0
20
40
60
80
100
120
140
TIME (min)

FIGURE 2.39

Least-Square Fifth-Order Polynomials Calculated From the YSI Probe Downstep Response Data by Program KOK2. The Oxygen Tension During Exposure Was 2.1×10^{-1} atm. O_2. The Exposure Durations Were: Curve 1 - 1 Minute; Curve 2 - 2 Minutes; Curve 3 - 3 Minutes Chart Speed Was 125 mm/min.

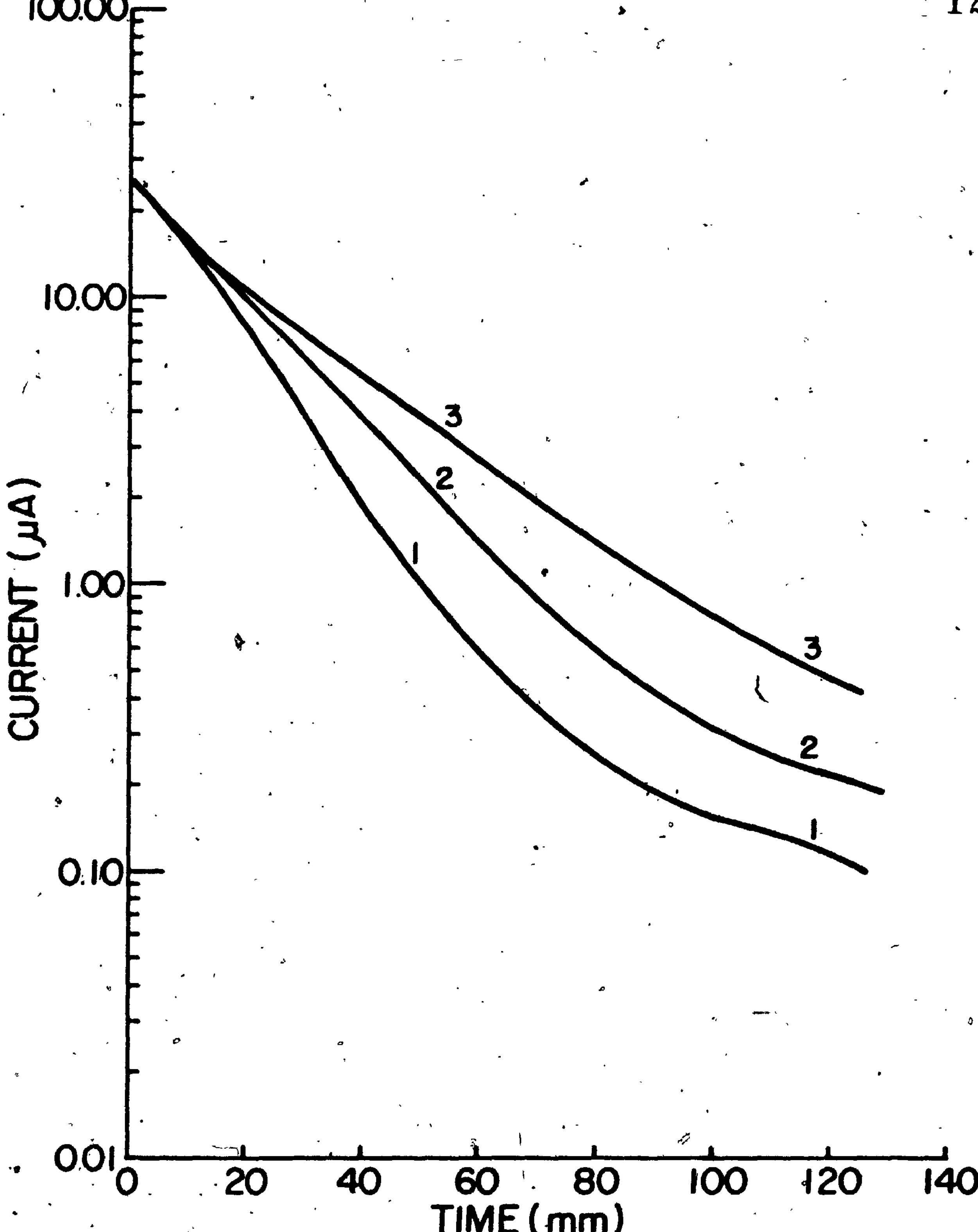
100.00
10.00
1.00
0.10
0.01
CURRENT (μA)
0
20
40
60
80
100
120
140
TIME (mm)
1
2
3
1
2
3

FIGURE 2.40

Comparison of the Least-Square Fifth-Order Polynomials Calculated From the YSI Probe Downstep Data By Program KOK2. The Exposure Duration was 1 Minute. The Oxygen Tensions During Exposure Were: Curve 1 - 3.0×10^{-3} atm. O_2; Curve 2 - 1.01×10^{-2} atm. O_2; Curve 3 - 9.26×10^{-4} atm. O_2; Curve 4 - 1.76×10^{-4} atm. O_2; Curve 5 - 3.02×10^{-2} atm. O_2; Curve 6 - 9.96×10^{-2} atm. O_2; Curve 7 - 2.1×10^{-1} atm. O_2

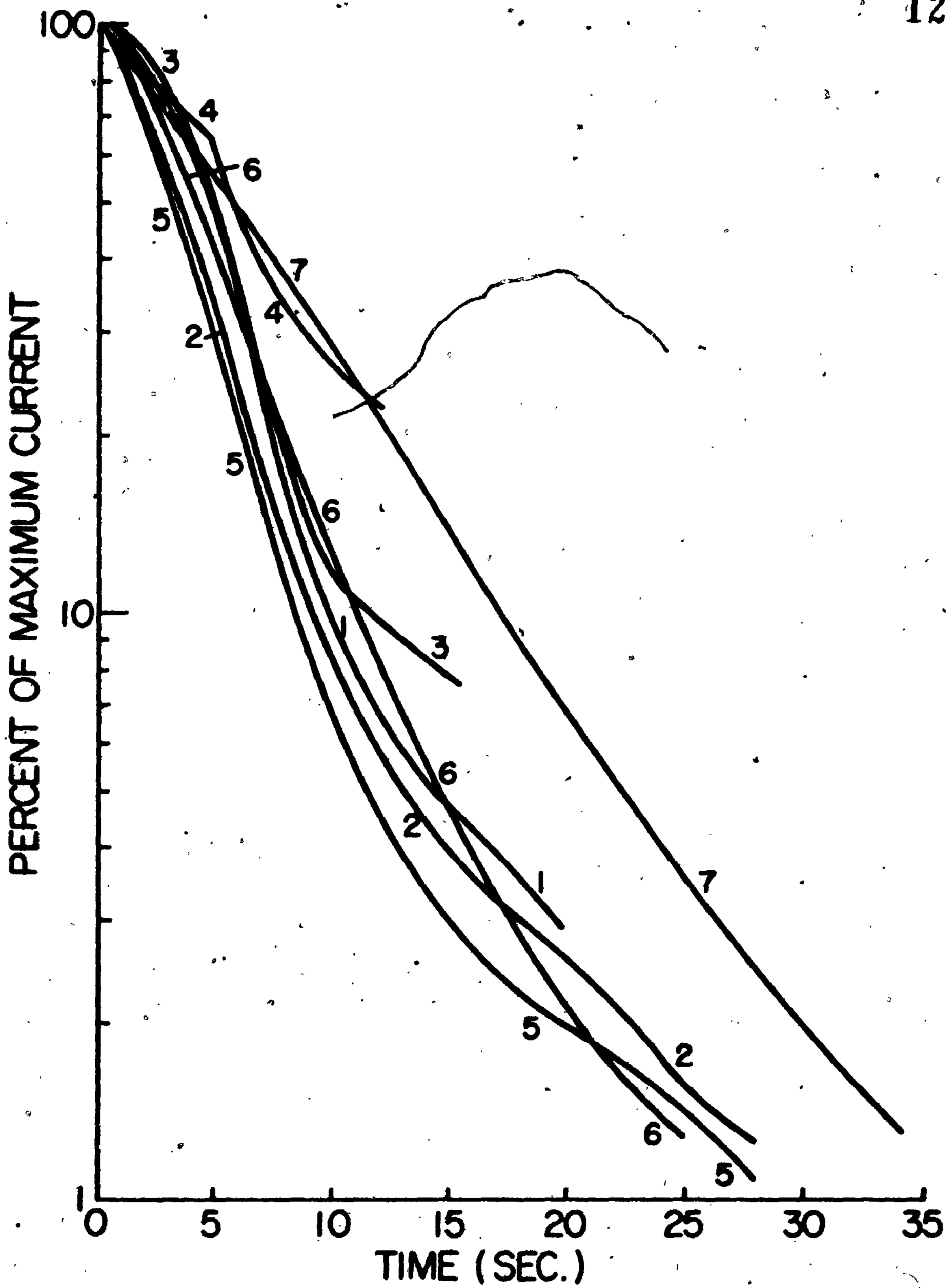
PERCENT OF MAXIMUM CURRENT
100
10
1
0
5
10
15
20
25
30
35
TIME (SEC.)
1
2
3
4
5
6
7

FIGURE 2.41

Comparison of the Least-Square Fifth-Order Polynomials Calculated From the YSI Probe Downstep Data By Program KOK2. The Exposure Duration Was 2 Minutes. The Oxygen Tensions During Exposure Were: Curve 1 - 3.0×10^{-3} atm. O_2; Curve 2 - 1.01×10^{-2} atm. O_2; Curve 3 - 9.26×10^{-4} atm. O_2; Curve 4 - 1.76×10^{-4} atm. O_2; Curve 5 - 3.02×10^{-2} atm. O_2; Curve 6 - 9.96×10^{-2} atm. O_2; Curve 7 - 2.1×10^{-1} atm. O_2

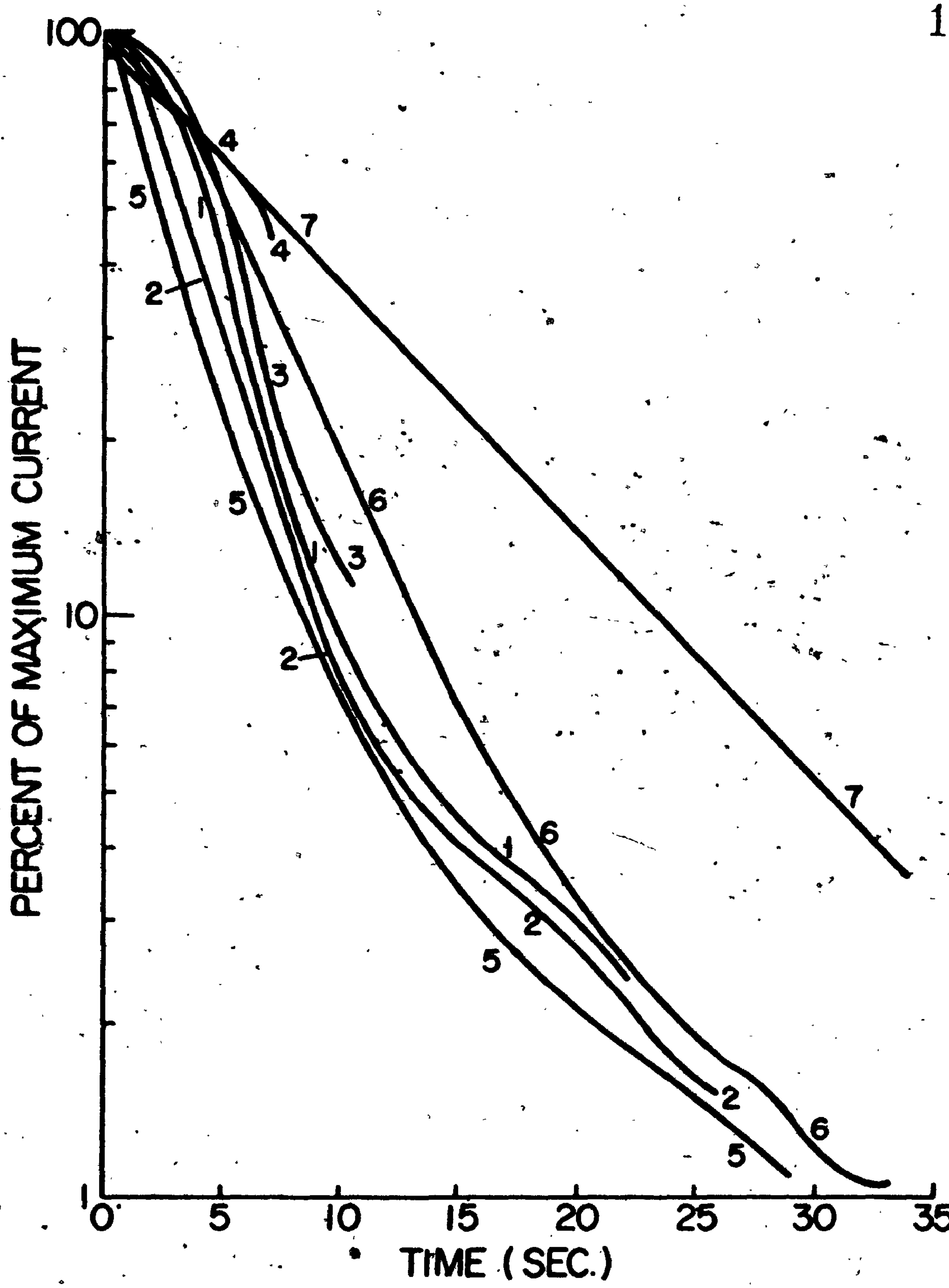
PERCENT OF MAXIMUM CURRENT
100
10
1
0
5
10
15
20
25
30
35
TIME (SEC.)
1
2
3
4
5
6
7

FIGURE 2.42

Comparison of the Least-Square Fifth-Order Polynomials Calculated From the YSI Probe Downstep Data By Program KOK2. The Exposure Duration Was 3 Minutes. The Oxygen Tensions During Exposure Were: Curve 1 - 3.0×10^{-3} atm. O_2; Curve 2 - 1.01×10^{-2} atm. O_2; Curve 3 - 9.26×10^{-4} atm. O_2; Curve 4 - 1.76×10^{-4} atm. O_2; Curve 5 - 3.02×10^{-2} atm. O_2; Curve 6 - 9.96×10^{-2} atm. O_2; Curve 7 - 2.1×10^{-1} atm. O_2

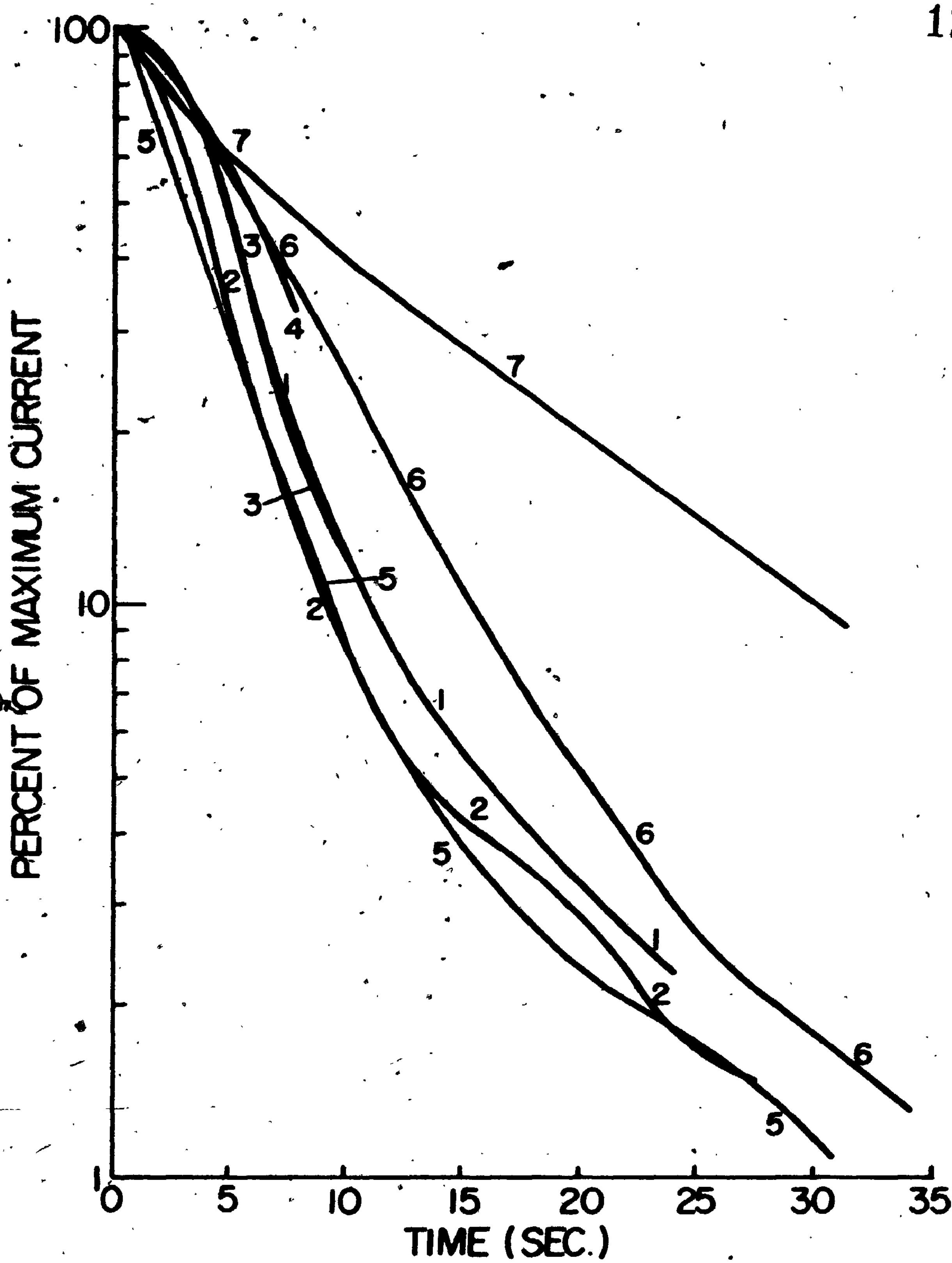

100
10
1
PERCENT OF MAXIMUM CURRENT
0
5
10
15
20
25
30
35
TIME (SEC.)
1
2
3
4
5
6
7

Cathode fouling occurred chiefly when the probe was submerged in a copper-containing solution. It was an unfortunate but unpreventable coincidence that the very serviceable reaction of sodium sulfite with oxygen is catalysed by cupric ion. The copper deposit affected the unsteady as well as the steady-state response. It could be removed by scouring the cathode with fine emery paper or a commercial brass cleaner (Brasso). The latter method proved problematic in use since the cleaning material was difficult to remove.

For the reasons cited above, probe performance varied a great deal during the course of the research. Benedek and Heideger [10] have also discussed the effect of age of the membrane on probe performance and have pointed out that the membrane slackens considerably over a period of a few days.

2.12.1 Temperature Dependence of Probe Output Current

The rate of change of the probe constant with temperature was found to be 3%/°C at 25°C. This is the same value as that obtained with the galvanic probe using the same type of membrane (YSI-nominal thickness 1 mil.). As has been mentioned, Johnson and Borkowski [38] obtained a value of 2%/°C. The difference in temperature coefficients may be ascribed to the difference in membrane materials. The galvanic probe had a probe constant of 320 microamp/atm. oxygen, whereas the polarographic probe had a constant of 77 microamp/atm. oxygen.

2.12.2 Steady-State Response

From the data in Table 2.2 it can be readily deduced that probe steady-state response was a linear function of oxygen tension over the range 1.76×10^{-4} atm. to 0.21 atm. oxygen. Values of the probe constant obtained during the unsteady-state experiments indicated linear operation only over the range 1.76×10^{-4} atm. to 3.02×10^{-2} atm. oxygen. Since the probe was submerged in cupric ion-containing sodium sulfite solution for twelve hours between downstep sets nos. V and VI, it was not unusual to observe this slight decrease in the probe constant over this period.

An important conclusion that also may be drawn from the data presented is that by subtracting a residual current even as large as the signal current from the total current (e.g. for the 1.76×10^{-4} atm. oxygen gas), a value of the probe constant may be obtained which closely agrees with other values of the probe constant obtained at much higher oxygen tensions. At these higher oxygen tensions the residual current was an insignificant fraction of the total current. This therefore gives substantial support to the method of obtaining the signal current from the total current by subtracting the residual current.

2.12.3 Unsteady-State Response

The downstep responses were always fairly reproducible and the polynomials fitted the data closely. From Figures 2.33 to 2.39 it is evident that for oxygen tensions of 1.76×10^{-4}, 9.26×10^{-4}, 3.0×10^{-3}, 1.01×10^{-2} and 3.02×10^{-2} atm. the duration of exposure had very little, if any effect on the downstep response, whereas for oxygen tensions of 9.96×10^{-2} and 0.21 atm. an increase in exposure duration considerably slowed down the downstep response.

As mentioned in the introduction of this section, it was physically impossible to obtain 'absolute reproducibility'. The accompanying figures define therefore the character of probe behavior rather than its absolute characteristics. Further quantification of the data to exactly describe the operating characteristics was therefore not attempted.

In Figures 2.40 to 2.42 the downstep responses from various oxygen tensions are compared after equal durations of exposure. After one minute exposure all curves except for the 1.76×10^{-4} atm. and 0.21 atm. oxygen had reached 10% of their average maximal currents within two seconds of each other. The 1.76×10^{-4} atm. oxygen curve probably deviated due to a large chain capacitance (1 microfarad) being present in the measuring circuit to suppress amplifier noise. It also lacked accuracy since even at a signal current of 50% of the average maximal current it was only half the residual current or one-third of the total recorded current. The 0.21 atm. oxygen curve was however clearly deviant and lagged 7.5 seconds behind the others at 90% response or 10% of the average maximal current. This lagging as compared to the other downstep responses increased in severity as the exposure duration increased and was also observable to a smaller extent for the 9.26 x 10^{-2} atm. oxygen curves as shown in Figures 2.41 and 2.42. The above-mentioned effects of oxygen tension and exposure duration on the polarographic probe's downstep response were similar to those exhibited by the galvanic probe as discussed in section 2.7. The galvanic probe's response to a downstep of 9.26 x 10^{-4} atm. oxygen after one minute exposure was however slower than to a downstep of 0.21 atm. oxygen.

In the following section several models are proposed to explain the observed behavior of the polarographic probe.

2.13 <u>Models of Probe Behavior</u>

2.13.1 Introduction

In the foregoing sections it was pointed out that the probe's downstep response was to some degree a function of the size of the downstep as well as of the duration of exposure. Invariably however, both in research reports and engineering specifications for commercial instruments only one time constant is quoted to describe a probe's performance. In other words, the assumption usually is that probe performance can be described in terms of a simple first-order lag system. From inspection of the experimental downstep responses on Figures 2.33 to 2.39 it may be concluded that even for the responses which were independent of both the exposure duration and oxygen tension, the response to a downstep input function was not a first-order lag since the plots are not straight lines on semilog paper. Since the ultimate aim of the investigation into probe behavior was to find a method of using the probe to accurately follow a slow decrease in oxygen tension, it was necessary to determine what influence the probe's transfer function had on the relationship between the actual and the observed oxygen tension decrease function. To assess this influence a mathematical model of the probe had to be constructed. A set of models of increasing complexity is described below. A simple model of steady-state behavior is described in section 2.13.2 for the sake of completeness and to elucidate the concepts used in the later models of dynamic behavior.

2.13.2 A Two-Layer Model of Steady-State Behavior

The steady-state current of a dissolved oxygen probe is given by Equation 2.5:

$$i = F\,n\,f \qquad (2.5)$$

The oxygen flux is proportional to the oxygen activity gradients in the membrane and electrolyte layer and is thus proportional to the oxygen tension in the external phase provided that the oxygen activity at the cathode is essentially zero (i.e. the diffusion limited situation). The resultant steady-state oxygen flux and current can be calculated using Equations 2.6 to 2.8:

$$k = \{ \frac{L_m}{D_m S_m} + \frac{L_e}{D_e S_e} \}^{-1} \quad (2.6)$$

$$f = P_{O_2} A^* k/32 \times 10^6 \quad (2.7)$$

$$i = 1.2062\ P_{O_2} A^* k \times 10^{10} \quad (2.8)$$

2.13.3 A Single Diffusion Layer Model of the Probe For Unsteady-State Behavior

If the membrane and electrolyte layer are modelled as a single mass-transfer resistance then the probe's response to a downstep from steady-state to zero oxygen tension is described by Equations 2.9 and 2.10:

$$i/i_\infty = 1 + 2 \sum_{n=1}^{\infty} (-1)^n \exp [-(\frac{n\pi}{B})^2 t] \quad (2.9)$$

$$i/i_\infty = 1 - \frac{2B}{\sqrt{\pi t}} \sum_{n=0}^{\infty} \exp [\frac{-B^2}{4t} (2n + 1)^2] \quad (2.10)$$

These equations were derived from Boelter's *et al.* [11] and Churchill's [16] equations for the concentration profile through an infinite slab of thickness L. The derivations are presented in Appendices 2.10 and 2.11. Response curves generated by Equations 2.9 and 2.10 for various values of B are graphed in Figure 2.43 together with the fifth-order best-fit polynomials for the experimental responses obtained for downsteps from 1.01×10^{-2} atm. and 3.02×10^{-2} atm. oxygen after 1 minute exposure. Both these were typical of the downstep responses obtained and were not affected by the oxygen tension or the duration of exposure.

2.13.4 A Double Diffusion Layer Model of the Probe For Unsteady-State Behavior

Benedek and Heideger [10] have presented Equation 2.11 as the Laplace transform of the activity profile through a two-layer system when the oxygen activity is kept at zero at $x = -a$ (cathode) and a step increase of amplitude P_1 is applied at the outside of the second layer at $x = b$ as illustrated in Figure 2.44.

$$P_{O_2}(x,s) = \{s^{-1}k_1P_1\sinh(\frac{x+a}{D_e^{\frac{1}{2}}}s^{\frac{1}{2}})\} \Big/$$

$$\{(\frac{D_e}{D_m})^{\frac{1}{2}} + k_2\}\sinh\{(\frac{b}{D_m^{\frac{1}{2}}} + \frac{a}{D_e^{\frac{1}{2}}})s^{\frac{1}{2}}\}$$

$$+ \{(\frac{D_e}{D_m})^{\frac{1}{2}} - k_2\}\sinh\{(\frac{b}{D_m^{\frac{1}{2}}} - \frac{a}{D_e^{\frac{1}{2}}})s^{\frac{1}{2}}\} \quad (2.11)$$

FIGURE 2.43

Comparison of Experimental YSI Probe Downstep Responses With the Responses Predicted By the Single Diffusion Layer Model. The Experimental Curves Shown Are the Least-Square Fifth-Order Polynomials Calculated By Program KOK2. The Exposure Duration Was 1 Minute. The Oxygen Tensions During Exposure Were: Curve 1 - 1.01×10^{-2} atm. O_2; Curve 2 - 3.02×10^{-2} atm. O_2

B is the Response Characteristics of a Single Diffusion Layer

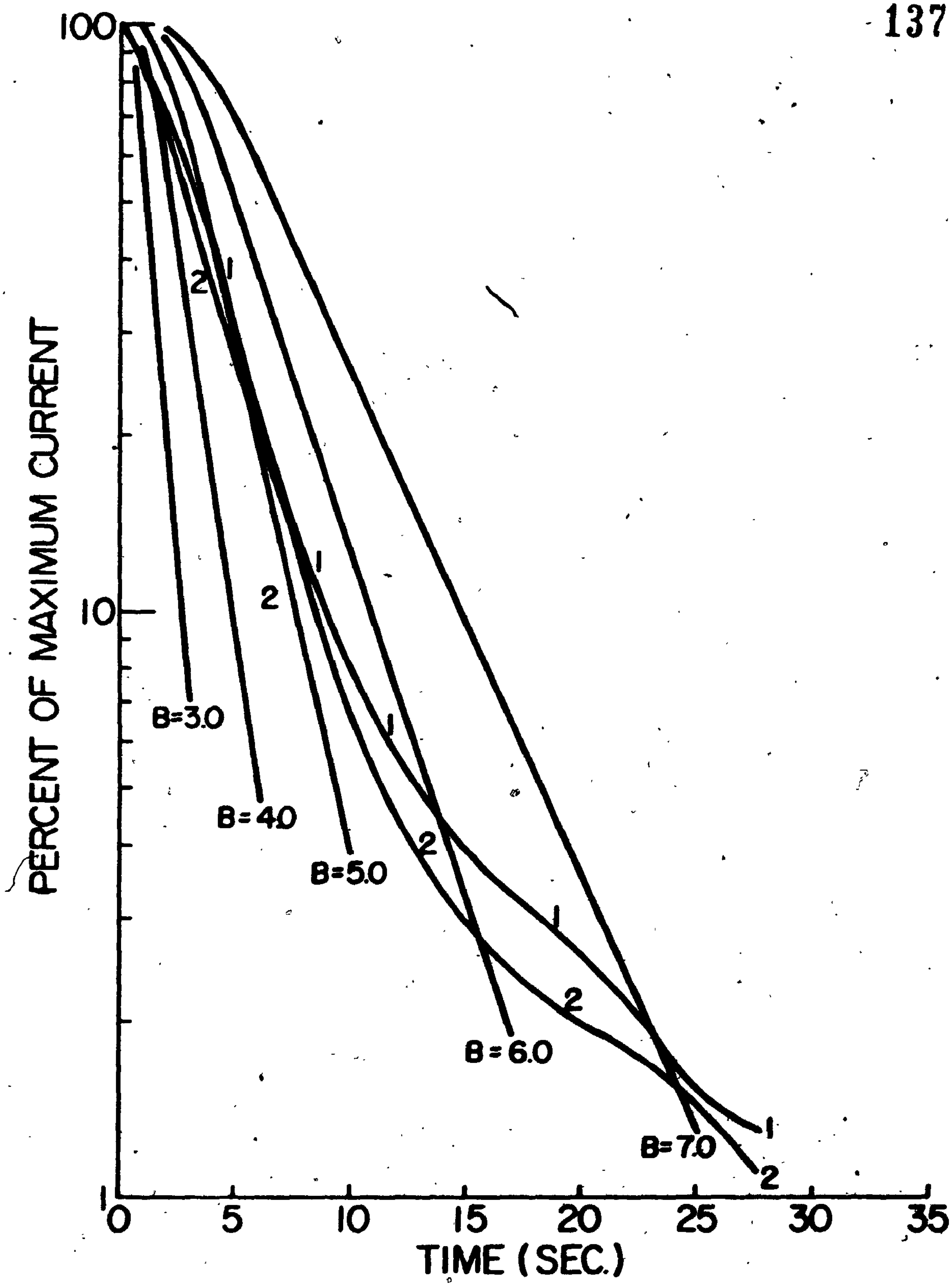

100
10
1
PERCENT OF MAXIMUM CURRENT
0
5
10
15
20
25
30
35
TIME (SEC.)
B=3.0
B=4.0
B=5.0
B=6.0
B=7.0
1
2

FIGURE 2.44

The Oxygen Concentration Profile Through a
2-Layer Diffusion System As Described
By Benedek and Heideger [10]

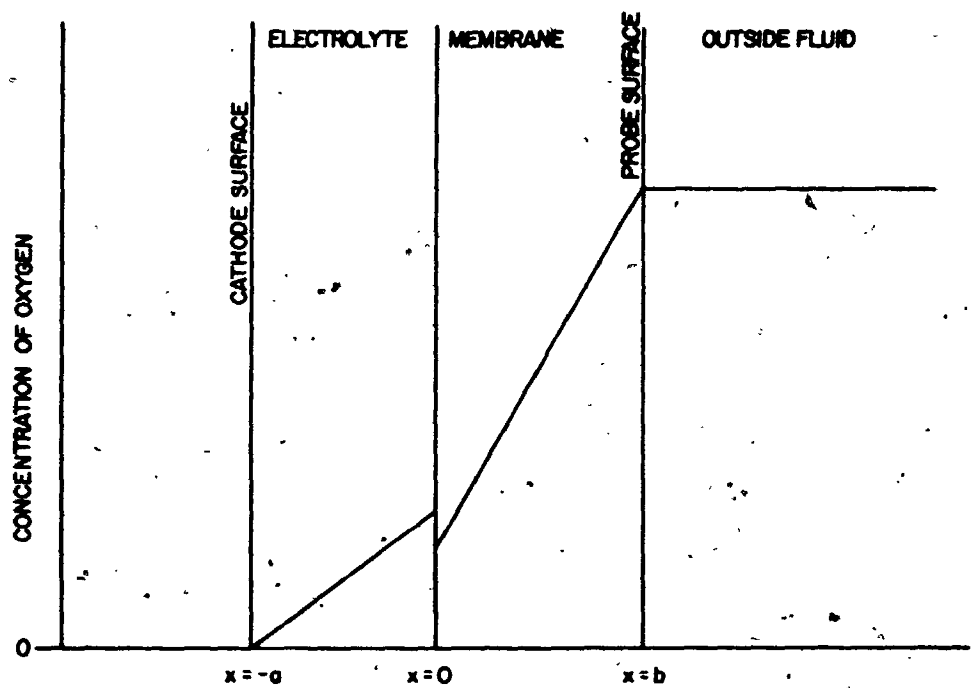
ELECTROLYTE
MEMBRANE
OUTSIDE FLUID
CATHODE SURFACE
PROBE SURFACE
CONCENTRATION OF OXYGEN
0
x = -a
x = 0
x = b

Due to difficulties in backtransforming this equation to the time domain they made some simplifying assumptions, reducing in effect, the problem to a one-layer system and obtained the same solution as presented in the previous section. The derivation from Equation 2.11 of the equation for the current as a fraction of steady-state current after an upstep in terms of the Laplace variable "s" is presented in Appendix 2.12. The solution is given in Equation 2.12:

$$L[i/i_\infty] = 2\{B_m^2C^* + B_e^2\}/s^{\frac{1}{2}}[(B_mC^* + B_e)\sinh\{(B_m+B_e)s^{\frac{1}{2}}\}$$
$$+ (B_mC^* - B_e)\sinh\{(B_m - B_e)s^{\frac{1}{2}}\}] \qquad (2.12)$$

The response to a downstep was obtained by inverting Equation 2.12 by Bellman's *et al.*[9] numerical method by quadrature and subtracting the solution from 1. This operation was performed by program KOK3, listed in Appendix 2.13. Sample solution curves generated by KOK3 for various combinations of B_e, B_m and C^* are presented in Figure 2.45 together with several curves generated from Equation 2.9 representing the single-layer model response. In Figure 2.46 several two-layer models are compared with experimental downstep responses from 1.01 x 10^{-2} atm. and 3.02 x 10^{-2} atm. oxygen.

FIGURE 2.45

Dissolved Oxygen Probe Downstep Responses

Predicted By the Single and Double Diffusion

Layer Models

Double Diffusion Layer Model:
(8 quadrature points)

Curve	B_e	B_m	C^*
1	2.5	2.5	1.0
2	2.5	2.5	2.0
3	2.5	2.5	0.05
4	3.0	2.0	1.0
5	3.0	2.0	2.0
6	3.0	2.0	0.05
7	2.0	3.0	1.0
8	2.0	3.0	2.0
9	2.0	3.0	0.05

Single Diffusion Layer Model

Symbol	B
✕	5.0
●	5.5
■	4.5

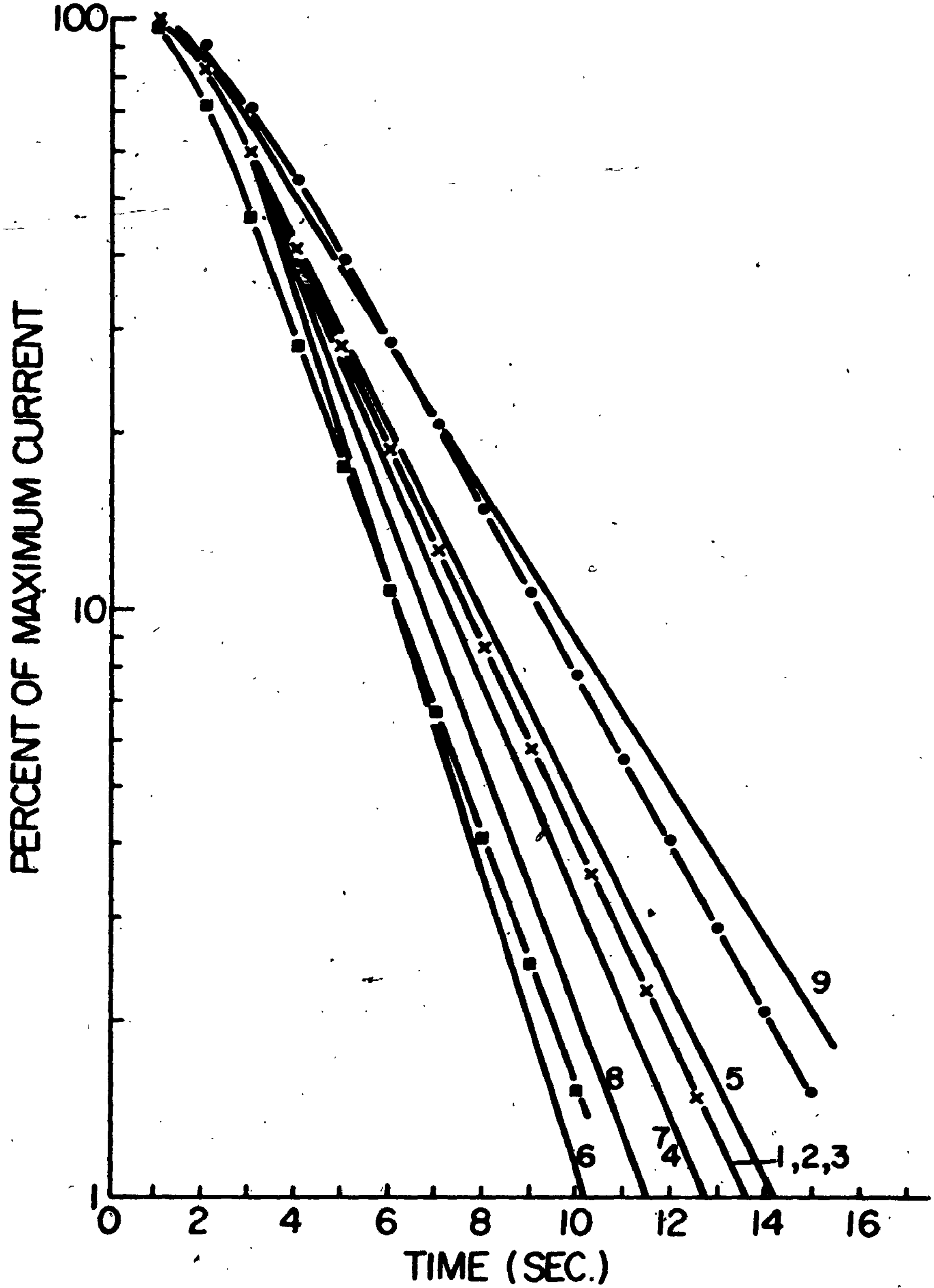

100
10
1
PERCENT OF MAXIMUM CURRENT
0
2
4
6
8
10
12
14
16
TIME (SEC.)
9
8
5
7
4
6
1,2,3

FIGURE 2.46

Comparison of the Least-Square Fifth-Order Polynomials Calculated From the YSI Probe Downstep Data By Program KOK2 and the Downstep Responses Predicted By the Double Diffusion Layer Model. The Exposure Duration Was 1 Minute. The Oxygen Tensions During Exposure Were: Curve 5 - 3.02×10^{-2} atm. O_2; Curve 6 - 1.01×10^{-2} atm. O_2

Double Diffusion Layer Model Parameters:
(8 quadrature points)

Curve	B_e	B_m	C^*
1	3.0	2.0	1.0
2	2.5	2.5	1.0
3	3.0	2.0	2.0
4	2.0	3.0	0.05

7

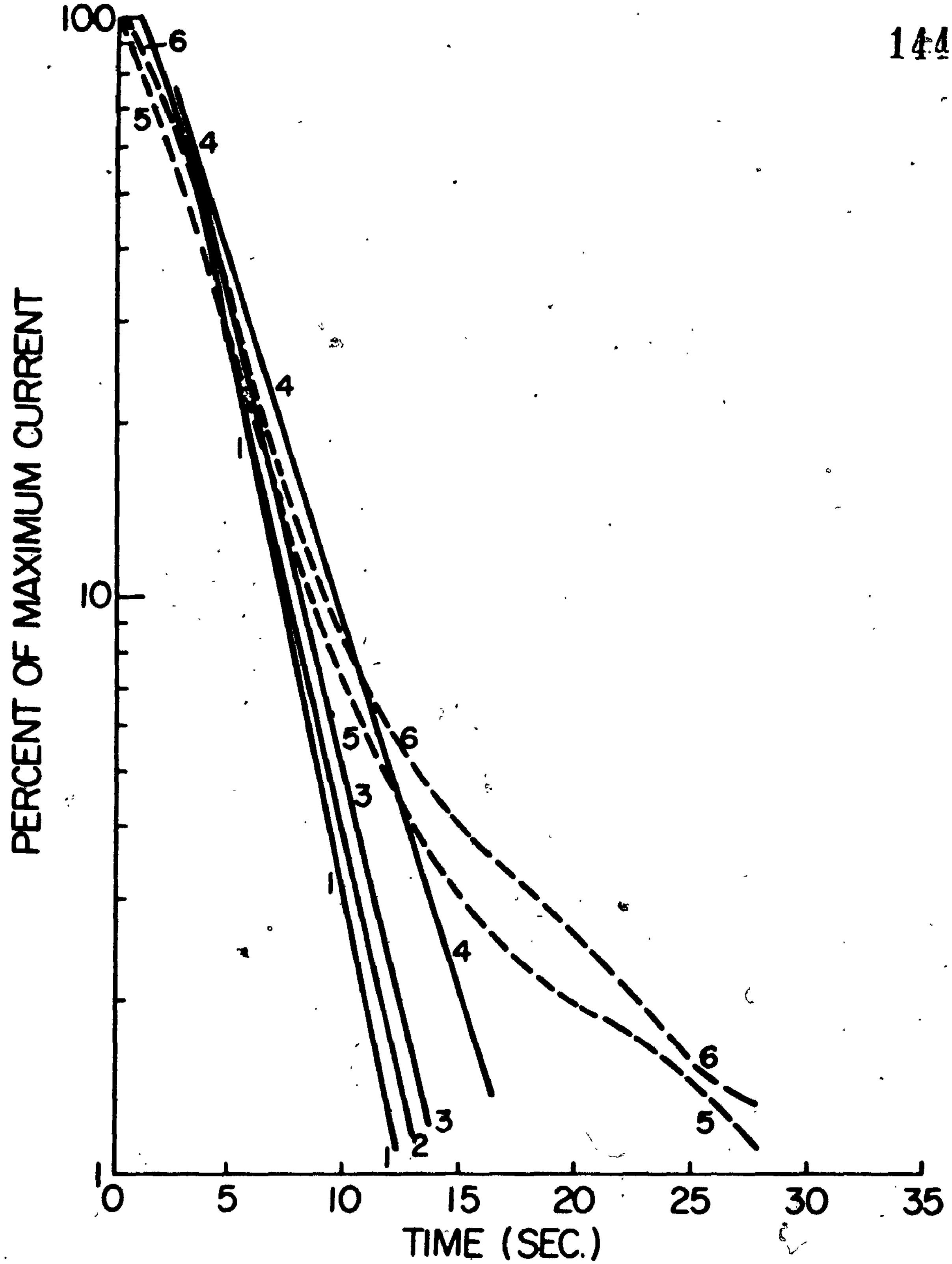

PERCENT OF MAXIMUM CURRENT
100
10
1
0
5
10
15
20
25
30
35
TIME (SEC.)
1
2
3
4
5
6

2.13.5 A Single Layer Diffusion Model With Oxygen Reservoir Correction

Deviation of the experimental results from the theoretically-predicted behavior for both the one-layer and two-layer systems occurred mainly when output currents less than ten percent of the steady-state current were reached. In this section the difference between the theoretical and experimental behavior is postulated to be due to a small current generated by an oxygen flux from a cylindrical semi-infinite oxygen reservoir. The YSI probe's central well containing the anode fulfilled this function. During exposure to an oxygen containing phase, oxygen diffused through the cylinder's face closest to the membrane into the cylinder's body and out through the wall of the cylinder to the cathode. After a downstep to zero oxygen tension, the flow of oxygen through the cylinder is reversed with the oxygen flowing out through the face nearest the membrane but also still flowing out through the wall to the cathode. The reservoir was modelled as semi-infinite since its length of approximately 0.5 cm was much larger than any of the layer thicknesses involved. Typical activity profiles during and after exposure are shown in Figure 2.47. The current contribution due to oxygen transfer from the reservoir was postulated to be directly proportional to the oxygen activity in the reservoir at a distance "$a*$" from the reservoir's face. As a simplification, the oxygen activity profiles in the membrane-electrolyte

FIGURE 2.47

Oxygen Concentration Profiles Along the Longitudinal Axis of the Semi-Infinite Cylindrical Reservoir: A) During Exposure; B) After Exposure Followed By a Downstep In Oxygen Tension

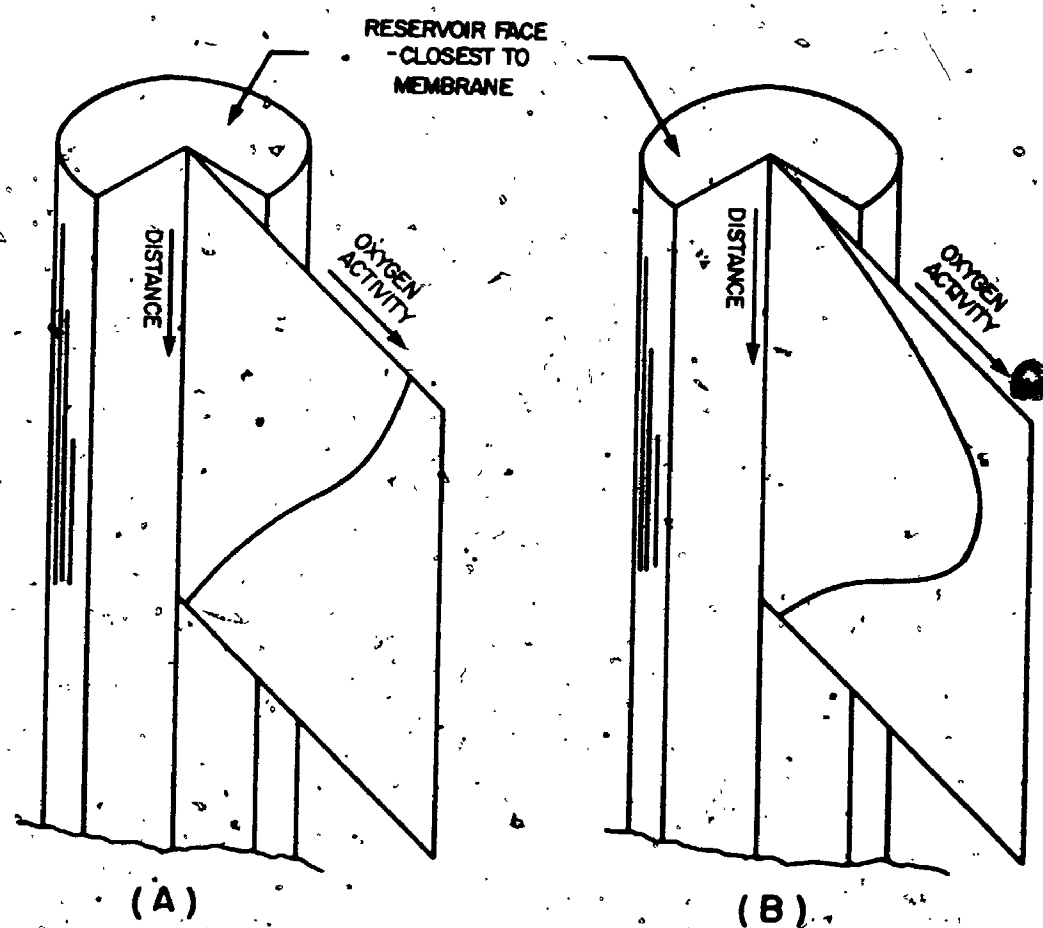
RESERVOIR FACE
-CLOSEST TO
MEMBRANE
DISTANCE
OXYGEN
ACTIVITY
(A)
(B)

system and the central well were assumed not to be interactive. The current output of a probe after a downstep is described by Equation 2.13:

$$i/i_A = (1-C_i)\{1-\frac{2B}{\sqrt{\pi t}}\sum_{n=0}^{\infty}\exp[\frac{-B^2}{4t}(2n+1)^2]\}$$

$$+ C_i\{\frac{\mathrm{erfc}(\frac{B_r}{\sqrt{t+A}}) - \mathrm{erfc}(\frac{B_r}{\sqrt{t}})}{\mathrm{erfc}(\frac{B_r}{\sqrt{A}})}\} \quad (2.13)$$

The development of Equation 2.13 is presented in Appendix 2.14. It was attempted to use a least-square regression technique to find the best-fit values for C_i, B and B_r for the experimental data. No absolute minimum could be found using this method. Program KOK5 uses a method of successive estimation of the parameters to reduce the difference between the model and the experimental values. It is listed in Appendix 2.16. A description of the method and equations used to write program KOK5 is given in Appendix 2.15. Results from program KOK5 for the one minute exposure downstep from 1.01×10^{-2} atm. oxygen are graphed in Figure 2.48 together with the fifth-order best-fit polynomial of the experimental results and the single-layer diffusion model for $B = 5.24$. Parameter values obtained for other exposure durations and downstep sizes are listed in Table 2.4.

FIGURE 2.48

Comparison of the Least-Square Fifth-Order Polynomial Calculated From the YSI Probe Downstep Data By Program KOK2 After 1 Minute Exposure To 1.01×10^{-2} atm. O_2 (Curve 1) With the Theoretical Downstep Responses Predicted By Two Models: Curve 2 - The Single Diffusion Layer With Central Well Correction Model For B=5.2395 sec^{-1}, C_i=0.11048, B_r=1.3249 sec^{-1}; Curve 3 - The Single Diffusion Layer Model For B=5.24

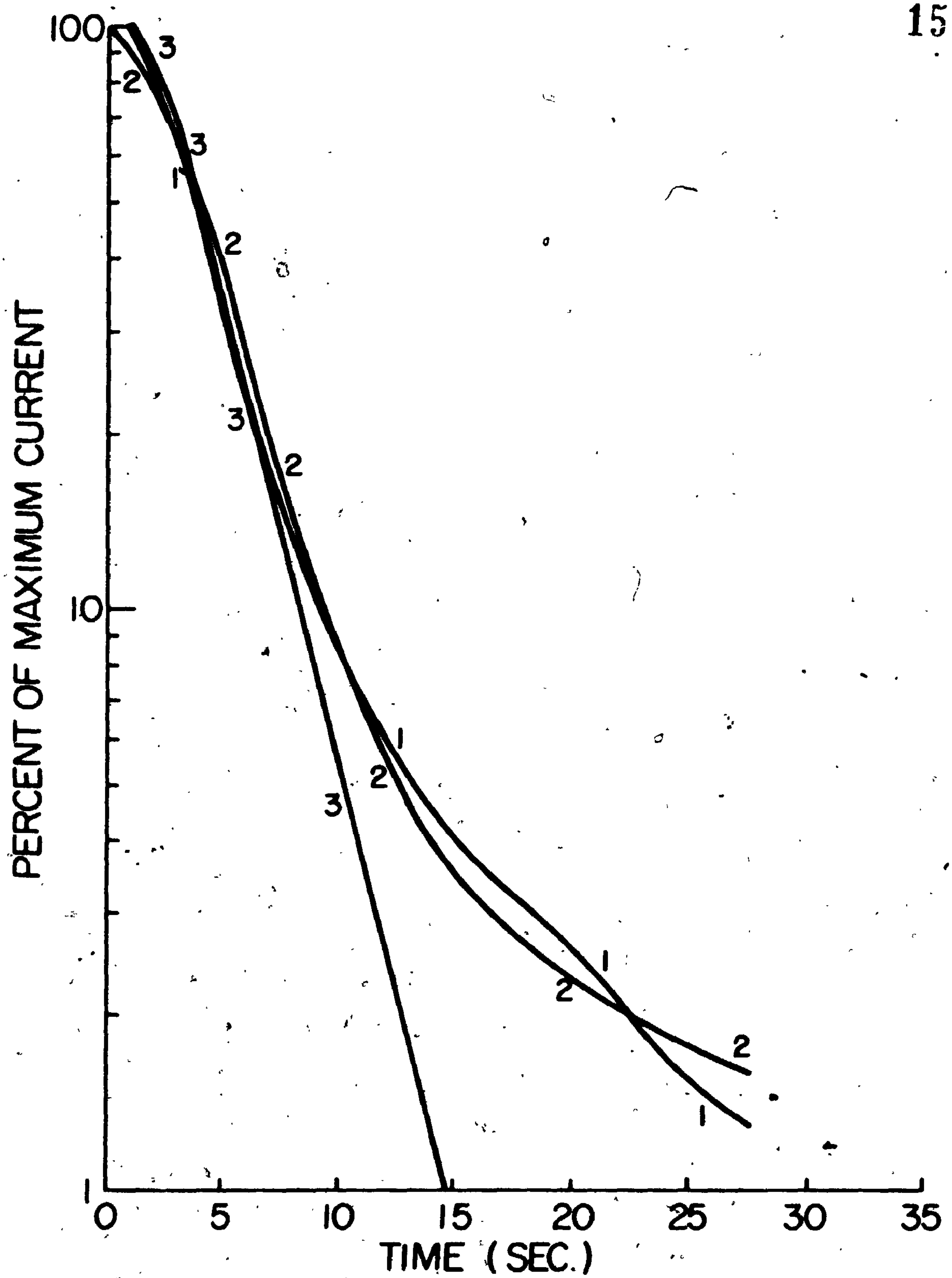
100
10
1
PERCENT OF MAXIMUM CURRENT
0
5
10
15
20
25
30
35
TIME (SEC.)
1
2
3

TABLE 2.4

Parameter Values Obtained From Program KOK5

Downstep Magnitude (atm.)	Exposure (secs.)	B ($sec^{\frac{1}{2}}$)	C_i	B_r ($sec^{\frac{1}{2}}$)	Average percent of deviation of model from data (%)
3.0×10^{-3}	60	5.46	0.109	1.55	13.1
1.01×10^{-2}	60	5.24	0.110	1.32	13.9
3.02×10^{-2}	60	5.27	0.096	0.97	26.2
3.0×10^{-3}	120	5.36	0.102	1.50	9.9
1.01×10^{-2}	120	5.19	0.128	1.05	14.6
3.02×10^{-2}	120	5.29	0.091	0.98	23.1
3.0×10^{-3}	180	5.67	0.090	1.63	9.5
1.01×10^{-2}	180	5.26	0.107	1.18	14.3
3.02×10^{-2}	180	5.48	0.086	1.04	21.5
average -	-				16.2

2.13.6 A Single Diffusion Layer Model with Oxygen Reservoir and Electrolyte Resistance Corrections

Although the model described in the previous section followed the experimental data reasonably well, it did not take into account the effect of step size on the dynamic response. This effect is partially accounted for below in terms of cell resistance. As the oxygen tension step size increased, probe output also increased. If the probe's ohmic resistance is considered to remain constant, then the ohmic voltage drop across the probe increases also with the step size thus decreasing the voltage drop available for oxygen reduction at the cathode. When the voltage available for oxygen reduction decreases sufficiently, it is no longer possible to maintain the diffusion-limited situation. A reservoir of oxygen then builds up in the membrane-electrolyte system. The following simplifying assumptions were made:

- The oxygen activity profile in the central well was not influenced by the oxygen activity gradient in the membrane-electrolyte system.

- The current contribution by the oxygen flux from the central well was directly proportional to the difference between the oxygen tension at a distance "$a*$" from the membrane in the central well and the oxygen tension at the cathode.

The relationship between the voltage available for oxygen reduction and the oxygen tension at the cathode surface could be modelled in terms of a simple Nernst-type relationship corrected for the irreversibility of the oxygen electrode.

The development of the implicit equations describing the model is presented in Appendix 2.17. Program KOK6, listed in Appendix 2.18, embodies these equations. It calculates the probe's output current after a downstep of P_1 atm. oxygen after "A" seconds of exposure. In addition to the constants B, C_i and B_r used before, it requires values of R and α which define the corrected Nernst relationship. No theoretical values were available for these parameters. In Figure 2.49 a comparison is made between the fifth-order best-fit polynomial and three models for the 3.02 x 10^{-2} atm. oxygen upstep followed by a downstep of the same magnitude after 60 seconds exposure. The values of the parameters used in each model are listed in Table 2.5. Only very small variations in probe dynamic response could be accounted for by manipulation of the values of α and R. Steady-state response was however much more drastically affected. When the electrolyte resistance was taken into account and if it was large enough, steady-state response was a function of the step size P_1. This is illustrated by the values of i_A and C_p calculated by program KOK6 and listed in Table 2.6. Values for the parameters used were the same as for model III

FIGURE 2.49

Comparison of the Least-Square Fifth-Order Polynomial Calculated From the YSI Probe Downstep Data By Program KQK2 After 1 Minute Exposure to 3.02×10^{-2} atm. O_2 (Curve 1) With the Theoretical Downstep Responses Predicted By Three Models: Curve 2 - The Single Diffusion Layer With Central Well Correction Model For $B=5.2665$ sec^{-1}, $C_i=0.09586$ and $B_r=0.96562$ sec^{-1}; Curve 3 - The Single Diffusion Layer Model For $B=5.267$ sec^{-1}; Curve 4 - The Single Diffusion Layer With Central Well and Nernst Equation Corrections For Values of B, C_i and B_r the Same as For Curve 2, $\alpha=8.07 \times 10^{-3}$ atm., $R=0.035$ μA^{-1}

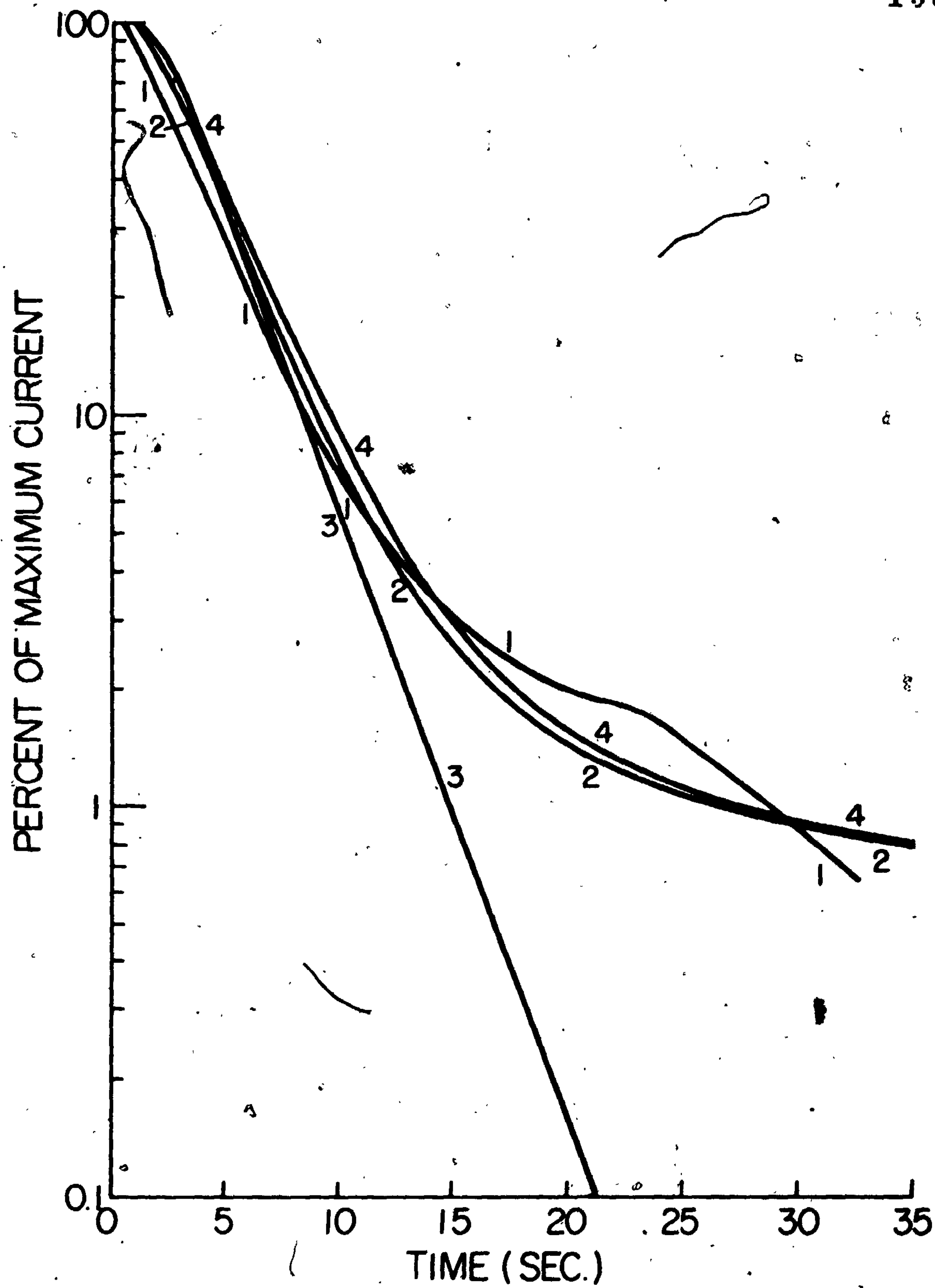
100
10
1
0.1
PERCENT OF MAXIMUM CURRENT
0
5
10
15
20
25
30
35
TIME (SEC.)
1
2
3
4

TABLE 2.5

Values of Parameters Used for the Mathematical Models in Figure 2.49

	Model I Single Diffusion Layer	Model II Single Diffusion Layer With Central Well Correction	Model III Single Diffusion Layer With Central Well and Electrolyte Resistance Corrections
B ($sec^{½}$)	5.267	5.2663	5.2663
C_i	-	0.095864	0.095864
C_p	-	-	135
C_r	-	-	15.074
B_r ($sec^{½}$)	-	0.96562	0.96562
α (atm. O_2)	-	-	8.07×10^{-3}
R (μA^{-1})	-	-	0.035
P_1 (atm. O_2)	-	3.02×10^{-2}	3.02×10^{-2}

TABLE 2.6

Effect of Electrolyte Resistance on Probe Output Current

P_1 (atm. O_2)	i_A (μA)	C_p (μA/atm. O_2)
	$\alpha = 8.07 \times 10^{-3}$ atm. O_2, $R = 0.035\ \mu A^{-1}$	
0.0302	3.9208	129.8
0.0996	12.839	128.9
0.2100	26.684	127.1
	$\alpha = 5.69 \times 10^{-6}$ atm. O_2, $R = 0.315\ \mu A^{-1}$	
0.0302	4.0819	135.2
0.0996	13.416	134.7
0.2100	25.772	122.7
	$\alpha = 0.00$ atm. O_2, $R = 0.01\ \mu A^{-1}$	
0.0302	4.0839	135.2
0.0996	13.468	135.2
0.2100	28.398	135.2

in Table 2.5.

2.13.7 Probe Response to a Slow Decrease in Oxygen Tension

Program KOK7 was written to investigate the anticipated response of the YSI probe to a simulated slow decrease in oxygen tension similar to a function that would be generated if the oxygen consumption rate of a microorganism were affected in a Michaelis-Menten manner by the oxygen tension. The following assumptions were made:

- The electrolyte resistance had no effect on the response
- The oxygen activity profiles in the membrane-electrolyte layer and in the central well were not interactive
- The current contribution by the oxygen flux from the central well was directly proportional to the oxygen tension at a point "a^*" from the membrane.

The single diffusion layer with central well correction model was used. The development of the relevant equations is presented in Appendix 2.19. Program KOK7 together with its subroutines is listed in Appendix 2.20. The results obtained from KOK7 for two simulated situations are graphed in Figures 2.50 and 2.51 together with the oxygen tension decrease curves, the lines of half-maximal slope and the graphical

FIGURE 2.50

Simulation of the Oxygen Probe Response According to the Single Diffusion Layer With Central Well Correction Model. Curve 1 - The Oxygen Tension Decrease Curve Calculated By Integrating the Michaelis-Menten Equation; $P_{O_{2}i}$ = 0.15 atm. O_2, Maximum Slope = 1.5×10^{-4} atm. O_2/sec, K_m' = 1.0×10^{-3} atm. O_2. Curve 2 - The Oxygen Tension-Time Curve Calculated By Program KOK7; B=5.0 sec^{-1}, C_i=0.1, B_r=1.0 sec^{-1}. Curve 3 is the curve of Half-Maximal Slope. Curve 4 is the Extrapolated Residual Current Line

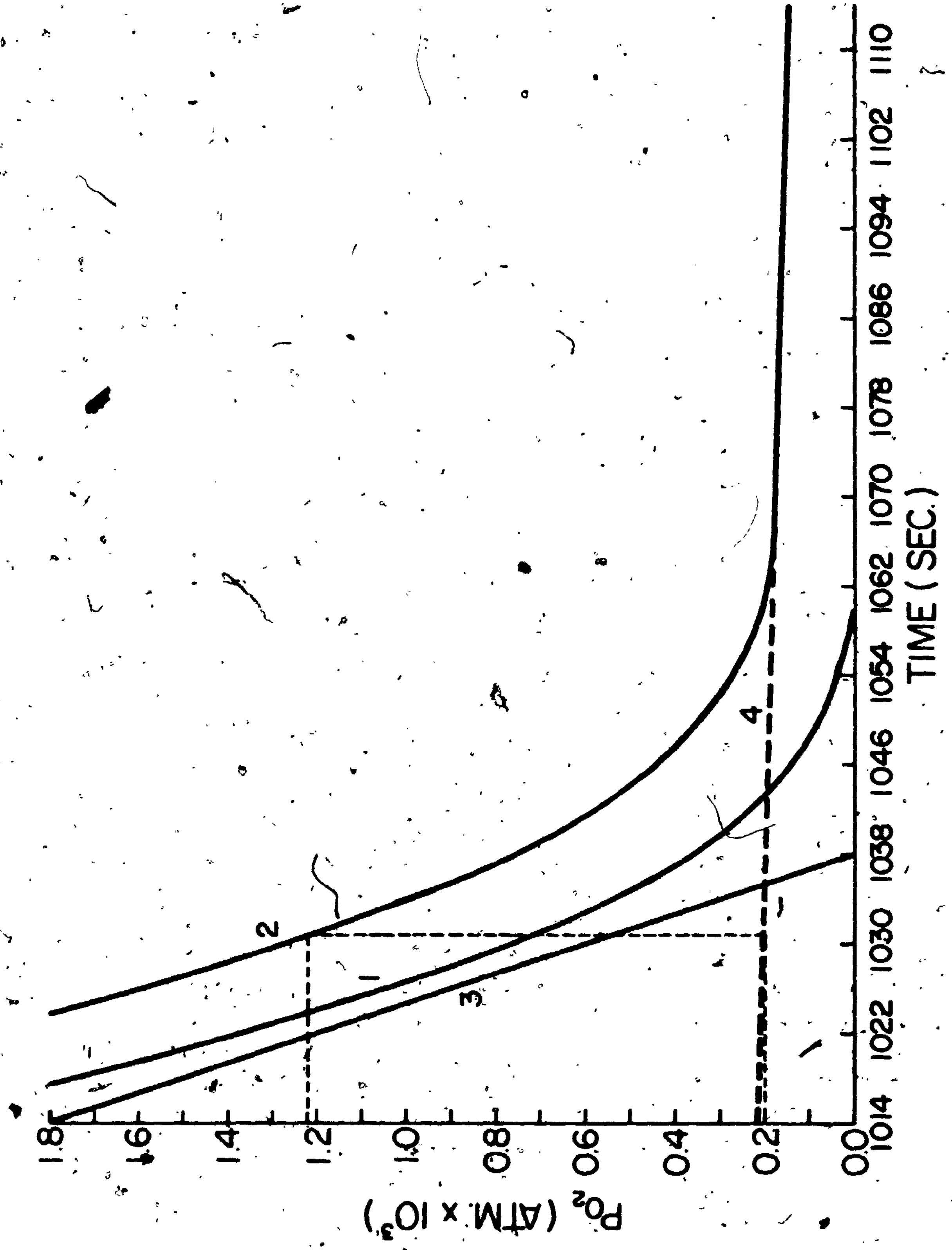

P_{O_2} (ATM x 10^3)
TIME (SEC.)
0.0
0.2
0.4
0.6
0.8
1.0
1.2
1.4
1.6
1.8
1014
1022
1030
1038
1046
1054
1062
1070
1078
1086
1094
1102
1110
1
2
3
4

FIGURE 2.51

Simulation of the Oxygen Probe Response According to the Single Diffusion Layer With Central Well Correction Model. Curve 1 - The Oxygen Tension Decrease Curve Calculated By Integrating the Michaelis-Menten Equation; P_{O_2} = 0.15 atm. O_2, Maximum Slope = 2.5×10^{-5} atm. O_2/sec, K_m = 2.0×10^{-4} atm. O_2. Curve 2 - The Oxygen Tension-Time Curve Calculated By Program MOK7; B=5.0 sec^{-1}, C_2=0.1, B_r=1.0 sec^{-1}. Curve 3 is the curve of Half-Maximal Slope. Curve 4 is the Extrapolated Residual Current Line

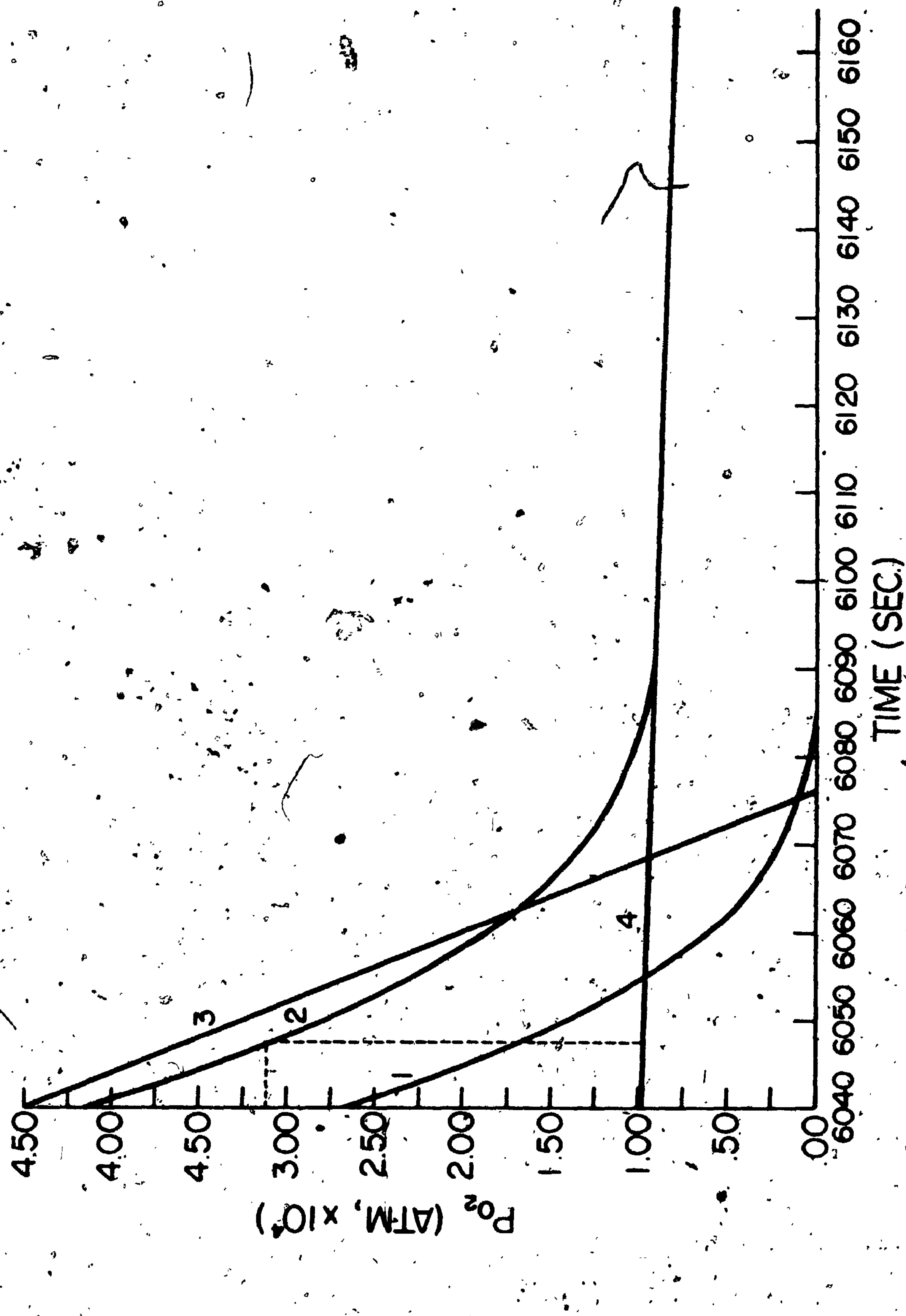

P_{O_2} (ATM, x10)
4.50
4.00
4.50
3.00
2.50
2.00
1.50
1.00
.50
.00
6040
6050
6060
6070
6080
6090
6100
6110
6120
6130
6140
6150
6160
TIME (SEC)
1
2
3
4

constructions necessary to obtain the K_m values from the response curves. The values of the parameters used are listed in Table 2.7. The values of K_m listed are the values used to calculate the oxygen tension decrease functions. The dynamic lag of the probe caused a residual current shown on Figures 2.50 and 2.51 as residual oxygen tensions. The K_m values were obtained from the response curves by finding the oxygen tension at which the probe response curve had a slope equal to half the maximal slope of the oxygen tension decrease curve by graphical means and subtracting the residual oxygen tension from this. The residual oxygen tension was obtained at this oxygen tension value by linear extrapolation of the tail of the response curve.

In Figure 2.50 the response curve was tangential to the half-maximal slope line at 1.22×10^{-3} atm. O_2. The residual oxygen tension was 0.20×10^{-3} atm., thus yielding a K_m value of 1.02×10^{-3} atm. O_2 as compared with the value of 1.00×10^{-3} atm. O_2 used to generate the oxygen tension decrease curve. In Figure 2.51 the tangential point occurred at 3.11×10^{-4} atm. The residual oxygen tension was 0.975×10^{-4} atm., yielding a K_m value of 2.13×10^{-4} atm. O_2 as compared to the value of 2.00×10^{-4} atm. O_2 used to generate the oxygen tension decrease curve.

TABLE 2.7

Values of the Parameters Used to Generate the YSI Probe Simulated Response Curves of Figures 2.50 and 2.51

Parameter	Figure 2.50	Figure 2.51
Maximum Rate of Oxygen Tension Decrease ($atm.\ O_2/sec.$)	-1.5×10^{-4}	-2.5×10^{-5}
P_0 ($atm.\ O_2$)	0.15	0.15
C_i	0.10	0.10
C_p (microamp/$atm.\ O_2$)	144	144
B ($sec^{\frac{1}{2}}$)	5.0	5.0
C_r (microamp/$atm.\ O_2$)	15	15
B_r ($sec^{\frac{1}{2}}$)	1.0	1.0
K_m ($atm.\ O_2$)	1.0×10^{-3}	2.0×10^{-4}

2.14 Discussion and Conclusions to Chapter 2

Both the galvanic and polarographic probe yielded a linear relationship between the bulk phase oxygen tension and the output current over a wide range of oxygen tension. The galvanic probe exhibited a disadvantageous characteristic in that its allowable output voltage decreased with oxygen tension if optimal response was to be retained. Dynamic response was also found to be slower at a lower oxygen tension than at a higher one. For these reasons the YSI polarographic probe was investigated. It was found to be superior in response speed and yielded very similar downstep responses for a wide range of downstep magnitudes.

The single diffusion layer with central well correction model could be used to represent the probe's behavior reasonably well. The use of a double diffusion layer model did not yield sufficient improvement to justify the increased complexity of an additional two parameters. Consideration of the electrolyte resistance had very little effect on the probe's response. By coupling the concentration profiles in the central well and the diffusion layer, the dependence of the probe's downstep response on the magnitude of the downstep could possibly be partly explained. The difficulties inherent in this procedure prevented its use in a model. It has been stressed earlier that the experiments described served only to elucidate the general performance of the YSI probe and to obtain reasonable estimates of its defining characteristic parameters. Using these values the anticipated probe response to a simulated oxygen tension decrease function was investigated. The oxygen tension decrease function used was obtained by integrating the Michaelis-Menten equation. It was found that the K_m value used to generate the oxygen tension decrease function could be recovered to within a few percent by subtracting the residual oxygen tension at the point of half-maximal slope. This justified the use of this technique to obtain a microorganism's K_m parameter from the experimental curves obtained with the YSI probe as described in Chapter 5.

CHAPTER 3

DISSOLVED OXYGEN MEASUREMENT WITH THE DROPPING MERCURY POLAROGRAPH

3.1 Introduction

A dropping mercury polarograph was employed to simultaneously obtain oxygen tension-time curves with the same samples as those used with the polarographic membrane-covered probe. A brief outline of its operation and previous uses similar to the author's is presented in section 3.2. It has been mentioned previously that this instrument has the disadvantage of producing a large and unpredictable residual current. For basic and complete descriptions of the polarographic method the reader is referred to Kirk-Othmer's [39] encyclopedia and Heyrovsky and Kuta's [34] original work.

3.2 Theory of Operation and Literature Review

Polarography was invented in 1922 [34] by Heyrovsky during his investigations of electrocapillary phenomena. Since then it has become the most widely used Faradaic electrochemical analytical technique [39], largely as a result of Ilkovic's mathematical treatment of the associated mass transfer problems. The direct current dropping mercury electrode (henceforth to be called the DME) was used for this investigation.

Mercury has classically been used as the electrode material because of its chemical nobility, its high hydrogen overvoltage and its ease of purification. By use of the DME, consisting of a fine-bore capillary, the mercury surface is continually renewed in an easily and accurately reproducible manner. The mercury falls off the tip of the capillary in droplets. When a potential is applied versus a nonpolarizable reference electrode to a DME submerged in a solution of reducible species the solutes are reduced at the DME (cathode). The current flowing then depends on the rate of diffusion of the material to the DME.

Four conditions must normally be satisfied to ensure that the observed current is a linear function of the concentration of the depolarizer in solution:

i) Convective mass transport must not contribute to the mass flux to the DME. Conventional polarographic analysis must therefore be conducted in unstirred solutions. This can be problematic during the study of metabolism of large cells which settle out rapidly.

ii) If the depolarizer is an electrolyte the migration current of the ions due to the imposed electric field affects the total current measured. This effect can be suppressed by adding an excess of indifferent electrolyte such as potassium chloride. Since oxygen is not an electrolyte this effect was however of no importance during this study.

iii) The electrostatic adsorption of reducible molecules on the surface of the mercury drop causes a current to flow which is greater than the limiting current determined by the diffusion rate. This effect produces 'maxima' [51]. They may be eliminated by the addition of small amounts of adsorbable material which is not reduced at the applied potential. Materials used for this purpose are colloids such as proteins, carbohydrates, polymers, soaps and dyes. Petering and Daniels [51] have found that for the analysis of oxygen in biological samples sufficient material of this type is present to eliminate the adsorption maximum of oxygen.

iv) The applied potential must be of such magnitude that the concentration of electroactive species at the DME surface is essentially zero. At this potential the limiting, or diffusion, current is obtained.

If conditions i) to iv) above are satisfied the current observed at the end of each drop life is the sum of three parts:

i) Charging Current

The mercury drop-solution interface forms a capacitor. As the drop grows in size, its surface area increases and the charge necessary to keep the capacitor charged up to the applied potential increases. Charging current is largest at the beginning of drop life and decreases parabolically thereafter.

ii) Polarographic Currents of No Interest

The reduction of species other than the one of interest cause polarographic currents which form part of the residual current.

iii) Polarographic Current of Interest

Reduction of the species of interest causes a polarographic current which forms the signal.

The sum of i) and ii) above is usually called the residual or background current and is determined in the absence of the species of interest by removing the latter. In the case of oxygen this can be accomplished by sparging the sample with water-saturated nitrogen. Polarographic waves of other species can sometimes interfere seriously with the determination of the species of interest. The hydrogen and oxygen waves overlap for example if a rotating solid platinum electrode instead of the DME is used [41]. The current at the end of drop life corrected for the residual current is directly proportional to the concentration of reducible species being investigated if the above conditions are satisfied.

Petering and Daniels [51] used the DME to measure oxygen concentration down to 0.016 ppm by weight. By experimentally determining the voltage at which oxygen reduction current was diffusion-limited they found a linear relationship between oxygen diffusion current and oxygen concentration. This apparatus was used to illustrate oxygen evolution and respiration by algae stimulated by the presence and absence of light. They also studied the respiration of yeast, homogenized rat liver tissue, red blood cells from chickens and blood from dogs. Moss [46] used the DME to study the effect of oxygen tension on respiration and cytochrome a_2 formation of *E. coli*. A linear relationship between current and oxygen tension was found. Baumberger [8] investigated the relationship between oxygen tension and yeast-cell respiration rate by means of the DME. The following were established:

i) Diffusion current is linearly related to oxygen tension at -0.5 volt vs a SCE half-cell.

ii) The residual current does not change over the course of an oxygen tension vs time test as a result of accumulation or disappearance of other metabolites; polarograms run on yeast suspensions from which all the dissolved oxygen had been removed by metabolism did not show any new substances to be present which were reducible on the DME at the voltage used for oxygen determination.

iii) Injury to the living cells by mercury could not be observed.

Winzler [71] also proved linearity between oxygen activity and polarographic current. This method was used to obtain critical oxygen tension and K_r values for *Saccharomyces cereviseae*.

3.3 Polarographic Apparatus

The polarographic apparatus used consisted of a Sargent XV Polarograph, a Sargent Micro Range Extender and a Leeds and Northrup 7736 Polarotron Dropping Mercury Electrode Assembly. The Sargent XV Polarograph produces a continuous record of either the current-voltage or current-time curve (with applied voltage held constant) depending on the mode of operation. Its output sensitivity can be varied from 0.003 to 1.00 microamp/mm. By switching the Micro Range Extender between the Polarograph and the Polarotron the sensitivity can be extended down to 0.0001 microamp/mm. The Polarotron is shown in Figure 3.1. It comprises the complete electrochemical assembly required for polarographic analysis. The reference cell is a saturated calomel electrode. The electrolysis assembly was held at constant temperature (23°C) by water from a controlled-temperature bath circulating through the water jacket. The purge valve allowed purge gas to be either bubbled through the test solution or sprayed over the surface of the sample, thus preventing air from diffusing into the solution. The Polarograph, the Micro Range Extender and the Polarotron are shown together in Photograph 3.1.

3.4 Polarograph Operating Parameters and Calibration

3.4.1 Oxygen Determination in Distilled Water

During the determination of oxygen in distilled water a dosing solution had to be added to suppress the maxima in the polarogram. The dosing solution had the following composition:

Sodium starch glycollate		54.6	gm
Sodium hexametaphosphate		20.0	gm
NaCl		300.0	gm
K_2CO_3		85.0	gm
KCl		35.0	gm
KNO_3		100.0	gm
Glycine		60.0	gm
H_2O (distilled)	to	1425	cc

FIGURE 3.1

The Polaratron

3 OF/DE 6

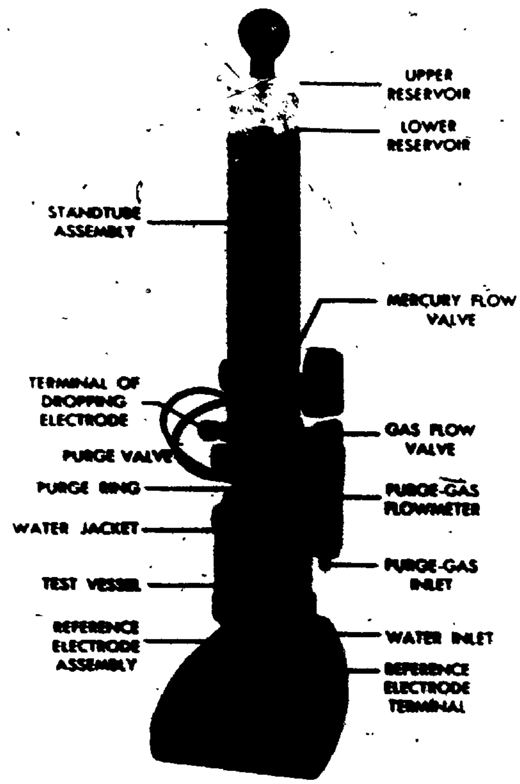
UPPER RESERVOIR
LOWER RESERVOIR
STANDTUBE ASSEMBLY
MERCURY FLOW VALVE
TERMINAL OF DROPPING ELECTRODE
PURGE VALVE
GAS FLOW VALVE
PURGE RING
PURGE-GAS FLOWMETER
WATER JACKET
PURGE-GAS INLET
TEST VESSEL
REFERENCE ELECTRODE ASSEMBLY
WATER INLET
REFERENCE ELECTRODE TERMINAL

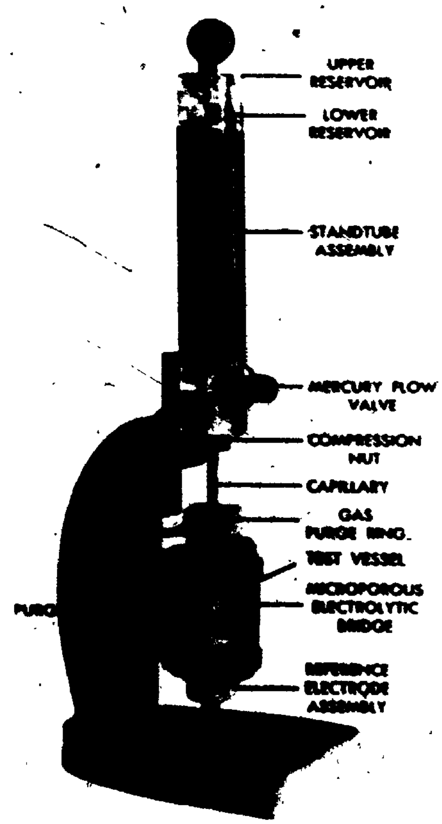
UPPER RESERVOIR
LOWER RESERVOIR
STANDTUBE ASSEMBLY
MERCURY FLOW VALVE
COMPRESSION NUT
CAPILLARY
GAS PURGE RING
TEST VESSEL
MICROPOROUS ELECTROLYTIC BRIDGE
REFERENCE ELECTRODE ASSEMBLY

PHOTOGRAPH 3.1

The Polarograph, the Micro-Range Extender
and the Polaratron

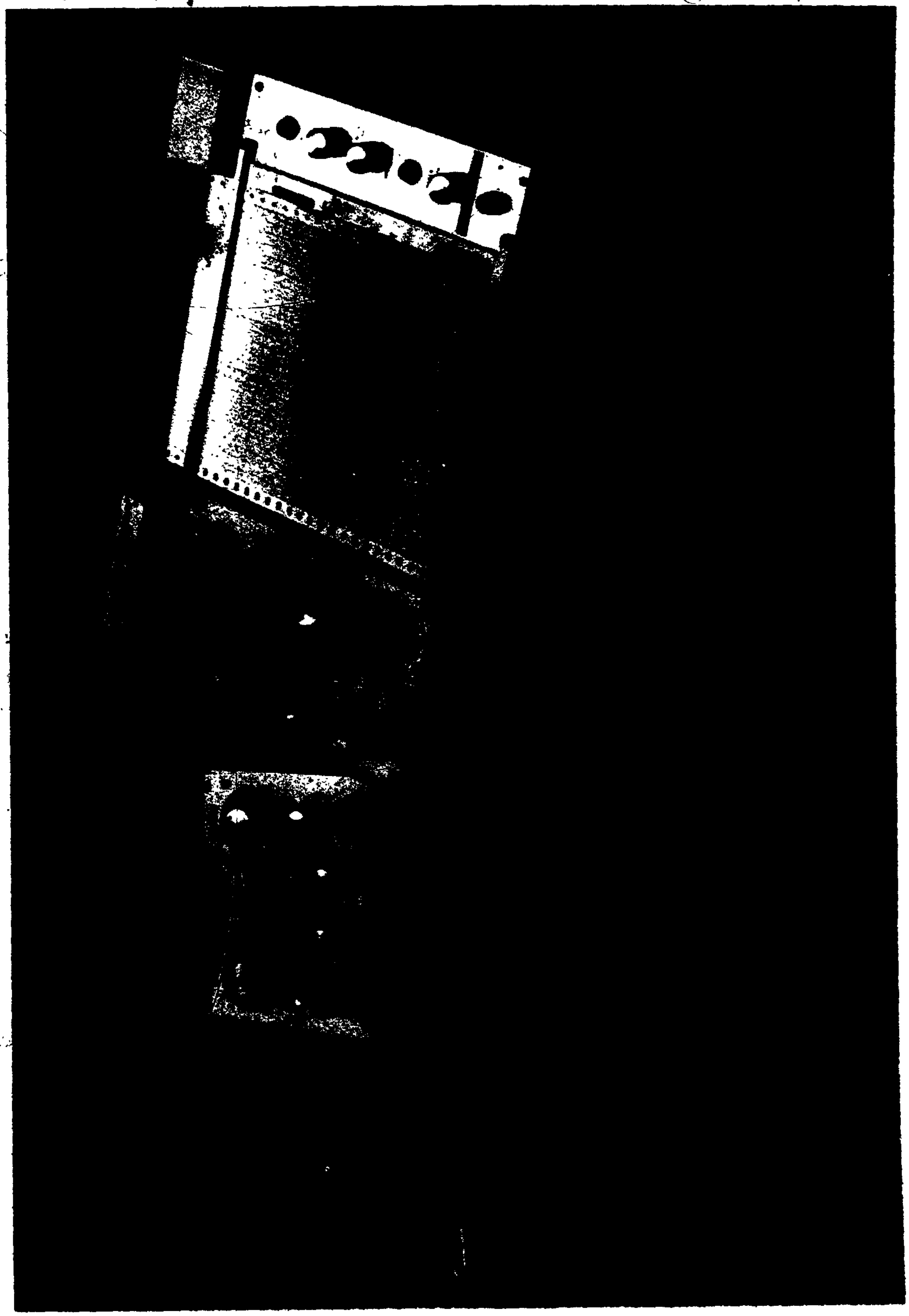

Two plateau's were observed at -0.5 volt and -1.5 volt vs SCE respectively. Baumberger [8] has proposed that these are due to the reactions:

$$O_2 + 2H^+ + 2e^- \rightarrow H_2O_2 \quad (3.1)$$

$$O_2 + 2H^+ + 4e^- \rightarrow 2OH^- \quad (3.2)$$

Since the second reaction involves twice as many electrons as the first the current is twice as high.

3.4.2 Current Measurement

In Figure 3.2 are shown the three different types of peaks observable on the polarograms. The shape of the peaks changed with oxygen tension. Part a) of Figure 3.2 illustrates the peaks obtained at high oxygen tension, part b) the peaks obtained at low oxygen tension and part c) the peaks obtained very close to zero oxygen tension. As the magnitude of the diffusion current due to oxygen reduction decreased, the charging current became an increasingly large fraction of the output signal. In interpreting the polarograms it was therefore important to observe the current at the end of drop life rather than the maximum deflection obtained.

FIGURE 3.2

Qualitative Differences Between the Peak Shapes Obtained With the Dropping Mercury Electrode. At a) High Oxygen Tension, b) Intermediate Oxygen Tension and c) Low Oxygen Tension

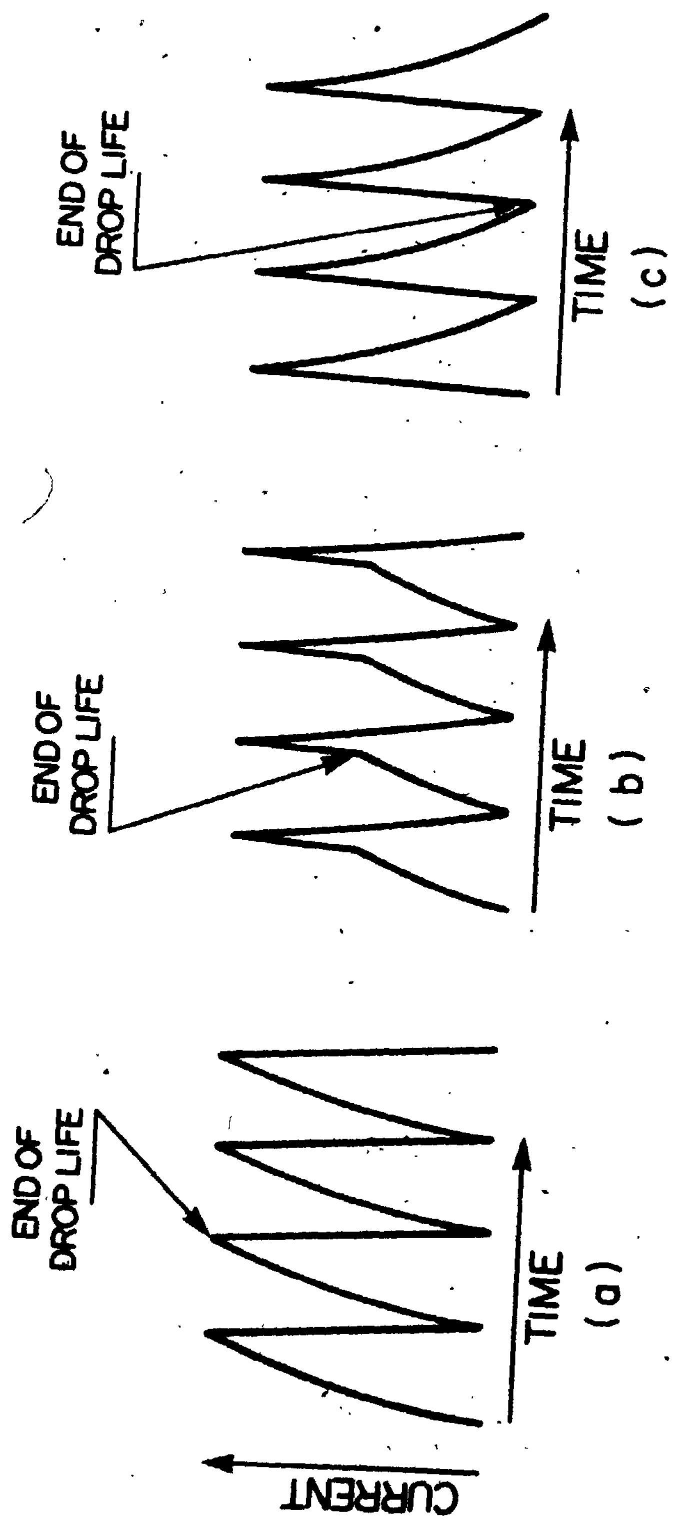

CURRENT
END OF DROP LIFE
TIME
(a)
END OF DROP LIFE
TIME
(b)
END OF DROP LIFE
TIME
(c)

3.4.3 Calibration With Distilled Water

Over a number of trials it became apparent that the charging current at -1.5v was approximately 0.2 microamp and at -0.5 volt was approximately 0.002 microamp. Using an applied voltage of -0.5 volt yielded therefore a far superior signal/noise ratio than operation at -1.5 volt and allowed the use of much lower sensitivities thus increasing the signal size and improving its readability and accuracy. Detailed experimental results are presented in Appendix 3.1. Results from the calibration procedure are presented in Table 3.1. The average calibration constant was 21.2 microamp/atm. oxygen with a standard deviation of 5.1%.

3.4.4 Oxygen Determination in Fermentation Liquid

It was found that the dosing solution reacted chemically with the supernatant of a centrifuged and filtered (0.8 micron-Millipore) sample from fermentation 1 (described in Chapter 5). For none of the tests presented below was any dosing solution therefore added. Detailed experimental results for the polarograph calibration with centrifuged and filtered supernatant are presented in Appendix 3.2. Results from the calibration procedure are presented below in Table 3.2. The average calibration constant was 21.3 microamp/atm. oxygen with a standard deviation of 4.1%.

TABLE 3.1

Results From Calibration With Distilled Water

Oxygen Tension (atm.)	Average Current (microamp)	Standard Deviation of Current (% of average current)	Calibration Constant (microamp/atm. O_2)
1.76×10^{-4}	0.0037	N.A.*	21.0
9.26×10^{-4}	0.0182	2.3	19.6
0.0030	0.0669	3.0	22.3
0.0101	0.232	0.2	23.0
0.0302	0.631	0.5	20.9
0.0996	2.04	0.3	20.5
0.21	4.26	0.3	20.3

*N.A. - Not available

TABLE 3.2

Results From The Calibration With Fermentation Supernatant

Oxygen Tension (atm.)	Average Current (microamp)	Standard Deviation of Current (% of average current)	Calibration Constant (microamp/atm. O_2)
1.76×10^{-4}	0.0035	5.5	19.7
9.26×10^{-4}	0.0204	2.8	22.1
0.0030	0.0677	2.2	22.6
0.0101	0.2104	0.9	20.8
0.0302	0.6491	0.7	21.5
0.0996	2.116	0.4	21.2
0.21	4.382	1.4	20.9

3.5 Conclusions

The dropping mercury polarograph was found to yield linear relationships between oxygen tension and diffusion current over the range 1.76 x 10^{-4} atm. oxygen to 0.21 atm. oxygen in both distilled water with dosing solution added and in centrifuged and filtered supernatant obtained from fermentation broth. This result agrees with the findings of Petering and Daniels [51], Moss [46], Baumberger [8] and Winzler [71].

During the calibration procedure no corrections were made for the atmospheric pressure being lower than 1 atm. or for the vapour pressure of water since the effect of these would be proportionally the same for all the calibration gases and only the linearity of the current-oxygen tension relationship was of interest.

The polarographic apparatus needed frequent standardization which could easily be accomplished by means of its internal circuitry. When properly standardized it could be used with confidence to detect changes as small as 0.0004 microamp in a total current of 0.1340 microamp. The accuracy of the baseline offset circuit was such that no difference could be observed between the original signal and the reconstituted signal obtained by adding the baseline offset to the reading obtained.

The residual current obtained in the fermentation liquid at -0.5 volt vs SCE was much larger than that obtained under the same conditions in distilled water with dosing solution added. This large residual current could be due to either a high charging current or a depolarizer other than oxygen being reduced. Since the charging current is influenced by the difference between the applied potential and the potential of the mercury-liquid interface [34] the large change in residual current could be due to the difference in chemical compositions of the two solutions. The larger residual current merely complicated the measuring of small oxygen diffusion currents and prevented the use of the lowest sensitivities of the polarograph.

CHAPTER 4

DISSOLVED OXYGEN CONTROL

4.1 Introduction

Molecular oxygen is in some ways very similar to other nutrients in submerged aerobic fermentations in that its limited availability may curtail growth. It is dissimilar from most other nutrients by virtue of its very limited solubility in water. Whereas other nutrients may be supplied in solution in sufficient concentration not to become growth-limiting during the course of a fermentation, the oxygen supply must be continuously renewed. This replenishment is usually accomplished by sparging with an oxygen-containing gas such as air or an artificial nitrogen-oxygen mixture. For oxygen not to be a growth-limiting factor, the oxygen supply must be sufficient to keep the dissolved oxygen tension at a level such that the oxygen consumption remains unaffected.

Many authors (e.g. Arnold and Steel [6]) have conceptualized the oxygen transfer system in terms of an interaction between the oxygen supply and the culture oxygen demand. Although this approach can be fruitful it contains some inherent dangers in that the oxygen supply and the culture oxygen demand are difficult to deal with and are often not well defined.

The oxygen supply to a fermentation depends on both the volumetric mass transfer coefficient and the mass transfer driving force. For example, should the mass transfer coefficient change due to the formation of a surface-active substance, the driving force would adjust itself by a lowering of the dissolved oxygen tension, possibly having as result an oxygen supply very close to that previous to the change in conditions. The result might also provide a drastic change in dissolved oxygen tension associated with an imperceptible change in oxygen supply. The fact that the exhaust gas composition does not fluctuate significantly at a steady aeration rate cannot be accepted as an indication that the conditions in the fermentor are not changing.

The culture oxygen demand is in itself a potentially misleading concept in that no chemical reaction 'demands' reactants. The demand is usually understood to be the maximum reaction rate possible under the given set of circumstances if the oxygen tension were to be increased sufficiently. The oxygen demand is however strongly influenced by temperature and by the concentration of other metabolites [71]. Should the demand change, the oxygen tension would adjust itself, thus affecting the supply. Such a shift in supply would not necessarily be noticeable since it is very difficult to obtain an accurate mass balance for a fermentor.

In both of the above instances it was pointed out that the dissolved oxygen tension could change without such an adjustment having a significant influence on the fermentor mass balance. Pirt [54] has aptly pointed out:

> "Unfortunately, the academic microbiologist seems little aware of the quantitative basis of aeration, with the result that he may have been unwittingly using anaerobic conditions thinking they were aerobic. The efficiency of aeration is stated in terms of the oxygen solution rate. Another parameter required to define the availability of oxygen is oxygen tension or activity in the medium."

Both the oxygen supply and the demand are determined by a number of factors. As such they are often not suitable as variables to be controlled directly. A variable which is much more easily measured and whose significance and effects are simpler to evaluate is the dissolved oxygen tension. It is obvious that for the purpose of process and fermentor design both the desired operating oxygen tension and the culture oxygen demand must be known.

4.2 Control Methods - Literature Review

Two major modes of dissolved oxygen control have evolved:

i) Control of the oxygen supply allowing the oxygen tension to find its own level.

ii) Control of oxygen tension by continuous monitoring and correcting the supply.

Minor modes such as adjustment of the fresh medium inflow according to an error signal from a dissolved oxygen readout device have not found wide acceptance. Brookes [13] used this method to match the oxygen "demand" to the supply.

4.2.1 Control of the Oxygen Supply

This system was used in its simplest form by Smith and Johnson [61] who determined the oxygen supply rate under various sets of conditions by the sulfite oxidation method and assumed the same quantities of oxygen were being supplied to a growing culture under the same conditions. Although no quantitative results could be obtained from this procedure since the mass transfer coefficients for the two solutions were different, a relationship between the aeration efficiency and the cell concentration of *Serratia marcescens* was found. Ecker and Lockhart [20] used a very similar approach in a study of the effects of limiting nutrients on physiological events during culture growth of *E. coli*. Tempest and Herbert [63] recorded oxygen uptake rates for *Candida utilis* under growth-limiting conditions imposed by glucose, xylose and ethanol. Maxon [44] also considered the 'effective aeration', determined by sodium sulfite oxidation as established by Cooper *et al.* [17], in an investigation of the effect of aeration on the propagation of Baker's yeast.

By means of measuring the outlet gas oxygen content and performing a mass balance, the real oxygen supply can be obtained. This method was used by Moss *et al.* [47]. Shu [60] has described a system using this approach to control oxygen utilization to follow a predetermined program. This system is illustrated in Figure 4.1.

The technique of controlling oxygen supply can be used with advantage under certain circumstances. Arnold and Steel [6] have pointed out a relationship between oxygen uptake rate and streptomycin production. Feren and Squires [23] have found that Cephalosporin C synthesis was depressed at an oxygen tension higher than the critical oxygen tension. In cases where a small change in oxygen tension can produce a large change in the type and quantity of antibiotic produced, it may be more appropriate to allow the dissolved oxygen to find its own level by controlling the oxygen supply. To effectively utilize this control strategy requires however a constant awareness that it is in reality the oxygen tension that controls the reaction rate and it should therefore be continuously monitored.

4.2.2 Control of the Dissolved Oxygen Tension

Brookes [13] has reviewed some of the dissolved oxygen control systems described in the literature. Two main mechanisms for controlling the dissolved oxygen tension are prevalent:

- manipulation of the oxygen dissolution driving force

FIGURE 4.1

The Dissolved Oxygen Control System

Described By Shu [60]

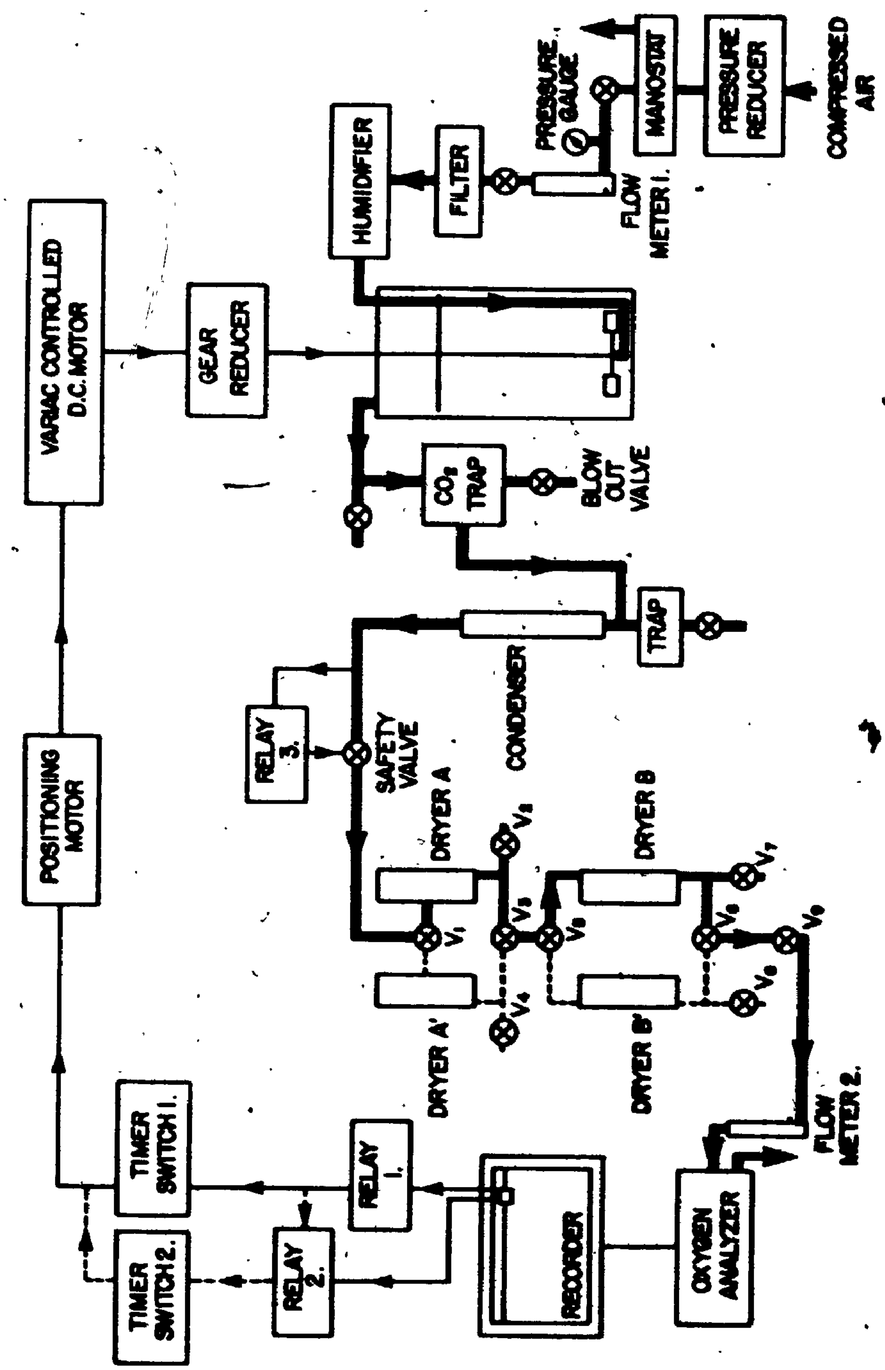
VARIAC CONTROLLED D.C. MOTOR
GEAR REDUCER
HUMIDIFIER
FILTER
PRESSURE GAUGE
MANOSTAT
PRESSURE REDUCER
COMPRESSED AIR
FLOW METER I.
CO2 TRAP
BLOW OUT VALVE
TRAP
CONDENSER
RELAY 3.
SAFETY VALVE
POSITIONING MOTOR
DRYER A
DRYER B
DRYER A'
DRYER B'
FLOW METER 2.
OXYGEN ANALYZER
RECORDER
RELAY 1.
RELAY 2.
TIMER SWITCH I.
TIMER SWITCH 2.

- manipulation of the mass transfer coefficient.

Terui *et al.* [64, 65, 67] has employed the former method by manipulating the composition of the sparging gas which was a mixture of oxygen and nitrogen. Harrison and Pirt [24] have used the same method to study the glucose metabolism of *Klebsiella aerogenes*. Moss, Babij and Rickard *et al.* [7, 47, 48, 56, 57] have also employed this method in conjunction with adjustment of the stirring rate to control oxygen tension. MacLennan and Pirt [42] controlled the oxygen tension at values from 0.26 mm Hg to 30 mm Hg oxygen by using a PID controller and a pneumatic valve to regulate the composition of an oxygen/nitrogen mixture. Their system is shown in Figure 4.2.

Manipulation of the volumetric mass transfer coefficient to control oxygen tension can be accomplished by two methods:

- adjustment of the sparging rate

- adjustment of the agitation rate

Herbert *et al.* [33] has implemented dissolved oxygen control by adjustment of the agitation rate. Terui and Konno *et al.* [65, 66, 67] have controlled oxygen tension by manipulation of the sparging rate of air without altering the gas composition. Flynn and Lilly [25] used a variable-depth sparging pipe to adjust the mass transfer coefficient. Commercial hardware is available (New Brunswick Scientific Company) which automatically controls oxygen tension by

FIGURE 4.2

The Dissolved Oxygen Control System

Described by MacLennan and Pirt [42]

F - filter
FR - flow regulator
G - pressure gauge
M - manometer
PR - pressure regulator
R_1, R_2 - rotameters

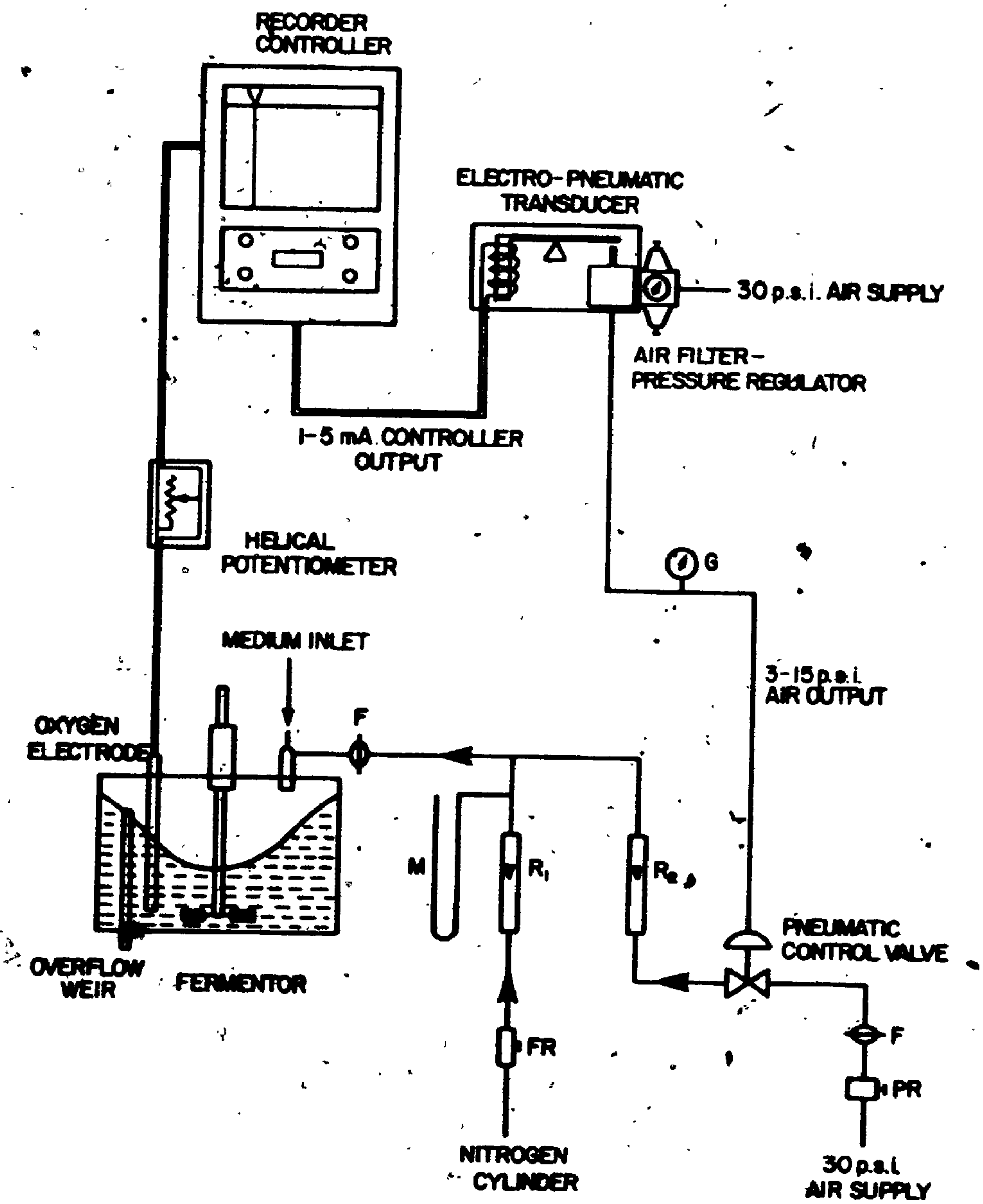
RECORDER CONTROLLER
ELECTRO-PNEUMATIC TRANSDUCER
30 p.s.i. AIR SUPPLY
AIR FILTER-PRESSURE REGULATOR
1-5 mA. CONTROLLER OUTPUT
HELICAL POTENTIOMETER
G
MEDIUM INLET
3-15 p.s.i. AIR OUTPUT
F
OXYGEN ELECTRODE
M
R1
R2
PNEUMATIC CONTROL VALVE
OVERFLOW WEIR
FERMENTOR
FR
F
PR
NITROGEN CYLINDER
30 p.s.i. AIR SUPPLY

means of sparging rates and agitation speed adjustments.

Oxygen tension control system design requirements include specifications of the desired oxygen control levels as well as culture oxygen demand. The necessary data for design may be obtained by the methods described by Chance [15] to obtain oxygen consumption vs oxygen tension curves. Terui *et al.* [65] has also described this method. The equipment described in Chapters 2 and 3 was designed for this purpose also. Depending on the type of fermentation, either oxygen supply or oxygen tension control may be appropriate.

4.3 A Mathematical Model of a Dissolved Oxygen Control System

During the course of several preliminary fermentations difficulties were encountered in finding the proper settings for the proportional-integral controller used to control the dissolved oxygen tension in the fermentor. The effect of antifoam addition to the fermentor was especially noticeable in that it always produced very large fluctuations in dissolved oxygen tension. The equipment utilized is described in Chapter 5. A mathematical model of the control system was drawn up. It is contained in Program KOK8 and its subroutines listed in Appendix 4.1 together with a sample output. The program as listed is self-explanatory. The assumptions made to develop the model are presented below.

These were:

i) Both the liquid phase and the gas phase in the head space are perfectly mixed. The oxygen tensions in these phases are uniform throughout.

ii) Oxygen enters the liquid phase from two sources: by absorption from the gas bubbles suspended in the liquid and through the interface between the liquid and gas phases.

iii) The only origin of gas bubbles in the liquid phase is sparging. No secondary gas bubbles are formed at the gas-liquid interface.

iv) The residence time distribution function of gas bubbles is a decaying exponential with a mean residence time independent of the gas sparging rate. Hanhart *et al.* [28] has partially justified this approach.

v) The volumetric mass transfer coefficient is related to the sparging rate by a simple relationship given by Aiba *et al.* [3]

$$K_v = 0.0635\, P^{0.95} V_s^{0.67} \qquad (4.1)$$

vi) The volumetric mass transfer coefficient K_v associated with the gas bubbles created by sparging during an incremental period Δt decreases exponentially at the same rate as the volume of bubbles remaining in suspension.

vii) Bubbles do not coalesce or break up after their initial formation so that the oxygen tension in the bubbles remaining in suspension can be calculated from the original oxygen content and the history of the liquid phase dissolved oxygen tension.

viii) The sparging gas flowrate remains steady throughout the iteration time interval as determined by the error signal coming to the controller at the end of the previous interval.

ix) Both the volumetric mass transfer coefficient and the mass transfer coefficient between the liquid surface and the gas head space are affected proportionally the same by the addition of surface-active material.

x) The behavior of the dissolved oxygen tension measuring probe is characterized by the single-diffusion layer and central well model developed in Chapter 2 and used in Programs KOK5 and KOK7.

xi) The oxygen consumption rate of the microorganisms is related to the oxygen tension in a manner which may be expressed by a hyperbolic function such as the Michaelis-Menten equation.

xii) During the initial steady-state the sparging gas flowrate is one-half the maximum air flow available through the control valve.

The liquid-phase oxygen tension was calculated at the end of each incremental period by an iterative procedure based on a mass balance for that period. The effective liquid-phase oxygen tension used to calculate the quantity of oxygen transferred and the oxygen tension remaining in the suspended bubbles was the arithmetic mean of the liquid phase oxygen tensions at the beginning and the end of the period.

The dynamic response of the dissolved oxygen tension to a sudden 40% decrease in both the volumetric mass transfer coefficient and the mass transfer coefficient between the liquid surface and the head space was investigated under various conditions of maximum organism growth rate, head space volume and the dissolved oxygen tension set point. Such a disturbance could be caused by the addition of an antifoam. All other operating parameters were kept constant. These are listed in Table 4.1. The values chosen for the operating parameters were arrived at by rough estimation of the actual observed process and by experience. The value of the gas-liquid interface mass transfer coefficient was obtained from

TABLE 4.1

Values of Operating Parameters Held Constant
During All Simulation Runs of KOK8

Parameter	Value	Units
Power input per unit volume	10.0	HP/m^3
Liquid phase volume	10.0	liter
Mass transfer coefficient head to liquid	0.04	cm/sec
Vessel diameter	25	cm
Sparging gas oxygen tension	0.21	atm.
Iteration time interval	1	sec
Michaelis-Menten constant for organism	0.001	atm. O_2
Organism concentration	10	gm/l
Oxygen consumption per cell growth	1	gm O_2/gm cells
Initial steady-state period	100	sec
Solubility of oxygen	0.040	gm/l/atm.
Mean residence time of bubbles	20	sec
Temperature	23	°C
Probe Constants: C_i	0.1	none
C_p	144	microamp/atm. O_2
C_r	15.5	microamp/atm. O_2
B	5.0	$sec^{1/2}$
B_r	1.0	$sec^{1/2}$
Number of intervals for integrations	60	none

Aiba *et al.*[3]. In Figure 4.3 the system open-loop response is compared with the responses obtained if only a proportional controller was modelled at various gains. The head space volume was 10 liters, the maximum organism growth rate was 0.1 hr^{-1} and the dissolved oxygen tension set point was 0.01 atmosphere. Dynamic responses at proportional gains of 0.0 (open-loop), 0.1, 0.2, 0.4, 0.75, 1.5, 2.5 and 5.0 m^3/hr/atm. of O_2 are shown. A block diagram of the system is presented in Figure 4.4.

Dynamic responses to the same disturbance under various conditions of head space volume, maximum organism growth rate and dissolved oxygen tension set point with a proportional-integral controller are shown in Figures 4.5 to 4.8. The proportional gain was 2.75 m^3/hr/atm. O_2; the integration gain was 0.236 m^3/hr/atm. O_2/sec. Values of the head space volume, maximum organism growth rate and the dissolved oxygen tension set point are shown in Table 4.2.

4.4 Discussion

Although the theoretical investigation into the behavior of the dissolved oxygen control system was by no means exhaustive several important operating principles were elucidated:

FIGURE 4.3

Dynamic Responses of the Simulated Dissolved Oxygen Control System (Proportional Control Only) To a 40% Step Decrease in Both Mass Transfer Coefficients. The Head Space Volume Was 10 l; the Maximum Organism Growth Rate Was 0.1 hr^{-1}; the Dissolved Oxygen Tension Set Point Was 0.01 atm. O_2. The Control System Gains Were: Curve 1 - 0.0; Curve 2 - 0.1; Curve 3 - 0.2; Curve 4 - 0.4; Curve 5 - 0.75; Curve 6 - 1.5; Curve 7 - 2.5; Curve 8 - 5.0. $m^3/hr/atm.\ O_2$

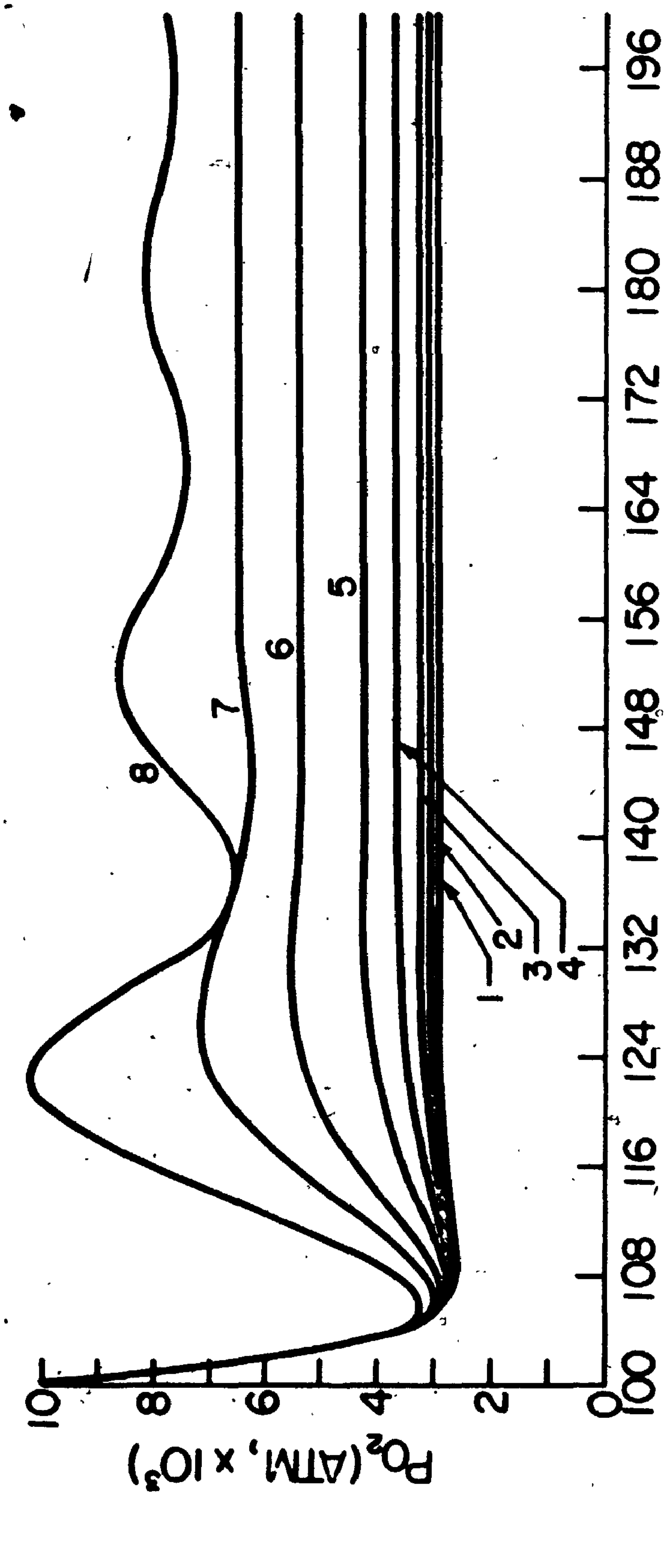

P_{O_2} (ATM, x 10^3)
TIME (SEC.)
0
2
4
6
8
10
100
108
116
124
132
140
148
156
164
172
180
188
196
1
2
3
4
5
6
7
8

FIGURE 4.4

Block Diagram of the Simulated Dissolved Oxygen Control System

The control system gain quoted in the text is the combined gain of all the units enclosed by the dashed line.

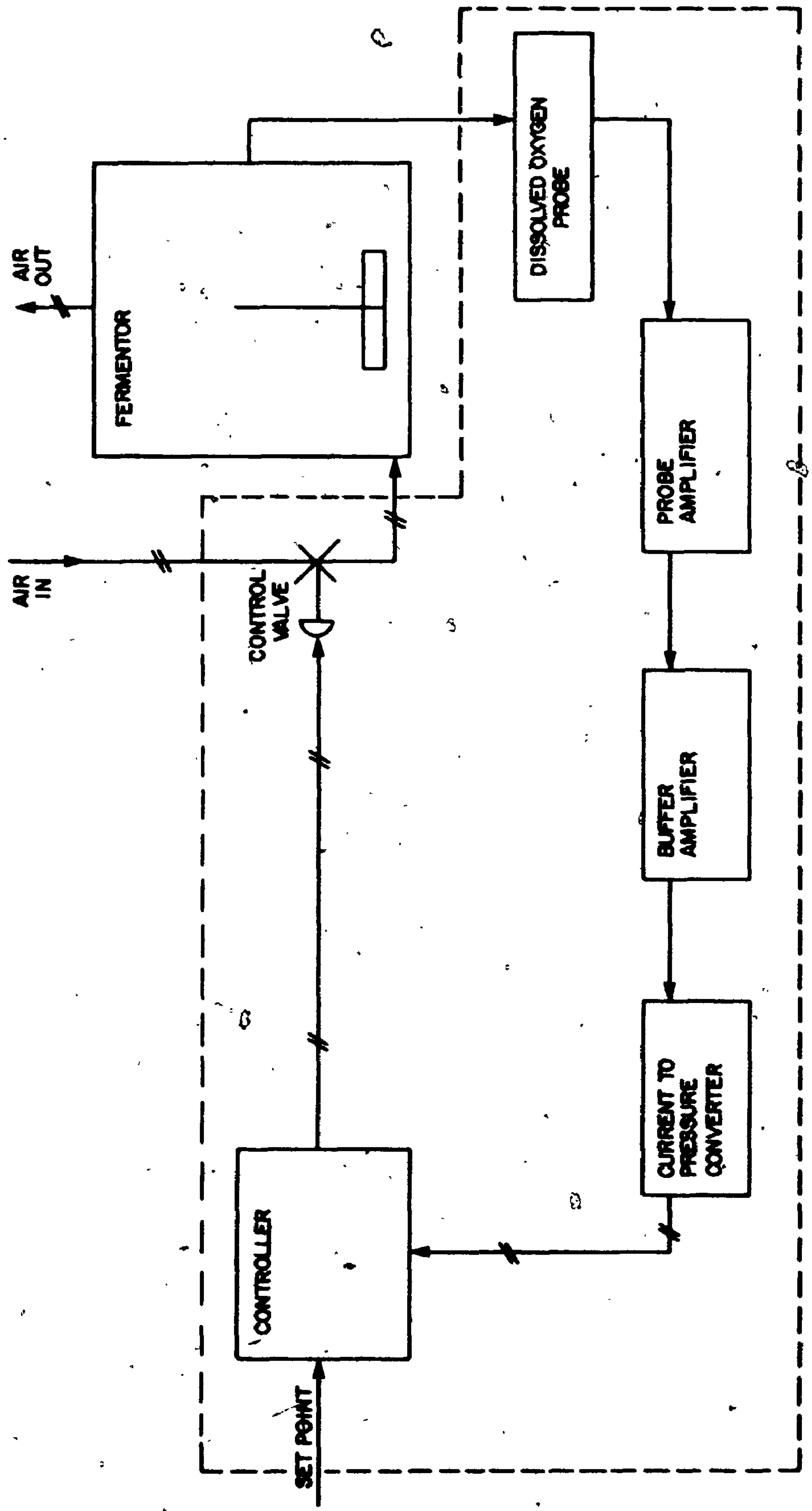
AIR OUT
FERMENTOR
DISSOLVED OXYGEN PROBE
AIR IN
CONTROL VALVE
PROBE AMPLIFIER
BUFFER AMPLIFIER
CURRENT TO PRESSURE CONVERTER
CONTROLLER
SET POINT

TABLE 4.2

Values of Head Space Volume, Maximum Organism Growth Rate and Dissolved Oxygen Tension Set Point Used to Generate Figures 4.5 - 4.8

Figure #	Curve #	Head Space (l.)	Maximum Growth Rate (hr^{-1})	Dissolved Oxygen Set Point (atm.)
4.5	1	10	0.1	0.01
	2	0.1	0.1	0.01
4.6	1	10	0.1	0.005
	2	0.1	0.1	0.005
4.7	1	10	0.2	0.01
	2	0.1	0.2	0.01
4.8	1	10	0.2	0.005
	2	0.1	0.2	0.005

FIGURE 4.5

Dynamic Responses of the Simulated Dissolved Oxygen Control System (Using a Proportional-Integral Controller) To a 40% Step Decrease in Both Mass Transfer Coefficients. Variable Values Are Listed in Tables 4.1 and 4.2

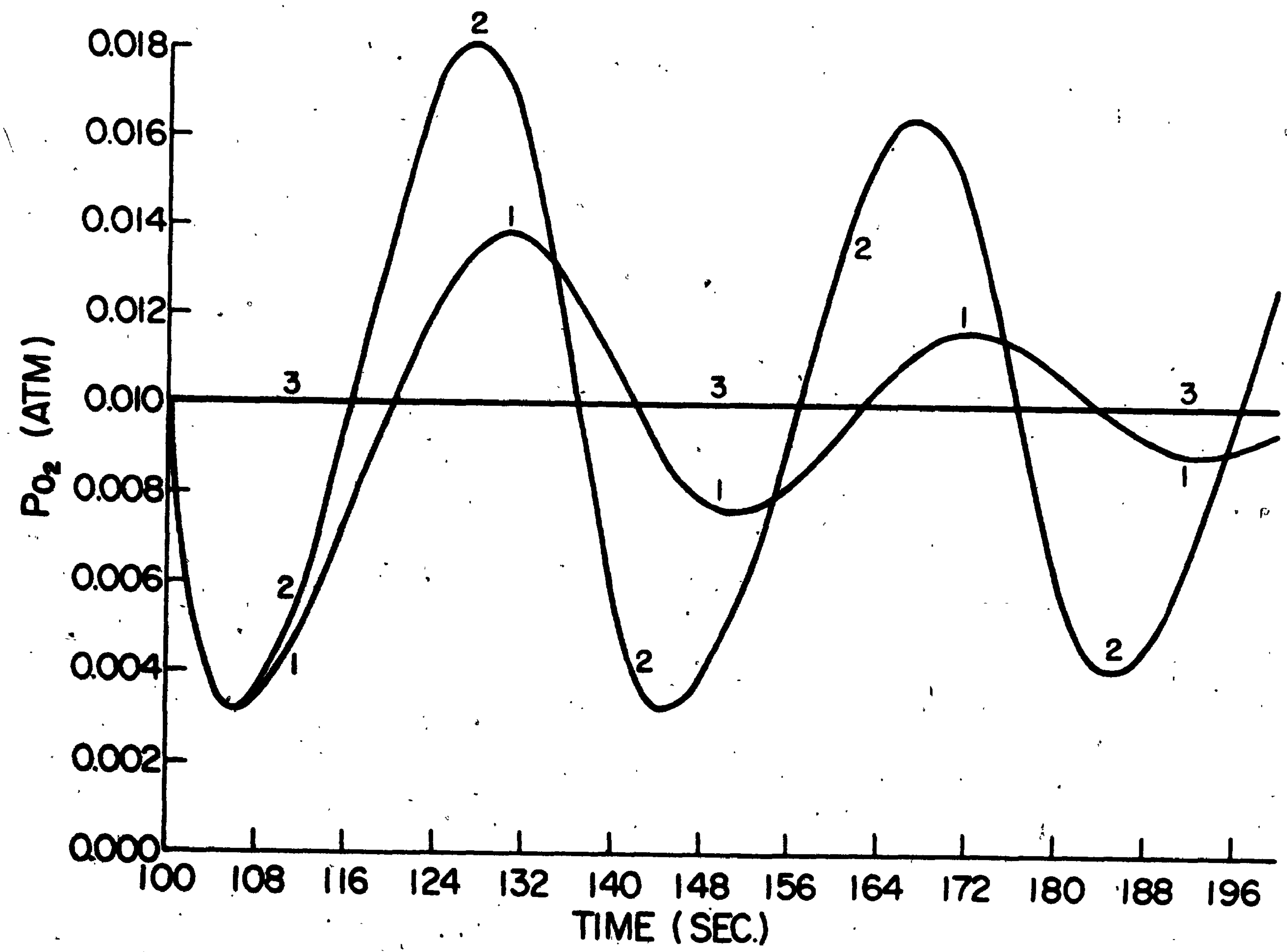

0.018
0.016
0.014
0.012
0.010
0.008
0.006
0.004
0.002
0.000
P_{O_2} (ATM)
100
108
116
124
132
140
148
156
164
172
180
188
196
TIME (SEC.)
1
2
3

FIGURE 4.6

Dynamic Responses of the Simulated Dissolved Oxygen Control System (Using a Proportional-Integral Controller) To a 40% Step Decrease in Both Mass Transfer Coefficients. Variable Values Are Listed in Tables 4.1 and 4.2

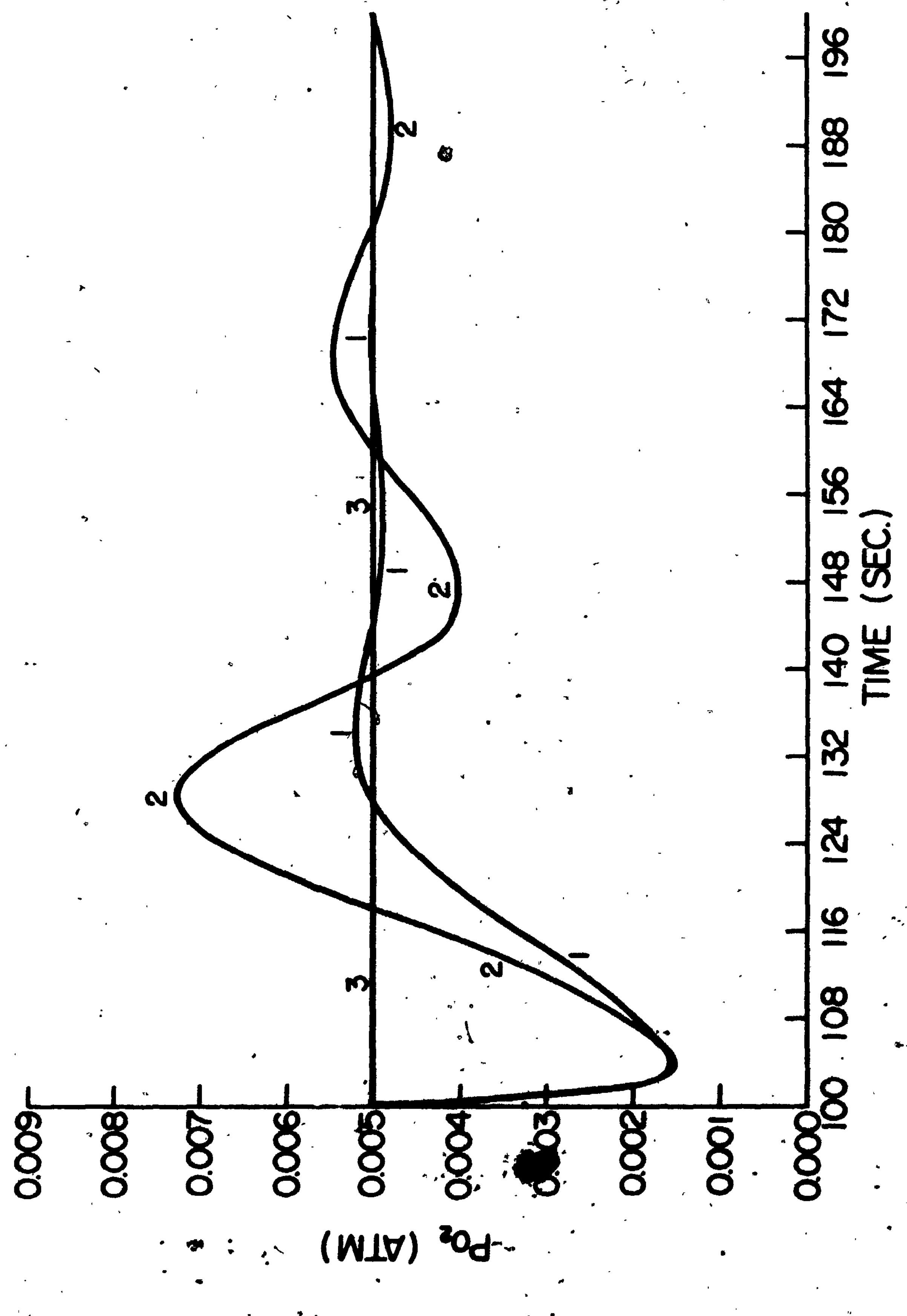

P_{O_2} (ATM)
0.009
0.008
0.007
0.006
0.005
0.004
0.003
0.002
0.001
0.000
100
108
116
124
132
140
148
156
164
172
180
188
196
TIME (SEC.)
1
2
3

FIGURE 4.7

Dynamic Responses of the Simulated Dissolved Oxygen Control System (Using a Proportional-Integral Controller) To a 40% Step Decrease in Both Mass Transfer Coefficients. Variable Values Are Listed in Tables 4.1 and 4.2

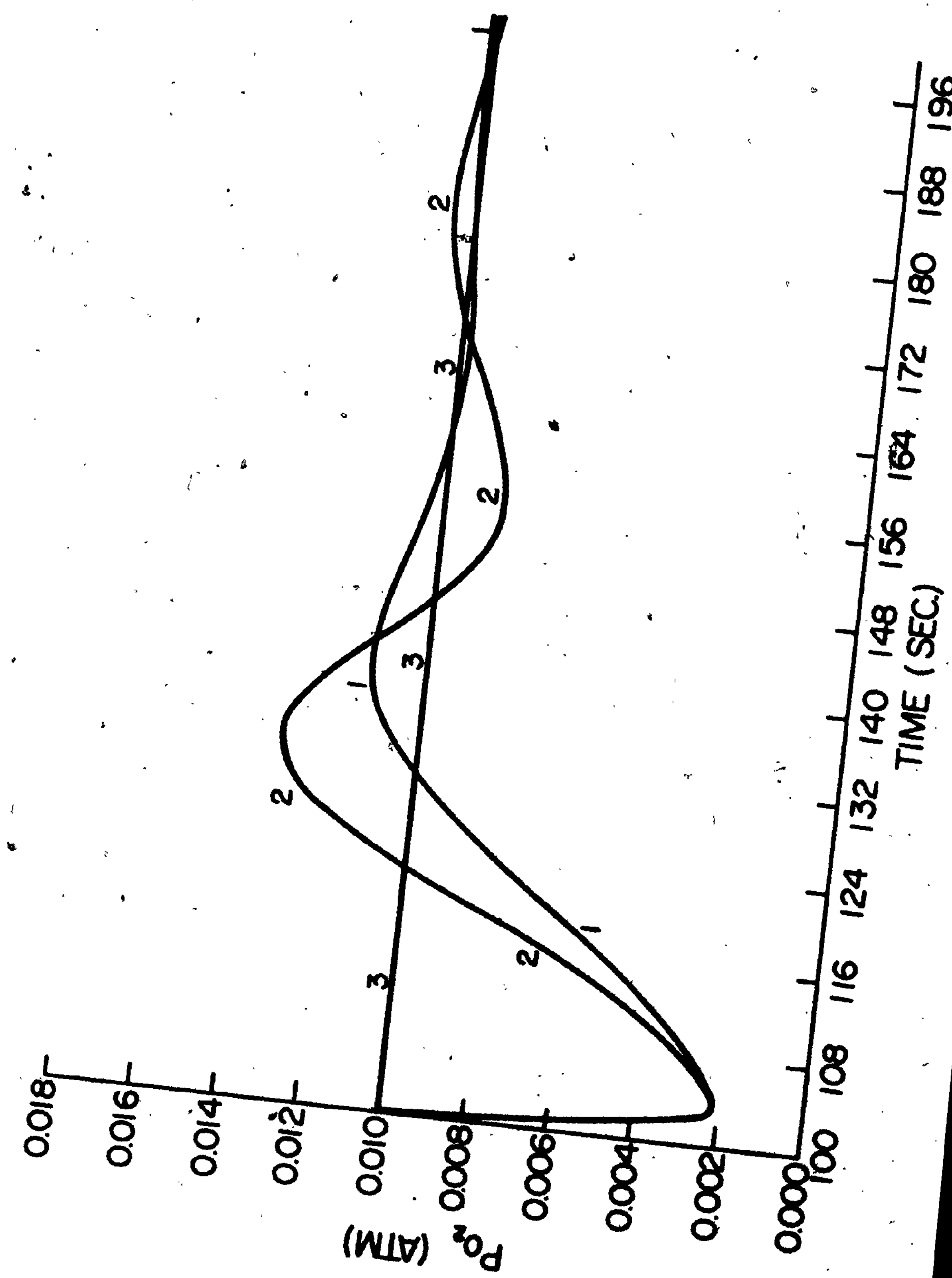
0.018
0.016
0.014
0.012
0.010
0.008
0.006
0.004
0.002
0.000
P_{O_2} (ATM)
100
108
116
124
132
140
148
156
164
172
180
188
196
TIME (SEC.)
1
2
3

FIGURE 4.8

Dynamic Responses of the Simulated Dissolved Oxygen Control System (Using a Proportional-Integral Controller) To a 40% Step Decrease in Both Mass Transfer Coefficients. Variable Values Are Listed in Tables 4.1 and 4.2

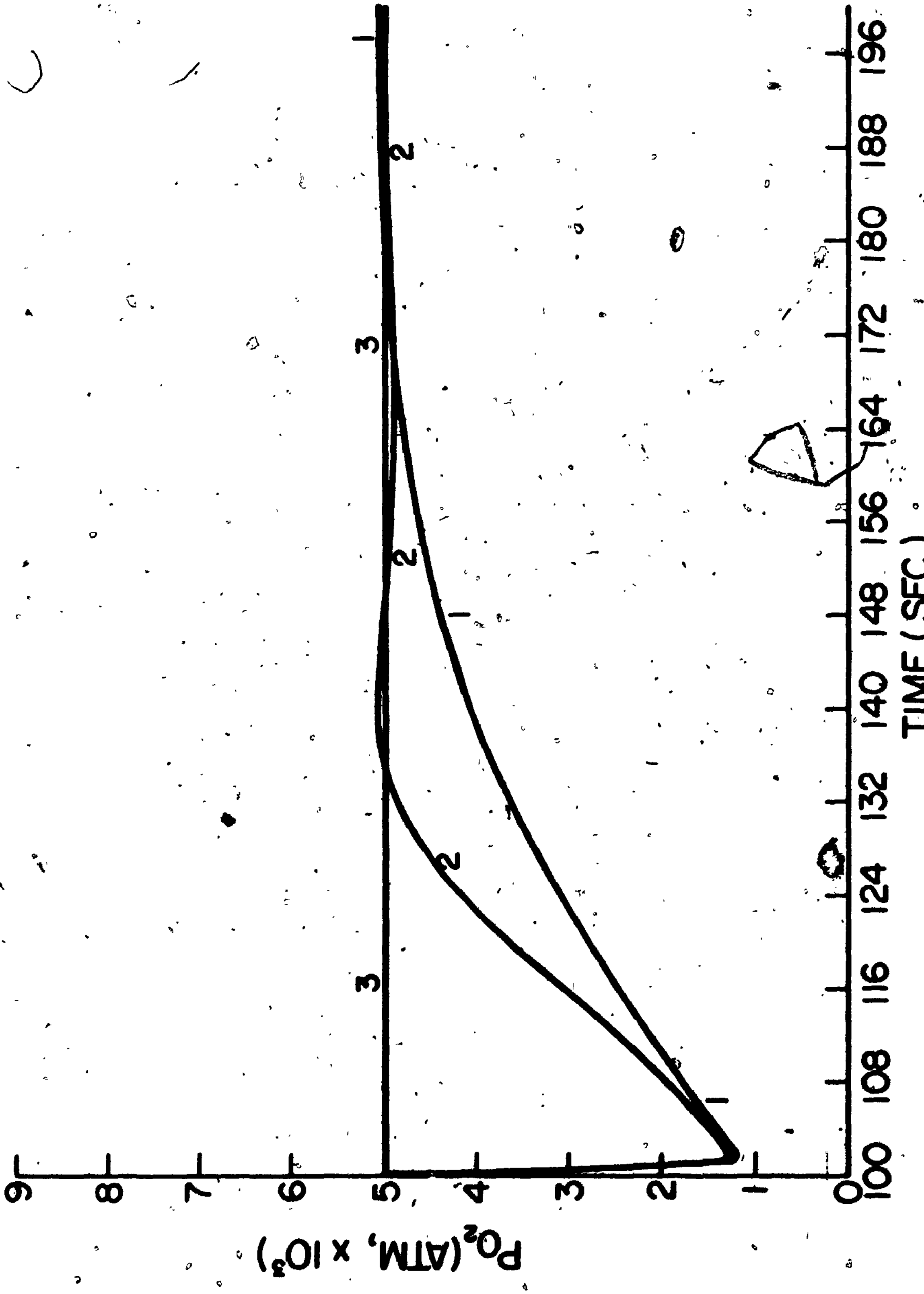

TIME (SEC.)
100 108 116 124 132 140 148 156 164 172 180 188 196
P_{O_2}(ATM, x 10^3)
0 1 2 3 4 5 6 7 8 9
1
2
3

i) Under all circumstances investigated the system having the larger head space was the more stable. The head space acted as a reservoir supplying oxygen to the liquid phase until the controller could take corrective action.

ii) The controller settings necessary to obtain a stable system having a desirable response (4:1 decay ratio) varied widely with the operating conditions such as the dissolved oxygen control set point and the maximum growth rate of the microorganisms. This may be deduced from the range of responses obtained (highly underdamped in Figure 4.5 and overdamped in Figure 4.8).

No direct experimental verification of these conclusions was obtained since the effort necessary for such a venture would have been excessive. From the simulations it was however apparent that the dissolved oxygen tension could be adequately controlled by sparging air instead of a much more costly artificial nitrogen-oxygen mixture. The dissolved oxygen control system described in Chapter 5 was designed on the basis of this conclusion. During operation of this system it was found that the controller settings had to be adjusted every time the operating conditions were changed to obtain stable operation.

From elementary considerations it is also obvious that the slower the probe response to a change in dissolved oxygen tension the lower the allowable maximum gain of the system would be and that the slower the system response the further the dissolved oxygen tension would deviate from its set point. The system is so complex due to the many operating parameters which affect it that the significance of the controller settings necessary to obtain stable operation in the real situation is difficult to evaluate. For this reason no values of the controller settings are reported in Chapter 5. One of the uncontrolled variables in the real system was for example the air supply pressure which although regulated, varied considerably with room temperature. This affected the gain of the system significantly as did the slow buildup of pressure drop across the air filtration system in the fermentor during the course of a fermentation lasting six weeks.

The most important points underscored by the simulation were the extreme sensitivity of a dissolved oxygen control system to a host of operating conditions and the importance of the head space gas phase in acting as a reservoir and stabilizing the system.

4.5 Conclusions to Chapter 4

In sections 4.1 and 4.2 two major modes of dissolved oxygen control were discussed and evaluated. It was pointed out that although under certain circumstances the control of oxygen supply might be the best control strategy available, in most cases the direct control of dissolved oxygen tension is preferable since it is the oxygen tension that determines the reaction rates in the fermentation. If oxygen supply control is used the oxygen tension should be continuously monitored, especially in processes where the culture oxygen demand is not very dependent on the oxygen tension but the production of metabolites is.

In sections 4.3 and 4.4 a dissolved oxygen tension control system was modelled and its dynamic response to a sudden addition of a surface-active material was investigated. It was found that the maximum organism growth rate and the dissolved oxygen tension set point very strongly influenced the system response. In all cases investigated the head-space filled with exhaust gas stabilized the system at the given controller settings.

CHAPTER 5

RESPIRATORY SYSTEM CHARACTERISTICS OF *CANDIDA LIPOLYTICA*

5.1 Introduction

The effect of oxygen on the behavior of yeast has been studied extensively. Most of the studies have been performed with yeasts which grow under both aerobic and anaerobic conditions. The interpretation of the results from such investigations has been complicated by the yeasts exhibiting the Pasteur effect. Studies performed on *Candida lipolytica* indicate that it cannot grow in an anaerobic environment [40].

In Chapter 5 the determination of the characteristics of the respiratory system of *C. lipolytica* is described and the results presented. Glucose was used as the substrate for growth although *C. lipolytica* is better known for its ability to utilize n-paraffins. All results were obtained after the organism was adapted to the growth conditions specified.

The literature review presented in sections 5.2 and 5.3 emphasizes only the most important works in the area since two very extensive reviews have recently been published by Wimpenny [70, 1969] and Harrison and Stouthamer [31, 1973].

5.2 Influence of Oxygen on Microbial Growth and Product Formation

It has long been recognized that oxygen has a profound influence on the growth and product formation by aerobic microorganisms. Examples illustrating the wide variety of effects that oxygen may have on microorganisms are discussed below.

Smith and Johnson [61] studied the aeration requirements of *Serratia marcescens* in batch culture and found that the final cell yield from glucose and citric acid increased with the aeration efficiency and levelled off at high efficiency. When 4% glucose (w/v) and 2% citric acid (w/v) was used as substrate the cell concentration varied from 9 gm/l at an effective aeration rate of 0.5 mM O_2/l/min to 23 gm/l at an aeration rate of 9 mM O_2/l/min. The live cell counts corresponding to these dry weights were 6.5×10^9 cells/ml and 1.7×10^{11} cells/ml. The aeration rates were obtained by the sulfite-oxidation method. The highest yield based on substrate utilized was 45% when the cell concentration on a dry weight basis was 29 gm/l and the live cell count 20×10^{11} cells/ml.

Pirt [54] has investigated the utilization of substrate-glucose by *Aerobacter cloacae*. When *Aerobacter cloacae* was grown anaerobically in continuous culture at a dilution rate of 0.3 hr^{-1} and a glucose feed concentration of 10.6 gm/l, the glucose carbon was divided as follows: 24% to butanediol, 21% to ethanol, 15% to carbon dioxide, 12% to formic acid, 9% to cell carbon, 7% to acetic acid and 3% to acetoin. Anaerobic metabolism was found to be largely independent of the dilution rate unless the growth rate was sufficiently close to the maximum value to cause glucose utilization to be appreciably incomplete.

When growth was fully aerobic at an oxygen absorption coefficient of 3.8 mM O_2/l/min, as measured by the sulfite oxidation method, 45% of the glucose carbon was diverted to cell carbon and 40% to carbon dioxide production. Only 3% of the glucose carbon was incorporated into volatile acids. At oxygen absorption coefficients of 1.4 and 0.4 mM O_2/l/min and a dilution rate of 0.3 hr^{-1}, the metabolic products were not significantly different from those obtained at an oxygen absorption coefficient of 3.8 mM O_2/l/min. The yield of metabolic products was however affected at higher dilution rates at these rates of oxygen supply.

Under anaerobic conditions the maximum percentage of glucose carbon incorporated as cell carbon was 9% at a dilution rate of 0.25 hr^{-1}. Under fully aerobic conditions this maximum was 55% at a dilution rate of 0.6 hr^{-1}.

At an oxygen absorption coefficient of 0 mM O_2/l/min, large quantities of volatile acids were produced at all dilution rates. When the oxygen absorption coefficient was 0.4 mM O_2/l/min, acetic acid was produced at dilution rates greater than 0.2 hr^{-1} and acetoin and butanediol production started at a dilution rate of 0.3 hr^{-1}. When the oxygen absorption coefficient was 1.4 mM O_2/l/min, acetic acid production did not start until the dilution rate was 0.45 hr^{-1}. At an oxygen absorption coefficient of 3.8 mM O_2/l/min acetic acid production started at a dilution rate of 0.6 hr^{-1}; formic acid and ethanol were only produced under anaerobic conditions.

A small oxygen deficiency led to acetic acid formation, a larger one caused butanediol and acetoin formation and a complete lack of oxygen caused formic acid and ethanol to be produced while the formation of acetic acid decreased.

The production of α-amylase and protease by *Bacillus amylosolvens* in batch culture has been investigated by Terui and Konno [67]. The batch cycle was divided into a proliferating phase (P-phase) and a hydrolase-producing phase (H-phase). It was found that in order to maximize enzyme production, the oxygen concentration during the P-phase should be at least 0.2 mM O_2/l to induce the formation of the hydrolase producing system to the greatest possible extent, but that during the H-phase an oxygen concentration of 0.02 mM O_2/l was sufficient for the formation of hydrolase.

The growth medium was starch, liquified by means of a bacterial α-amylase. After 30 hours the amylase and protease concentrations were as follows:

Oxygen Concentration $mM\ O_2/l$	amylase activity (arbitrary units)	protease activity (arbitrary units)
0.5	4000	2500
0.2	3700	2400
0.05	2400	1500
0.02	400	300

The formation of amylase and protease during the P-phase was hardly affected by the oxygen concentration during this phase; when the oxygen concentration was lowered from 0.2 to 0.02 $mM\ O_2/l$ after approximately 20 hrs, the subsequent hydrolase production was approximately 15% lower than when the oxygen concentration was kept constant at 0.2 $mM\ O_2/l$.

Ecker and Lockhart [20] compared the sequences of physiological events in batch culture of *E. coli* (strain K12) at the time of growth cessation caused by the limited availability of either the carbon source, the nitrogen source or oxygen. Glucose was used as the carbon source and ammonium sulfate as the nitrogen source. When glucose became growth limiting, growth ceased together with nitrogen utilization. When the nitrogen source became limiting, growth stopped but the glucose utilization continued and the pH of the culture decreased. When the availability of oxygen decreased to 6 to 8 x 10^{-12} $mM\ O_2$/cell/hr (as determined by the sulfite oxidation method), growth and nitrogen utilization stopped but glucose consumption continued and acid formation was observed.

The above was interpreted as an indication that oxygen had a no less profound effect on the metabolism of *E. coli* than either the nitrogen source or the carbon substrate.

Harrison and Pirt [29,30] have described the influence of dissolved oxygen tension on the metabolism and respiration of *Klebsiella aerogenes*. *K. aerogenes* was grown in continuous culture using glucose as the energy substrate and ammonium as the source of nitrogen. The dissolved oxygen tension was controlled by means of varying the oxygen content of the sparging gas, thus allowing the culture dissolved oxygen tension to find its own level as dictated by the culture oxygen demand. Three states of the culture were described.

At a dissolved oxygen tension greater than 15 mm Hg (the 'excess oxygen state') the respiration rate was independent of the dissolved oxygen tension.

When the dissolved oxygen tension was brought below 15 mm Hg, complex oscillations in the dissolved oxygen tension occurred, although the aeration conditions were kept constant. This was called the 'transition state'. The oscillations reflected an alternate inhibition and stimulation of the respiration rate. A decrease in the dissolved oxygen tension to below 5 mm Hg increased the respiration rate; an increase in the dissolved oxygen tension from 5 to 10 mm Hg decreased the respiration rate. The oscillations were observed under conditions of glucose-limited and nitrogen-limited growth and over the pH range 6.0 to 7.4. The pattern of oscillations was influenced by the growth rate. Oscillations could be observed at dilution rates between 0.2 and 0.5 hr^{-1} but not at 0.1 hr^{-1}. The range of the fluctuations also depended on the history of the culture. The authors ascribed the variations in oxygen uptake rates causing the oscillations in dissolved oxygen tension to the uncoupling of oxidative phosphorylation at a dissolved oxygen tension of approximately 5 mm Hg.

The third state was the "limited oxygen state". In this state the oxygen tension stabilized at a value below 5 mm Hg.

In the excess oxygen state when the growth was limited by the ammonium supply, 95% of the glucose carbon could be accounted for as carbon dioxide, pyruvate and cell mass. Some ethanol and 2,3-butanediol was also produced. Pyruvate was not accumulated when growth was glucose-limited. In the limited oxygen state, acetic acid, formic acid and lactic acid accumulated as well as ethanol and 2,3-butanediol. The proportions of the glucose carbon incorporated into the volatile compounds varied with the conditions of growth and whether the growth was glucose or ammonium-limited.

The filamentous fungus *Aspergillus nidulans* was found by Carter and Bull [14] to exhibit an increased activity of the hexose monophosphate (HMP) pathway under certain conditions. When *A. nidulans* was grown in continuous culture at a dilution rate of 0.5 hr^{-1}, the activity of the HMP pathway was found to be 2.2 times as great at a dissolved oxygen tension of 2 mm Hg as it was at 160 mm Hg. The HMP pathway activity was inferred from the levels of glucose-6-phosphate dehydrogenase present. At a dissolved oxygen tension of 2 mm Hg, 54% of the substrate-glucose was metabolized via the HMP pathway vs 25% at a dissolved oxygen tension of 160 mm Hg.

Feren and Squires [23] have described the effect of various dissolved oxygen tensions on the production of Capreomycin and Cephalosporin C. The organisms used or the conditions of growth were not specified other than that the batch culture technique was used.

Capreomycin synthesis was at a maximum when the dissolved oxygen tension was maintained at 10% of saturation with air. At 0% saturation a lag of 30 hours in the start of antibiotic synthesis was observed and the titer at harvest was only 60% of the control.

During the Cephalosporin C fermentations only 55% of the control titer was obtained when the dissolved oxygen was 10% of saturation with air and the control was run at 45% saturation.

For both the Capreomycin and Cephalosporin fermentations the critical oxygen tensions for respiration and for antibiotic production were different.

Nagai and Aiba [49] found that the growth yield of *Azotobacter vinelandii* was inversely related to the dissolved oxygen tension in continuous culture under both glucose and oxygen-limited conditions. The cell yield of *A. vinelandii* increased to 0.24 gm cells/gm glucose at very low dissolved oxygen tension (approximately 0.02 ppm) from 0.035 gm cells/gm glucose at 4 ppm oxygen. The rate of carbon dioxide evolution increased from 0.02 mole CO_2/gm cells/hr at very low dissolved oxygen tension to 0.11 mole CO_2/gm cells/hr at an oxygen tension equivalent to 4 ppm. This phenomenon was related to the inductive increase in aldolase which accompanied an increase in dissolved oxygen tension.

Babij *et al.* [7] have investigated the effects of glucose and oxygen concentration on the lipid composition of *Candida utilis* grown in a turbidostat.

When the glucose level was kept constant at 0.001%, the lipid composition was very little affected by changes of dissolved oxygen concentration in the range 0 to 0.235 mM O_2/l. The three most abundant fatty acids were linoleic, oleic and palmitic acid. These fatty acids comprised approximately 46%, 37% and 10% respectively of the total fatty acids present.

At high glucose concentrations (1-6%) the most significant changes occurred in the oleic and linolenic acid concentrations as the oxygen concentration changed. At very low dissolved oxygen concentration (smaller than 0.001 mM O_2/l) oleic acid and linolenic acid accounted for 48% and 2% respectively of the total fatty acids; at high dissolved oxygen concentration (0.16 mM O_2/l) they accounted for 22% and 23% respectively. Linoleic acid remained relatively constant at 40%. Palmitic acid accounted for 10% of the total fatty acid pool.

During an investigation of the metabolism of *Saccharomyces carlsbergensis*, Moss *et al.* [48] found that both the oxygen tension and the glucose concentration strongly influenced the division between aerobic and anaerobic metabolism.

At a glucose uptake rate between 1.2 and 2.8 mM glucose/hr/gm yeast, the division between aerobic and anaerobic metabolism was controlled by the oxygen tension. At an oxygen tension of 0.21 atm, metabolism was 98% aerobic; at an oxygen tension of 0.01 atm it was 80% anaerobic, having ethanol as a major end product. When the glucose uptake rate was between 7.6 and 18.2 mM glucose/hr/gm yeast, the metabolism was mainly anaerobic, even at an oxygen tension of 0.21 atm.

The oxygen uptake was variable and fluctuated between 0 and approximately 4 mM O_2/hr/gm yeast when the oxygen tension was 1.8×10^{-3} atm in cultures containing low glucose concentrations or when the oxygen tension was below 4.0×10^{-2} atm in cultures containing high glucose concentrations. The change between aerobic and anaerobic metabolism was spontaneous.

The same authors also investigated the behavior of *Candida utilis* as affected by the oxygen tension and glucose concentration [47].

At a low glucose concentration the oxygen consumption rate of *C. utilis* remained steady at approximately 7 mM O_2/hr/gm yeast independently of the dissolved oxygen tension for values of the latter between 1.3×10^{-4} atm to 4.5×10^{-2} atm. The oxygen consumption rate increased however to 13 mM O_2/hr/gm yeast when the oxygen tension was increased to 0.21 atm.

In the presence of a high glucose concentration, the oxygen consumption rate increased from 1.2 mM O_2/hr/gm yeast at a dissolved oxygen tension of 1.3×10^{-4} atm to 25 mM O_2/hr/gm yeast at a dissolved oxygen tension of 0.21 atm. The terms 'high' and 'low' glucose concentration were not defined.

The cell yield in a low glucose concentration diminished from 0.7 gm cells/gm glucose at a dissolved oxygen tension of 0.21 atm to 0.24 gm cells/gm glucose under anaerobic conditions. At a high glucose concentration the cell yield was not significantly influenced by the oxygen tension and remained almost constant at 0.40 gm cells/gm glucose.

When *C. utilis* was grown under glucose-limiting conditions, ethanol was produced only at very low oxygen tensions (below 1.3×10^{-4} atm) whereas at high glucose concentrations, ethanol was produced at all oxygen tensions.

5.3 The Respiratory System of Microorganisms

The study of microbial respiration has compelled successive generations of researchers to build increasingly complex models of the respiratory system to explain their observations. In this section the work of the major contributors is reviewed in chronological order. For recent, excellent reviews of the area the reader is referred to the publications by Wimpenny [70] and Harrison and Stouthamer [31].

Winzler [71, 1941] studied the effects of temperature, substrate concentration and carbon monoxide on the relationship between the dissolved oxygen tension and the respiration rate of *Saccharomyces cerevisiae*. By use of a dropping mercury polarograph values of K_m were obtained under a wide variety of conditions. Below are presented some of the K_m values and maximum respiration rates of *S. cerevisiae* when the glucose concentration in the suspending medium was 0.1M:

Temperature (°C)	Maximum respiration rate (mm^3/hr/mg dry wt)	K_m (mm Hg)
34.3	86	1.26
26.8	66	0.89
23.4	43	0.47
15.8	20	0.29
9.5	9	0.14
5.0	5	0.07

A plot of the maximum respiration rate vs the inverse of the absolute temperature yielded a straight line. The activation energy for the respiration process was found to be 17.25 Kcal/mole.

The influence of the substrate concentration on the value of K_m was also investigated. At 20°C the values of K_m obtained were 2.5 mm Hg and 0.2 mm Hg when the glucose concentration of the suspending medium was 0.1M and 0.0M respectively.

Winzler [71] postulated that the factor limiting the rate of oxygen consumption was the degree of unsaturation of the 'oxygen activating enzyme' and not the resistance to diffusion through the cell material. Under conditions of low glucose concentration the oxygen requirement would be lower than when the glucose concentration was high, since in the former case the cell's metabolism would be slower. At the lower glucose concentration the degree of unsaturation of the oxygen activating enzyme necessary for the oxygen consumption rate not to be affected by the oxygen tension would therefore also be lower than at a higher glucose concentration.

To substantiate that it was the unsaturation of the oxygen terminal enzyme and not diffusion that limited the oxygen consumption rate at low oxygen tension an ingenious experiment was devised, utilizing the competitive inhibition of the oxygen terminal enzyme by carbon monoxide. The carbon monoxide thus displaced oxygen, thereby lowering the degree of saturation of the oxygen activating enzyme at equivalent oxygen tensions. The oxygen tension at which the respiration rate decreased was therefore much higher than when no carbon monoxide was present. At these higher oxygen tensions the diffusional resistance to oxygen through the cell material could not be rate-limiting. When the inhibition by carbon monoxide was taken into account, the respiration rate-oxygen tension curves obtained at carbon monoxide tensions of 0, 0.04, 0.10 and 0.16 atm were all identical (at 20°C and 0.1 M glucose in the suspending medium). Identical curves were also obtained under conditions of carbon monoxide inhibition and no inhibition regardless whether the glucose concentration was 0.0 or 0.1 M glucose.

Winzler [71] concluded therefore that it was the unsaturation of the oxygen activating enzyme that caused a decrease in the respiration rate as the oxygen tension dropped below the critical oxygen tension.

Moss [46, 1952] investigated the influence of oxygen tension on the respiration rate and the cytochrome formation by *E. coli*. The oxygen consumption of *E. coli* was measured after the culture had been grown anaerobically and was then subjected to various oxygen tensions. The organism was grown in continuous culture. The respiration rates are recorded below. The units used were not communicated by the author.

Oxygen Tension (atm)	Oxygen Consumption After Hours of Aeration 0	1½	3	4½
0.90-0.95	670	960	1090	950
0.75-0.87	540	890	1000	940
0.42-0.45	640	-	970	980
0.1-0.3	520	830	910	1020
Anaerobic	650	650	680	-

The final respiration rates obtained were not significantly affected by the oxygen tension but the higher oxygen tensions stimulated an increase in respiration faster than did the lower ones.

The amount of cytochrome a_2 present in the cells was also measured. The cytochrome a_2 content of the cells grown at an oxygen tension of 0.1 atm after 4½ hours of aeration was twice that of the cells grown at 0.75 atm oxygen tension. Cytochrome development was however faster at the higher oxygen tension; after 1½ hours of aeration the cytochrome content of cells grown at 0.75 atm O_2 was 1.6 times that of the cells grown at 0.1 atm O_2. The phenomena described above were much more thoroughly investigated by Terui and Konno [65, 66, 67] and will be described in more detail later in this section.

Longmuir [41, 1954] obtained K_m values for a variety of microorganisms. The bacteria and yeast were suspended in a solution of 1% glucose, 0.05 M KCl and 0.05 M phosphate buffer at a pH of 7.3; for the heart-muscle preparation a 0.004 M succinate solution and no glucose was used. The K_m

values are listed in Table 5.1 together with those obtained by other authors. The K_m values were related to the cell diameter in the following manner:

$$K_m = G\, d^h \tag{5.1}$$

where $G = 9.0 \times 10^{-8}$ mole O_2/l/micron, d is the cell diameter in microns, $h = 2.6032$ and K_m is expressed in mole O_2/l. Baker's yeast did not fit this relationship.

The author ascribed the increase in K_m observed with increasing cell size to the increased diffusional resistance of the cell material. K_m values for several cell-free preparations were also found. These were approximately the same for the various organisms and not very much smaller than that obtained for the smallest organism, *Aerobacter aerogenes*. Some of the K_m values are shown below:

Organism	diameter (microns)	K_m (mole/l x 10^6)	
		whole cells	cell-free preparation
Aerobacter aerogenes	0.6	4.01×10^{-2}	3.83×10^{-2}
Bacillus megatherium	2.0	7.13×10^{-1}	2.87×10^{-2}
Bacillus megatherium (grown on glycine)	4.0	1.34	3.68×10^{-2}

TABLE 5.1

Some K_m Values For Microorganisms

Author	Organism	K_m (μmole O_2/l)
Winzler [71]	*S. cerevisiae**	8.0×10^{-1}
Longmuir [41]	*Aerobacter aerogenes*	3.1×10^{-2}
	Micrococcus candidans	1.1×10^{-2}
	Bacillus megatherium	6.0×10^{-1}
	Azotobacter indicum	3.0×10^{-1}
	Acetobacter suboxydans	1.6
	Serratia marcescens	3.6×10^{-2}
	Escherichia coli	2.2×10^{-2}
	Baker's yeast	6.4×10^{-1}
	Pig-heart preparation	1.9×10^{-2}
	Ox-heart preparation	2.4×10^{-2}
Chance [15]	Heart-muscle preparation	1.0
Terui *et al.* [65]	*S. cerevisiae*	1.0
Terui and Konno [66]	*Aspergillus oryzae*	2.0
Terui and Konno [67]	*Bacillus amylosolvens*	3.5×10^{-1}
Johnson [37]	*Candida utilis*	1.3

* recalculated from original data

The K_m values obtained by Longmuir [41] were considerably smaller than those obtained by other authors. Chance [15] has severely criticized his work and claimed that the extremely low K_m values were due to inactivation of the cells prior to or during the experiments.

Chance [15, 1957] attempted to provide a biochemical basis for the observed relationship between the respiration rate and the oxygen tension in a manner similar to Winzler's [71]. The model used was however more complex than the latter's. Chance [15] considered respiration as the consequence of the integrated action of a series of enzymes instead of as the result of the reaction between oxygen and the terminal oxidase which was considered to be cytochrome a_3. The author described how the sequence of action of the various components of the respiratory chain could be determined by measuring the relative speeds with which the absorption bands of the reduced compounds present during anaerobiosis would disappear upon rapidly adding oxygen.

By use of the spectrophotometric determination of reduced cytochrome a_3 and succinate and the polarographic measurement of dissolved oxygen, the effect of the addition of succinate on the level of cytochrome a_3 reduction and oxygen consumption of heart-muscle preparation was investigated. Initially no succinate was present, the oxygen concentration was 0.240 mM O_2/l and the cytochrome a_3 was totally oxidized as measured at 4450-4600 Å. When 12 mM/l succinate was added, the oxidation level of cytochrome a_3 fell rapidly to 80% and remained almost steady at that value while oxygen and succinate utilization and fumarate production proceeded at a constant rate. Just before the oxygen was exhausted the oxidation level of the cytochrome dropped and decreased to a very low level upon complete depletion of the oxygen supply. Above the critical oxygen tension the degree of reduction of the terminal oxidase was largely independent of the oxygen concentration and depended on the substrate supply. As long as the oxygen concentration was above 4 micromole O_2/l the rate of fumarate production was constant. The half-maximal fumarate production rate occurred at an oxygen concentration of 1 micromole O_2/l. An appreciable reduction of cytochrome a_3 beyond the steady-state level occurred however above the 4 micromole O_2/l level; the oxidase was 50% reduced at 2 micromole O_2/l whereas one-half the maximum respiration occurred at 1 micromole O_2/l. This phenomenon meant that there was an overabundance of terminal oxidase. The respiration rate depended on the concentration of oxidized terminal oxidase and not on the ratio of oxidized to reduced oxidase.

Chance [15] incorporated this concept of the respiratory system into a mathematical model representing a chain of four reactions by means of nonlinear differential equations. In this model, after the oxygen tension was suddenly increased at the beginning of a calculation, the terminal oxidase level of oxidation decreased first and before any perceivable change in the respiration rate occurred. The enzyme at the substrate end of the chain maintained an almost constant, fairly low level of oxidation until the oxygen tension had decreased to a very low level. It then became very abruptly totally reduced.

With a similar model consisting of three components the effect of the substrate concentration on K_m was studied. As the substrate concentration decreased, the K_m also decreased since a lower concentration of oxidized terminal oxidase was required to maintain the steady-state respiration rate.

Terui *et al.* [65, 1960] divided the effect of oxygen tension on microorganisms into two parts:

- the influence of the oxygen concentration during growth on cell composition
- the action of the oxygen concentration on the metabolism of existing cells.

Starting with 48-hour old cultures of anaerobically-grown *Saccharomyces cerevisiae* (30°C), the adaptive increase in respiratory activity at various levels of oxygen concentration was measured. Some of the values obtained for the respiration rate and the K_m of *S. cerevisiae* after 12 hours of growth at various oxygen concentrations are given below:

Oxygen Concentration mM O_2/l	Respiration Rate μl O_2/mg yeast/hr	K_m O_2/l x 10^3
0.01	17	0.71
0.02	30	1.30
0.05	57	2.41
0.20	67	3.03
0.50	69	3.43

It is not clear whether the adaptation took place under continuous or a batch cultivation condition. The specific rate of increase in respiratory activity S_r, as defined in Equation 5.2, was found to follow Michaelis-Menten kinetics with respect to oxygen.

$$S_r = \frac{1}{m} \frac{dZ}{dt} \qquad (5.2)$$

where S_r = the specific rate of oxygen adaptation

m = cell weight/unit volume

Z = respiratory activity/unit volume

The oxygen concentration required to produce one-half the maximum rate of adaptation was approximately 4.2×10^{-5} M O_2. The critical oxygen concentration for oxygen adaptation was between 2 and 5×10^{-4} M O_2.

During adaptation to 0.20mM O_2 the cytochrome *c* content of *S. cerevisiae* was found to increase parallel to the respiration rate. After 12 hours the cytochrome *c* content had risen from nil under anaerobic conditions to 59 μg/gm yeast (dry wt). The FAD content also rose sharply during the initial adaptation phase. It reached 14 μg/gm yeast after 5½ hours, but had decreased slightly to 9 μg/gm yeast after 12 hours.

It was also observed that the K_m of the cells adapted to a higher oxygen concentration was larger than of those adapted to a lower oxygen concentration.

Terui and Konno [66] also investigated the oxygen adaptation of *Aspergillus oryzae*. After inoculation at a density of 1 mg spores/ml, the respiration rate of *A. oryzae* was observed during batch culture. Starting with an initial glucose concentration of 3%, the following respiration rates were observed after 8 hours:

Oxygen Concentration During Growth (mM O_2/l)	Respiratory Activity (μl O_2/mg/hr)
0.01	20
0.02	31
0.05	42
0.20	55
0.50	70

For normal spore germination an oxygen concentration greater than 0.05 mM O_2/l was required. The specific rate of adaptation of the respiration rate with respect to oxygen exhibited Michaelis-Menten kinetics; the half-rate constant was 8×10^{-5} M O_2.

As the oxygen adaptation proceeded, the K_m was increased; the higher the oxygen concentration maintained in the culture, the more quickly the value of K_m increased.

Some data are presented below:

Oxygen Concentration During Growth ($mM\ O_2/l$)	K_m (mole $O_2/l \times 10^6$) after:		
	4 hours	6 hours	8 hours
0.011	1.93	1.95	2.00
0.023	1.91	2.05	2.16
0.050	2.02	5.27	5.64
0.234	2.18	5.42	5.80
0.568	3.16	5.55	5.87

The above data were obtained when the *A. oryzae* spores were germinated in submerged culture and consumed oxygen dissolved in the growth medium. When the spores were however incubated and germinated in a surface culture and respired gaseous oxygen, a second, cytochrome-independent respiration pathway was observed. This second pathway was insensitive to azide inhibition. The authors proposed that a flavin compound was the terminal oxygen enzyme of the second respiration pathway.

Part of the study by Terui and Konno [67, 1961] on the effect of oxygen on the hydrolase-producing capacity of *Bacillus amylosolvens* is described in section 5.2. When *B. amylosolvens* was grown in batch culture at 30°C on a hydrolyzed-starch medium two growth phases were observed: the proliferating phase (P-cells) and the hydrolase-producing phase (H-cells). The P-cells exhibited a K_m of 3.5×10^{-7} M O_2; the H-cells had two K_m values, being 5.8×10^{-7} and 3.0×10^{-4} M O_2 respectively. The oxygen concentration maintained during these experiments was not reported. The authors interpreted their observations as an indication of the existence of two independent respiratory systems in the H-cells. The oxygen terminal enzyme exhibiting the lower K_m was azide-sensitive; the other was not. The respiration of P-cells was 90% inhibited by 0.002 M azide; the respiration of H-cells was only inhibited 40% at this azide concentration. The cytochrome and flavin contents of P-cells and H-cells are compared below. Concentrations are expressed in μg/gm dry wt.:

	P-cells (7 hr culture)	H-cells (20 hr culture)
cytochrome oxidase	210	82
FAD	53	71
cytochrome *c*	190	130

The larger K_m observed, presumably due to the flavin terminal oxidase, was very close in value to the Michaelis-Menten constants observed for other flavin enzymes.

The specific rate of oxygen concentration adaptation of *B. amylosolvens* was related to the oxygen concentration maintained during growth in a Michaelis-Menten manner. The half-rate constant was 7×10^{-5} M O_2. The maximum respiration rates attained by the P-cells are presented below. The units of the respiration rate were not presented.

Oxygen Concentration During Growth (mM O_2/l)	Respiration Rate
0.02	189
0.05	289
0.20	397
0.50	419

The authors described the half-rate constant of the specific oxygen adaptation rate as the dissociation constant of a complex which controls the rate of oxygen adaptation. This complex was thought to dissociate reversibly into dissolved oxygen and an unknown intracellular entity.

Upon investigating the relationship between the oxygen tension and the respiration rate of *Bacillus megatherium*, Herbert [32, 1965] obtained the following results:

- When the organism was grown under high dissolved oxygen tension, cytochromes a_1 and a_2 were undetectable but cytochrome b_1 was detectable.

- At low dissolved oxygen tension both the a-cytochromes appeared and the cytochrome b_1 concentration remained constant.

- At very low dissolved oxygen tension all cytochromes decreased to concentrations found in anaerobically-grown cells.

No numerical data were reported by the author.

Johnson [37, 1967] grew *Candida utilis* in continuous culture on acetate medium (30°C) using oxygen as the limiting nutrient. A hyperbolic relationship of the Michaelis-Menten type was obtained between the growth rate and the oxygen concentration. The maximum growth rate was 0.44 hr^{-1} and the half-rate constant was 1.34 x 10^{-6} M O_2. Some data from this study are presented below:

Oxygen Concentration During Growth (mole O_2/l x 10^6)	Growth Rate (hr^{-1})	Maximum Respiration Rate (μM O_2/l/min)	K_m (mole O_2/l x 10^6)
0.62	0.105	0.59	0.46
0.97	0.190	0.91	0.67
2.84	0.293	1.12	0.80

The substrate levels present at the various oxygen concentrations were however not reported. The K_m values reported are therefore of doubtful significance. From the shape of the curves obtained during the measurement of K_m, the author deduced that the decrease in respiration rate, observed when the oxygen tension was allowed to fall as a result of metabolism, was caused by diffusional resistance through the cell material. Harrison and Stouthamer [31] and Terui and Sugimoto [64] have however sharply criticized Johnson's [37] reasoning. The latter [64] showed that the behavior observed by Johnson [37] could also be observed for *Saccharomyces cerevisiae* and *Hansenula anomala* but that such behavior was due to a combination of substrate and oxygen limitation. The behavior reverted to normal Michaelis-Menten type behavior when the substrate limitation was eliminated by decreasing respiratory pathway activity with Antimycin *A*.

Johnson [37] also compared the maximum rates at which *C. utilis* was capable of consuming oxygen when grown at different oxygen concentrations. Cells grown at higher oxygen concentrations could use oxygen at a more rapid rate in the presence of excess oxygen than when grown at lower oxygen concentrations:

Oxygen Concentration During Growth (mole O_2/l x 10^6)	Oxygen Uptake Rate During Growth (μ mole O_2/l/min)	Maximum Oxygen Uptake Rate (μ mole O_2/l/min)
0.234	0.195	0.312
0.62	0.399	0.594
0.97	0.721	0.912
1.29	0.788	0.942
2.84	1.11	1.12

Cells grown at a low oxygen concentration were able to (immediately, without adaptation) use oxygen more rapidly than the rate at which it was used during growth. During the above determinations the author again failed to consider the differing substrate concentrations of the cultures which had been grown at different oxygen concentrations and therefore at different growth rates. The conclusions made are therefore questionable.

Moss and Rickard *et al.* [47, 48, 56, 57, 1969-71] have extensively investigated the effects of oxygen and glucose concentration on yeast growth in both batch and continuous culture. A massive amount of data but little interpretation was presented; the significance of their work is difficult to judge since in many instances it is not clear how the experiments were performed and under what conditions the measurements were made.

Saccharomyces cerevisiae and *Saccharomyces carlsbergensis* [56] were grown in batch culture under various conditions of aeration and initial glucose concentration. For *S. cerevisiae* the *a*, *b* and *c*-type cytochrome content was maximal when the initial glucose and oxygen concentrations were both low. *S. carlsbergensis* had a maximum cytochrome content after the initial glucose concentration had been low but the oxygen concentration had been high. The cytochrome content of *Candida utilis* [57] was decreased regardless of the oxygen concentration, when the initial glucose concentration was increased. The *a*-type cytochromes were more affected than either the *b*-type or *c*-type. The authors failed to measure either the oxygen concentration in the medium or the respiration rate of the organisms. The differences between the final pH values of the cultures with low and high initial glucose concentrations were also not taken into account.

During the continuous culture of *C. utilis* by Moss *et al.* [47], the yeast was grown both in a chemostat and a turbidostat to obtain conditions of 'high' and 'low' glucose concentration. However, the glucose concentration varied considerably as the dissolved oxygen was controlled at certain steady-state levels. It is therefore difficult to determine whether the observed fluctuations in cytochrome content were due to the changes in oxygen tension or the glucose concentration. The 'low' glucose concentration was not known. In addition, comparison between the data from the chemostat and the turbidostat is difficult since during the former the growth rate was controlled at 0.1 hr^{-1} while during the latter the growth rate adjusted itself as controlled by the turbidity. For the above reasons no more than a qualitative description of the work is presented here. There was an inverse relationship between the dissolved oxygen tension and the cytochrome content and between the glucose concentration and the cytochrome content. A step change from high to low dissolved oxygen tension indicated that there was a lag of about ten hours during which there was little change in the cytochrome content of the cells. This was followed by rapid oscillatory changes in cytochrome content and a change to a more anaerobic metabolism, with ethanol as the end product.

The cytochrome content of *Saccharomyces carlsbergensis* as a function of glucose concentration and oxygen tension was also investigated by Moss *et al.* [48] in a manner similar to that described above. The problems encountered in evaluating the significance of the data collected were also similar. Cytochrome aa_3 varied directly with oxygen concentration in low glucose. The quantity present of this cytochrome was always lower in cells grown in high glucose than in those grown in low glucose concentration. When the glucose concentration was high, the cytochrome aa_3 content was not affected by the oxygen tension. The *b*-type cytochromes were inversely related to the glucose concentration and were not affected by the oxygen tension. The *c*-type cytochromes were depressed by a high glucose concentration and at low glucose concentrations increased as the oxygen tension decreased.

From the work of all the authors quoted above a general view of the respiratory system as it is influenced by dissolved oxygen may be constructed. The influence of oxygen can be divided into two parts:

- The effect of oxygen on the chemical composition of a microbial cell such as its cytochrome content.

- The effect of oxygen on the respiration rate of adapted cells and the degree of oxidation of the components of its respiratory system.

The specific rate of oxygen adaptation is a function of the oxygen tension; below the critical oxygen tension for adaptation, the adaptation rate is increased as the oxygen tension is increased. The total quantity of cytochromes developed in a cell increases as the oxygen tension is lowered unless anaerobic metabolism becomes predominant. The final respiration rate when adaptation is complete is a function of the oxygen tension if the latter is below the critical oxygen tension for the respiration rate. The functions relating the specific adaptation rate and the respiration rate to oxygen seem to be hyperbolic functions of the Michaelis-Menten type. The terminal oxidase is usually a cytochrome but several microorganisms have been observed having an azide-insensitive flavin terminal oxidase.

For cells adapted to a given oxygen tension, when the energy-substrate is not rate-limiting, the respiration rate is related to the oxygen tension in a hyperbolic manner, resembling the Michaelis-Menten equation. The half-rate constant in this relationship, K_m, depends on the amount of terminal oxidase present since a minimal concentration of oxidized oxidase is required to maintain the respiration rate independent of the oxygen tension. When the maximum respiration rate is controlled by the supply of energy-substrate, K_m is lowered compared to the non-limiting situation since the critical concentration of oxidized oxidase is lowered. The lower the substrate concentration, the lower the K_m. For yeasts, and probably also for other microbes, the respiration rate is not limited by the mass transfer of oxygen but by the rate of electron transfer in the respiratory chain.

5.4 The Interpretation of the Oxygen Tension Versus Time Curves

To elucidate the anticipated effect of double substrate inhibition on the oxygen tension versus time curves, Program KOK9 was written to numerically solve the implicit function resulting from the integration of the double substrate Michaelis-Menten equation. Program KOK9 is listed in Appendix 5.1. Both Deindorfer [18] and Fredrickson *et al.* [26] have presented Equation 5.3 describing the growth rate of a microorganism under conditions of double substrate inhibition:

$$\mu = \mu_{max} \frac{S_1 S_2}{(K_1 + S_1)(K_2 + S_2)} \qquad (5.3)$$

By analogy Equation 5.4 may be written for the reaction rate of the respiratory system:

$$\frac{dP_{O_2}}{dt} = \left(\frac{dP_{O_2}}{dt}\right)_{max} \frac{S_1 P_{O_2}}{(K_1 + S_1)(K_m + P_{O_2})} \qquad (5.4)$$

In Equation 5.4, S_1 represents the glucose concentration in the medium in which *Candida lipolytica* was suspended during the respiration-rate experiments. K_1 represents the Michaelis-Menten constant of the most reduced end of the metabolic chain with respect to glucose; K_m is the Michaelis-Menten constant of the least-reduced end of the respiratory chain with respect to oxygen. The parameters K_1 and K_m are not the same as the Michaelis-Menten constants exhibited by the organism with respect to glucose and oxygen for the regulation of its growth rate. They essentially reflect the state of the cells' metabolic system as adapted to the physical and chemical conditions during the fermentation. During the respiration rate measurements the dissolved oxygen tension was monitored in a closed chamber containing yeast suspension to which various concentrations of glucose had been added to adjust the initial glucose concentration. By assuming a constant ratio Y to exist between the consumption of glucose and oxygen as expressed by equation 5.5, Equation 5.4 can be integrated to yield the simulated oxygen tension versus time relationship in the chamber.

$$\frac{dS_1}{dt} = Y\,Q\,\frac{dP_{O_2}}{dt} \qquad (5.5)$$

The integrated form of Equation 5.4 is shown in Equation 5.6:

$$P_{O_2} + \frac{A_3}{A_1}\ln P_{O_2} + \left(\frac{A_4}{A_2} - \frac{A_1}{A_2} - \frac{A_3}{A_1}\right)\ln(A_1 + A_2 P_{O_2})$$

$$= \left(\frac{dP_{O_2}}{dt}\right)_{max} t + P_{O_{2_i}}$$

$$+ \left(\frac{A_4}{A_2} - \frac{A_1}{A_2} - \frac{A_3}{A_1}\right)\ln(A_1 + A_2 P_{O_{2_i}}) \qquad (5.6)$$

where: $A_1 = S_{1_i} - Q\,Y\,P_{O_{2_i}}$

$A_2 = Q\,Y$

$A_3 = K_1 K_m + K_m S_{1_i} - Q\,Y\,P_{O_{2_i}} K_m$

$A_4 = Q\,Y\,K_m + K_1 + S_{1_i} - Q\,Y\,P_{O_{2_i}}$

Equation 5.6 was solved by Program KOK9 for values of time. Four simulated oxygen tension decrease curves are shown in Figure 5.1 together with their lines of maximum slope. The only parameter varied was the initial glucose concentration. Y was assumed to be equal to 6. Program KOK9 also calculated the oxygen tensions at which the slopes of the curves were one-half their maximum slopes. These values are the K_m values. They are presented in Table 5.2 for values of 2 and 6 for Y.

To prevent substrate inhibition completely would require a high initial glucose concentration. During the experiments, four different initial glucose concentrations were used and four K_m values obtained for each set of growth conditions. To obtain a K_m value the oxygen tension in a sample was measured continuously and recorded as a function of time. These curves are referred to as the oxygen tension-time curves. Ideally, the maximum respiration rate should occur at the beginning of the oxygen tension-time curve. In practice however, the initial slopes of the oxygen tension-time curves were somewhat lower than the maximum slopes.

FIGURE 5.1

Simulated Oxygen Tension-Time Curves and the Lines of Maximum Slope

The initial oxygen tension was 0.15 atm. O_2.

K_1 = 0.03 gm/l , K_m = 0.001 atm. O_2

Y = 6.0 gm glucose/gm O_2

maximum slope = 1.0×10^{-4} atm. O_2/sec

Initial Glucose Concentrations:

□	0.31 gm/l
o	0.11 gm/l
●	0.075 gm/l
x	0.050 gm/l

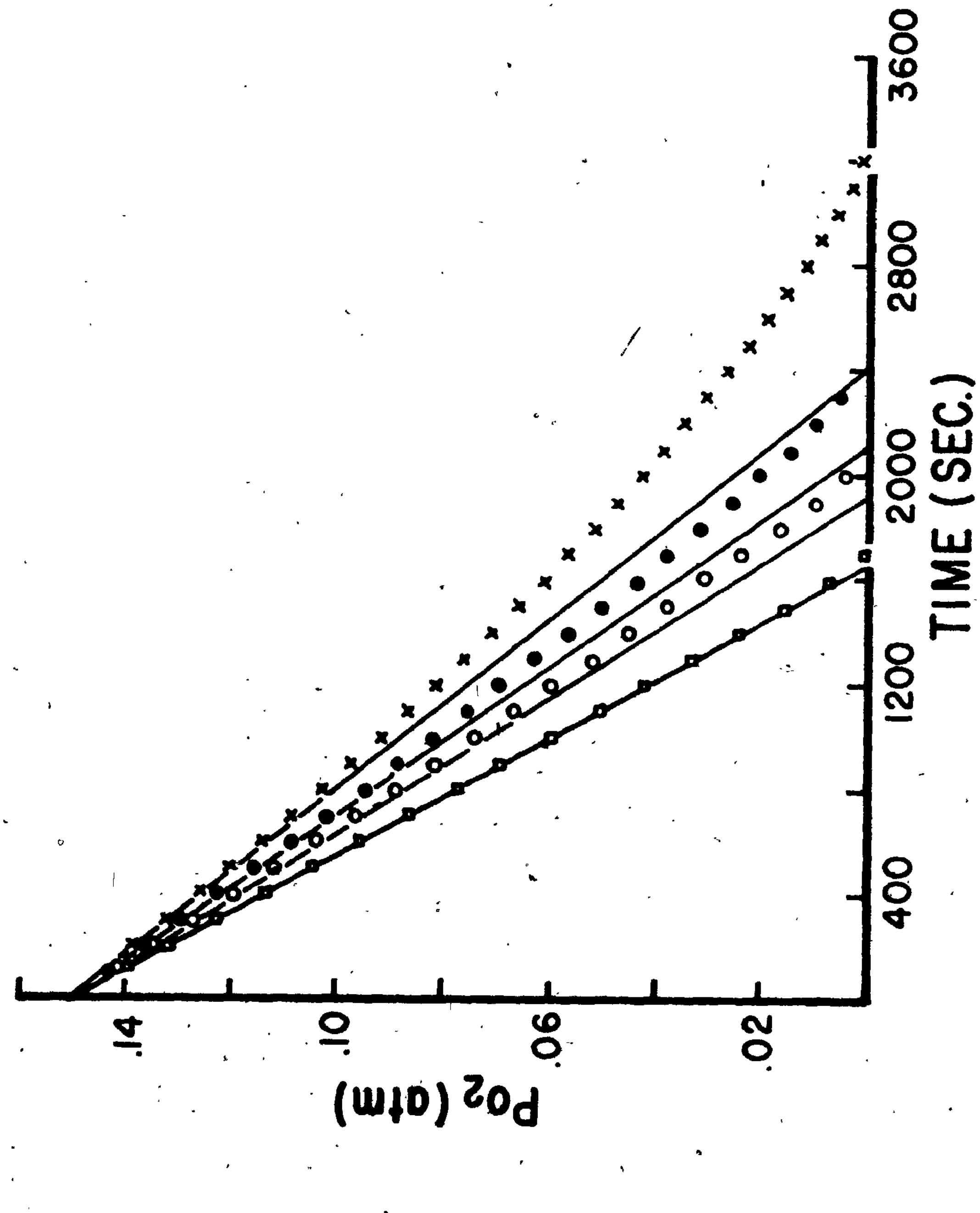

.14
.10
.06
.02
P_{O_2} (atm)
400
1200
2000
2800
3600
TIME (SEC.)

TABLE 5.2

Oxygen Tensions At Which The Simulated Oxygen Tension-Time Curves Reach Half Their Maximum Slopes. (K_1=0.03 gm/l, K_m=1.0 x 10^{-3} atm O_2, initial oxygen tension = 0.15 atm)

Y (gm glucose/gm O_2)	Initial Glucose Concentration (gm/l)	Oxygen Tension at Half-Initial Slope (atm x 10^3)
2	0.310	0.99
2	0.110	1.04
2	0.075	1.10
2	0.050	1.25
6	0.310	1.01
6	0.110	1.21
6	0.075	1.67
6	0.050	8.32

The K_m value was obtained by finding the oxygen tension at which the slope of an oxygen tension-time curve was one-half the maximum slope observed in that curve. The K_m values are therefore also referred to in the text as the 'oxygen tension at half-maximal slope'.

During the recording of the oxygen tension-time curves, the glucose concentrations in the samples changed due to the metabolism of *C. lipolytica*. The oxygen tension-time curves obtained at low glucose concentrations therefore reflected the double-substrate inhibition by both oxygen and glucose while the concentrations of both these substrates were changing. The glucose concentration at the point of half-maximal slope was not known and the K_m values obtained from these curves were therefore of questionable value.

5.5 *Candida Lipolytica*; Culture Maintenance and Inoculum Preparation

Lodder *et al.* [40] have described two varieties of *C. lipolytica*: variety *lipolytica* and variety *deformans*. *C. lipolytica* can grow by budding like a typical yeast, by producing pseudomycelium or by forming a true, septate mycelium [40]. Under conditions of intense agitation during submerged fermentation it grows as a typical yeast and by forming some pseudomycelium. Neither variety can grow anaerobically. Abe and Tabuchi [1] have reported that significant quantities of citric acid are produced in submerged culture. Both varieties require thiamin to stimulate growth.

The strain of *C. lipolytica* used was ATCC #8661. The varietal form of this culture was not specified.

The culture was maintained on agar plates at room temperature and was transferred to new plates every two weeks. The composition of the growth medium used for both the inoculum and the agar plates is presented in Table 5.3. The composition of the medium was derived from descriptions given by Dostalek [19] and Ingram [36]. 2.0% (w/v) of Bacto-agar (Difco Laboratories) was added for plate preparation. All other reagents used were 'Baker Analyzed' reagent grade (J.T. Baker Chemical Co.). The glucose solution was sterilized separately from the mineral and vitamin solution. The inoculum was grown in 100 cc batches in 500 cc Erlenmeyer flasks covered with lint squares on a rotary shaker at 200 rpm. (New Brunswick Scientific Co.). The inoculum was started 2 days before it was required to inoculate a fermentation.

5.6 The Fermentor and Support Systems

5.6.1 The Fermentor

The fermentor used was a Model CMF-128S (New Brunswick Scientific Co.). The maximum working volume of the vessel was 24 liters. The vessel contents and all ports could be sterilized in place. Temperature control (±0.5°C) was

TABLE 5.3

Composition of the Growth Medium For Agar Plate and Inoculum Preparation

KH_2PO_4	7.0 gm
NH_4Cl	5.0 gm
$MgSO_4$	0.2 gm
NaCl	0.1 gm
D-Glucose (Dextrose)	10.0 gm
$ZnSO_4 \cdot 7H_2O$	11 mgm
$MnSO_4 \cdot H_2O$	6 mgm
$FeSO_4 \cdot 7H_2O$	1 mgm
EDTA·di-Na	7.3 mgm
$CoCl_2$	180 microgram
$CuSO_4 \cdot 5H_2O$	40 microgram
Thiamine dihydrochloride	100 mgm
Distilled H_2O to	1000 cc

achieved by means of a hollow-baffle heat exchanger. The vessel contents were agitated by a disc turbine impeller of 4.5 inch diameter. A 1/8-inch single-orifice sparger was used to aerate the vessel. The sparging air was sterilized by filtration through a steam-heated glass-wool filter. The fermentor is shown in Photograph 5.1.

5.6.2 The pH Controller

A pH-152 pH-controller-recorder (New Brunswick Scientific Co.) was used. It controlled the pH in the fermentor vessel to within ±0.1 pH unit by the addition of either acid or base solution. The steam-sterilizable electrodes used were a #117143 Silver Chloride Reference Electrode and a #117123 Calomel Measuring Electrode (Leeds and Northrup). 2.5 N NaOH solution was used to control the pH. When the pH controller detected a difference between the set point pH and the fermentor pH it added pH control solution for the duration of the addition cycle, followed by a stirring cycle, before a new addition was made.

5.6.3 The Level Control System

The fermentor contained the necessary circuitry to switch on a pump whenever contact occurred between a level probe and the liquid surface in the fermentor vessel. The level probe used is shown in Figure 5.2. This probe was

PHOTOGRAPH 5.1

The CMF 1285 Fermentor

FIGURE 5.2

The Level Probe

A) enlarged section of one probe end

B) the double-ended probe

1. 316-stainless-steel tube
2. glass tubing
3. epoxy resin ('5-min epoxy', Devcon Corp.)
4. gold rod
5. connecting wire

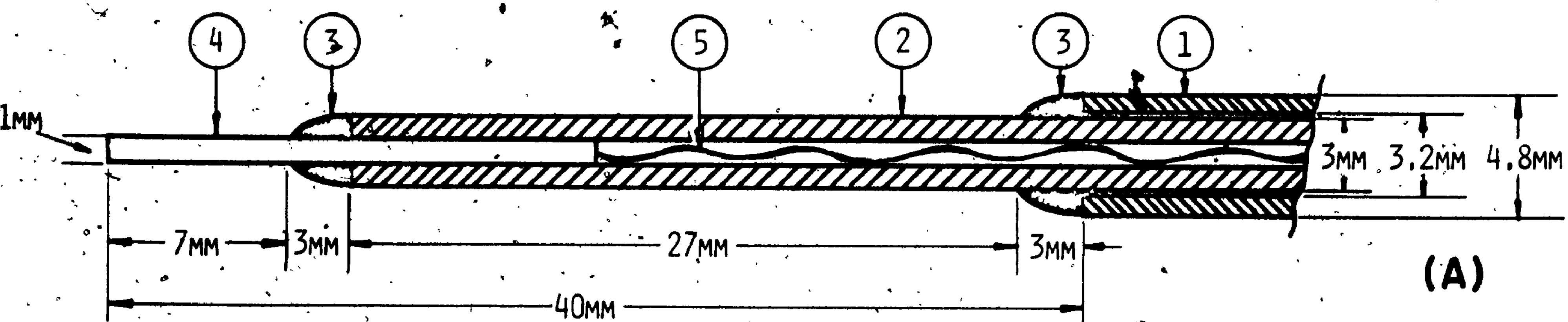

(A)

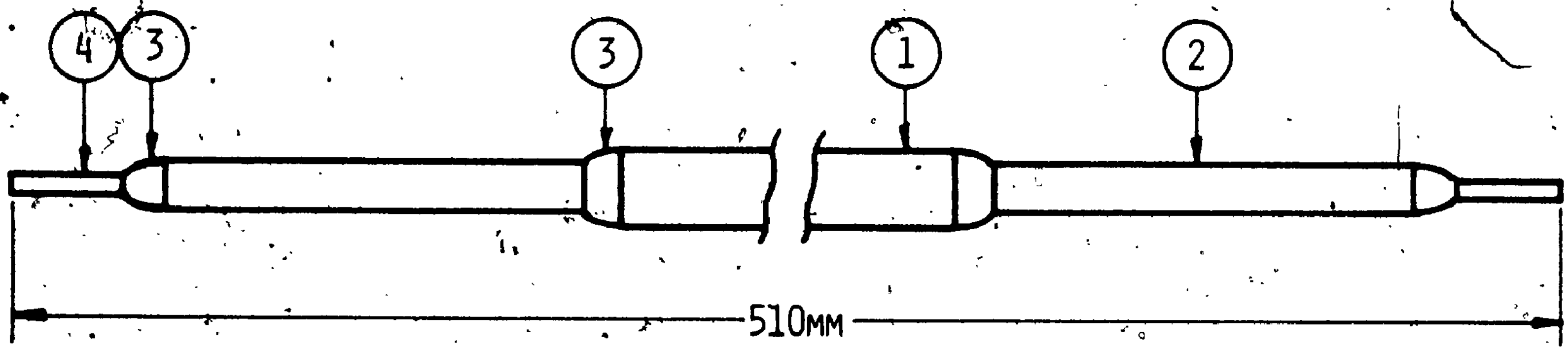

(B)

found to differentiate better between the foam and the liquid than the stainless steel probe supplied with the fermentor did. Whenever contact occurred continuously for more than 10 seconds a Sigmamotor pump (Model A1·4·E, Sigmamotor Inc.) was switched on until a 10 second continuous lack of contact occurred.

5.6.4 The Foam Control System

The fermentor had provisions for the automatic addition of an antifoam solution. It was found however that the addition of antifoam adversely affected the quality of the dissolved oxygen control. Also, during several attempts to suppress foam formation with Antifoam C (Dow Corning) *C. lipolytica* was found to preferentially metabolize the antifoam compound rather than the substrate glucose. Foam was therefore destroyed by means of a mechanical foam breaker rotating at 500 rpm. It is shown in Photograph 5.2. The layer of foam was always kept less than 1/2 inch in thickness by this method if the foam breaker was mounted so that its bottom was at exactly the same level as the tip of the level control probe.

PHOTOGRAPH 5.2

The Mechanical Foam Breaker

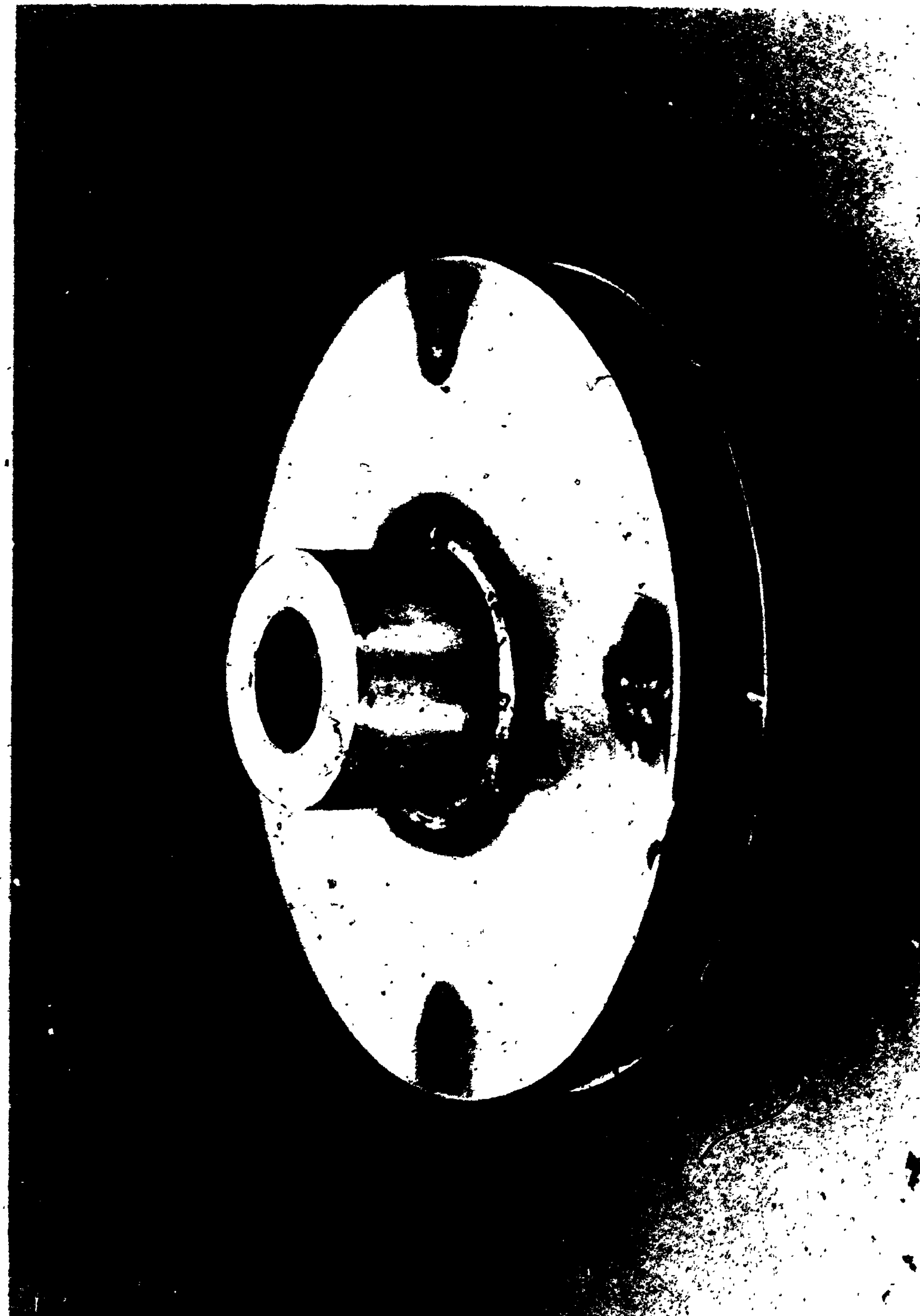

5.6.5 The Continuous Feed System

Two 40-l stainless steel tanks were used as feed solution reservoirs. These were autoclaved separately from the fermentor. During continuous culture the feed solution was transferred from the reservoir to the fermentor vessel by a Sigmamotor pump (Model A1.4.E, Sigmamotor Inc.) having a maximum pumping capacity of 900 ml/hr. The feed vessel was mounted on a scale so that its weight could be read off at any time.

5.7 The Dissolved Oxygen Control System

Dissolved oxygen was measured with a membrane-covered polarographic oxygen electrode (Model #27567-03, Instrumentation Laboratory) in conjunction with an Oxygen Amplifier (Model #27564-02, IL) and an Oxygen Indicator (Model #27565-02, IL). The oxygen probe's response time was 45 seconds and was linear to within ±1% (manufacturer's specifications). The Oxygen Amplifier's output signal was 0-20 mA. The ground-isolation requirement of the amplifier was found to be much more severe than the manufacturer's specifications seemed to indicate. The only grounding point of the dissolved oxygen control system was the electrode itself. All amplifiers and other instruments which required line voltage were fed through an isolation transformer. All ground cables were removed from these instruments. The instruments were mounted on a 1/2-inch thick acrylic plate. A grounded shield covered the instrument assembly. The output from the Oxygen Amplifier was fed simultaneously to the Oxygen Indicator (a visual read-out device), a Foxboro amplifier (Model #693AT-0A-SD) and a voltage-to-current transmitter (Model #821-BX-U, Acromag). The signal from the Foxboro amplifier was fed to a recorder (Model #6420HF-0-A, Foxboro). The signal from the Acromag transmitter was fed to a current-to-air transducer (Model #1767-69TA-Style B, Foxboro) which in turn supplied an air pressure signal to a pneumatic proportional-integral controller (Model #1923-130M, Foxboro). Sparging air was regulated by a pneumatic control valve (Type 75, Badger Meter Inc.). The signal flow is illustrated in Figure 5.3.

5.8 The Respiration Rate Test Chamber

The respiration rate test chamber is shown in Photograph 5.3. It was constructed of acrylic and consisted of three sections. These are shown separated in Photograph 5.4.

The bottom section had a central raised spindle with a slightly tapered side to form a water-tight seal with the middle section. The spindle's top was machined concave except for a small flat plateau in its centre to allow a magnetic stirrer to turn freely. The concave shape of the spindle's top allowed maximum drainage of the liquid through a 1/4-inch hole at the lowest point. This hole connected with a 1/8-inch diameter hole leading sideways so that the

FIGURE 5.3

Signal Flow In the Dissolved Oxygen Control System

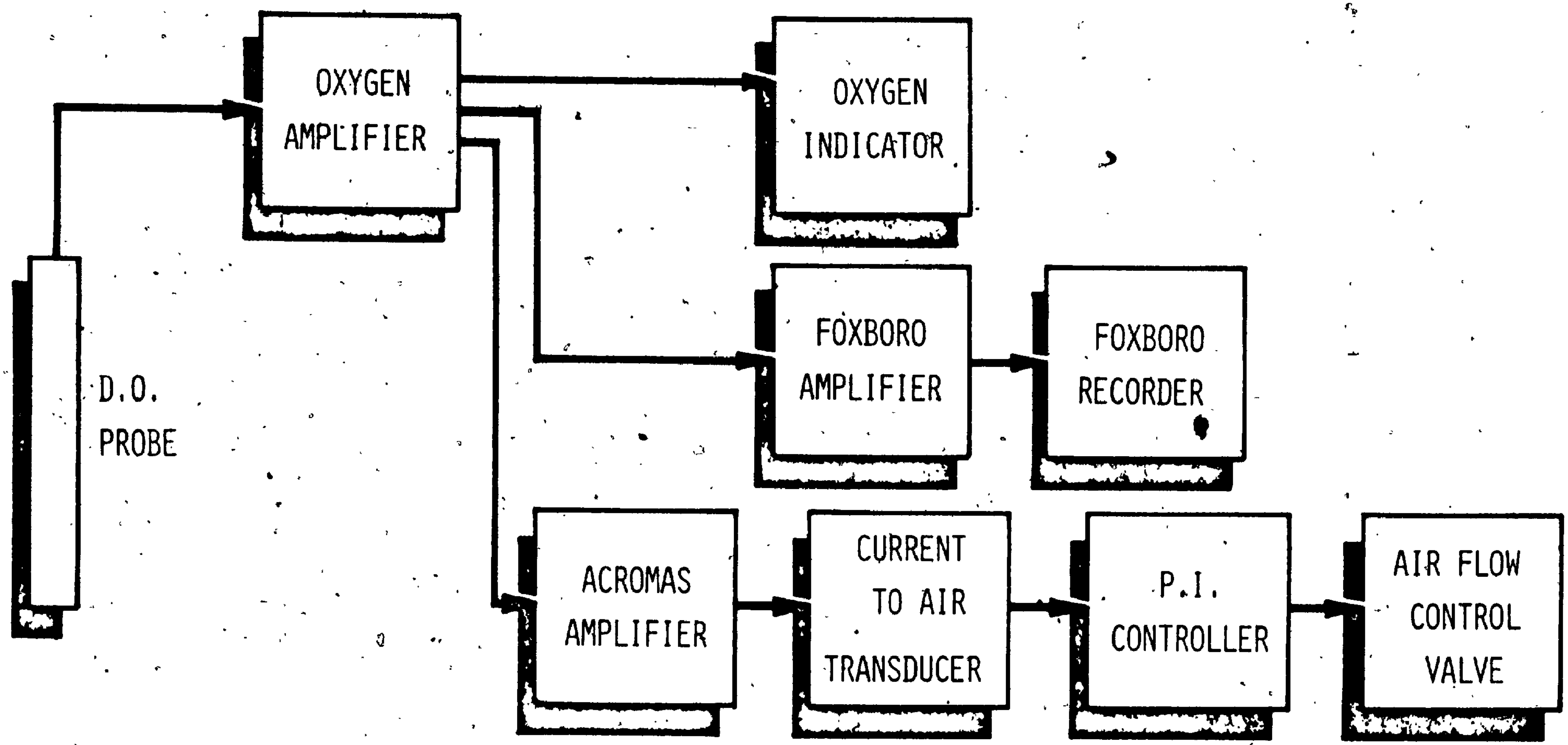
OXYGEN AMPLIFIER
OXYGEN INDICATOR
FOXBORO AMPLIFIER
FOXBORO RECORDER
D.O. PROBE
ACROMAS AMPLIFIER
CURRENT TO AIR TRANSDUCER
P.I. CONTROLLER
AIR FLOW CONTROL VALVE

PHOTOGRAPH 5.3

The Respiration Rate Test Chamber

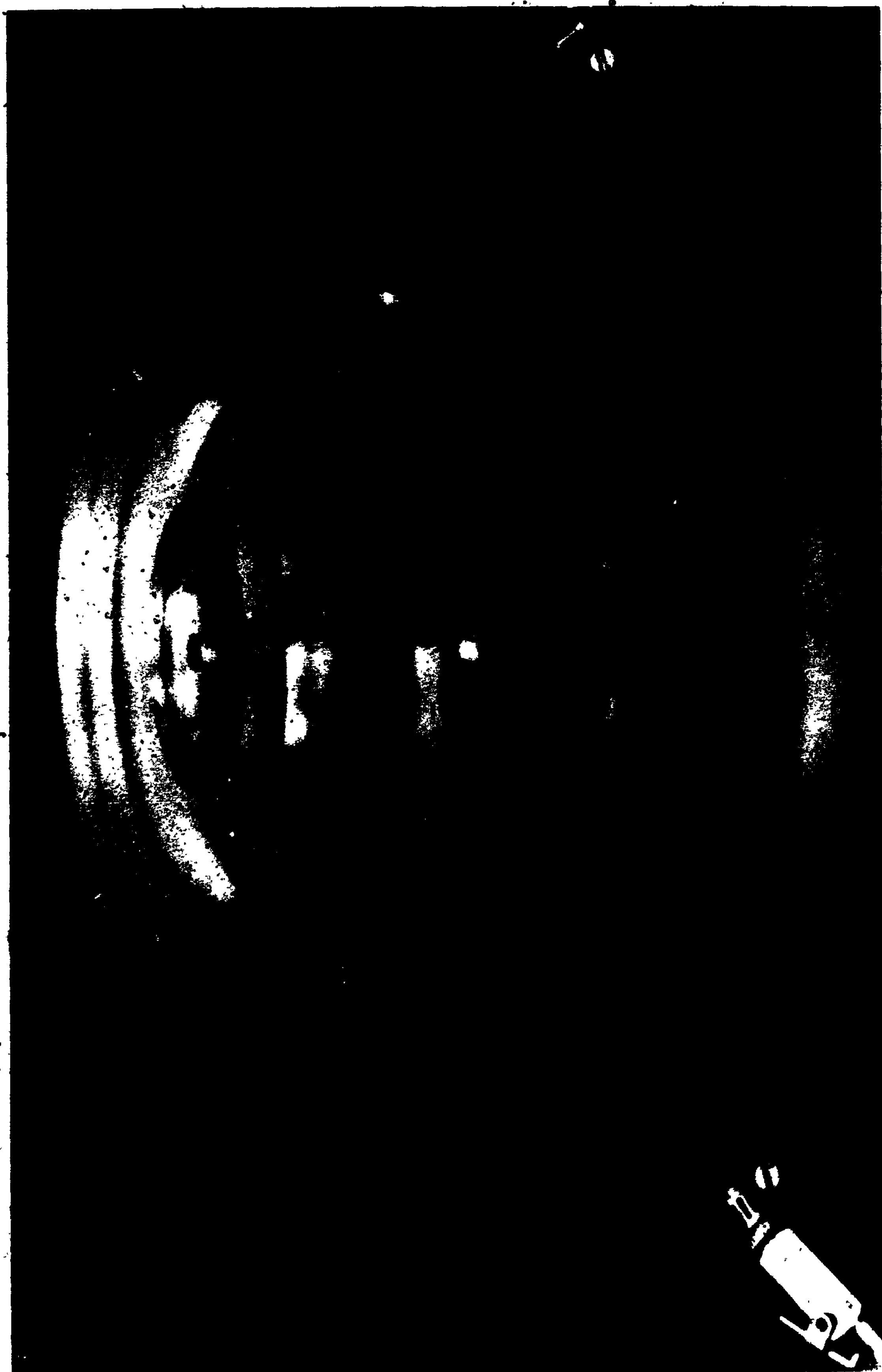

4 OF/DE 6

PHOTOGRAPH 5.4

The Three Parts of the Respiration
Rate Test Chamber Separated.

From Top to Bottom:
Bottom section, Top section, Middle section

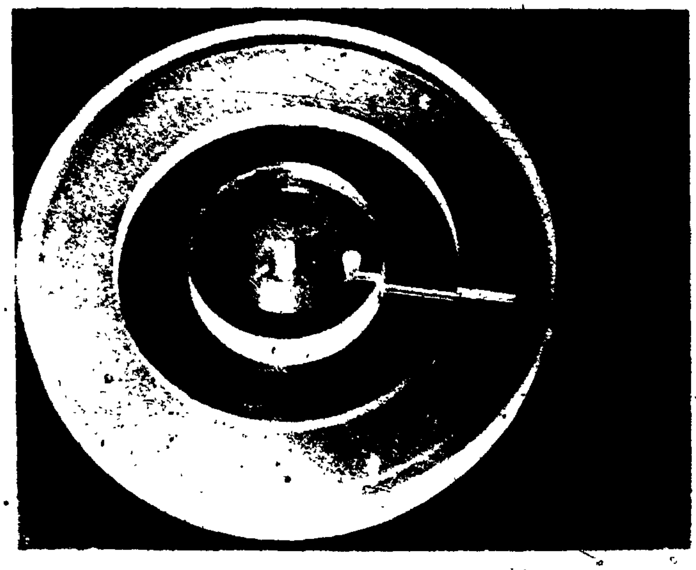

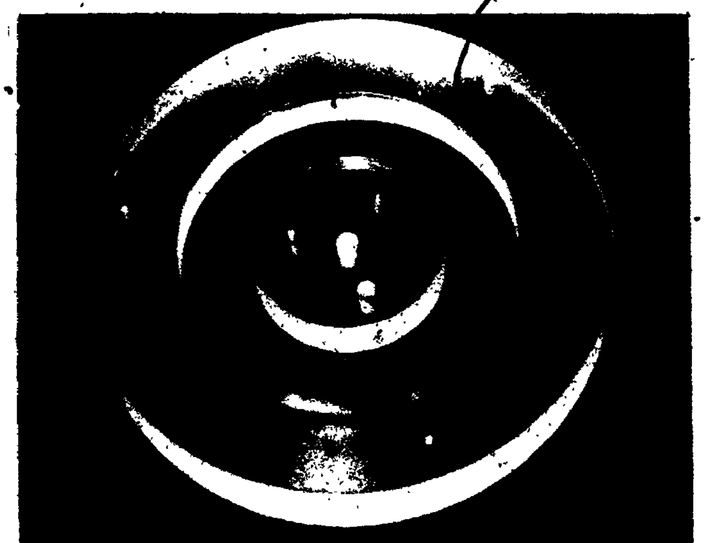

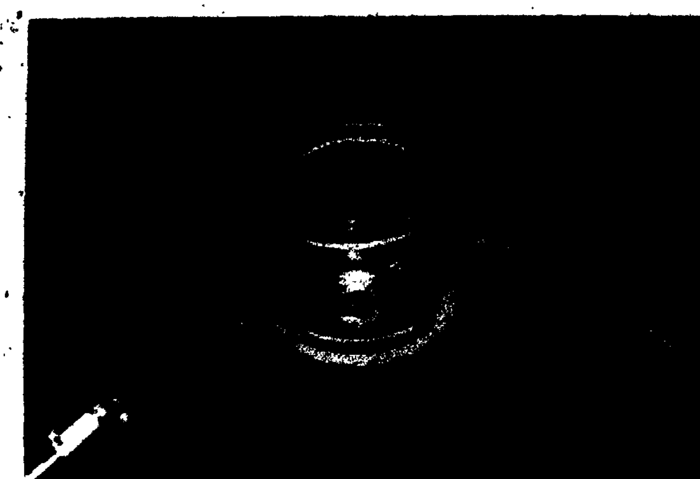

liquid draining from the chamber emerged through the side of the bottom section. A slight vacuum could be applied at the liquid exit to hasten the drainage process. The liquid exit could be blocked by a stopcock during respiration rate determinations. The rest of the bottom section was shaped to contain small accidental spills.

The middle section consisted of a double-walled annulus. Water from a controlled-temperature bath was pumped through the space between the walls. A tapered, upward slanting hole was machined through the walls to mount the YSI dissolved oxygen probe. When mounted, the probe's face was at a 30° angle with the vertical. This was found to minimize bubble adherence to the probe's membrane while the chamber was being filled. At both the top and the bottom on the inside of the middle section were small tapers to mate with the bottom and top sections. The inside diameter of the middle section was 2.5 inches.

The top section had a spindle with a tapered side protruding downward similar to the bottom section. Its face was concave with the highest point being in the centre where a 1/4-inch hole was located to receive a funnel during filling. The face was concave to allow trapped air bubbles to slide to the central hole and escape during filling. A second 1/4-inch hole was located off-centre to receive a thermometer or a nitrogen sparging tube. The upper face of the top section was also concave with its lowest point located at the central funnel hole to allow a small pool of stagnant liquid to cover the funnel and thermometer holes and thus effectively seal them.

The chamber had an internal volume of 200 ml when assembled. The contents were agitated with a 1-1/2-inch long Teflon-coated magnetic stirring rod driven by a variable-speed stirrer (Model PC 353, Corning Glass Works).

5.9 Method For Running a Continuous Fermentation

5.9.1 Initial Batch Culture

The maintenance of the *C. lipolytica* culture and the preparation of the inoculum were described in section 5.5. The fermentor and its support systems were described in sections 5.6 and 5.7. The medium composition for the initial batch culture is given in Table 5.4.

The fermentor containing the complete medium except the dextrose, was sterilized as described in the fermentor's manual with the pH electrodes, the dissolved oxygen electrode and the level probe in place. The dextrose solution was autoclaved separately. After cooling, the pH control system was recalibrated by obtaining a small sample from the fermentor. The dissolved oxygen control system was calibrated by sparging the fermentor contents with sterile air for 2 hours. The dextrose solution was then added and the fermentation inoculated. All operations were carried out using standard sterile

TABLE 5.4

Composition of Medium For the Initial Batch Culture

KH_2PO_4		1.0 gm
NH_4Cl		2.75 gm
$MgSO_4$		150 mg
NaCl		75 mg
Thiamine hydrochloride		225 mg
Dextrose		1.5 gm
$ZnSO_4 \cdot 7H_2O$		25 mg
$MnSO_4 \cdot H_2O$		13.5 mg
$FeSO_4 \cdot 7H_2O$		2.25 mg
EDTA-di-Na		16.5 mg
$CoCl_2$		405 microgm
$CuSO_4 \cdot 5H_2O$		90 microgm
Distilled H_2O	to	1000 ml

procedures. The fermentor temperature was controlled at 23°C at all times. After one day of operation substantial growth was always visible and the continuous phase was started.

5.9.2 Operation of the Continuous Fermentation

The composition of the medium used for the continuous feed is given in Table 5.5. The medium was prepared in stainless-steel tanks in 29 liter lots containing all the necessary minerals and vitamin for 30 liters of medium. The tanks were autoclaved for 2 hours at 121°C. The dextrose solution was autoclaved separately. It was added to the feed tank by aseptic methods and thoroughly mixed in by sparging with sterile air.

Upon starting the continuous phase of the fermentation the liquid level control system was switched on, the feed tank connected to the fermentor and the pump feed rate adjusted to the desirable feed rate. The feed tanks were switched whenever necessary.

During the continuous fermentation the dry cell weight, the glucose concentration and the pH were measured four times daily. Descriptions of the methods used are given in Appendix 5.2. The dissolved oxygen tension and the feed rate were adjusted during the fermentation as required.

Two continuous fermentations were completed, lasting 870 hours (36.2 days) and 812 hours (33.8 days), respectively.

TABLE 5.5

Composition of the Continuous Feed Medium

KH_2PO_4	0.33 gm
NH_4Cl	0.92 gm
$MgSO_4$	30 mg
NaCl	25 mg
Thiamine Hydrochloride	75 mg
Dextrose	5 gm
$ZnSO_4 \cdot 7H_2O$	8 mg
$MnSO_4 \cdot H_2O$	4.5 mg
$FeSO_4 \cdot 7H_2O$	750 microgm
EDTA-di-Na	5.5 mg
$CoCl_2$	135 microgm
$CuSO_4 \cdot 5H_2O$	30 microgm
Distilled H_2O to	1000 cc

During the first fermentation only the YSI probe was used to obtain oxygen tension-time curves; during the second both the YSI probe and the dropping mercury polarograph were used simultaneously. The detailed procedure is presented in the next section.

5.10 Method For the Oxygen Tension-Time Experiments

For both fermentations, under each set of conditions of dissolved oxygen tension and dilution rate, four oxygen tension-time curves were obtained at different concentrations of glucose in the samples. The procedure followed is described below.

Eighteen hours before the start of the tests the YSI probe was fitted with a new 1/2-mil thick Teflon membrane. It was then stored in a 5% (w/v) sodium sulfite solution while connected to a 0.800 volt polarizing voltage. At the same time 1200 ml of fermentation broth was collected, centrifuged at 6,000 rpm for 30 minutes and filtered twice through 0.8 μ Millipore filters. This material was collected to dilute the samples without changing the chemical environment of the yeast except for the glucose concentration. 108 mg of dextrose (D-glucose) was dissolved in 300 ml of the supernatant. This resulted in a glucose concentration of 2.0×10^{3} M higher than that present originally in the supernatant. The rest of the supernatant (solution A), the supernatant with the glucose added (solution B) and 300 cc of distilled water were separately aerated at 23°C for 1/2 hour. They were then covered and left standing overnight. No loss of glucose was found to occur during this period. Just before the start of the tests four mixtures of solutions A and B were prepared in the manner as shown in Table 5.6. Two down-step responses of the YSI probe were obtained by quickly submerging it into a 5% (w/v) solution of sodium sulfite with 1.0×10^{-5} M copper sulfate added. The YSI probe was then mounted in the chamber described in section 5.8. The chamber was sparged with oxygen-free nitrogen until the probe current reached a low steady value. For the experiments during which the oxygen tension-time curves were also determined polarographically, the mercury flow through the Polarotron capillary was also started at this time. A 100 ml sample was obtained from the fermentor and 62.5 cc of this material was added to one of the supernatant mixtures. The mixture was stirred briefly. The nitrogen flow to the chamber was stopped and 200 cc of sample was added through a funnel so that no gas bubbles remained in the chamber and a small pool of liquid on the top of the chamber sealed the spaces between the holes and the funnel stem and the thermometer. The stirring rate in the chamber was set at 300 rpm. 10 ml of the sample mixture was added to the sampling vessel of the Polarotron and the dropping mercury electrode lowered. The head space in the sampling vessel was constantly sparged with nitrogen.

TABLE 5.6

The Preparation of Samples For the Oxygen Tension-Time Curves

Sample #	Solution A (ml)	Solution B (ml)	Fermentor Broth (ml)	Glucose Added (Mole/l x 10^3)
a	0	187.5	62.5	1.5
b	137.5	50	62.5	0.4
c	162.5	25	62.5	0.2
d	182.5	5	62.5	0.04

The sensitivities of the YSI probe amplifier and recording system and of the polarograph were adjusted when necessary to obtain the largest possible recorded output.

When the oxygen was completely exhausted in both the test chamber and the polarograph sampling vessel, the contents were removed and both were washed twice with distilled water. Nitrogen was then sparged through the test chamber again to bring the probe back to its residual current and the next sample was inserted.

After all four samples had been analysed the YSI probe was calibrated with distilled water saturated with air at 23°C. The polarograph was calibrated with supernatant at 23°C. All determinations of oxygen tension-time curves were performed at 23°C.

5.11 Operating Conditions and Results For Fermentation 1

5.11.1 Conditions During the Fermentation

The time-invariant operating conditions for Fermentation 1 are listed in Table 5.7. Results from the dry weight, carbohydrate and pH analyses are recorded in Appendix 5.3.

Fermentation 1 was divided into thirteen periods. The time-variant operating parameters were determined at the beginning of each period. The first period comprised the batch fermentation. The time-variant operating conditions during the continuous fermentation were the dissolved oxygen

TABLE 5.7

Time-Invariant Operating Conditions For Fermentation 1

Inoculation	11:30 a.m. April 12, 1973
Operating Temperature	23°C ± 0.5°C
pH Control Addition Cycle	5 seconds
pH Control Stirring Cycle	15 seconds
Agitator Speed	500 rpm
Start of Continuous Feed	11:59 a.m. April 14, 1973
Operating Volume	10.0 liters

tension and the dilution rate. The values of these parameters are listed in Table 5.8 together with the observed average values of carbohydrate (as glucose) and dry weight concentrations and pH. Confidence intervals are recorded together with the average values of carbohydrate and dry weight at a confidence level of 0.95. These were calculated by use of the Student's t-distribution [62]. No values of pH, carbohydrate or dry weight were included when these were obtained within a twelve hour period after either of the time-variant operating conditions were adjusted. The dissolved oxygen tension remained within 2% of full scale (full scale = 100% = saturation with air at 1 atm) of the set point at all the set points employed. Settings of the dissolved oxygen controller are not reported since they have no useful function. These had to be adjusted every time a new operating point was chosen for the fermentation. The operation of this system was discussed in Chapter 4. The equivalent of at least two reactor residence times were allowed for process stabilization and adaptation of *C. lipolytica* after a change in time-variant operating conditions before a set of oxygen tension-time curves was obtained.

5.11.2 Shapes and Initial Slopes of Oxygen Tension-Time Curves

At the end of each period four oxygen tension-time curves were obtained with various initial glucose

TABLE 5.8

Time-Variant Operating Conditions And Parameters For Fermentation 1. Confidence Intervals Calculated at 0.95 Confidence Level

Period No.	Time (Hrs. After Inoculation) Start	Finish	Samples Included	Time Variant Operating Conditions: Dissolved Oxygen Tension (% Saturation)	Average Dilution Rate (Hr^{-1}) ± 5%	Observed Parameters: Carbohydrate Concentration (As Glucose mg/l) And Confidence Interval	Dry Weight Concentration (gm/l) And Confidence Interval	Average pH
2	48.5	145.7	1-10	25 ± 2	0.039	38.7 ± 1.5	0.92 ± 0.08	5.3
3	145.7	196.7	13-20	50 ± 2	0.043	40.0 ± 0.7	0.93 ± 0.12	5.3
4	196.7	296.0	21-36	35 ± 2	0.044	40.2 ± 1.3	1.34 ± 0.05	5.3
5	296.0	337.8	37-42	20 ± 2	0.045	38.2 ± 1.1	1.53 ± 0.04	5.4
6	337.8	387.3	45-51	10 ± 2	0.045	37.2 ± 2.2	1.26 ± 0.07	N.A.*
7	387.3	434.7	53-59	5 ± 2	0.045	36.3 ± 2.1	1.38 ± 0.14	N.A.
8	434.7	531.0	61-75	50 ± 2	0.031	41.2 ± 1.0	1.23 ± 0.04	5.4
9	531.0	603.2	77-87	20 ± 2	0.031	43.8 ± 1.3	1.21 ± 0.03	5.3
10	603.2	673.7	89-98	5 ± 2	0.031	39.0 ± 0.8	1.25 ± 0.02	5.3
11	673.7	768.8	101-114	50 ± 2	0.056	43.4 ± 1.9	1.82 ± 0.03	5.3
12	768.8	818.5	117-123	20 ± 2	0.058	39.1 ± 1.6	1.85 ± 0.06	5.2
13	818.5	867.0	125-131	5 ± 2	0.059	34.9 ± 1.0	1.67 ± 0.03	5.3

*N.A. - Not Available

concentration as described in section 5.10. The initial parts of the four curves obtained at the end of period 3 are shown in Figure 5.4. These curves were representative of the curves obtained during the rest of the experiments. The oxygen tension-time curves obtained when 1.5×10^{-3}, 0.4×10^{-3} and 0.2×10^{-3} M. of glucose were added (parts a, b and c) typically displayed an initial non-linear part. The oxygen tension-time curves obtained when 0.04×10^{-3} M. of glucose was added (part d) were completely non-linear. The maximum slopes of the latter curves were therefore difficult to judge. They were approximated by the slope of the straight line between the first two tabulated observations, usually spaced at 480 seconds (1000 mm at a chart speed of 125 mm/min.). The maximum slopes of the other curves were obtained graphically by measuring the slopes of the lines drawn through the linear portions of the curves and dividing by the dry weight concentration. These are recorded in Table 5.9 together with the time-variant operating conditions and the initial glucose concentrations.

5.11.3 Oxygen Tensions at Half-Maximum Slope

The method to obtain the oxygen tension at half-maximum slope and to compensate for the YSI probe's residual current by graphical means was developed at the end of Chapter 2. In Figures 5.5 to 5.10 are shown the final parts of the oxygen tension-time curves during tests 2a-2c and

FIGURE 5.4

Initial Parts of the Oxygen Tension-Time Curves Obtained At the End of Period 3 (Fermentation 1)

	Part
□	a
○	b
●	c
X	d

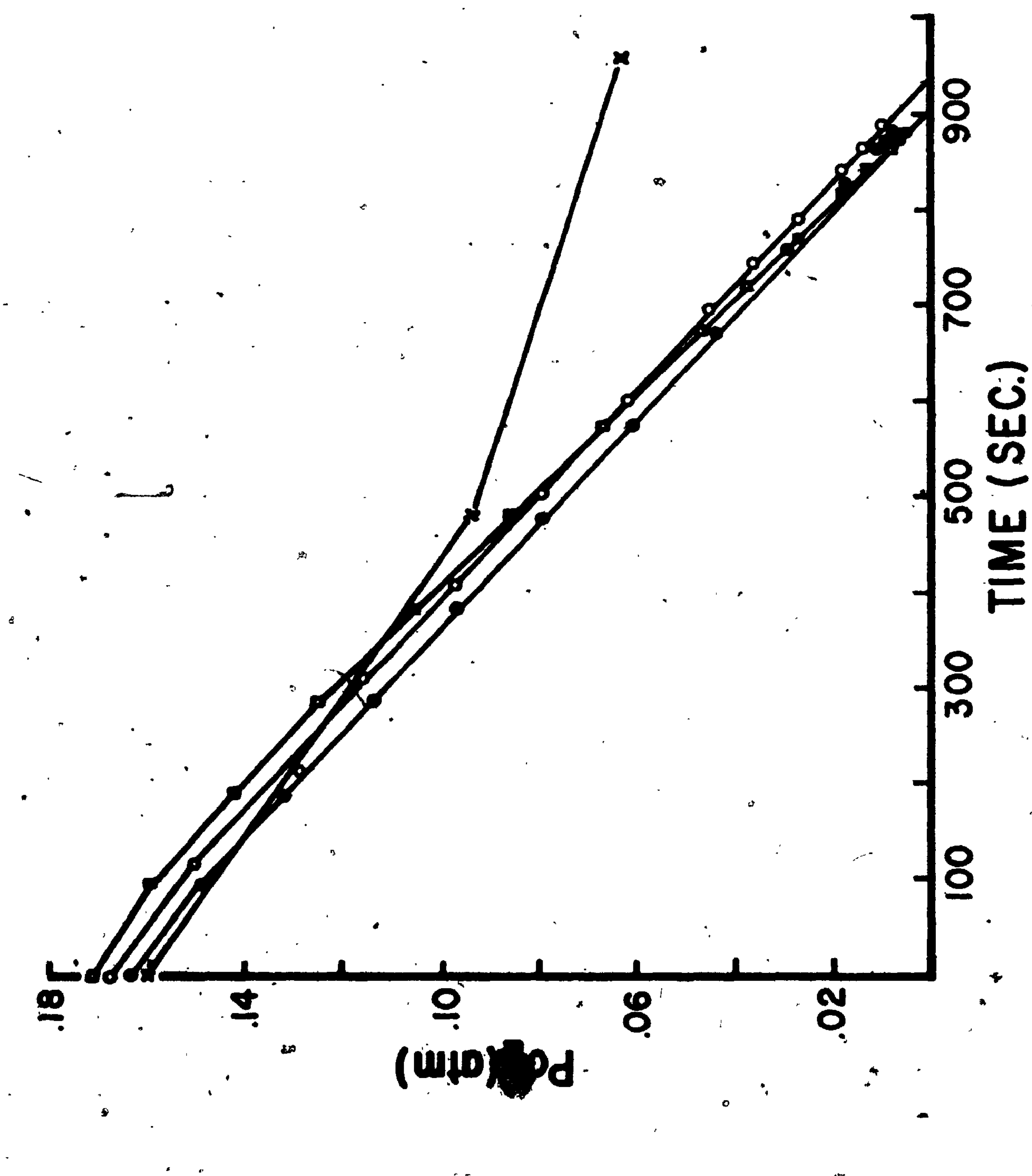

.18
.14
.10
.06
.02
Po (atm)
100
300
500
700
900
TIME (SEC.)

TABLE 5.9

Maximum Slopes of Oxygen Tension-Time Curves, Fermentation 1

Test and Period No.	Part No.	Oxygen Tension During Growth (% Air Saturation) (±2%)	Dilution Rate (Hr^{-1})	Initial Glucose Concentration (mg/l)	Maximum Slope (Atm O_2/sec/(gm/l)) x 10^4
2	a	25	0.039	309	6.34
	b			111	5.76
	c			75	5.90
	d			46	N.A.*
3	a	50	0.043	310	8.71
	b			112	7.92
	c			76	7.66
	d			47	5.94**
4	a	35	0.044	310	7.10
	b			112	6.29
	c			76	6.04
	d			47	4.67**
5	a	20	0.045	308	7.84
	b			110	6.41
	c			74	6.05
	d			45	2.11**
6	a	10	0.045	307	8.33
	b			109	7.07
	c			73	6.18
	d			44	3.94**
7	a	5	0.045	306	8.26
	b			108	7.12
	c			72	6.45
	d			44	4.45**

TABLE 5.9 (continued)

Test and Period No.	Part No.	Oxygen Tension During Growth (% Air Saturation) (±2%)	Dilution Rate (Hr^{-1})	Initial Glucose Concentration (mg/l)	Maximum Slope (Atm O_2/sec/(gm/l)) x 10^4
8	a	50	0.031	311	5.98
	b			113	5.29
	c			77	5.23
	d			48	3.56**
9	a	20	0.031	314	6.64
	b			116	N.A.*
	c			80	6.10
	d			51	3.32**
10	a	5	0.031	309	8.49
	b			111	8.24
	c			75	7.83
	d			46	3.97**
11	a	50	0.056	314	7.19
	b			116	6.24
	c			79	6.27
	d			51	4.43**
12	a	20	0.056	309	8.55
	b			111	7.62
	c			75	7.42
	d			46	4.49**
13	a	5	0.056	305	8.56
	b			107	7.59
	c			71	7.18
	d			42	4.46**

*N.A. - Not Available

**Obtained from first two tabulated points

FIGURE 5.5

The Final Part of the Oxygen Tension-Time
Curve Obtained During Test 2a (Fermentation 1)
Together With the Geometrical Construction
To Determine the Oxygen Tension At
Half-Maximum Slope

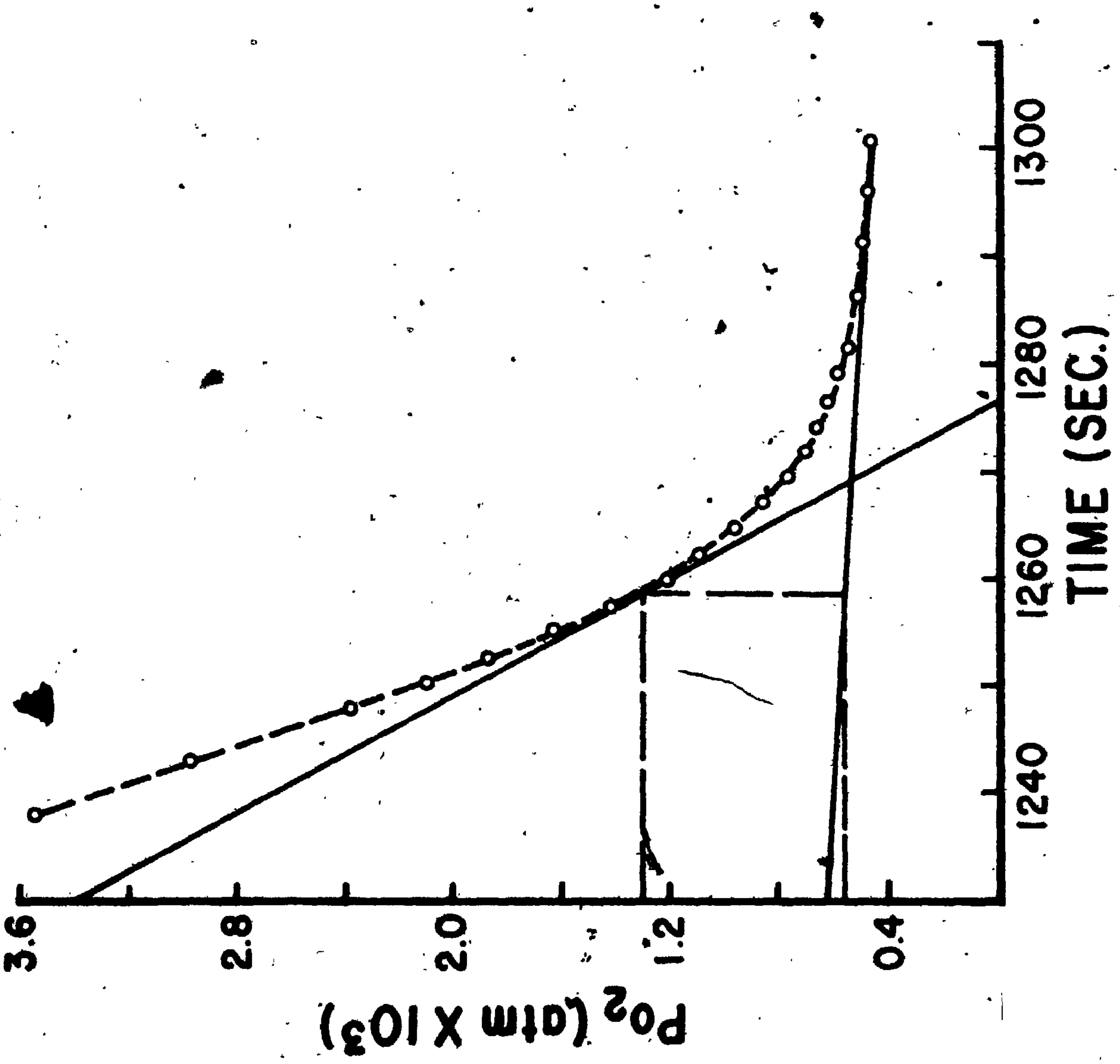

3.6
2.8
2.0
1.2
0.4
P_{O_2} (atm X 10^3)
1240
1260
1280
1300
TIME (SEC.)

FIGURE 5.6

The Final Part of the Oxygen Tension-Time Curve Obtained During Test 2b (Fermentation 1) Together With the Geometrical Construction To Determine the Oxygen Tension At Half-Maximum Slope

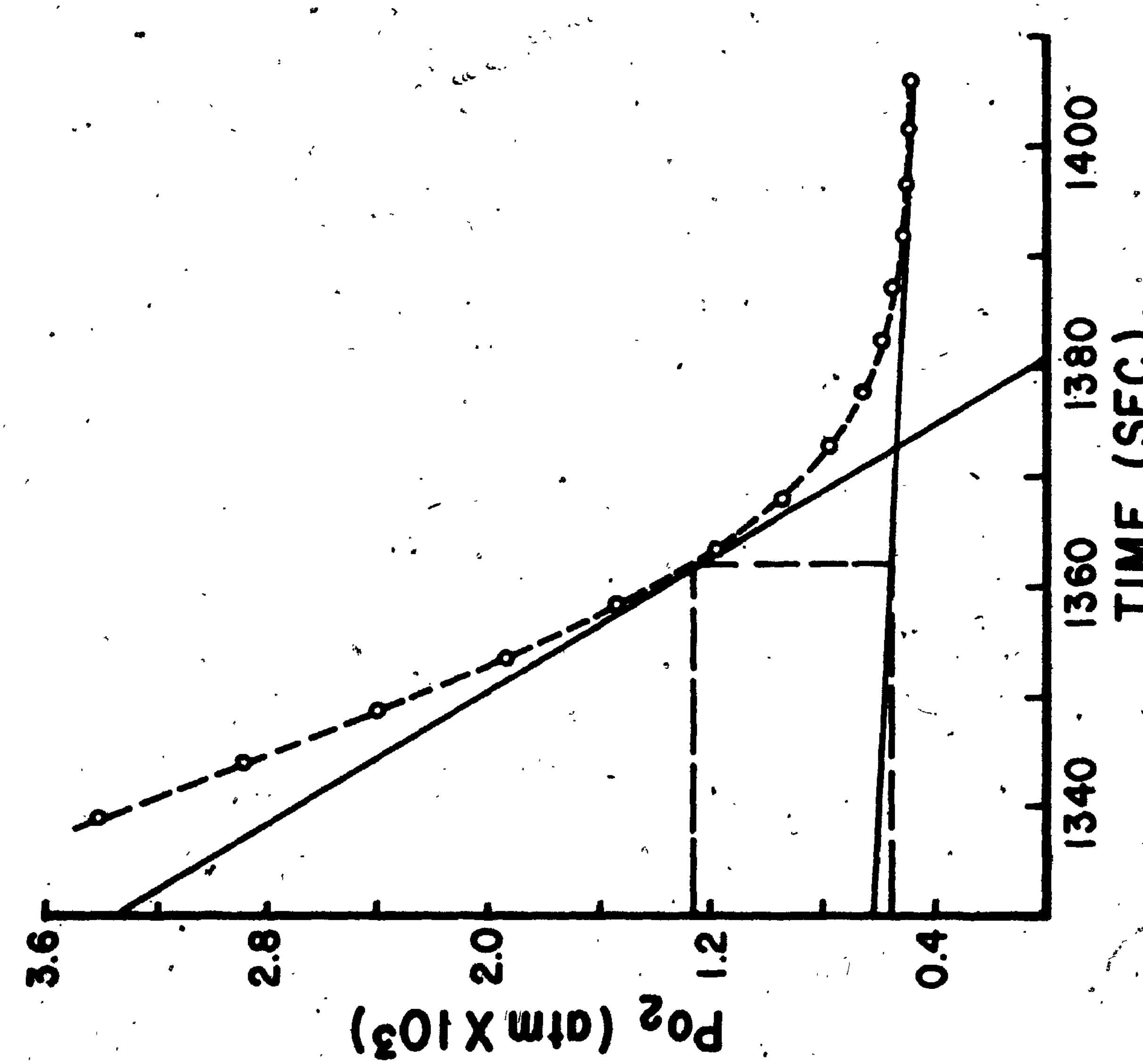
3.6
2.8
2.0
1.2
0.4
P_{O_2} (atm X 10^3)
1340
1360
1380
1400
TIME (SEC.)

FIGURE 5.7

The Final Part of the Oxygen Tension-Time Curve Obtained During Test 2c (Fermentation 1) Together With the Geometrical Construction To Determine the Oxygen Tension At Half-Maximum Slope

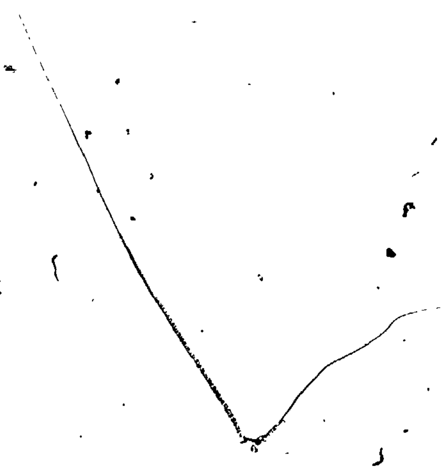

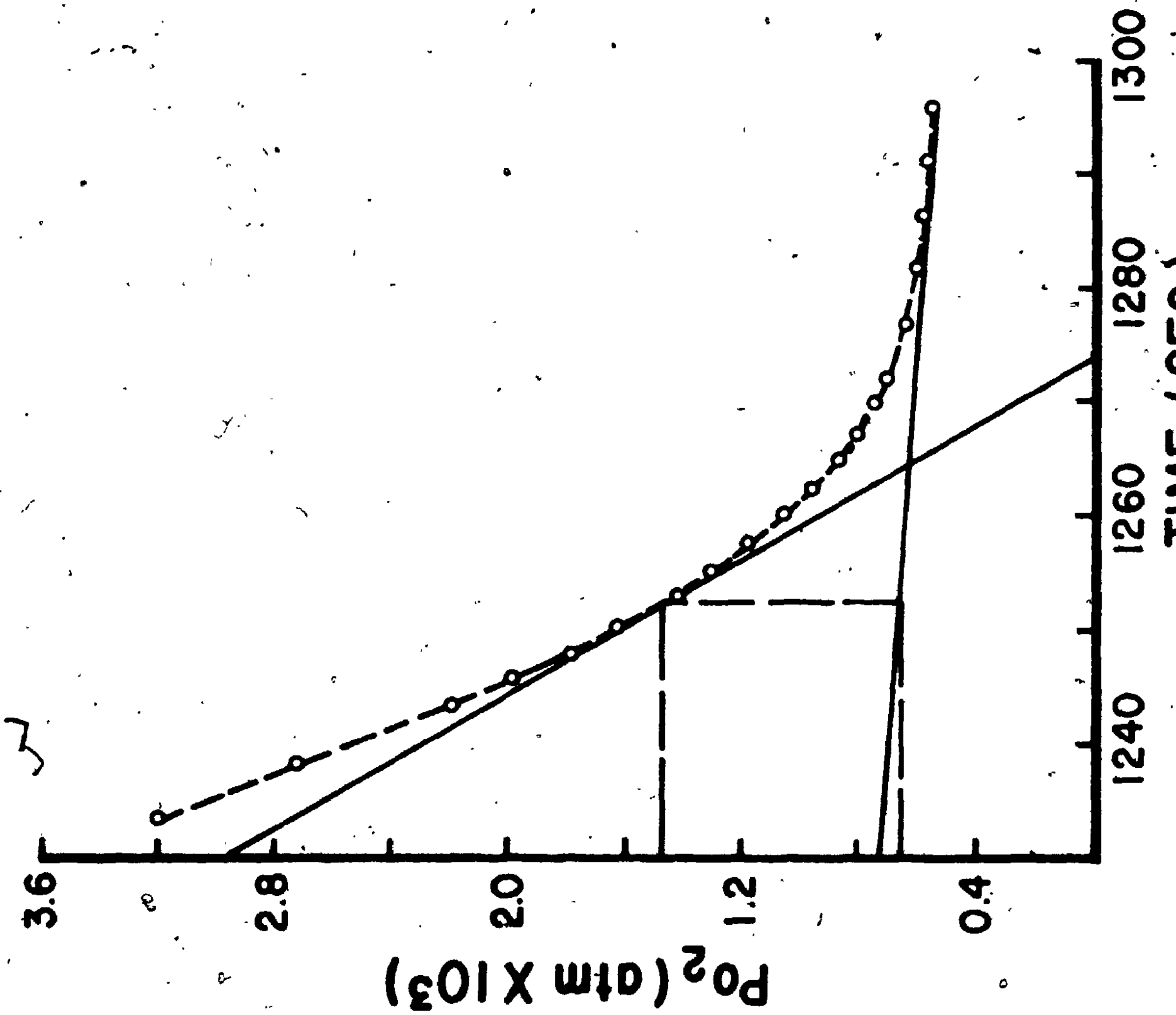

P_{O_2} (atm X 10³)
3.6
2.8
2.0
1.2
0.4
1240
1260
1280
1300
TIME (SEC.)

FIGURE 5.8

The Final Part of the Oxygen Tension-Time
Curve Obtained During Test 4a (Fermentation 1)
Together With the Geometrical Construction
To Determine the Oxygen Tension At
Half-Maximum Slope

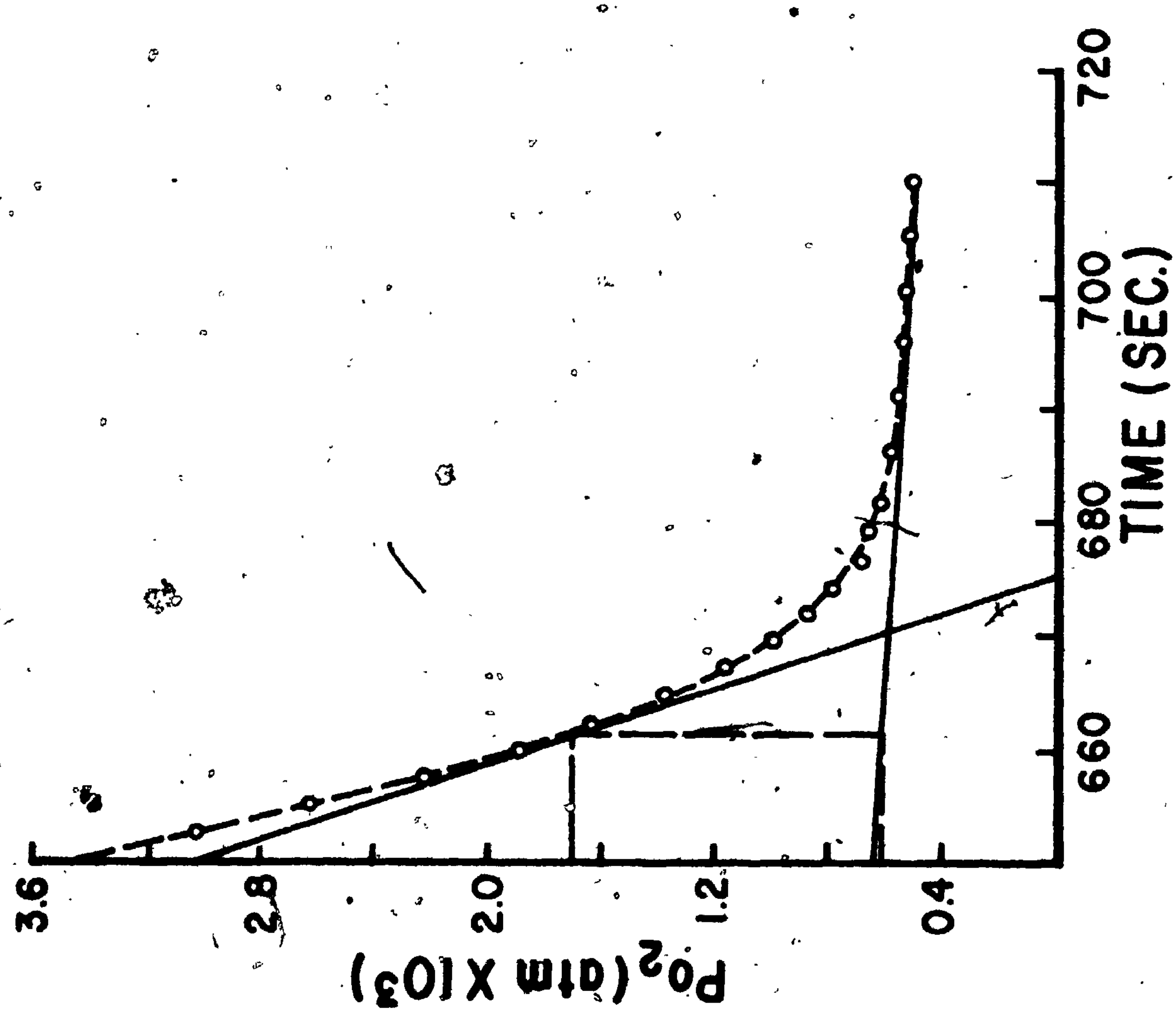

P_{O_2} (atm X 10³)
3.6
2.8
2.0
1.2
0.4
TIME (SEC.)
660
680
700
720

FIGURE 5.9

The Final Part of the Oxygen Tension-Time Curve Obtained During Test 4b (Fermentation 1) Together With the Geometrical Construction To Determine the Oxygen Tension At Half-Maximum Slope

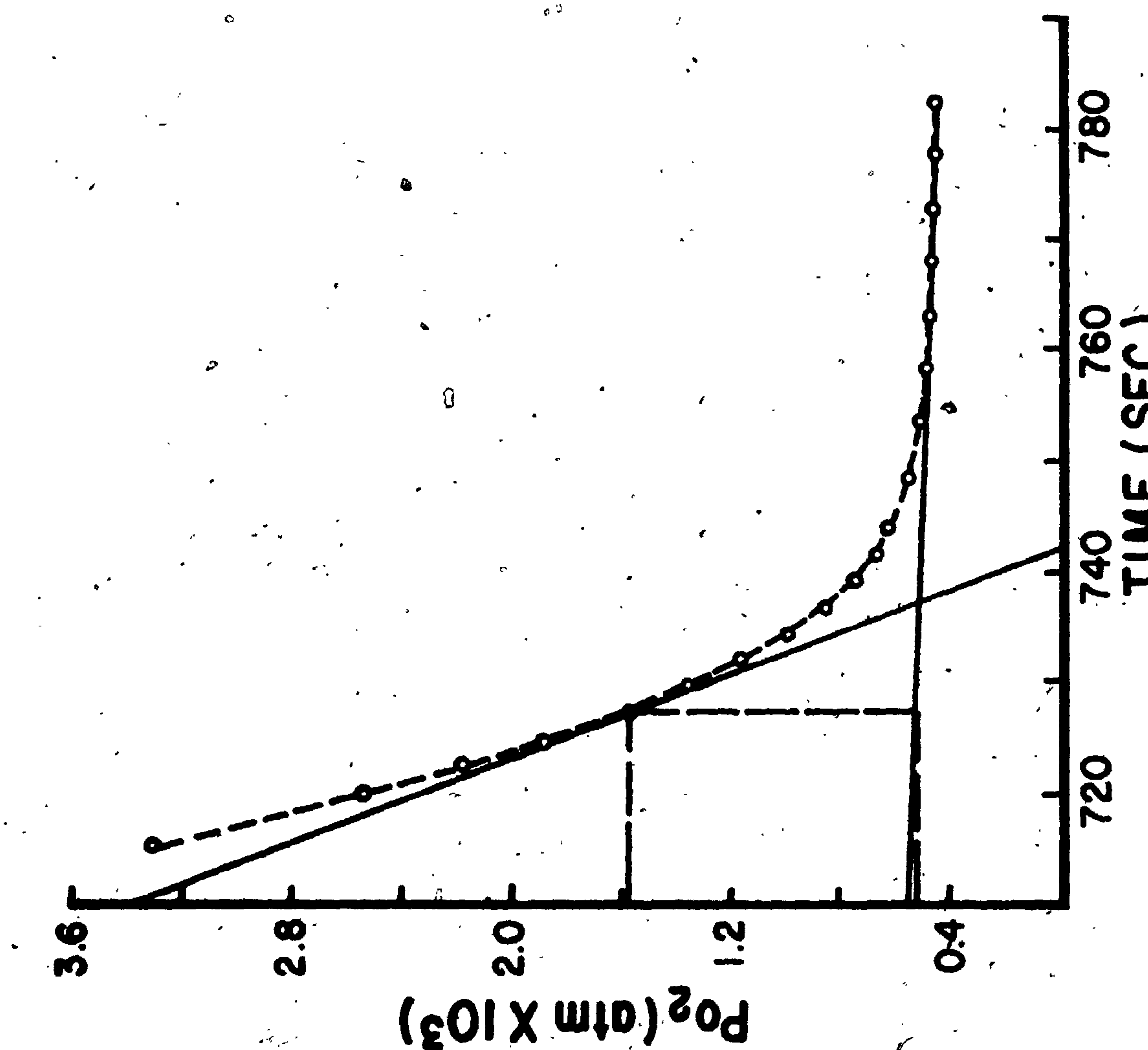

TIME (SEC.)
720
740
760
780
3.6
2.8
2.0
1.2
0.4
Po2 (atm X 10³)

FIGURE 5.10

The Final Part of the Oxygen Tension-Time Curve Obtained During Test 4c (Fermentation 1) Together With the Geometrical Construction To Determine the Oxygen Tension At Half-Maximum Slope

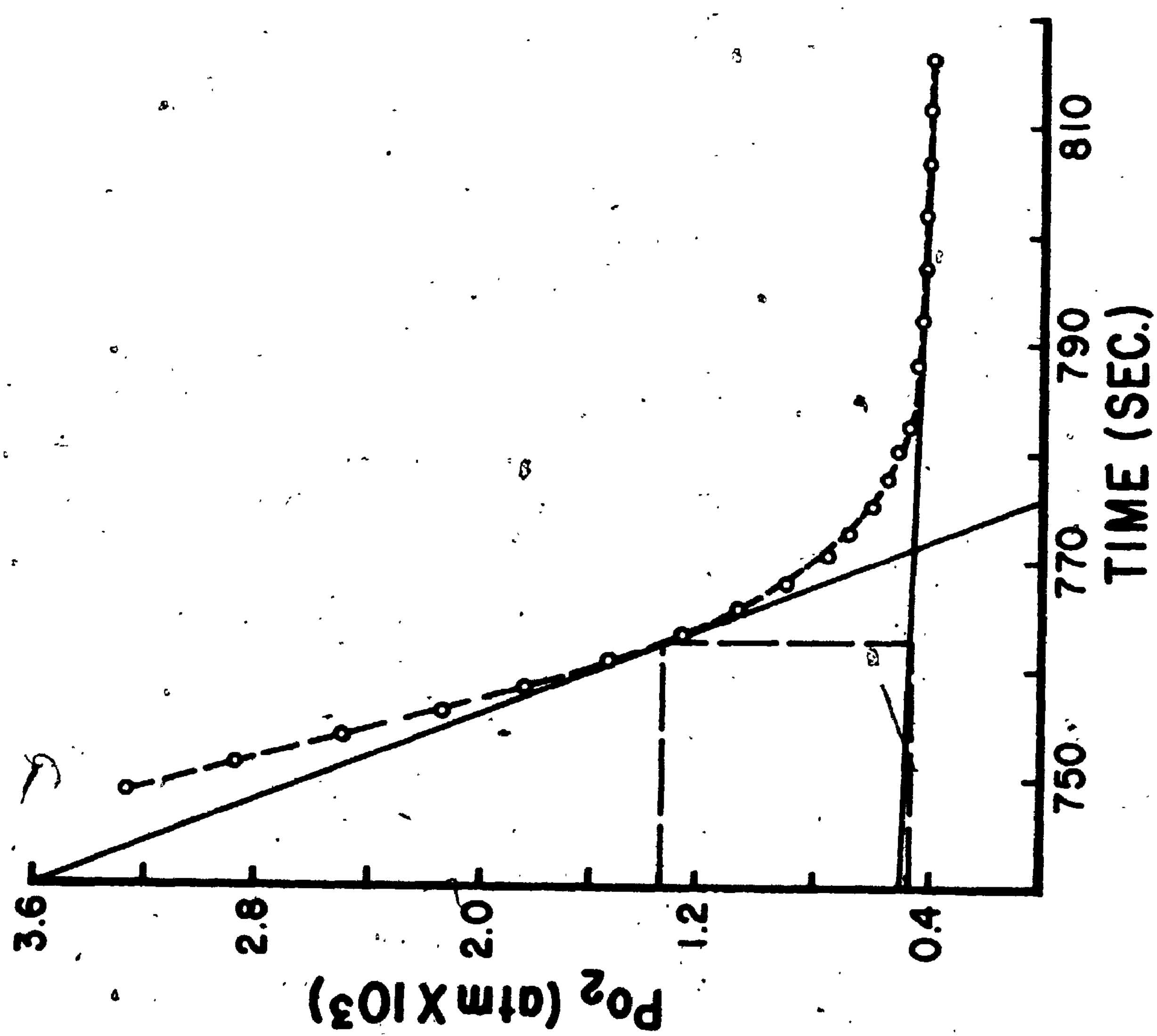

P_{O_2} (atm X 10^3)
3.6
2.8
2.0
1.2
0.4
750
770
790
810
TIME (SEC.)

4a-4c together with their lines of half-maximum slope and the extrapolated residual current lines. These curves were representative of the oxygen tension-time curves obtained during the rest of the experiments. No other detailed data for these experiments are presented due to their bulk.

Especially in Figures 5.7 to 5.10 the tangential points between the experimental curves and the lines of half-maximum slope are difficult to locate accurately.

Program KOK10 was written to find the points of half-maximum slope by three different numerical means:

- By plotting a sixth-order least-square polynomial through all points below a probe current of 1 micro-amp and algebraically finding the point at which the slope of this polynomial is half the maximum slope.

- By numerically differentiating the data below a current of 1 microamp, obtaining the least-square hyperbola by Hohmann and Lockhart's [35] method and algebraically finding the point of half-maximum slope.

- By plotting the least-square sixth-order polynomial through the numerical derivatives and algebraically finding the point of half-maximum slope.

Only parts a, b and c of each test set were thus analysed. For each of the above methods the graphically-obtained residual current signal was subtracted from the total current at half-maximum slope to obtain the oxygen tension equivalent at the point of half-maximum slope.

Program KOK10 is listed in Appendix 5.4. In Figure 5.11 is shown the last part of the oxygen tension-time curve obtained during test 2a together with its sixth-order least-square polynomial; the least-square hyperbola and polynomial of the numerical derivatives of test 2a are shown in Figure 5.12.

The oxygen tensions at the points of half-maximum slope obtained graphically and by means of Program KOK10 are compared in Table 5.10.

The differences between the oxygen tensions obtained by the graphical method and each of the three numerical methods are listed in Table 5.11 as percentages of the graphically-obtained results.

The average absolute differences were 115%, 149% and 7.4% respectively for methods 2, 3 and 4. During 33 calculations, methods 2 and 3 obtained 4 and 6 estimates respectively which were within 10% of the graphically-obtained values. Method 4 obtained 26 estimates of the oxygen tension at half-maximum slope within 10% of the graphically-obtained values during 35 calculations. Three estimates obtained with method 4 were not within 20% of the values obtained with method 1.

Both methods 2 and 3 yielded results so different from the graphically-obtained ones that the effectiveness

FIGURE 5.11

Comparison of the Last Part of the Oxygen Tension-Time Curve Obtained During Test 2a (Fermentation 1)(o) With the Least-Square Sixth-Order Polynomial Calculated By Program KOK10

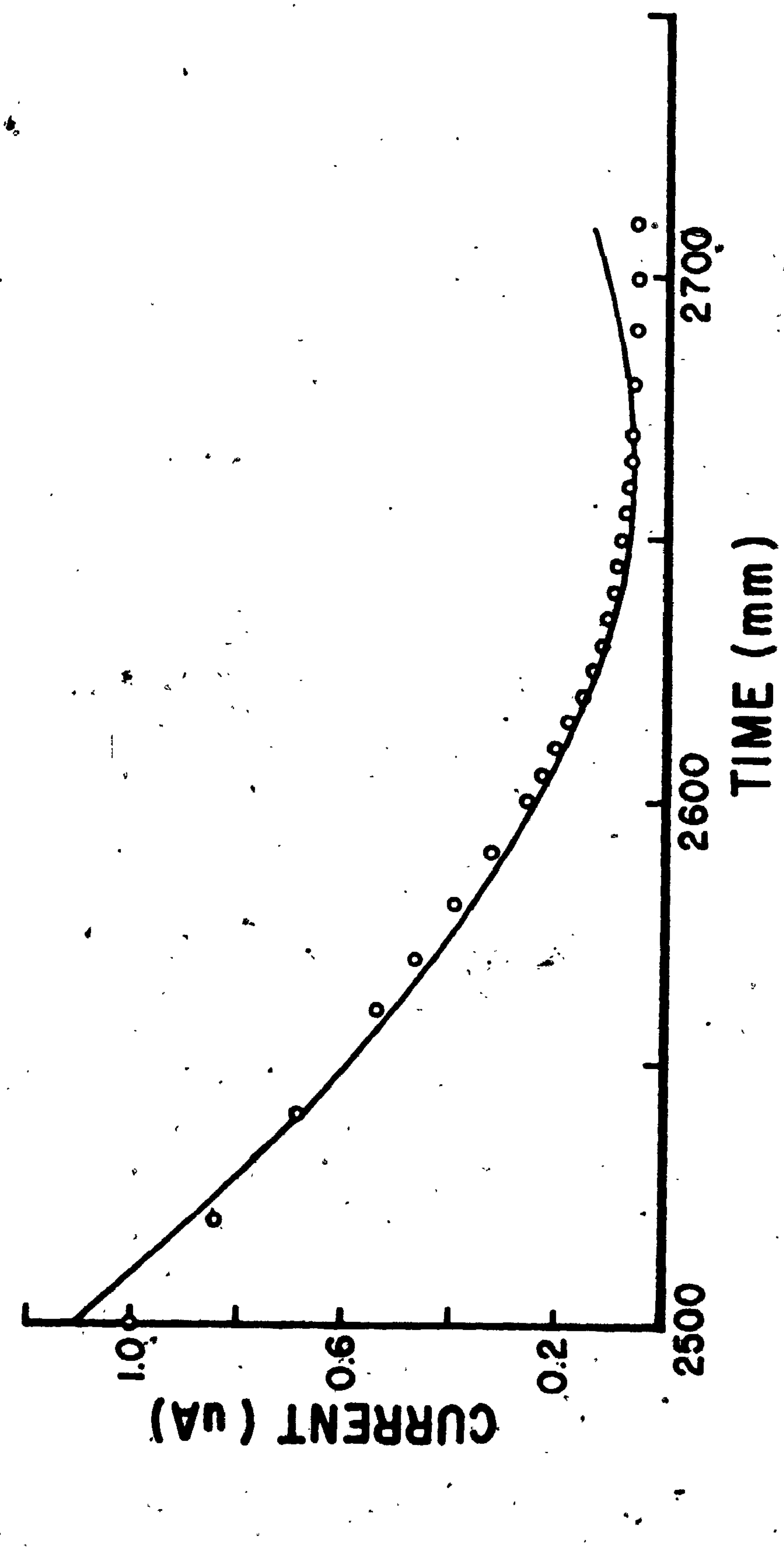

CURRENT (uA)
1.0
0.6
0.2
2500
2600
2700
TIME (mm)

FIGURE 5.12

The Numerical Derivatives of the Last Part of the Oxygen Tension-Time Curve Obtained During Test 2a (Fermentation 1) (o) and the Least-Square Hyperbola (Curve 1) and the Least-Square Sixth-Order Polynomial (Curve 2) Calculated By Program KOK10

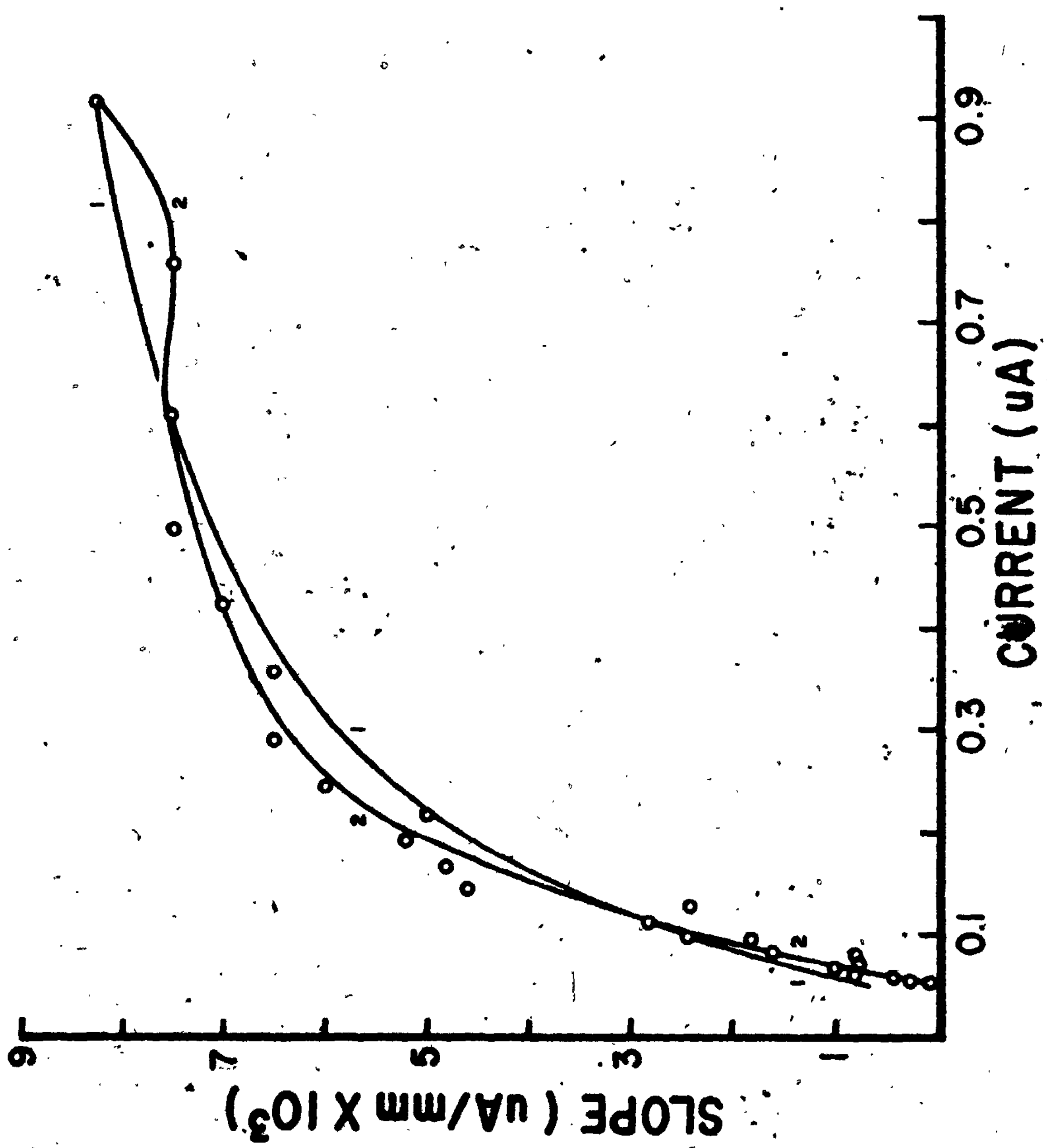
SLOPE (uA/mm X 10³)
1
3
5
7
9
CURRENT (uA)
0.1
0.3
0.5
0.7
0.9
1
2

TABLE 5.10

Oxygen Tensions At Points of Half-Maximum Slope. Method 1-Graphical; Method 2-Derivative of the Fitting Polynomial; Method 3-Hyperbola Plotted Through the Numerical Derivatives; Method 4-Polynomial Plotted Through the Numerical Derivatives

Test and Period No.	Part No.	Oxygen Tensions At Points of Half-Maximum Slope ($Atm \times 10^4$) Method 1	Method 2	Method 3	Method 4
2	a	7.45	8.09	8.63	7.63
	b	7.63	9.73	8.72	8.00
	c	8.73	45.99	20.90	9.00
3	a	11.66	80.39	12.88	11.98
	b	12.31	10.93	17.20	12.31
	c	12.15	16.55	13.37	12.47
4	a	13.06	160.59	13.24	12.14
	b	11.64	21.01	11.70	10.53
	c	8.56	12.57	10.23	9.18
5	a	9.95	9.05	10.52	9.29
	b	8.48	10.35	66.69	8.97
	c	7.83	11.66	29.11	8.56
6	a	6.27	7.37	N.A.*	6.93
	b	5.91	8.90	7.66	6.06
	c	6.71	9.19	8.68	6.20

TABLE 5.10 (continued)

Test and Period No.	Part No.	Oxygen Tensions At Points of Half-Maximum Slope (Atm x 10^4) Method 1	Method 2	Method 3	Method 4
7	a	6.35	9.66	82.89	7.87
	b	5.37	7.42	10.64	6.80
	c	6.08	8.85	N.A.	6.08
8	a	12.52	52.42	12.68	12.52
	b	12.43	52.58	16.38	12.26
	c	10.84	17.81	12.43	10.92
9	a	6.59	10.04	15.83	7.39
	b	N.A.	N.A.	N.A.	N.A.
	c	6.75	8.60	52.07	7.23
10	a	6.09	6.40	11.95	6.32
	b	5.00	5.15	41.15	6.25
	c	6.64	10.85	10.23	7.34
11	a	12.85	20.06	14.52	13.99
	b	11.62	16.02	12.50	12.06
	c	11.88	20.59	14.96	13.20
12	a	12.01	N.A.	12.15	10.87
	b	10.95	13.36	33.48	9.60
	c	9.74	13.22	31.91	9.60
13	a	7.96	9.03	10.55	8.05
	b	6.44	N.A.	8.05	7.60
	c	7.24	10.10	13.32	7.15

*N.A. - Not Available

TABLE 5.11

Differences Between The Oxygen Tensions At The Half-Maximum Slopes Obtained By Graphical and Numerical Means As Percentages of the Graphical Results

Test And Period No.	Part No.	Differences (%)		
		Method 2	Method 3	Method 4
2	a	8.6	15.8	2.4
	b	27.5	14.3	4.8
	c	426.8	139.4	3.1
3	a	589.4	10.5	2.7
	b	-11.2	39.7	0.0
	c	36.2	10.0	2.6
4	a	1129.6	1.4	-7.0
	b	80.5	0.5	-9.5
	c	46.8	19.5	7.2
5	a	0.0	5.7	-6.7
	b	22.1	686.4	5.8
	c	48.9	271.8	9.3
6	a	17.5	N.A.*	10.5
	b	50.6	29.6	2.5
	c	37.0	29.4	-7.6

TABLE 5.11 (continued)

Test And Period No.	Part No.	Differences (%)		
		Method 2	Method 3	Method 4
7	a	52.1	1205.9	23.9
	b	38.2	98.1	26.6
	c	45.6	N.A.	0.0
8	a	318.7	1.3	0.0
	b	323.0	31.8	1.4
	c	64.3	14.7	0.7
9	a	52.4	140.2	12.1
	b	N.A.	N.A.	N.A.
	c	27.4	671.4	7.1
10	a	5.1	96.2	3.8
	b	3.0	723.0	25.0
	c	63.4	54.1	10.5
11	a	56.1	13.0	8.9
	b	37.9	7.6	3.8
	c	73.3	25.9	11.1
12	a	N.A.	1.2	-9.5
	b	22.0	205.8	-12.3
	c	35.7	227.6	-1.4
13	a	18.44	32.5	1.1
	b	N.A.	25.0	18.0
	c	39.5	84.0	-1.2

*N.A. - Not available

of these methods could be readily dismissed.

The average difference between the oxygen tension values obtained by graphical means and by plotting the least-square sixth-order polynomials through the numerical derivatives is useful in estimating the error in the graphically determined values. Since the same residual current signal was used to compute both these values and its error is not known, a reasonable estimate of the error in the oxygen tension at half-maximal slope would be 20%.

5.12 Operating Conditions and Results For Fermentation 2

5.12.1 Conditions During the Fermentation

The time-invariant operating conditions for Fermentation 2 are listed in Table 5.12. Results from the dry weight, carbohydrate and pH analyses are recorded in Appendix 5.5.

Fermentation 2 was divided into seven periods. The time-variant parameters were determined at the beginning of each period. The first period comprised the batch fermentation. The time-variant operating conditions during the continuous fermentation were the dissolved oxygen tension and the dilution rate. The values of these variables are listed in Table 5.13 together with the observed average values of carbohydrate (as glucose) and dry weight concentrations and pH. All calculations were performed in the same manner as described in section 5.11.1. Data obtained

TABLE 5.12

Time-Variant Operating Conditions For Fermentation 2

Inoculation	1:00 p.m. June 20, 1973
Operating Temperature	23°C ± 0.5°C
pH Control Addition Cycle	5 seconds
pH Control Stirring Cycle	15 seconds
Agitator Speed	500 rpm
Start of Continuous Feed	1:00 p.m. June 21, 1973
Operating Volume	9.5 liters

TABLE 5.13

Time-Variant Operating Conditions And Parameters For Fermentation 2, Confidence Intervals Calculated At 0.95 Confidence Level

Period No.	Time (Hrs. After Inoculation)		Samples Included	Time Variant Operating Conditions		Observed Parameters		
	Start	Finish		Dissolved Oxygen Tension (% Saturation)	Average Dilution Rate (Hr^{-1}) ± 5%	Carbohydrate Concentration (As Glucose mg/l) And Confidence Interval	Dry Weight Concentration (gm/l) And Confidence Interval	Average pH
2	242.5	335.0	41-54	50 ± 2	0.054	43.1 ± 0.9	1.45 ± 0.03	5.1
3	361.0	433.0	59-71	10 ± 2	0.054	40.9 ± 0.9	1.30 ± 0.05	5.1
4	457.0	527.0	75-86	5 ± 2	0.054	35.8 ± 1.0	1.13 ± 0.04	5.1
5	553.0	623.0	91-102	50 ± 2	0.068	44.0 ± 1.8	1.51 ± 0.06	5.0
6	648.3	719.0	107-118	10 ± 2	0.068	40.7 ± 3.6	1.38 ± 0.04	5.1
7	745.0	812.0	123-135	5 ± 2	0.068	38.8 ± 1.6	1.34 ± 0.04	5.1

during the first 24 hours after a change in time-variant operating conditions were not used in the calculations. This was twice the period allowed during Fermentation 1. The equivalent of at least four reactor residence times were allowed for process stabilization and adaptation of *C. lipolytica* after a change in time-variant operating conditions before a set of oxygen tension-time curves was obtained. Two reactor residence times had been allowed for stabilization during Fermentation 1.

5.12.2 Shapes and Initial Slopes of the Oxygen Tension-Time Curves (YSI Probe)

The oxygen tension-time curves were obtained in the manner described in section 5.10..

The initial parts of the four curves obtained at the end of period 4 are shown in Figure 5.13. The curves had the same general shape as those obtained during Fermentation 1 but exhibited a shorter linear portion. This decreased the certainty with which the maximum slopes could be obtained. The maximum slopes are recorded in Table 5.14 together with the time-variant operating conditions and the initial glucose concentrations.

FIGURE 5.13

Initial Parts of the Oxygen Tension-Time Curves Obtained At the End of Period 4 With the YSI Probe (Fermentation 2)

	Part
□	a
○	b
●	c
×	d

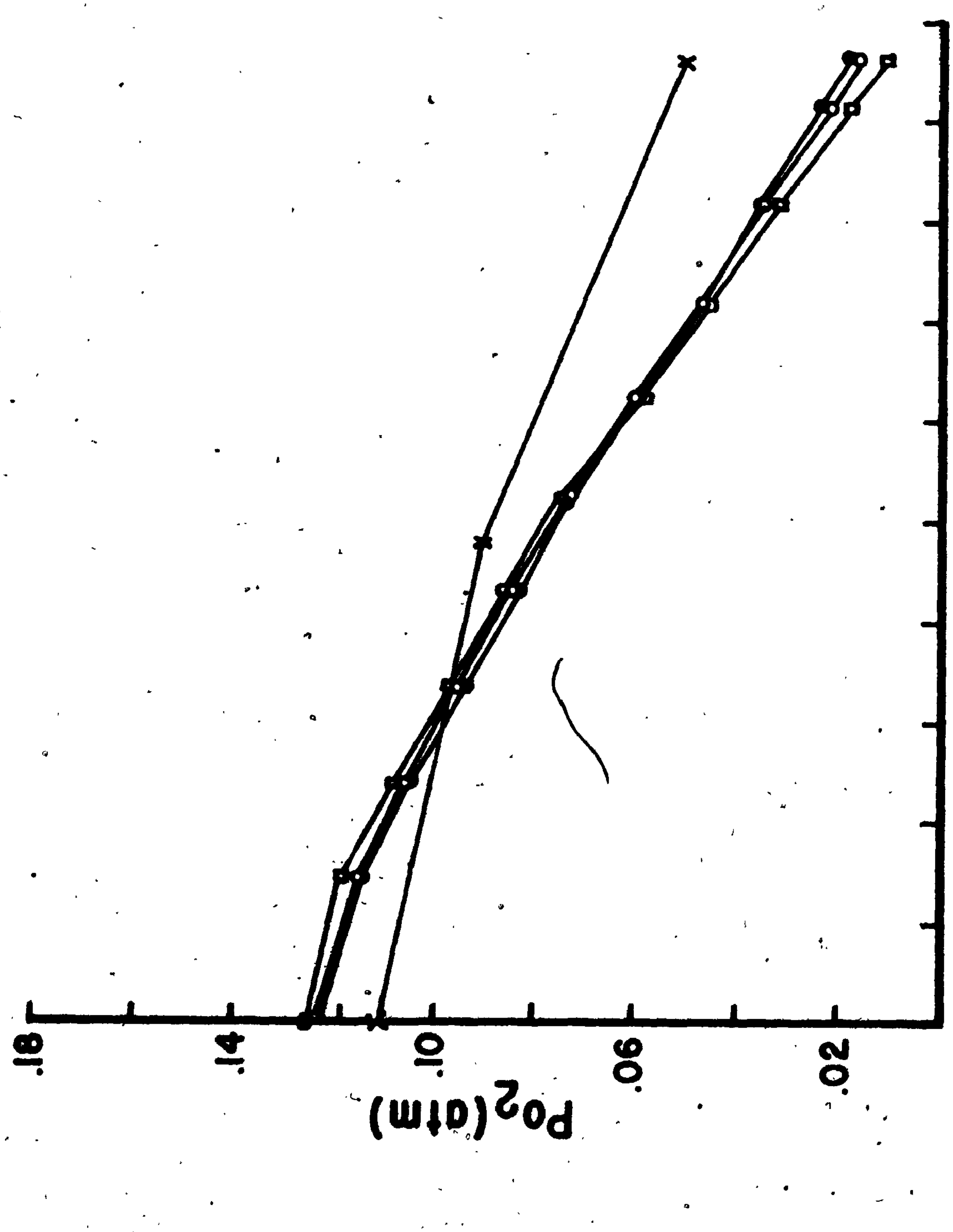
.18
.14
.10
.06
.02
P_{O_2}(atm)
50
150
250
350
450
TIME (SEC.)

TABLE 5.14

Maximum Slopes of Oxygen Tension-Time Curves (YSI Probe)

Test and Period No.	Part No.	Oxygen Tension During Growth (% Air Saturation) (±2%)	Dilution Rate (Hr^{-1})	Initial Glucose Concentration (mg/l)	Maximum Slope (Atm O_2/sec/(gm/l)) x 10^4
2	a	50	0.054	313	5.65
	b			115	4.97
	c			79	5.01
	d			50	3.74**
3	a	10	0.054	311	7.23
	b			113	6.57
	c			77	6.56
	d			48	3.53**
4	a	5	0.054	306	10.39
	b			108	9.30
	c			72	8.98
	d			43	3.02**
5	a	50	0.068	314	6.94
	b			116	6.73
	c			80	6.85
	d			51	8.12**
6	a	10	0.068	314	8.53
	b			113	8.26
	c			77	8.04
	d			48	5.04**
7	a	5	0.068	309	8.98
	b			111	9.08
	c			75	9.65
	d			46	6.44**

** Obtained from first two tabulated points

5.12.3 Oxygen Tensions at Half-Maximum Slope (YSI Probe)

The method to obtain the oxygen tensions at the points of half-maximum slope was discussed in section 5.11.

The final parts of the curves obtained during tests 4a to 4c are shown in Figures 5.14 to 5.16.

The oxygen tensions at half-maximum slope obtained graphically and by means of Program KOK10 from the least-square sixth-order polynomial plotted through the numerical derivatives are compared in Table 5.15 together with their differences as percentages of the graphically obtained oxygen tensions.

The absolute average difference was 6.9%. Out of 18 calculations Program KOK10 yielded 14 values within 10% of the graphically obtained ones. Only one value was not within 20%.

5.13 Results For Fermentation 2 With the Dropping Mercury Polarograph

5.13.1 Shapes and Initial Slopes of the Oxygen Tension-Time Curves (DME)

The oxygen tension-time curves were obtained by measuring the polarograph's current output, subtracting the residual current at the end of each test and dividing by the polarograph's calibration constant. The initial parts of the four curves obtained at the end of period 6 are shown in Figure 5.17. The maximum slopes are recorded in Table 5.16

FIGURE 5.14

The Final Part of the Oxygen Tension-Time Curve Obtained With the YSI Probe During Test 4a (Fermentation 2) Together With the Geometrical Construction To Determine the Oxygen Tension At Half-Maximum Slope

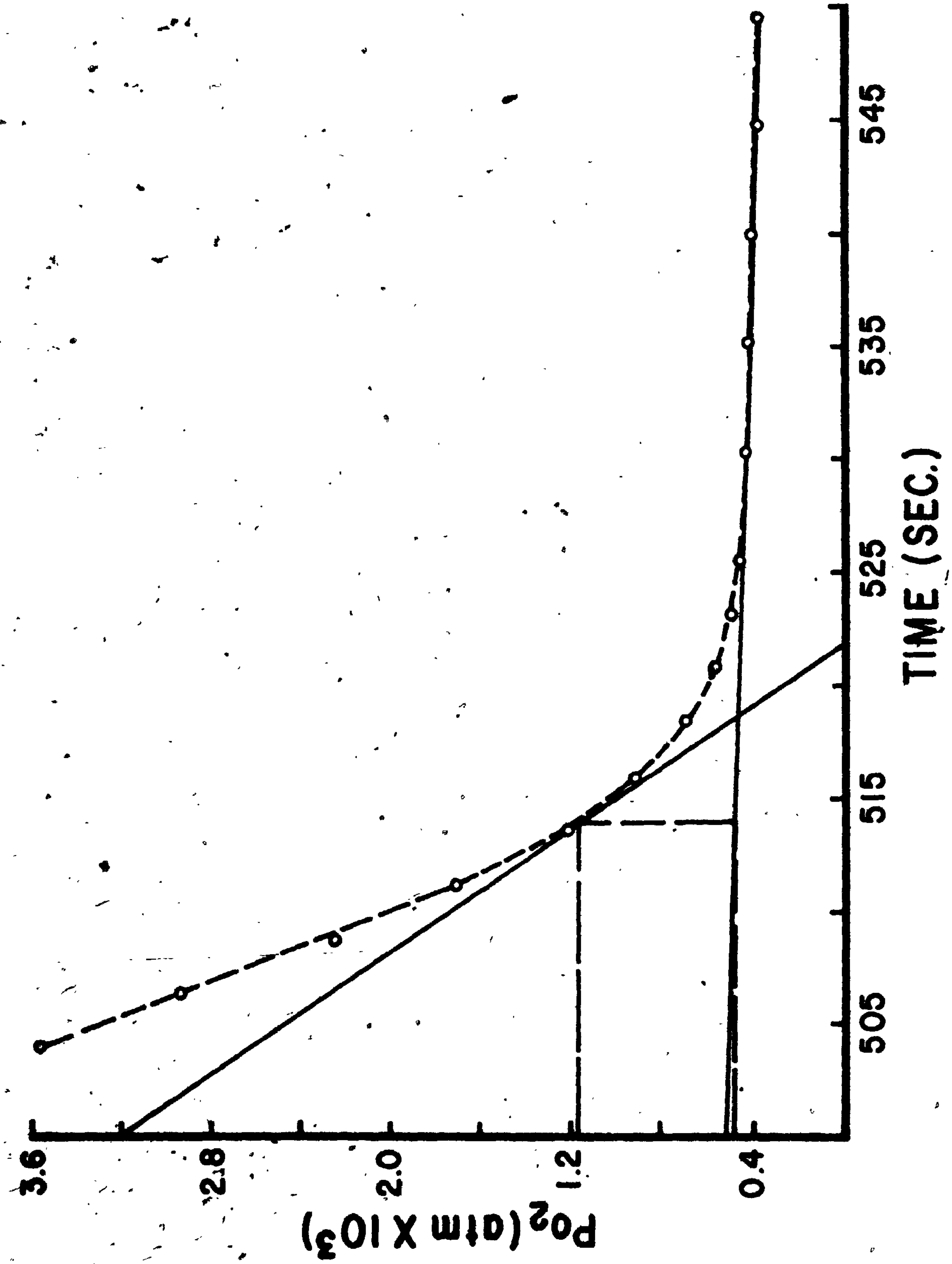
TIME (SEC.)
505
515
525
535
545
P_{O_2} (atm X 10^3)
3.6
2.8
2.0
1.2
0.4

FIGURE 5.15

The Final Part of the Oxygen Tension-Time Curve Obtained With the YSI Probe During Test 4b (Fermentation 2) Together With the Geometrical Construction To Determine the Oxygen Tension At Half-Maximum Slope

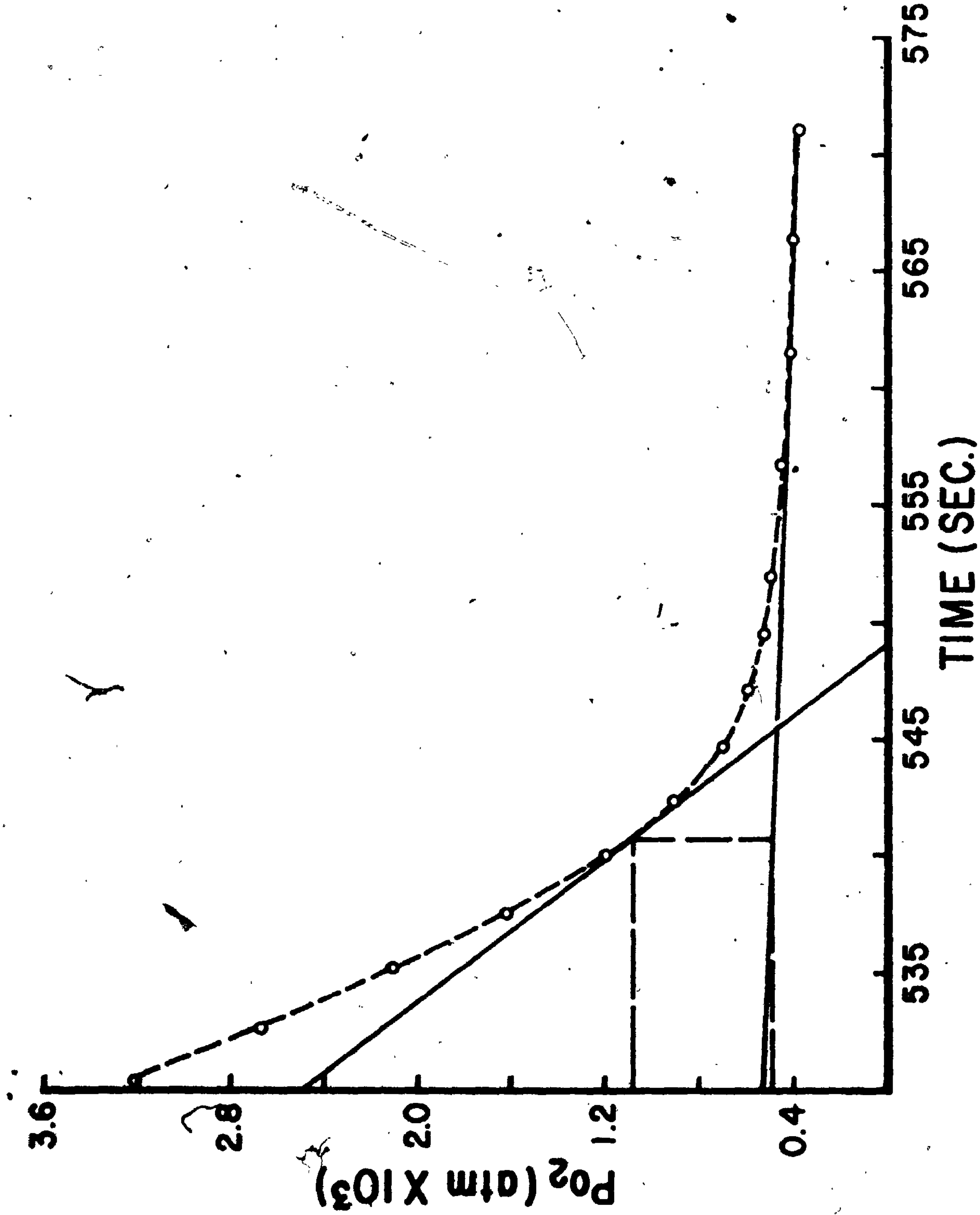

575
565
555
545
535
TIME (SEC.)
3.6
2.8
2.0
1.2
0.4
P_{O_2} (atm X 10^3)

FIGURE 5.16

The Final Part of the Oxygen Tension-Time Curve Obtained With the YSI Probe During Test 4c (Fermentation 2) Together With the Geometrical Construction To Determine the Oxygen Tension At Half-Maximum Slope

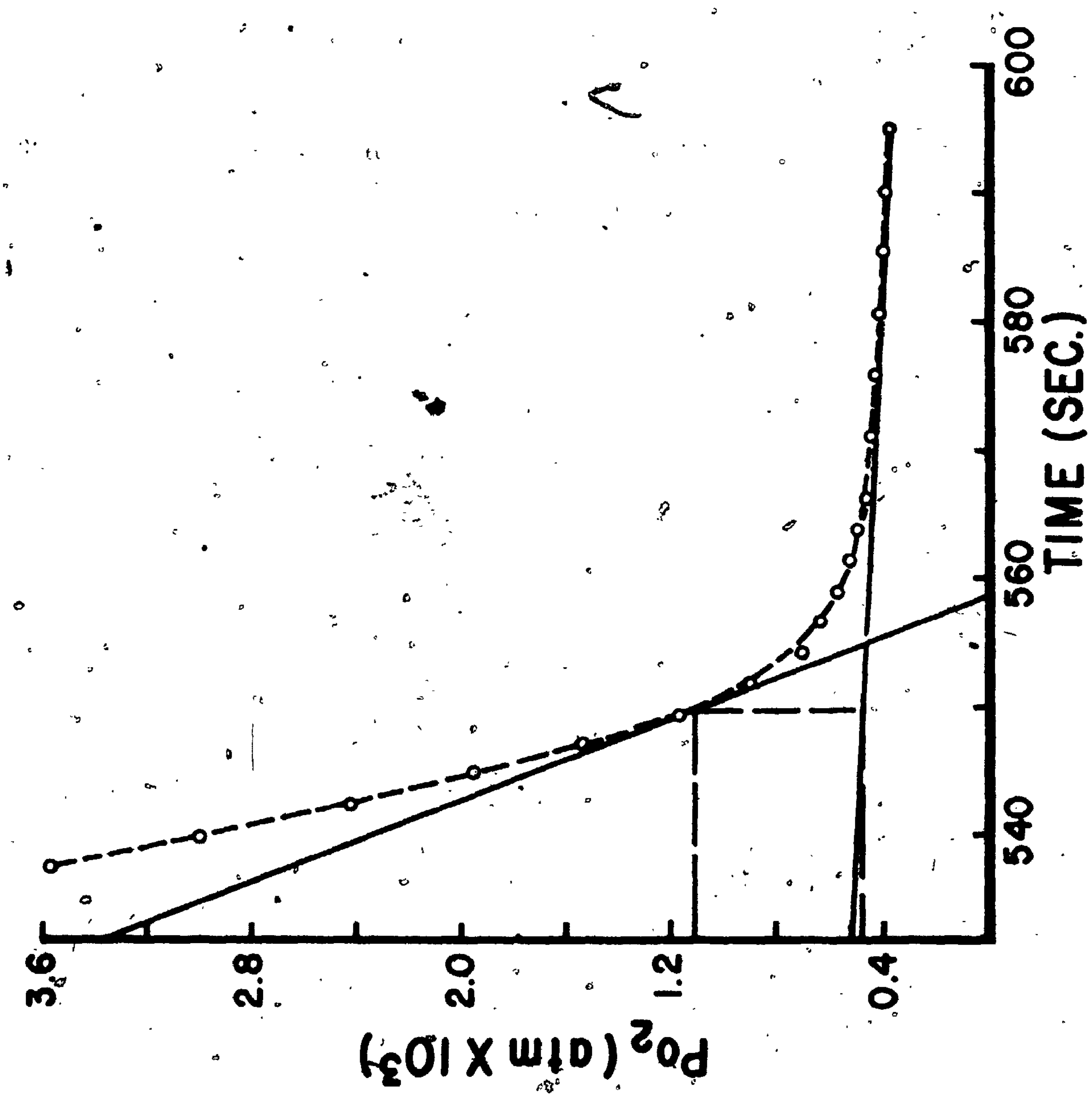

3.6
2.8
2.0
1.2
0.4
Po2 (atm X 10³)
540
560
580
600
TIME (SEC.)

TABLE 5.15

Oxygen Tensions At Points of Half-Maximum Slope and Their Differences As Percentages of the Graphically-Obtained Values

Test and Period No.	Part No.	Oxygen Tensions At Points of Half-Maximum Slope ($Atm \times 10^4$): Obtained By Graphical Means	Oxygen Tensions At Points of Half-Maximum Slope ($Atm \times 10^4$): Obtained From Program KOK10 (Method 4)	Differences (%)
2	a	9.99	9.60	-3.9
	b	10.31	10.46	1.5
	c	9.37	9.76	4.2
3	a	6.17	6.79	10.0
	b	6.01	6.64	10.5
	c	6.17	6.56	6.3
4	a	6.87	7.18	4.5
	b	6.30	6.17	-2.1
	c	6.30	6.80	7.9
5	a	12.49	12.35	-1.1
	b	11.67	11.67	0.0
	c	12.99	11.75	-9.5
6	a	7.06	6.68	-5.4
	b	6.84	6.99	2.2
	c	5.47	6.91	26.3
7	a	8.06	8.43	4.6
	b	7.39	6.95	-6.0
	c	6.65	7.84	17.9

FIGURE 5.17

Initial Parts of the Oxygen Tension-Time Curves Obtained At the End of Period 4 With the DME (Fermentation 2)

	Part
□	a
o	b
●	c
×	d

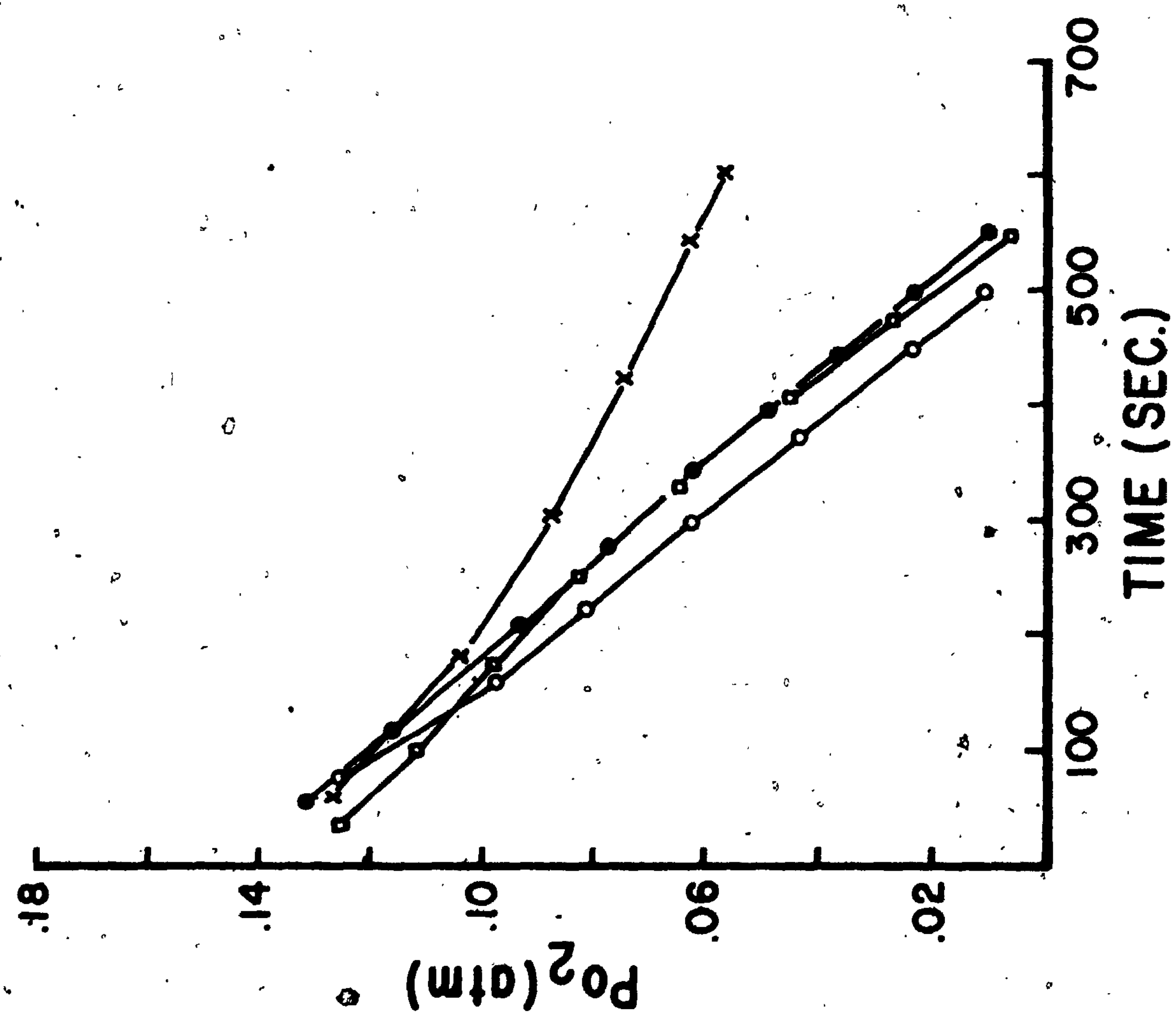

TIME (SEC.)
100
300
500
700
P_{O_2} (atm)
.18
.14
.10
.06
.02

TABLE 5.16

Maximum Slopes of Oxygen Tension-Time Curves (DME)

Test And Period No.	Part No.	Oxygen Tension During Growth (% Air Saturation) ±2%	Dilution Rate (Hr^{-1})	Initial Glucose Concentration (mg/l)	Maximum Slope (Atm O_2/sec/(gm/l)) x 10^4
2	a	50	0.054	313	5.72
	b			115	6.44
	c			79	6.16
	d			50	4.08**
3	a	10	0.054	311	7.80
	b			113	7.84
	c			77	7.16
	d			48	4.44**
4	a	5	0.054	306	8.56
	b			108	10.24
	c			72	8.72
	d			43	3.04**
5	a	50	0.068	314	6.64
	b			116	6.80
	c			80	6.56
	d			51	3.36**
6	a	10	0.068	311	7.60
	b			113	7.44
	c			77	7.20
	d			48	3.32**
7	a	5	0.068	309	8.20
	b			111	8.24
	c			75	8.24
	d			46	3.68**

**Obtained from PTS at 200 and 500 seconds.

together with the time-variant operating conditions and the initial glucose concentrations. The maximum slopes for the d-parts of the tests were calculated from the coordinates of the observations made after 200 and 500 seconds. The observations obtained during the initial 200 second period could not be used since the liquid swirling in the polarograph's test vessel took at least that long to subside.

5.13.2 Oxygen Tensions at Half-Maximum Slope (DME)

The oxygen tensions at the points of half-maximum slope were obtained graphically and by the three numerical methods by means of Program KOK10. Program KOK10 utilized only those data below an oxygen tension of 8.35×10^{-3} atm oxygen for these calculations.

The final parts of the curves obtained during tests 2a to 2c are shown in Figures 5.18 to 5.20 together with their lines of half-maximum slope.

The oxygen tensions at half-maximum slope obtained graphically and by means of Program KOK10 are compared in Table 5.17. The differences between the oxygen tensions obtained by the graphical method and each of the three numerical methods are listed in Table 5.18 as percentages of the graphically obtained results.

The average absolute differences were 19.3%, 120.7% and 6.9% respectively for methods 2, 3 and 4. Method 4 obtained 14 out of 18 estimates within 10% of the graphical

FIGURE 5.18

The Final Part of the Oxygen Tension-Time Curve Obtained With the DME During Test 2a (Fermentation 2) Together With the Geometrical Construction To Determine the Oxygen Tension At Half-Maximum Slope

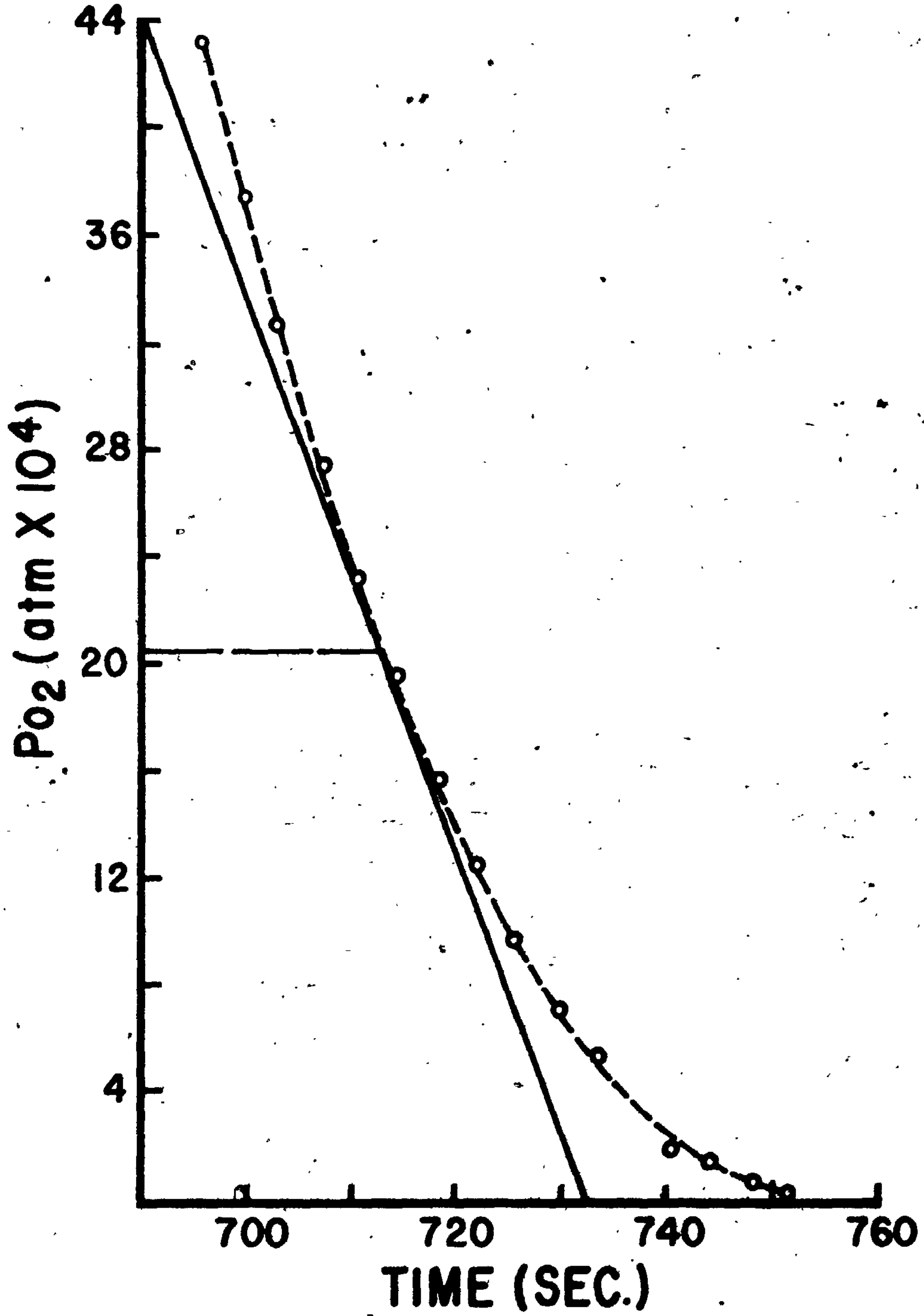
44
36
28
20
12
4
P_{O_2} (atm X 10^4)
700
720
740
760
TIME (SEC.)

FIGURE 5.19

The Final Part of the Oxygen Tension-Time Curve Obtained With the DME During Test 2b (Fermentation 2) Together With the Geometric Construction To Determine the Oxygen Tension At Half-Maximum Slope

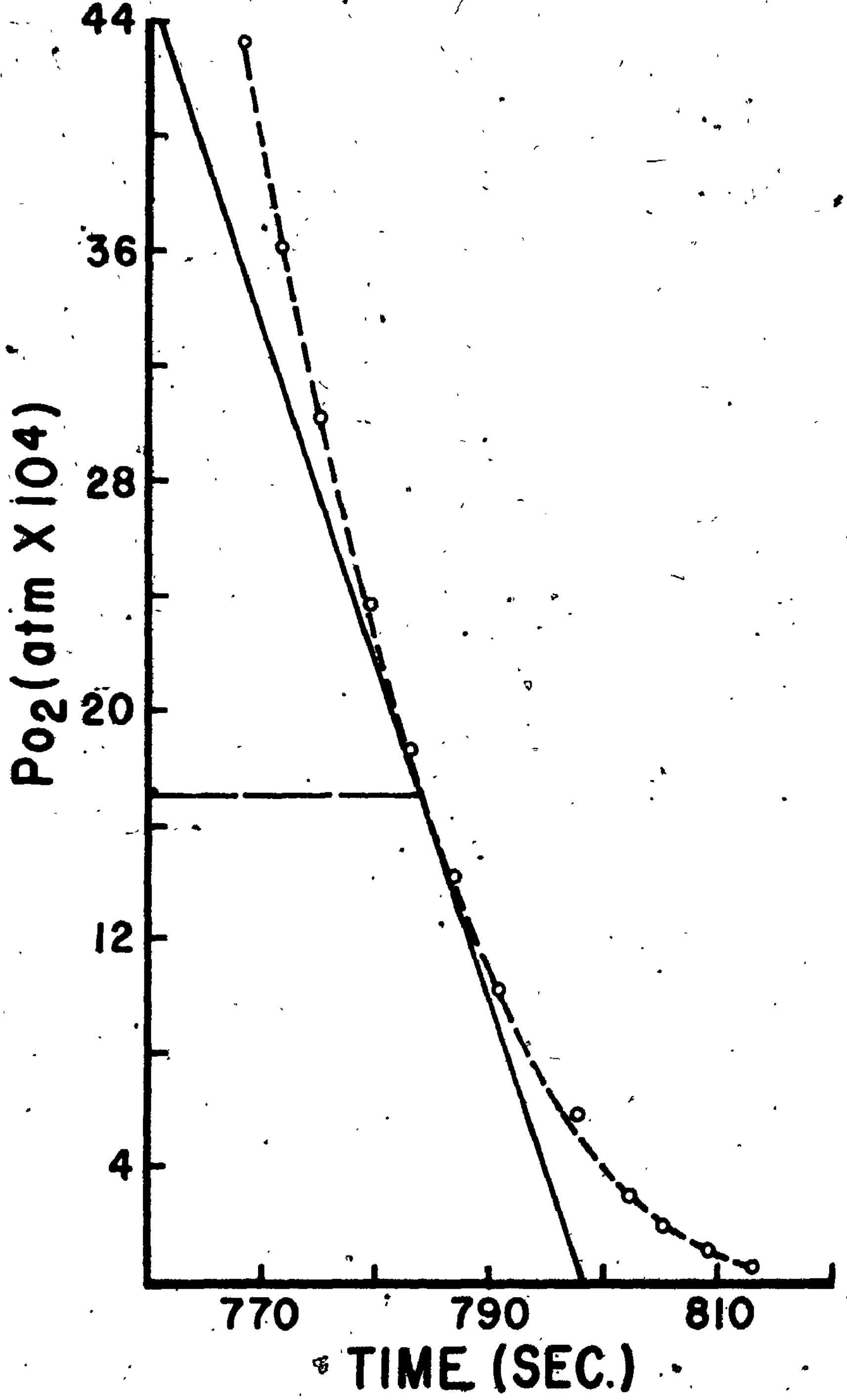
44
36
28
20
12
4
Po2 (atm X 104)
770
790
810
TIME (SEC.)

FIGURE 5.20

The Final Part of the Oxygen Tension-Time Curve Obtained With the DME During Test 2c (Fermentation 2) Together With the Geometric Construction To Determine the Oxygen Tension At Half-Maximum Slope

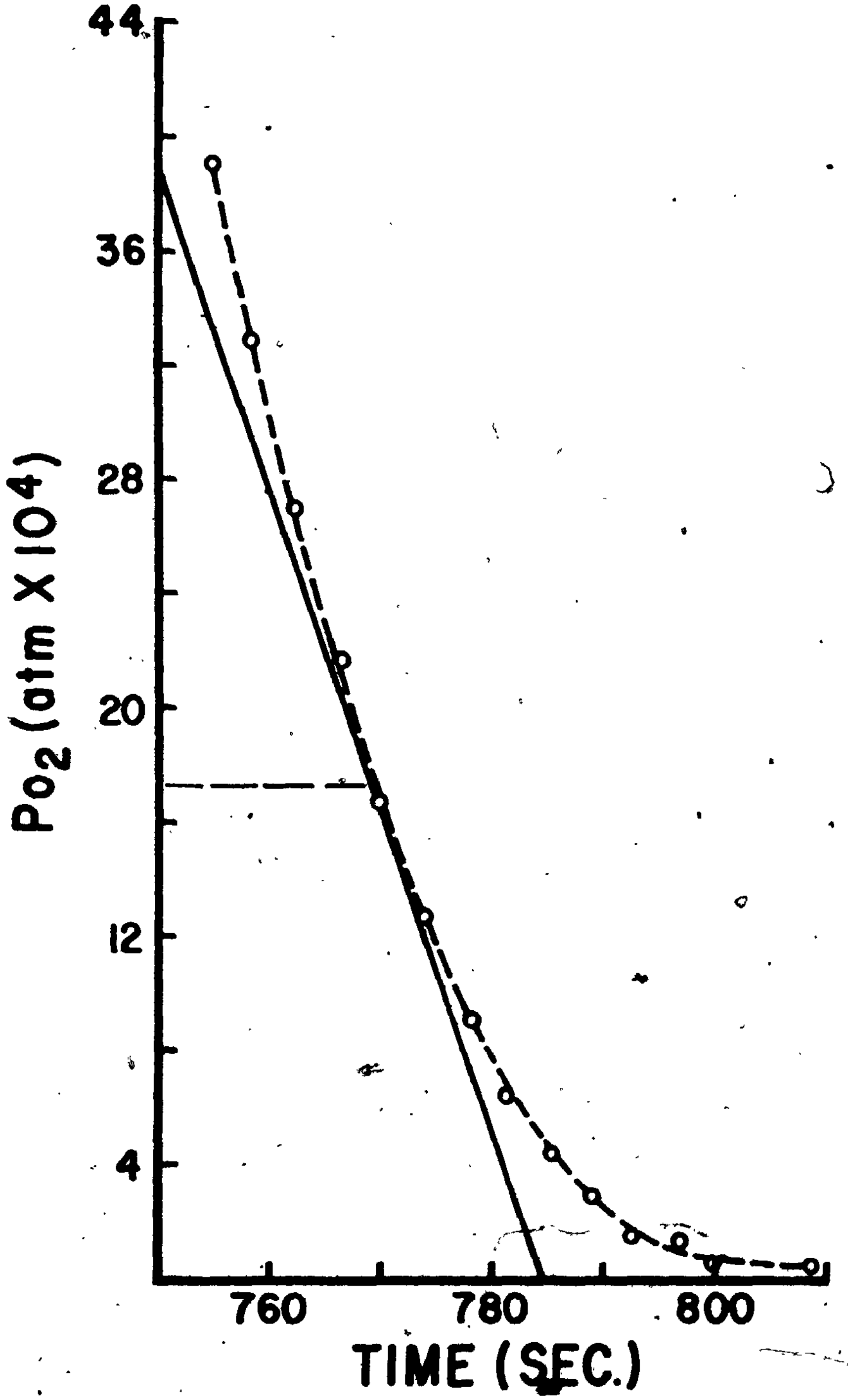
44
36
28
20
12
4
Po_2 (atm X 10^4)
760
780
800
TIME (SEC.)

TABLE 5.17

Oxygen Tensions At Points of Half-Maximum Slope Obtained With the Dropping Mercury Polarograph. Method 1-Graphical; Method 2-Derivative of the Fitting Polynomial; Method 3-Hyperbola Plotted Through the Numerical Derivatives; Method 4-Polynomial Plotted Through the Numerical Derivatives

Test and Period No.	Part No.	Oxygen Tensions At Points of Half-Maximum Slope ($Atm \times 10^4$) Method 1	Method 2	Method 3	Method 4
2	a	19.6	20.1	35.3	17.2
	b	15.7	16.5	32.5	15.3
	c	16.4	16.3	23.4	15.5
3	a	10.4	11.3	16.3	10.7
	b	11.0	14.2	23.7	13.0
	c	9.7	6.0	46.8	10.5
4	a	13.8	20.2	51.9	13.7
	b	19.5	21.9	31.9	19.6
	c	12.7	3.9	48.8	10.1
5	a	33.8	36.0	48.8	32.5
	b	32.4	33.8	50.8	30.7
	c	25.7	25.3	40.9	27.3
6	a	22.7	26.9	35.5	24.5
	b	25.2	38.3	36.2	25.6
	c	22.6	23.9	25.8	22.4
7	a	9.4	10.8	12.5	10.9
	b	11.4	10.0	51.2	12.3
	c	9.0	10.7	18.6	8.6

TABLE 5.18

Differences Between The Oxygen Tensions At The Half-Maximum Slopes

Obtained By Graphical and Numerical Means As Percentages of The Graphical Result

Test and Period No.	Part No.	Differences (%) Method 2	Method 3	Method 4
2	a	2.6	80.1	-12.2
	b	5.1	107.0	- 2.5
	c	-0.6	42.7	- 5.5
3	a	8.7	56.7	2.9
	b	29.1	115.5	18.2
	c	-38.1	382.5	8.2
4	a	46.4	276.1	0.7
	b	12.3	63.6	0.5
	c	-69.3	284.3	-20.5
5	a	6.5	44.4	- 3.2
	b	4.3	56.8	- 5.2
	c	-1.6	-59.1	6.2
6	a	18.5	56.4	7.9
	b	52.0	43.7	1.6
	c	5.8	14.2	- 0.9
7	a	14.9	33.0	16.0
	b	-12.3	349.1	7.9
	c	18.9	106.7	- 4.4

values. Only one estimate was not within 20%.

5.14 Discussion

5.14.1 The Effect of Dissolved Oxygen Tension and Dilution Rate on Cell Concentration

The carbohydrate and dry weight concentrations obtained during both Fermentations 1 and 2 are listed together with the dilution rates and dissolved oxygen tensions in Table 5.19. The linear coefficients of partial correlation [62] between the time-variant operating conditions and the observed parameters are listed in Table 5.20. The best correlation was obtained between the oxygen tension and the glucose concentration. This could be interpreted as an indication that the dissolved oxygen tension to which *C. lipolytica* was adapted influenced the cells' metabolism so as to alter the glucose concentration-growth rate relationship. However, the latter seemed to be influenced by other, unknown factors since no correlation of significance could be found between the dilution rate and the glucose concentration. Any such effect of the dilution rate on the glucose concentration would have been rather small since the maximum value of the dilution rate was only 0.068 hr^{-1}. It could easily be substantially masked by the uncertainty of the glucose measurement.

TABLE 5.19

Time Variant Operating Conditions and Parameters For Fermentations 1 and 2 - Confidence Intervals Were Calculated At 0.95 Confidence Level

		Time Variant Operating Conditions		Observed Parameters	
Fermentation No.	Period No.	Dissolved Oxygen Tension (% Air Saturation)	Dilution Rate (Hr^{-1}, ±5%)	Carbohydrate Concentration As Glucose (mg/1)	Dry Weight Concentration (gm/1)
1	3	50 ± 2	0.043	40.0 ± 0.7	0.93 ± 0.12
	5	20 ± 2	0.045	38.2 ± 1.1	1.53 ± 0.04
	7	5 ± 2	0.045	36.3 ± 2.1	1.38 ± 0.14
1	8	50 ± 2	0.031	41.2 ± 1.0	1.23 ± 0.04
	9	20 ± 2	0.031	43.8 ± 1.3	1.21 ± 0.03
	10	5 ± 2	0.031	39.0 ± 0.8	1.25 ± 0.02
1	11	50 ± 2	0.056	43.4 ± 1.9	1.82 ± 0.03
	12	20 ± 2	0.058	39.1 ± 1.6	1.85 ± 0.06
	13	5 ± 2	0.059	34.9 ± 1.0	1.67 ± 0.03
2	2	50 ± 2	0.054	43.1 ± 0.9	1.45 ± 0.03
	3	10 ± 2	0.054	40.9 ± 0.9	1.30 ± 0.05
	4	5 ± 2	0.054	35.8 ± 1.0	1.13 ± 0.04
2	5	50 ± 2	0.068	44.0 ± 1.8	1.51 ± 0.06
	6	10 ± 2	0.068	40.7 ± 3.6	1.38 ± 0.04
	7	5 ± 2	0.068	38.8 ± 1.6	1.34 ± 0.04

TABLE 5.20

Linear Coefficients of Partial Correlation Between The Time-Variant Operating Conditions and Observed Parameters For Fermentations 1 and 2

	Glucose Concentration	Cell Concentration
Oxygen Tension	0.695	0.090
Dilution Rate	0.037	0.450

The oxygen tension did not appreciably influence the dry weight, or cell concentration. The correlation coefficient of 0.450 between the cell concentration and the dilution rate is in itself not sufficiently large to warrant the drawing of a definite conclusion. If however this coefficient is calculated separately for Fermentations 1 and 2, values of 0.787 and 0.778 are obtained. This indicates that in both fermentations the dilution rate had a strong influence on the cell concentration; cell concentration and the efficiency of substrate glucose utilization increased markedly with dilution rate. The decrease in the correlation coefficient upon combination of the data from Fermentations 1 and 2 is an indication that the two fermentations were not comparable in operation.

5.14.2 Maximum Slopes of the Oxygen-Tension-Time Curves (YSI Probe)

The maximum slopes of the oxygen tension-time curves obtained with the YSI Probe are listed in Tables 5.9 and 5.14 for Fermentations 1 and 2 respectively.

During Fermentation 1 in all tests the maximum slopes of the oxygen tension-time curves decreased appreciably with a decreasing initial glucose concentration. During all tests starting at an initial glucose concentration of approximately 75 mg/l or higher (parts a-c) the initial parts of the curves were typically non-linear and increased in slope until a maximum value was reached. This slope (the 'maximum slope') was then maintained until the oxygen tension or glucose concentration became rate limiting. The tests performed with an initial glucose concentration of approximately 45 mg/l (parts d) yielded non-linear curves, which gradually decreased in slope. The behavior observed was very similar to that predicted by the double-substrate Michaelis-Menten model described in section 5.4.

During Fermentation 2 the decrease in maximum slope with decreasing initial glucose concentration was not nearly as pronounced nor as regular as it had been during Fermentation 1. The non-linear portion of the curves was much more extensive and a good estimate of the maximum slope was therefore difficult to obtain.

The initial non-linear portions of the curves are ascribed to the short-term adaptation of *C. lipolytica* to the sudden increase in glucose concentration and oxygen tension at the beginning of the test. This adaptation would comprise the establishment of steady-state diffusion gradients and the repression or induction of enzyme systems operation but not a decrease or increase in the cells' enzyme content.

The linear coefficients of partial correlation between the maximum slopes, the dissolved oxygen tension during growth, the dilution rate and the initial glucose concentration are listed in Table 5.21. For both Fermentation 1 and 2, negative correlation coefficients were obtained between the dissolved oxygen tension and the maximum slope. If the maximum slope of the oxygen tension-time curve is taken to be an indication of the potential respiration rate of *C. lipolytica* and thereby as a measure of the quantity of enzymes available in the respiratory system, the result obtained is that a lower dissolved oxygen tension during growth resulted in a higher respiratory system content of *C. lipolytica* cells. This result is in agreement with the results obtained by Moss [46] for *E. coli*, by Terui *et al.* [65] for *S. cerevisiae*, by Herbert [32] for *Bacillus megatherium* and by Moss and Rickard *et al.* [47, 48, 56, 57] for several yeasts. The higher correlation coefficient for Fermentation 2 could be due to the longer adaptation period allowed (four residence times as opposed to two during Fermentation 1).

Weak positive correlations were obtained between the dilution rate and the maximum slope. Following analogous reasoning to the above, an increase in dilution rate resulted in an increased respiratory system content of *C. lipolytica*. The positive correlations obtained between the initial glucose concentration and the maximum slope are in accordance with both the double-substrate Michaelis-Menten model presented in section 5.4 and Chance's [15] more complex model consisting of four interacting reactions.

TABLE 5.21

Linear Coefficients of Partial Correlation Between The Dissolved Oxygen Tension, The Dilution Rate, The Initial Glucose Concentration And the Maximum Slope of the Oxygen Tension-Time Curve

(Parts "d" not included)

Maximum Slope and:	Fermentation 1*	Fermentation 2
Dissolved Oxygen Tension	-0.465	-0.829
Dilution Rate	0.317	0.490
Initial Glucose Concentration	0.521	0.237

*Only results at 50, 20 and 5% air saturation included.

The low correlation coefficient between the maximum slope and the initial glucose concentration obtained for Fermentation 2 was again an indication that the tests performed during Fermentation 2 suffered from a severe, unidentified interference. During Fermentation 1 for all tests except 11c the maximum slope decreased as the initial glucose concentration was decreased. During Fermentation 2 tests 2c, 5c, 7b and 7c did not follow this pattern.

5.14.3 Oxygen Tensions at Half-Maximum Slope

The oxygen tensions obtained at half-maximum slope with the YSI probe are listed in Tables 5.10 and 5.15 for Fermentations 1 and 2, respectively. The linear coefficients of partial correlation between the graphically obtained values of oxygen tension at half-maximum slope and the dissolved oxygen tension during growth, the dilution rate and the initial glucose concentration are listed in Table 5.22.

A very strong correlation was obtained between the dissolved oxygen tension maintained during growth and the oxygen tension at half-maximum slope for both fermentations. If this phenomenon is considered in light of the model proposed by Chance [15] it would infer that a high oxygen tension during growth resulted in a low respiratory content in *C. lipolytica*. This conclusion concurs with that obtained in the previous section.

TABLE 5.22

Linear Coefficients of Partial Correlation Between The Dissolved Oxygen Tension, The Dilution Rate, The Initial Glucose Concentration and the Oxygen Tensions at Half-Maximum Slope (parts "d" not included)

Oxygen Tension At Half-Maximum Slope And:	Fermentation 1*	Fermentation 2
Dissolved Oxygen Tension	0.929	0.937
Dilution Rate	0.615	0.621
Initial Glucose Concentration	0.340	0.289

*Only results at 50, 20 and 5% air saturation included.

A positive correlation was obtained between the dilution rate and the oxygen tension at half-maximum slope. Again, if this result is interpreted in terms of Chance's [15] model it would signify a decrease in the respiratory system content. This conclusion is however at variance with the result obtained in the previous section. This apparent paradox can be explained by considering the effect of the oxygen consumption rate on the oxygen tension at half-maximum slope. Since the oxygen consumption rate (or maximum slope) was found to increase with the dilution rate at which *C. lipolytica* was grown, and since the oxygen tension at half-maximum slope was a function of the consumption rate, the observed correlation may be a secondary one, resulting from the effect of the dilution rate influencing the initial slope which was in turn then affecting the oxygen tension at which the slope was one-half its maximal value. The same consideration may of course also be applied to the conclusion drawn above concerning the effect of the oxygen tension during growth on the oxygen tension at half-maximum slope.

A weak positive correlation was obtained between the initial glucose concentration and the oxygen tension at half-maximum slope. The rather substantial error in the measurement of the oxygen tension at half-maximum slope (estimated 20%), combined with the fairly small variations expected in this variable as a result of the changes in initial glucose concentration within each test set, could account for the low correlation coefficients obtained. For the calculation of the correlation coefficients only the data from parts a, b and c of each test set were used. The oxygen tensions at half-maximum slope for the d-parts were very high as predicted by the model described in section 5.4. For the higher initial glucose concentrations the results were in variance with this model which predicted increased oxygen tensions at half-maximum slope as the initial glucose concentration was decreased. The assumptions on which the model was based were therefore not entirely in keeping with reality. The results were however in agreement with the predictions of Chance's [15] model.

5.14.4 Comparison of the Data Obtained With the YSI Probe and the Dropping Mercury Electrode

The maximum slopes and oxygen tensions at half-maximum slope determined simultaneously with the YSI probe and the dropping mercury electrode during Fermentation 2 are compared in Table 5.23. The linear correlation coefficient between the two sets of maximum slopes was 0.814; the average absolute percentage difference between the values was 11%. The linear correlation coefficient between the two sets of oxygen tensions at half-maximum slope was 0.637; the average absolute percentage difference between the values was 122%. The values of the oxygen tensions at half-maximum slope obtained with the

TABLE 5.23

Comparison of Maximum Slopes and Oxygen Tension of Half-Maximum Slope Obtained With the YSI Probe and the DME (Fermentation 2)

		YSI Probe		DME	
Test and Period No.	Part No.	Maximum Slope Atm O_2/Sec/(gm/l) x 10^4	Oxygen Tension at Half-Maximum Slope (Atm x 10^4)	Maximum Slope Atm O_2/Sec/(gm/l) x 10^4	Oxygen Tension at Half-Maximum Slope (Atm x 10^4)
2	a	5.65	9.99	5.72	19.6
	b	4.97	10.31	6.44	15.7
	c	5.01	9.37	6.16	16.4
	d	3.74	-	4.08	-
3	a	7.23	6.17	7.80	10.4
	b	6.57	6.01	7.84	11.0
	c	6.57	6.17	7.16	9.7
	d	3.53	-	4.44	-
4	a	10.39	6.87	8.56	13.8
	b	9.30	6.30	10.24	19.5
	c	8.98	6.30	8.72	12.7
	d	3.02	-	3.04	-
5	a	6.94	12.49	6.64	33.8
	b	6.73	11.67	6.80	32.4
	c	6.85	12.99	6.56	25.7
	d	8.12	-	3.36	-
6	a	8.53	7.06	7.60	22.7
	b	8.26	6.84	7.44	25.2
	c	8.04	5.47	7.20	22.6
	d	5.04	-	3.32	-
7	a	8.98	8.06	8.20	9.4
	b	9.08	7.39	8.24	11.4
	c	9.65	6.65	8.24	9.0
	d	6.44	-	3.68	-

polarograph were always higher than those obtained with the YSI probe.

Had it been the dynamic lag of the YSI probe interfering with the measurement, the oxygen tension-time curves obtained with the probe would have decreased at a higher oxygen tension than the ones obtained with the polarograph. Therefore the oxygen tensions obtained at half-maximum slope with the YSI probe would have been the higher.

If it were assumed that the residual current signals subtracted from the YSI probe signals were erroneously large, it is pointed out that even if the former are substantially reduced the difference between the two sets of oxygen tensions at half-maximum slope are not much affected. For Fermentation 2 the average residual current of the YSI probe was 0.38 of the total current at half-maximum slope. For the polarograph this fraction was 0.82. An error in the determination of the residual current would have had therefore a much more pronounced effect on the results obtained with the polarograph than on those obtained with the YSI probe.

The most likely source of error in the determination of the oxygen tension at half-maximum slope by means of the polarograph is however the interpretation of the polarographic traces. The current proportional to the oxygen tension is the current at the end of the life of the mercury drop. As was pointed out in Chapter 3, the peak current observed on the polarographic trace is not necessarily coincident with the end of the drop life. This is especially so when the charge current is much larger than the signal current. On the polarographic traces obtained, no clear difference between the peak signal and the end of the drop life was apparent. Consequently, the peak current was used as being representative of the oxygen tension in solution, since a means of discriminating between this current and the current at the end of the drop life was lacking. This lack of differentiation could lead to considerable error.

Neither the derivatives of the oxygen tension-time curves produced by the YSI probe nor those produced by the polarograph could be satisfactorily fitted with a hyperbola. For the YSI data this was understandable enough since they were affected by the dynamic lag of the probe. That the data obtained with the polarograph suffered from a similar shortcoming casts further doubt upon their validity.

5.15 Conclusions to Chapter 5

A correlation coefficient of 0.695 was obtained between the oxygen tension during growth and the glucose concentration in the medium, whereas no correlation was found to exist between the oxygen tension and the cell concentration. The oxygen tension during growth therefore altered the relationship between the growth rate of *C. lipolytica* and the glucose concentration; the glucose concentration necessary to maintain a certain growth rate (assumed to be the same as the fermentor's dilution rate at steady state) increased slightly as the oxygen tension increased. The efficiency of conversion of glucose to cell substance was not influenced by the oxygen tension at the dilution rates tested. This efficiency was however affected by the dilution rate as indicated by a correlation coefficient of 0.450 between the dilution rate and the cell concentration. As pointed out in section 5.14.1, correlation coefficients of 0.787 and 0.778 are obtained between these two variables if they are calculated separately for the two fermentations. The decrease in substrate utilization efficiency with decreasing dilution rate can be ascribed to the increasing importance of endogenous metabolism as the dilution rate decreased.

Although close agreement between the oxygen tensions at half-maximum slope obtained with the YSI probe and the polarograph could not be found, a correlation coefficient of 0.814 was obtained between the maximum slopes of the curves. The absolute average percentage difference was 11%. In view of the unfavourable conditions (very extensive non-linear regions) this difference is not surprising. The straight lines drawn to determine the maximum slopes could not be calculated statistically since the inclusion and exclusion of data in this process would have been as subjective as the drawing of the lines themselves. The oxygen tension-time curves obtained during Fermentation 1 were of substantially more favourable nature for the purpose than those obtained during Fermentation 2. The discrepancy between the types of curves obtained during the two fermentations might be due to the difference in the period allowed for process stabilization after a change in time-variant operating parameters. These periods were two and four residence times respectively for the two fermentations. The nature of such a relationship between the shape of the oxygen tension-time curves and the stabilization period is not understood.

The data obtained during Fermentation 1 with the YSI probe were consistent and regular, thus at least partially justifying the argument that it was the polarograph which was in error and not the YSI probe. At worst, the results are only credible in a qualitative rather than a quantitative sense. The conclusions reached by the interpretation of the YSI probe data are therefore at least qualitatively sound.

From the values of the maximum slopes it was deduced that as the dissolved oxygen tension during growth was decreased, the respiratory system content of the *C. lipolytica* cells increased. This result was further supported by the trends of the oxygen tensions at half-maximum slope as determined with the YSI probe.

There was some indication that an increase in dilution rate resulted in an increase in respiratory system content of *C. lipolytica*. This was indicated by the positive correlation coefficient between the dilution rate and the maximum slope of the oxygen tension-time curves. The oxygen consumption rate acted as an intervening variable between the dilution rate and the oxygen tension obtained at half-maximum slope so that the relationship obtained between the latter two variables could not be considered significant. This intervention could have been accounted for by further statistical manipulation but in view of the small sample size and the large errors it was not deemed worthwhile.

The influence of the initial glucose concentration on the maximum slope and the oxygen tension at half-maximum slope was in accordance with Chance's [15] model of the respiratory system. The latter relationship was marred by the large uncertainties in the values for the oxygen tension at half-maximum slope. Chance [15] did not take into account the decreasing substrate concentration during a test so that the results obtained during the tests starting with an approximate glucose concentration of 45 mg/l did not conform to his theoretical results. They were however in agreement with the predictions of the model described in section 5.4 which, although much simpler than Chance's [15], did correct for this factor.

CHAPTER 6

CONCLUSIONS

Three major topics have been treated herein:

i) The static and dynamic behavior of two types of dissolved oxygen probes and the mathematical modelling of the response characteristics of the polarographic membrane-covered probe.

ii) The control of the dissolved oxygen tension in a typical pilot-plant fermentor.

iii) The effect of the dissolved oxygen tension and the dilution rate during the continuous cultivation of *C. lipolytica* on its maximum rate of respiration and its affinity for oxygen.

6.1 The Oxygen Probe

6.1.1 The Galvanic Probe

For the galvanic probe it was found that the steady-state output current at a given oxygen tension was a function of the external resistive load and the temperature. If the above two factors were adequately controlled, it yielded a linear relationship between the oxygen tension and the output current. The dynamic response of the probe was influenced by the external resistive load, the duration of the exposure prior to a downstep and the oxygen tension to which the probe was exposed. The effect of the temperature on the dynamic response was not investigated.

The maximum allowable voltage output signal from the galvanic probe to retain an optimal dynamic response, was found to vary with the oxygen tension being measured. This allowable voltage output decreased as the oxygen tension decreased. For the system studied it was approximately 10 mv at 0.21 atm. of oxygen and considerably below 1 mv at 9.26×10^{-4} atm. of oxygen. This characteristic of the galvanic probe caused considerable difficulty in the measurement of very low oxygen tensions since it necessitated the measuring of very low voltages.

6.1.2 The Polarographic YSI Probe

The polarographic YSI probe yielded a linear relationship at steady state between the oxygen tension and the output current over the range 1.76×10^{-4} atm. to 0.21 atm. of oxygen.

Its dynamic responses to downsteps in oxygen tension were very similar over a wide range of downstep magnitudes.

The dynamic behavior of the polarographic probe could be adequately modelled in terms of a combination of a single diffusion layer and a central well oxygen reservoir. The model contained three fitting parameters all of which had a clear physical significance. A more complex model incorporating a modified Nernst equation to account for the effect of the downstep magnitude on the dynamic response was only moderately successful. It is believed that the modest effect observed was mainly due to the aging of the membrane. The effect of the single diffusion layer and central well model on the response to a slowly decreasing oxygen tension function obtained by integrating the Michaelis-Menten equation was calculated. It was found that on the basis of the proposed model the effect of the dynamic lag of the probe could be calculated.

6.1.3 The Problems Encountered in the Measurement of the Oxygen Tension

The two main problems encountered in measuring the dissolved oxygen tension with both the galvanic and the polarographic probes were the storage of oxygen inside the probes and the gradual change in the static and dynamic behavior as the membrane aged. The former problem caused the probes to exhibit a dynamic lag considerably more complex and of greater duration than was due to oxygen diffusion through the membrane and the electrolyte layer.

The second problem can be alleviated considerably by the use of a mechanically sturdier membrane. A membrane reinforced with a stainless steel mesh was for example mounted on the oxygen probe used in the fermentor. This probe never exhibited signs of aging over periods of up to six weeks. The disadvantage inherent in this solution is the increased dynamic lag of the probe due to an increased membrane thickness. To overcome this negative aspect a membrane material would be required combining the properties of impermeability to water and large molecules and of chemical inertness with a diffusivity coefficient for oxygen much larger than the presently used Teflon membranes possess. The solution to the first problem is readily apparent but at present not feasible; the prevention of any and all oxygen reservoirs in the design of a dissolved oxygen probe is no easy matter.

6.2 The Dropping Mercury Polarograph

The dropping mercury polarograph was found to yield a linear relationship between the oxygen tension and the diffusion current over the range of 1.76×10^{-4} atm. to 0.21 atm. of oxygen in both distilled water with dosing solution added and in centrifuged and filtered supernatant obtained from Fermentation 1. At high ratios of the charging current to the signal current the maximum readings obtained on the polarographic trace were not proportional to the oxygen tension since they were not coincident with the times at which the drops fell off the capillary. During the calibration procedure, when the oxygen tension remained constant, the end of drop life could be differentiated from the peak reading and the true signal current could be obtained. Under dynamic conditions this differentiation proved extremely problematic.

6.3 The Dissolved Oxygen Control System

A theoretical study of a dissolved oxygen control system underscored the sensitivity of the performance of such a system to the dissolved oxygen set point and the maximum organism growth rate. It was found that the head space in a fermentor considerably stabilized the operation of the control system by acting as an oxygen reservoir. The dynamic lag of the oxygen probe is also of paramount importance since it is the slowest unit in the feedback circuit.

6.4 The Respiratory System of *Candida lipolytica*

It was found that the respiratory system content of *C. lipolytica* was increased as the oxygen tension maintained during growth was decreased. Both the relationships between the oxygen tension during culture and the maximum slope of the oxygen tension-time curves and between the oxygen tension during culture and the oxygen tension at half-maximum slope obtained with the YSI probe supported this conclusion.

There was also evidence that the respiratory system content of *C. lipolytica* increased with the dilution rate.

The influence of the glucose concentration at the start of a test on the oxygen tension obtained at half-maximum slope was in accordance with Chance's [15] model of the respiratory system.

The values of the maximum slopes obtained simultaneously with the polarograph and the YSI probe were in good agreement. The lack of agreement between the values for the oxygen tensions at half-maximum slope obtained with the two instruments was probably due to the use of the polarographic peak currents rather than the currents which were flowing at the end of drop life.

The significance of the findings reported above is that they lend further support to the presently-held views of the method of adaptation to environmental factors by microorganisms. Such knowledge could be of great practical significance for the optimization of e.g. microbial cytochrome production. *C. lipolytica* might be a particularly suitable organism for such a process since it cannot switch to an anaerobic metabolism. The effect of using a hydrocarbon substrate instead of glucose would also be of the greatest interest.

APPENDIX 2.1

AN APPRAISAL OF THE CUPRIC ION-CATALYSED REACTION BETWEEN SODIUM SULFITE AND OXYGEN-ITS EFFECTIVENESS IN PROVIDING AN OXYGEN-FREE ENVIRONMENT

Finn [24] has stated:

> "In the presence of copper or cobalt salts, which act as catalysts, the reaction [of sodium sulfite] with oxygen proceeds rapidly and irreversibly to completion in the liquid phase. The reaction rate is .... independent of the sulfite ion concentration at a sodium sulfite concentration greater than 0.015 M."

Fuller and Crist [27] have found that the rate of the cupric ion-catalysed sulfite ion oxidation by oxygen in the aqueous phase was independent of the cupric ion concentration when the latter exceeded 10^{-8} M at an oxygen tension of 1 atm. There is however some question as to whether this oxygen tension was really maintained in their apparatus. If it were not, it would be of interest to know at what tension oxygen became the rate-limiting reactant.

No further information on the kinetic role of oxygen at low tension in this reaction could be found in the literature. Under static conditions, it was observed that a dissolved oxygen probe would exhibit roughly the same residual current when submerged in copper-catalysed sodium sulfite solution as when suspended in nitrogen gas. It is however not known how fast a sodium sulfite solution reduced small amounts of air accidentally brought in contact with it e.g. during the downstep response experiments.

APPENDIX 2.2

PROBE CONSTANT vs TEMPERATURE DATA FOR THE GALVANIC PROBE WHEN SUBMERGED IN AIR-SATURATED WATER

C_p = probe constant (microamp/atm. O_2)

T = temperature (°C)

Load resistors: I - 10 ohms
II - 24 ohms
III - 120 ohms
IV - 620 ohms

I		II		III		IV	
T	C_p	T	C_p	T	C_p	T	C_p
22.9	292	22.9	290	22.6	270	22.8	285
22.8	291	23.0	292	23.0	294	23.0	289
23.0	293	24.0	298	24.0	303	23.1	293
23.0	295	24.6	305	24.8	308	24.0	301
24.0	300	25.1	310	25.1	314	24.5	302
24.2	306	25.9	317	26.0	319	25.3	311
24.9	309	26.1	327	26.8	325	26.0	315
25.1	314	27.2	332	27.7	333	27.0	328
25.8	317	27.3	330	27.3	330	28.5	342
26.0	322	27.8	335	28.0	338	29.5	347
27.0	330	28.4	337	28.7	345	30.1	351

I		II		III		IV	
T	C_p	T	C_p	T	C_p	T	C_p
27.3	333	29.5	350	29.8	353	31.0	360
27.6	336	30.0	358	30.1	356	31.5	365
28.2	342	31.0	363	31.1	368	32.0	370
28.8	347	31.1	363	30.9	364	3[illegible].1	370
29.0	350	28.0	337	27.8	331	31.7	365
29.9	356	25.5	316	25.1	312	31.1	362
30.3	358	24.7	305	24.1	303	30.5	352
31.3	370	23.7	296	23.0	294	29.9	347
31.1	367	22.6	294	22.1	287	29.0	338
28.7	345	21.4	281	21.0	281	27.0	324
27.2	328	20.9	276	20.7	276	25.8	311
25.0	311	20.9	276	21.1	281	25.0	302
24.0	302	22.1	291	22.9	294	24.2	298
22.9	292					23.0	289
22.0	287					22.7	285
21.0	281					22.0	277
20.4	274					21.2	276
21.8	287					20.8	268
23.0	295					21.0	276
						21.9	280
						22.7	289
						23.1	293
						24.0	297

The least-square lines were:

I - $C_p = 91.1 + 8.85\,T$

II - $C_p = 94.4 + 8.66\,T$

III - $C_p = 90.8 + 8.80\,T$

IV - $C_p = 88.0 + 8.76\,T$

APPENDIX 2.3

SPECIFICATIONS OF THE YSI POLAROGRAPHIC PROBE PROVIDED BY THE MANUFACTURER (YELLOW SPRINGS INSTRUMENT CO., MODEL #YSI 5331)

Range: Full Scale for air or oxygen saturated solutions

Consumption Rate: Less than 7 to 1500 microliters of oxygen/hr.

Response Time: 90% of reading in 10 secs. approximately.

APPENDIX 2.4

EXPERIMENTAL RESULTS FOR THE STEADY-STATE CALIBRATION OF THE POLAROGRAPHIC YSI PROBE

Conditions:

Temperature: 22°C

Atmospheric Pressure: 758 mm Hg

Currents were measured after 1 minute of exposure to the gas phase.

Gas #	Oxygen Tension (atm. of O_2)
0	0^*
1	1.76×10^{-4}
2	9.26×10^{-4}
3	3.00×10^{-3}
4	1.01×10^{-2}
5	3.02×10^{-2}
6	9.96×10^{-2}
7	2.1×10^{-1}

*Sodium Sulfite Solution - 50 gm/l - Cu^{++} catalyzed

5 OF/DE 6

TEST #	GAS #	CURRENT (μA)	SIGNAL CURRENT (μA)
I-a-i	0	0.010	
I-a-ii	1	0.036	0.026
I-b-i	0	0.006	
I-b-ii	1	0.030	0.024
I-c-i	0	0.008	
I-c-ii	1	0.033	0.025
II-a-i	0	0.008	
II-a-ii	2	0.140	0.132
II-b-i	0	0.008	
II-b-ii	2	0.135	0.127
II-c-i	0	0.007	
II-c-ii	2	0.135	0.128
III-a-i	0	0.008	
III-a-ii	3	0.400	0.392
III-b-i	0	0.009	
III-b-ii	3	0.390	0.381
III-c-i	0	0.010	
III-c-ii	3	0.395	0.385
IV-a-i	0	0.010	
IV-a-ii	4	1.450	1.440
IV-b-i	0	0.010	
IV-b-ii	4	1.425	1.415
IV-c-i	0	0.010	
IV-c-ii	4	1.425	1.415
V-a-i	0	0.011	
V-a-ii	5	4.167	4.156
V-b-i	0	0.011	
V-b-ii	5	4.167	4.156
V-c-i	0	0.012	
V-c-ii	5	4.259	4.247
VI-a-i	0	0.012	
VI-a-ii	6	13.000	12.988
VI-b-i	0	0.011	

TEST #	GAS #	CURRENT (μA)	SIGNAL CURRENT (μA)
VI-b-ii	6	13.125	13.113
VI-c-i	0	0.011	
VI-c-ii	6	12.750	12.739
VII-a-i	0	0.012	
VII-a-ii	7	29.167	29.155
VII-b-i	0	0.012	
VII-b-ii	7	29.545	29.533
VII-c-i	0	0.011	
VII-c-ii	7	29.545	29.534

APPENDIX 2.5

PROGRAM KOK1

Program KOK1 Checked the Data Obtained During the Polarographic Probe Characterization

```
PAGE   1

// JCB    1122

LOG DRIVE    CART SPEC    CART AVAIL   PHY DRIVE
  0000         1122          1122         0000

V2 M10   ACTUAL  8K  CONFIG  8K

// DUP

*DELETE              KCK1
CART ID 1122   DB ACDR  4930   DB CNT    0025

// FOR
* IOCS (CARD,1403 PRINTER)
* ONE WORD INTEGERS
* LIST SOURCE PROGRAM
* NAME KCK1
C ROBERT KOK ---PROGRAM KOK1 TO ORGANIZE AND CHECK DATA FOR THE POLAROGRAPHIC
C PROBE CHARACTERIZATION---VARIABLES AS FOLLOWS---N1=NUMBER OF DOWNSTEP
C RESPONSES OBTAINED---A1,A2,A3,A4=DUMMY VARIABLES FOR TITLES ETC---IDUR=
C DURATION OF EXPOSURE IN MINUTES---RES=RESIDUAL CURRENT IN MICROAMPS---
C N2=NO. PTS IN EACH RESPONSE---I,I1,I2,DUMMY=DO-LOOP VARIABLES---TIME=
C TIME IN MM---TTIME=TIME IN SECS---CURR=CURRENT IN MICROAMPS---MWH=IS A
C VECTOR FOR THE PLOTTING SUBROUTINE CURV9
C GRAPHIC OUTPUT CAN BE SUPPRESSED BY MEANS OF DATA SWITCH NO. 1
      DIMENSION A1(20),A2(10),A3(2),A4(30),TIME(30),TTIME(30),CURR(30)
      DIMENSION MWH(5)
      READ(2,100)N1,A3
  100 FORMAT(I2,2A1)
      READ(2,101)A1
  101 FORMAT(20A4)
      A4(1)=A3(2)
      WRITE(5,104)
      DO 10 I1=1,N1
      READ(2,102)(A2(I),I=1,5),IDUR,RES,(A2(J),J=6,10),N2
  102 FORMAT(5A2,I1,F9.3,5A2,I2)
      READ(2,103)(TIME(I),CURR(I),I=1,N2)
  103 FORMAT(3F10.3)
      WRITE(5,108)
  108 FORMAT(///)
  104 FORMAT(1H1)
      WRITE(5,101)A1
      WRITE(5,105)(A2(I),I=1,5),IDUR,RES,(A2(J),J=6,10),N2
  105 FORMAT(14H RESPONSE NUMBER5A2,/23H DURATION OF EXPOSURE  I1,5H  MI
     1N/23H RESIDUAL CURRENT WAS  F6.3,10H  MICROAMP/21H OXYGEN CONCENTR
     2ATION5A2,10H O2 IN N2 /29H NUMBER OF POINTS IN DOWNSTEP I2)
      DO 20 I2=2,N2
      IF (TIME(I2)-TIME(I2-1))12,12,11
   11 IF (CURR(I2)-CURR(I2-1))13,13,12
   13 A4(I2)=A3(2)
      GO TO 20
   12 A4(I2)=A3(1)
   20 TTIME(I2)=TIME(I2)*0.48
      WRITE(5,106)
  106 FORMAT(///45H    TTIME(SECS)        TIME(MM)    CURR(MICROA))
      WRITE(5,107)(TTIME(I),TIME(I),CURR(I),A4(I),I=1,N2)
  107 FORMAT(3F15.3,A1)
      CALL DATSW(1,II)
      GO TO (10,11),II
```

```
C PLOTTING USING CURV9
    1 WRITE(5,106)
      XMIN=CURR(N2)*0.9
      XMAX=CURR(1)*1.1
      YMIN=TIME(1)-1.
      YMAX=TIME(N2)+3.
      MWH(1)=N2
      CALL CURV9(CURR,TIME,XMIN,XMAX,YMIN,YMAX,N2,1,MWH,1)
   10 CONTINUE
      CALL EXIT
      END

FEATURES SUPPORTED
 ONE WORD INTEGERS
 IOCS

CORE REQUIREMENTS FOR KOK1
 COMMON      0  VARIABLES     330  PROGRAM     550

END OF COMPILATION

// DUP

*STORE      WS  UA  KOK1
CART ID 1122   DB ADDR  4930   DB CNT   0025

// XEQ KOK1
```

APPENDIX 2.6

RESULTS FROM THE POLAROGRAPHIC PROBE CHARACTERIZATION TESTS

For each downstep response the following are listed below:

- chart speed - mm/minute
- downstep response number
- duration of exposure - minutes
- residual current - microamp
- oxygen tension to which the probe was exposed - % O_2 in N_2 or ppm O_2 in N_2
- number of data points tabulated.

The following are presented in tabular form:

- time since the downstep - secs
- time since the downstep - mm
- current signal obtained corrected for the residual current - microamp.

POLAROGRAPHIC PROBE CHARACTERIZATION -CHART SPEED 125 MM/MIN -APRIL 4 1973
RESPONSE NUMBER I-1
DURATION OF EXPOSURE 1 MIN
RESIDUAL CURRENT WAS 0.021 MICROAMP
OXYGEN CONCENTRATION 0.3P O2 IN N2
NUMBER OF POINTS IN DOWNSTEP 9

TTIME(SECS)	TIME(MM)	CURR(MICROA)
-0.000	0.000	0.454
2.580	6.000	0.314
5.279	11.000	0.184
7.680	16.000	0.064
10.079	21.000	0.046
12.479	26.000	0.024
14.879	31.000	0.020
17.279	36.000	0.015
19.680	41.000	0.012

POLAROGRAPHIC PROBE CHARACTERIZATION -CHART SPEED 125 MM/MIN -APRIL 4 1973
RESPONSE NUMBER I-2
DURATION OF EXPOSURE 1 MIN
RESIDUAL CURRENT WAS 0.022 MICROAMP
OXYGEN CONCENTRATION 0.3P O2 IN N2
NUMBER OF POINTS IN DOWNSTEP10

TTIME(SECS)	TIME(MM)	CURR(MICROA)
-0.000	0.000	0.443
3.360	7.000	0.323
5.760	12.000	0.193
8.159	17.000	0.065
10.559	22.000	0.039
12.959	27.000	0.031
15.360	32.000	0.020
17.760	37.000	0.016
20.159	42.000	0.013
22.560	47.000	0.010

POLAROGRAPHIC PROBE CHARACTERIZATION -CHART SPEED 125 MM/MIN -APRIL 4 1973
RESPONSE NUMBER I-3
DURATION OF EXPOSURE 1 MIN
RESIDUAL CURRENT WAS 0.023 MICROAMP
OXYGEN CONCENTRATION 0.3P O2 IN N2
NUMBER OF POINTS IN DOWNSTEP10

TTIME(SECS)	TIME(MM)	CURR(MICROA)

-C.000	0.000	0.437
3.340	8.000	0.262
6.239	13.000	0.129
8.639	18.000	0.052
11.040	23.000	0.038
13.440	28.000	0.023
15.840	33.000	0.018
18.240	38.000	0.014
20.639	43.000	0.011
23.040	48.000	0.008

POLAROGRAPHIC PROBE CHARACTERIZATION -CHART SPEED 125 MM/MIN -APRIL 4 1973
RESPONSE NUMBER I-4
DURATION OF EXPOSURE 2 MIN
RESIDUAL CURRENT WAS 0.023 MICROAMP
OXYGEN CONCENTRATION 0.3P O2 IN N2
NUMBER OF POINTS IN DOWNSTEP10

TTIME(SECS)	TIME(MM)	CURR(MICROA)
-C.000	0.000	0.437
2.980	6.000	0.302
5.279	11.000	0.184
7.680	16.000	0.062
10.079	21.000	0.041
12.479	26.000	0.028
14.879	31.000	0.019
17.279	36.000	0.016
19.680	41.000	0.013
22.080	46.000	0.010

POLAROGRAPHIC PROBE CHARACTERIZATION -CHART SPEED 125 MM/MIN -APRIL 4 1973
RESPONSE NUMBER I-5
DURATION OF EXPOSURE 1 MIN
RESIDUAL CURRENT WAS 0.023 MICROAMP
OXYGEN CONCENTRATION 0.3P O2 IN N2
NUMBER OF POINTS IN DOWNSTEP11

TTIME(SECS)	TIME(MM)	CURR(MICROA)
-0.000	0.000	0.437
1.440	3.000	0.372
3.840	8.000	0.232
6.239	13.000	0.054
8.639	18.000	0.049
11.040	23.000	0.034
13.440	28.000	0.022
15.840	33.000	0.018
18.240	38.000	0.014
20.639	43.000	0.010
23.040	48.000	0.008

POLAROGRAPHIC PROBE CHARACTERIZATION -CHART SPEED 125 MM/MIN -APRIL 4 1973
RESPONSE NUMBER 1-6
DURATION OF EXPOSURE 2 MIN
RESIDUAL CURRENT WAS 0.023 MICROAMP
OXYGEN CONCENTRATION 0.3P O2 IN N2
NUMBER OF POINTS IN DOWNSTEP10

TTIME(SECS)	TIME(MM)	CURR(MICROA)
-0.000	0.000	0.437
3.160	7.000	0.272
5.760	12.000	0.154
8.159	17.000	0.060
10.559	22.000	0.038
12.959	27.000	0.027
15.360	32.000	0.019
17.760	37.000	0.014
20.159	42.000	0.013
22.560	47.000	0.010

POLAROGRAPHIC PROBE CHARACTERIZATION -CHART SPEED 125 MM/MIN -APRIL 4 1973
RESPONSE NUMBER 1-7
DURATION OF EXPOSURE 1 MIN
RESIDUAL CURRENT WAS 0.023 MICROAMP
OXYGEN CONCENTRATION 0.3P O2 IN N2
NUMBER OF POINTS IN DOWNSTEP11

TTIME(SECS)	TIME(MM)	CURR(MICROA)
-0.000	0.000	0.432
2.400	5.000	0.342
4.800	10.000	0.217
7.199	15.000	0.079
9.600	20.000	0.046
12.000	25.000	0.032
14.399	30.000	0.024
16.799	35.000	0.018
19.200	40.000	0.014
21.599	45.000	0.011
24.000	50.000	0.008

POLAROGRAPHIC PROBE CHARACTERIZATION -CHART SPEED 125 MM/MIN -APRIL 4 1973
RESPONSE NUMBER 1-8
DURATION OF EXPOSURE 3 MIN
RESIDUAL CURRENT WAS 0.025 MICROAMP
OXYGEN CONCENTRATION 0.3P O2 IN N2
NUMBER OF POINTS IN DOWNSTEP11

TTIME(SECS)	TIME(MM)	CURR(MICROA)
-0.000	0.000	0.432

2.400	5.000	0.357
4.800	10.000	0.227
7.199	15.000	0.097
9.600	20.000	0.048
12.000	25.000	0.035
14.399	30.000	0.028
16.799	35.000	0.017
19.200	40.000	0.015
21.599	45.000	0.012
24.000	50.000	0.010

POLAROGRAPHIC PROBE CHARACTERIZATION -CHART SPEED 125 MM/MIN -APRIL 4 1973
RESPONSE NUMBER 1-9
DURATION OF EXPOSURE 1 MIN
RESIDUAL CURRENT WAS 0.023 MICROAMP
OXYGEN CONCENTRATION 0.3P O2 IN N2
NUMBER OF POINTS IN DOWNSTEP10

TTIME(SECS)	TIME(MM)	CURR(MICROA)
-0.000	0.000	0.432
3.840	8.000	0.262
6.239	13.000	0.144
8.639	18.000	0.058
11.040	23.000	0.037
13.440	28.000	0.028
15.840	33.000	0.020
18.240	38.000	0.017
20.639	43.000	0.013
23.040	48.000	0.010

POLAROGRAPHIC PROBE CHARACTERIZATION -CHART SPEED 125 MM/MIN -APRIL 4 1973
RESPONSE NUMBER 1-10
DURATION OF EXPOSURE 3 MIN
RESIDUAL CURRENT WAS 0.023 MICROAMP
OXYGEN CONCENTRATION 0.3P O2 IN N2
NUMBER OF POINTS IN DOWNSTEP11

TTIME(SECS)	TIME(MM)	CURR(MICROA)
-0.000	0.000	0.432
2.400	5.000	0.362
4.800	10.000	0.237
7.199	15.000	0.109
9.600	20.000	0.055
12.000	25.000	0.036
14.399	30.000	0.026
16.799	35.000	0.020
19.200	40.000	0.016
21.599	45.000	0.012
24.000	50.000	0.010

POLAROGRAPHIC PROBE CHARACTERIZATION -CHART SPEED 125 MM/MIN -APRIL 4 1973
RESPONSE NUMBER I-11
DURATION OF EXPOSURE 1 MIN
RESIDUAL CURRENT WAS 0.023 MICROAMP
OXYGEN CONCENTRATION 0.3P O2 IN N2
NUMBER OF POINTS IN DOWNSTEP10

TTIME(SECS)	TIME(MM)	CURR(MICROA)
-0.000	0.000	0.432
3.840	8.000	0.242
6.239	13.000	0.122
8.639	18.000	0.056
11.040	23.000	0.039
13.440	28.000	0.028
15.840	33.000	0.019
18.240	38.000	0.015
20.639	43.000	0.012
23.040	48.000	0.009

POLAROGRAPHIC PROBE CHARACTERIZATION -CHART SPEED 125 MM/MIN -APRIL 4 1973
RESPONSE NUMBER I-12
DURATION OF EXPOSURE 1 MIN
RESIDUAL CURRENT WAS 0.023 MICROAMP
OXYGEN CONCENTRATION 0.3P O2 IN N2
NUMBER OF POINTS IN DOWNSTEP11

TTIME(SECS)	TIME(MM)	CURR(MICROA)
-0.000	0.000	0.432
2.400	5.000	0.342
4.800	10.000	0.232
7.199	15.000	0.104
9.600	20.000	0.054
12.000	25.000	0.036
14.399	30.000	0.027
16.799	35.000	0.018
19.200	40.000	0.015
21.599	45.000	0.012
24.000	50.000	0.009

POLAROGRAPHIC PROBE CHARACTERIZATION -CHART SPEED 125 MM/MIN -APRIL 4 1973
RESPONSE NUMBER II-1
DURATION OF EXPOSURE 1 MIN
RESIDUAL CURRENT WAS 0.020 MICROAMP
OXYGEN CONCENTRATION 1.01P O2 IN N2
NUMBER OF POINTS IN DOWNSTEP12

TTIME(SECS)	TIME(MM)	CURR(MICROA)
-0.000	0.000	1.442

3.840	8.000	0.790
6.239	13.000	0.300
8.639	18.000	0.157
11.040	23.000	0.097
13.440	28.000	0.075
15.840	33.000	0.053
18.240	38.000	0.042
20.639	43.000	0.033
23.040	48.000	0.026
25.439	53.000	0.022
27.840	58.000	0.018

POLAROGRAPHIC PROBE CHARACTERIZATION -CHART SPEED 125 MM/MIN -APRIL 4 1973
RESPONSE NUMBER 11-2
DURATION OF EXPOSURE 1 MIN
RESIDUAL CURRENT WAS 0.021 MICROAMP
OXYGEN CONCENTRATION 1.01P O2 IN N2
NUMBER OF POINTS IN DOWNSTEP12

TTIME(SECS)	TIME(MM)	CURR(MICROA)
-0.000	0.000	1.441
3.840	8.000	0.749
6.239	13.000	0.279
8.639	18.000	0.146
11.040	23.000	0.124
13.440	28.000	0.068
15.840	33.000	0.055
18.240	38.000	0.042
20.639	43.000	0.033
23.040	48.000	0.026
25.439	53.000	0.019
27.840	58.000	0.017

POLAROGRAPHIC PROBE CHARACTERIZATION -CHART SPEED 125 MM/MIN -APRIL 4 1973
RESPONSE NUMBER 11-3
DURATION OF EXPOSURE 1 MIN
RESIDUAL CURRENT WAS 0.021 MICROAMP
OXYGEN CONCENTRATION 1.01P O2 IN N2
NUMBER OF POINTS IN DOWNSTEP12

TTIME(SECS)	TIME(MM)	CURR(MICROA)
-0.000	0.000	1.441
2.400	5.000	1.004
4.800	10.000	0.579
7.199	15.000	0.199
9.600	20.000	0.116
12.000	25.000	0.084
14.399	30.000	0.062
16.799	35.000	0.049
19.200	40.000	0.036
21.599	45.000	0.031

24.000	50.000	0.025
26.400	55.000	0.019

POLAROGRAPHIC PROBE CHARACTERIZATION -CHART SPEED 125 MM/MIN -APRIL 4 1973
RESPONSE NUMBER II-4
DURATION OF EXPOSURE 2 MIN
RESIDUAL CURRENT WAS 0.021 MICROAMP
OXYGEN CONCENTRATION 1.01P O2 IN N2
NUMBER OF POINTS IN DOWNSTEP12

TTIME(SECS)	TIME(MM)	CURR(MICROA)
-0.020	0.000	1.429
1.920	4.000	1.029
4.319	9.000	0.619
6.720	14.000	0.204
9.120	19.000	0.129
11.520	24.000	0.091
13.920	29.000	0.065
16.319	34.000	0.049
18.720	39.000	0.042
21.119	44.000	0.033
23.520	49.000	0.025
25.919	54.000	0.022

POLAROGRAPHIC PROBE CHARACTERIZATION -CHART SPEED 125 MM/MIN -APRIL 4 1973
RESPONSE NUMBER II-5
DURATION OF EXPOSURE 1 MIN
RESIDUAL CURRENT WAS 0.021 MICROAMP
OXYGEN CONCENTRATION 1.01P O2 IN N2
NUMBER OF POINTS IN DOWNSTEP12

TTIME(SECS)	TIME(MM)	CURR(MICROA)
-0.000	0.000	1.416
2.400	5.000	0.979
4.800	10.000	0.589
7.199	15.000	0.199
9.600	20.000	0.121
12.000	25.000	0.086
14.399	30.000	0.061
16.799	35.000	0.048
19.200	40.000	0.038
21.599	45.000	0.030
24.000	50.000	0.024
26.400	55.000	0.019

POLAROGRAPHIC PROBE CHARACTERIZATION -CHART SPEED 125 MM/MIN -APRIL 4 1973
RESPONSE NUMBER II-6
DURATION OF EXPOSURE 2 MIN

RESIDUAL CURRENT WAS 0.021 MICROAMP
OXYGEN CONCENTRATION 1.01P O2 IN N2
NUMBER OF POINTS IN DOWNSTEP12

TTIME(SECS)	TIME(MM)	CURR(MICROA)
-0.000	0.000	1.416
2.400	5.000	1.004
4.800	10.000	0.589
7.199	15.000	0.201
9.600	20.000	0.126
12.000	25.000	0.086
14.399	30.000	0.064
16.799	35.000	0.051
19.200	40.000	0.040
21.599	45.000	0.034
24.000	50.000	0.027
26.400	55.000	0.021

POLAROGRAPHIC PROBE CHARACTERIZATION -CHART SPEED 125 MM/MIN -APRIL 4 1973
RESPONSE NUMBER 11-7
DURATION OF EXPOSURE 1 MIN
RESIDUAL CURRENT WAS 0.022 MICROAMP
OXYGEN CONCENTRATION 1.01P O2 IN N2
NUMBER OF POINTS IN DOWNSTEP12

TTIME(SECS)	TIME(MM)	CURR(MICROA)
-0.000	0.000	1.415
2.880	6.000	0.903
5.279	11.000	0.428
7.680	16.000	0.178
10.079	21.000	0.111
12.479	26.000	0.076
14.879	31.000	0.056
17.279	36.000	0.047
19.680	41.000	0.036
22.080	46.000	0.031
24.479	51.000	0.026
26.880	56.000	0.021

POLAROGRAPHIC PROBE CHARACTERIZATION -CHART SPEED 125 MM/MIN -APRIL 4 1973
RESPONSE NUMBER 11-8
DURATION OF EXPOSURE 3 MIN
RESIDUAL CURRENT WAS 0.021 MICROAMP
OXYGEN CONCENTRATION 1.01P O2 IN N2
NUMBER OF POINTS IN DOWNSTEP12

TTIME(SECS)	TIME(MM)	CURR(MICROA)
-0.000	0.000	1.416
3.360	7.000	0.849

5.760	12.000	0.354
8.159	17.000	0.174
10.559	22.000	0.109
12.959	27.000	0.081
15.360	32.000	0.060
17.760	37.000	0.048
20.159	42.000	0.039
22.560	47.000	0.032
24.959	52.000	0.025
27.360	57.000	0.022

POLAROGRAPHIC PROBE CHARACTERIZATION -CHART SPEED 125 MM/MIN -APRIL 4 1973
RESPONSE NUMBER II-9
DURATION OF EXPOSURE 1 MIN
RESIDUAL CURRENT WAS 0.022 MICROAMP
OXYGEN CONCENTRATION 1.01P O2 IN N2
NUMBER OF POINTS IN DOWNSTEP12

TTIME(SECS)	TIME(MM)	CURR(MICROA)
-0.000	0.000	1.415
2.400	5.000	1.028
4.800	10.000	0.608
7.179	15.000	0.213
9.600	20.000	0.123
12.000	25.000	0.090
14.379	30.000	0.064
16.799	35.000	0.051
19.200	40.000	0.041
21.579	45.000	0.032
24.000	50.000	0.026
26.400	55.000	0.021

POLAROGRAPHIC PROBE CHARACTERIZATION -CHART SPEED 125 MM/MIN -APRIL 4 1973
RESPONSE NUMBER II-10
DURATION OF EXPOSURE 3 MIN
RESIDUAL CURRENT WAS 0.022 MICROAMP
OXYGEN CONCENTRATION 1.01P O2 IN N2
NUMBER OF POINTS IN DOWNSTEP12

TTIME(SECS)	TIME(MM)	CURR(MICROA)
-0.000	0.000	1.415
3.360	7.000	0.778
5.760	12.000	0.308
8.159	17.000	0.158
10.559	22.000	0.105
12.959	27.000	0.080
15.360	32.000	0.059
17.760	37.000	0.047
20.159	42.000	0.037
22.560	47.000	0.031
24.959	52.000	0.024

27.360	57.000	0.021

POLAROGRAPHIC PROBE CHARACTERIZATION -CHART SPEED 125 MM/MIN -APRIL 4 1973
RESPONSE NUMBER II-11
DURATION OF EXPOSURE 1 MIN
RESIDUAL CURRENT WAS 0.022 MICROAMP
OXYGEN CONCENTRATION 1.01P O2 IN N2
NUMBER OF POINTS IN DOWNSTEP12

TTIME(SECS)	TIME(MM)	CURR(MICROA)
-0.000	0.000	1.415
2.840	6.000	0.888
5.279	11.000	0.458
7.680	16.000	0.180
10.079	21.000	0.110
12.479	26.000	0.080
14.879	31.000	0.057
17.279	36.000	0.047
19.680	41.000	0.037
22.080	46.000	0.031
24.479	51.000	0.026
26.880	56.000	0.022

POLAROGRAPHIC PROBE CHARACTERIZATION -CHART SPEED 125 MM/MIN -APRIL 4 1973
RESPONSE NUMBER II-12
DURATION OF EXPOSURE 1 MIN
RESIDUAL CURRENT WAS 0.022 MICROAMP
OXYGEN CONCENTRATION 1.01P O2 IN N2
NUMBER OF POINTS IN DOWNSTEP12

TTIME(SECS)	TIME(MM)	CURR(MICROA)
-0.000	0.000	1.415
3.360	7.000	0.838
5.760	12.000	0.378
8.159	17.000	0.170
10.559	22.000	0.105
12.959	27.000	0.078
15.360	32.000	0.059
17.760	37.000	0.045
20.159	42.000	0.038
22.560	47.000	0.030
24.959	52.000	0.023
27.360	57.000	0.018

POLAROGRAPHIC PROBE CHARACTERIZATION -CHART SPEED 125 MM/MIN -APRIL 4 1973
RESPONSE NUMBER III-1
DURATION OF EXPOSURE 1 MIN
RESIDUAL CURRENT WAS 0.021 MICROAMP

OXYGEN CONCENTRATION 926 PPM O2 IN N2
NUMBER OF POINTS IN DOWNSTEP 7

TTIME(SECS)	TIME(MM)	CURR(MICROA)
-0.000	0.000	0.119
3.360	7.000	0.094
5.760	12.000	0.055
8.159	17.000	0.022
10.559	22.000	0.015
12.959	27.000	0.012
15.360	32.000	0.010

POLAROGRAPHIC PROBE CHARACTERIZATION -CHART SPEED 125 MM/MIN -APRIL 4 1973
RESPONSE NUMBER III-2
DURATION OF EXPOSURE 1 MIN
RESIDUAL CURRENT WAS 0.022 MICROAMP
OXYGEN CONCENTRATION 926 PPM O2 IN N2
NUMBER OF POINTS IN DOWNSTEP 7

TTIME(SECS)	TIME(MM)	CURR(MICROA)
-0.000	0.000	0.121
3.360	7.000	0.083
5.760	12.000	0.045
8.159	17.000	0.018
10.559	22.000	0.013
12.959	27.000	0.010
15.360	32.000	0.008

POLAROGRAPHIC PROBE CHARACTERIZATION -CHART SPEED 125 MM/MIN -APRIL 4 1973
RESPONSE NUMBER III-3
DURATION OF EXPOSURE 1 MIN
RESIDUAL CURRENT WAS 0.021 MICROAMP
OXYGEN CONCENTRATION 926 PPM O2 IN N2
NUMBER OF POINTS IN DOWNSTEP 7

TTIME(SECS)	TIME(MM)	CURR(MICROA)
-0.000	0.000	0.122
3.840	8.000	0.076
6.239	13.000	0.034
8.639	18.000	0.019
11.040	23.000	0.012
13.440	28.000	0.010
15.840	33.000	0.008

POLAROGRAPHIC PROBE CHARACTERIZATION -CHART SPEED 125 MM/MIN -APRIL 4 1973
RESPONSE NUMBER III-4

DURATION OF EXPOSURE 2 MIN
RESIDUAL CURRENT WAS 0.022 MICROAMP
OXYGEN CONCENTRATION 926 PPM O2 IN N2
NUMBER OF POINTS IN DOWNSTEP 7

TTIME(SECS)	TIME(MM)	CURR(MICROA)
-0.000	0.000	0.121
3.360	7.000	0.090
5.760	12.000	0.053
8.159	17.000	0.021
10.559	22.000	0.014
12.959	27.000	0.012
15.360	32.000	0.010

POLAROGRAPHIC PROBE CHARACTERIZATION -CHART SPEED 125 MM/MIN -APRIL 4 1973
RESPONSE NUMBER III-5
DURATION OF EXPOSURE 1 MIN
RESIDUAL CURRENT WAS 0.022 MICROAMP
OXYGEN CONCENTRATION 926 PPM O2 IN N2
NUMBER OF POINTS IN DOWNSTEP 7

TTIME(SECS)	TIME(MM)	CURR(MICROA)
-0.000	0.000	0.123
3.840	8.000	0.075
6.239	13.000	0.033
8.639	18.000	0.016
11.040	23.000	0.012
13.440	28.000	0.009
15.840	33.000	0.007

POLAROGRAPHIC PROBE CHARACTERIZATION -CHART SPEED 125 MM/MIN -APRIL 4 1973
RESPONSE NUMBER III-6
DURATION OF EXPOSURE 2 MIN
RESIDUAL CURRENT WAS 0.022 MICROAMP
OXYGEN CONCENTRATION 926 PPM O2 IN N2
NUMBER OF POINTS IN DOWNSTEP 7

TTIME(SECS)	TIME(MM)	CURR(MICROA)
-0.000	0.000	0.123
3.360	7.000	0.093
5.760	12.000	0.049
8.159	17.000	0.021
10.559	22.000	0.015
12.959	27.000	0.012
15.360	32.000	0.009

PCLARCGRAPHIC PROBE CHARACTERIZATION -CHART SPEED 125 MM/MIN -APRIL 4 1973
RESPCNSE NUMBER III-7
CURATICN CF EXPOSURE 1 MIN
RESIDUAL CURRENT WAS 0.022 MICROAMP
OXYGEN CONCENTRATICN 926 PPM O2 IN N2
NUMBER CF POINTS IN DOWNSTEP 7

TTIME(SECS)	TIME(MM)	CURR(MICROA)
-C.000	0.000	0.123
2.400	5.0C0	0.1C3
4.8C0	10.C00	0.059
7.199	15.000	0.023
9.600	20.C00	0.017
12.0C0	25.CC0	0.013
14.399	30.000	0.010

PCLAROGRAPHIC PROBE CHARACTERIZATION -CHART SPEED 125 MM/MIN -APRIL 4 1973
RESPCNSE NUMBER III-8
CURATICN CF EXPOSURE 3 MIN
RESIDUAL CURRENT WAS 0.022 MICROAMP
OXYGEN CONCENTRATION 926 PPM O2 IN N2
NUMBER CF PCINTS IN DOWNSTEP 7

TTIME(SECS)	TIME(MM)	CURR(MICROA)
-C.CC0	0.CC0	0.123
2.880	6.C00	0.098
5.279	11.000	0.055
7.680	16.000	0.022
1C.C79	21.CC0	0.C16
12.479	26.C00	0.012
14.879	31.000	0.010

PCLARCGRAPHIC PROBE CHARACTERIZATION -CHART SPEED 125 MM/MIN -APRIL 4 1973
RESPCNSE NUMBER III-9
CURATICN CF EXPCSURE 1 MIN
RESIDUAL CURRENT WAS 0.022 MICROAMP
OXYGEN CONCENTRATION 926PPM O2 IN N2
NUMBER CF PCINTS IN DOWNSTEP 7

TTIME(SECS)	TIME(MM)	CURR(MICROA)
-0.000	0.000	0.123
3.840	8.000	0.088
6.239	13.CC0	0.C49
8.639	18.C00	0.021
11.040	23.000	0.013
13.440	28.000	0.012
15.840	33.CC0	0.010

PCLAROGRAPHIC PROBE CHARACTERIZATION -CHART SPEED 125 MM/MIN -APRIL 4 1973
RESPONSE NUMBER III-10
DURATICN CF EXPOSURE 3 MIN
RESICUAL CURRENT WAS 0.022 MICROAMP
CXYGEN CONCENTRATICN 926 PPM O2 IN N2
NUMBER CF PCINTS IN DOWNSTEP 7

TTIME(SECS)	TIME(MM)	CURR(MICROA)
-0.000	0.000	0.123
2.880	6.000	0.095
5.279	11.000	0.055
7.680	16.000	0.024
10.079	21.000	0.017
12.479	26.000	0.014
14.879	31.000	0.011

POLAROGRAPHIC PROBE CHARACTERIZATION -CHART SPEED 125 MM/MIN -APRIL 4 1973
RESPONSE NUMBER III-11
DURATICN CF EXPCSURE 1 MIN
RESIDUAL CURRENT WAS 0.022 MICROAMP
CXYGEN CONCENTRATION 926 PPM O2 IN N2
NUMBER CF PCINTS IN DOWNSTEP 7

TTIME(SECS)	TIME(MM)	CURR(MICROA)
-0.000	0.000	0.123
2.400	5.000	0.100
4.800	10.000	0.059
7.199	15.000	0.026
9.600	20.000	0.016
12.000	25.000	0.012
14.399	30.000	0.010

PCLAROGRAPHIC PROBE CHARACTERIZATION -CHART SPEED 125 MM/MIN -APRIL 4 1973
RESPONSE NUMBER III-12
DURATICN CF EXPOSURE 1 MIN
RESIDUAL CURRENT WAS 0.023 MICROAMP
CXYGEN CONCENTRATION 926 PPM O2 IN N2
NUMBER OF PCINTS IN DOWNSTEP 7

TTIME(SECS)	TIME(MM)	CURR(MICROA)
-0.000	0.000	0.122
3.840	8.000	0.077
6.239	13.000	0.041
8.639	18.000	0.018
11.040	23.000	0.013
13.440	28.000	0.010
15.840	33.000	0.008

POLAROGRAPHIC PROBE CHARACTERIZATION -CHART SPEED 125 MM/MIN -APRIL 4 1973
RESPONSE NUMBER IV-1
DURATION OF EXPOSURE 1 MIN
RESIDUAL CURRENT WAS 0.019 MICROAMP
OXYGEN CONCENTRATION 176 PPM O2 IN N2
NUMBER OF POINTS IN DOWNSTEP 6

TTIME(SECS)	TIME(MM)	CURR(MICROA)
-0.000	0.000	0.025
2.400	5.000	0.020
4.800	10.000	0.018
7.199	15.000	0.013
9.600	20.000	0.009
12.000	25.000	0.008

POLAROGRAPHIC PROBE CHARACTERIZATION -CHART SPEED 125 MM/MIN -APRIL 4 1973
RESPONSE NUMBER IV-2
DURATION OF EXPOSURE 1 MIN
RESIDUAL CURRENT WAS 0.019 MICROAMP
OXYGEN CONCENTRATION 176 PPM O2 IN N2
NUMBER OF POINTS IN DOWNSTEP 6

TTIME(SECS)	TIME(MM)	CURR(MICROA)
-0.000	0.009	0.025
2.400	5.000	0.019
4.800	10.000	0.015
7.199	15.000	0.009
9.600	20.000	0.008
12.000	25.000	0.006

POLAROGRAPHIC PROBE CHARACTERIZATION -CHART SPEED 125 MM/MIN -APRIL 4 1973
RESPONSE NUMBER IV-3
DURATION OF EXPOSURE 1 MIN
RESIDUAL CURRENT WAS 0.019 MICROAMP
OXYGEN CONCENTRATION 176 PPM O2 IN N2
NUMBER OF POINTS IN DOWNSTEP 6

TTIME(SECS)	TIME(MM)	CURR(MICROA)
-0.000	0.000	0.024
2.400	5.000	0.020
4.800	10.000	0.013
7.199	15.000	0.009
9.600	20.000	0.006
12.000	25.000	0.005

POLAROGRAPHIC PROBE CHARACTERIZATION -CHART SPEED 125 MM/MIN -APRIL 4 1973
RESPONSE NUMBER IV-4
DURATION OF EXPOSURE 2 MIN
RESIDUAL CURRENT WAS 0.019 MICROAMP
OXYGEN CONCENTRATION 176 PPM O2 IN N2
NUMBER OF POINTS IN DOWNSTEP 6

TTIME(SECS)	TIME(MM)	CURR(MICROA)
-0.000	0.000	0.025
2.400	5.000	0.018
4.800	10.000	0.015
7.199	15.000	0.011
9.600	20.000	0.008
12.000	25.000	0.006

POLAROGRAPHIC PROBE CHARACTERIZATION -CHART SPEED 125 MM/MIN -APRIL 4 1973
RESPONSE NUMBER IV-5
DURATION OF EXPOSURE 1 MIN
RESIDUAL CURRENT WAS 0.019 MICROAMP
OXYGEN CONCENTRATION 176 PPM O2 IN N2
NUMBER OF POINTS IN DOWNSTEP 6

TTIME(SECS)	TIME(MM)	CURR(MICROA)
-0.000	0.000	0.024
2.400	5.000	0.020
4.800	10.000	0.015
7.199	15.000	0.009
9.600	20.000	0.007
12.000	25.000	0.006

POLAROGRAPHIC PROBE CHARACTERIZATION -CHART SPEED 125 MM/MIN -APRIL 4 1973
RESPONSE NUMBER IV-6
DURATION OF EXPOSURE 2 MIN
RESIDUAL CURRENT WAS 0.019 MICROAMP
OXYGEN CONCENTRATION 176 PPM O2 IN N2
NUMBER OF POINTS IN DOWNSTEP 6

TTIME(SECS)	TIME(MM)	CURR(MICROA)
-0.000	0.000	0.024
2.400	5.000	0.020
4.800	10.000	0.017
7.199	15.000	0.011
9.600	20.000	0.008
12.000	25.000	0.006

POLAROGRAPHIC PROBE CHARACTERIZATION -CHART SPEED 125 MM/MIN -APRIL 4 1973

RESPONSE NUMBER IV-7
DURATION OF EXPOSURE 1 MIN
RESIDUAL CURRENT WAS 0.019 MICROAMP
OXYGEN CONCENTRATION 176 PPM O2 IN N2
NUMBER OF POINTS IN DOWNSTEP 6

TTIME(SECS)	TIME(MM)	CURR(MICROA)
-0.000	0.000	0.025
2.400	5.000	0.020
4.800	10.000	0.015
7.199	15.000	0.010
9.600	20.000	0.007
12.000	25.000	0.006

POLAROGRAPHIC PROBE CHARACTERIZATION -CHART SPEED 125 MM/MIN -APRIL 4 1973
RESPONSE NUMBER IV-8
DURATION OF EXPOSURE 3 MIN
RESIDUAL CURRENT WAS 0.020 MICROAMP
OXYGEN CONCENTRATION 176 PPM O2 IN N2
NUMBER OF POINTS IN DOWNSTEP 6

TTIME(SECS)	TIME(MM)	CURR(MICROA)
-0.000	0.000	0.023
2.880	6.000	0.014
5.279	11.000	0.010
7.680	16.000	0.005
10.079	21.000	0.003
12.479	26.000	0.003

POLAROGRAPHIC PROBE CHARACTERIZATION -CHART SPEED 125 MM/MIN -APRIL 4 1973
RESPONSE NUMBER IV-9
DURATION OF EXPOSURE 1 MIN
RESIDUAL CURRENT WAS 0.018 MICROAMP
OXYGEN CONCENTRATION 176 PPM O2 IN N2
NUMBER OF POINTS IN DOWNSTEP 6

TTIME(SECS)	TIME(MM)	CURR(MICROA)
-0.000	0.000	0.025
2.400	5.000	0.021
4.800	10.000	0.018
7.199	15.000	0.010
9.600	20.000	0.006
12.000	25.000	0.005

POLAROGRAPHIC PROBE CHARACTERIZATION -CHART SPEED 125 MM/MIN -APRIL 4 1973
RESPONSE NUMBER IV-10

DURATION OF EXPOSURE 3 MIN
RESIDUAL CURRENT WAS 0.017 MICROAMP
OXYGEN CONCENTRATION 176 PPM O2 IN N2
NUMBER OF POINTS IN DOWNSTEP 6

TTIME(SECS)	TIME(MM)	CURR(MICROA)
-0.000	0.000	0.025
2.400	5.000	0.022
4.800	10.000	0.017
7.199	15.000	0.013
9.600	20.000	0.010
12.000	25.000	0.007

POLAROGRAPHIC PROBE CHARACTERIZATION -CHART SPEED 125 MM/MIN -APRIL 4 1973
RESPONSE NUMBER IV-11
DURATION OF EXPOSURE 1 MIN
RESIDUAL CURRENT WAS 0.018 MICROAMP
OXYGEN CONCENTRATION 176 PPM O2 IN N2
NUMBER OF POINTS IN DOWNSTEP 6

TTIME(SECS)	TIME(MM)	CURR(MICROA)
-0.000	0.000	0.025
2.400	5.000	0.022
4.800	10.000	0.015
7.199	15.000	0.009
9.600	20.000	0.007
12.000	25.000	0.005

POLAROGRAPHIC PROBE CHARACTERIZATION -CHART SPEED 125 MM/MIN -APRIL 4 1973
RESPONSE NUMBER IV-12
DURATION OF EXPOSURE 1 MIN
RESIDUAL CURRENT WAS 0.018 MICROAMP
OXYGEN CONCENTRATION 176 PPM O2 IN N2
NUMBER OF POINTS IN DOWNSTEP 6

TTIME(SECS)	TIME(MM)	CURR(MICROA)
-0.000	0.000	0.024
3.360	7.000	0.018
5.760	12.000	0.014
8.159	17.000	0.007
10.559	22.000	0.006
12.959	27.000	0.003

POLAROGRAPHIC PROBE CHARACTERIZATION -CHART SPEED 125 MM/MIN -APRIL 4 1973
RESPONSE NUMBER V-1
DURATION OF EXPOSURE 1 MIN

RESIDUAL CURRENT WAS 0.018 MICROAMP
OXYGEN CONCENTRATION 3.02P O2 IN N2
NUMBER OF POINTS IN DOWNSTEP17

TTIME(SECS)	TIME(MM)	CURR(MICROA)
-0.000	0.000	4.149
1.440	3.000	3.362
3.840	8.000	2.019
6.239	13.000	0.507
8.639	18.000	0.337
11.040	23.000	0.227
13.440	28.000	0.162
15.840	33.000	0.114
18.240	38.000	0.084
20.639	43.000	0.069
23.040	48.000	0.051
25.439	53.000	0.041
27.840	58.000	0.032
30.239	63.000	0.025
32.639	68.000	0.022
35.040	73.000	0.020
37.440	78.000	0.018

POLAROGRAPHIC PROBE CHARACTERIZATION -CHART SPEED 125 MM/MIN -APRIL 4 1973
RESPONSE NUMBER V-2
DURATION OF EXPOSURE 1 MIN
RESIDUAL CURRENT WAS 0.018 MICROAMP
OXYGEN CONCENTRATION 3.02P O2 IN N2
NUMBER OF POINTS IN DOWNSTEP16

TTIME(SECS)	TIME(MM)	CURR(MICROA)
-0.000	0.000	4.102
3.360	7.000	2.112
5.760	12.000	0.592
8.159	17.000	0.372
10.559	22.000	0.239
12.959	27.000	0.169
15.360	32.000	0.126
17.760	37.000	0.099
20.159	42.000	0.072
22.560	47.000	0.060
24.959	52.000	0.048
27.360	57.000	0.039
29.759	62.000	0.034
32.160	67.000	0.029
34.559	72.000	0.022
36.959	77.000	0.020

POLAROGRAPHIC PROBE CHARACTERIZATION -CHART SPEED 125 MM/MIN -APRIL 4 1973
RESPONSE NUMBER V-3
DURATION OF EXPOSURE 1 MIN

RESIDUAL CURRENT WAS 0.019 MICROAMP
OXYGEN CONCENTRATION 3.02P O2 IN N2
NUMBER OF POINTS IN DOWNSTEP16

TTIME(SECS)	TIME(MM)	CURR(MICROA)
-0.000	0.000	4.101
1.920	4.000	3.129
6.720	14.000	0.521
9.120	19.000	0.306
11.520	24.000	0.213
13.920	29.000	0.158
16.319	34.000	0.116
18.720	39.000	0.091
21.119	44.000	0.072
23.520	49.000	0.055
25.919	54.000	0.046
28.319	59.000	0.037
30.720	64.000	0.032
33.120	69.000	0.028
35.520	74.000	0.023
37.919	79.000	0.019

POLAROGRAPHIC PROBE CHARACTERIZATION -CHART SPEED 125 MM/MIN -APRIL 4 1973
RESPONSE NUMBER V-4
DURATION OF EXPOSURE 2 MIN
RESIDUAL CURRENT WAS 0.017 MICROAMP
OXYGEN CONCENTRATION 3.02P O2 IN N2
NUMBER OF POINTS IN DOWNSTEP15

TTIME(SECS)	TIME(MM)	CURR(MICROA)
-0.000	0.000	4.103
2.400	5.000	2.853
7.139	15.000	0.483
9.600	20.000	0.298
12.000	25.000	0.218
14.399	30.000	0.160
16.739	35.000	0.125
19.200	40.000	0.095
21.599	45.000	0.078
24.000	50.000	0.062
26.400	55.000	0.050
28.799	60.000	0.046
31.200	65.000	0.039
33.599	70.000	0.033
36.000	75.000	0.030

POLAROGRAPHIC PROBE CHARACTERIZATION -CHART SPEED 125 MM/MIN -APRIL 4 1973
RESPONSE NUMBER V-5
DURATION OF EXPOSURE 1 MIN
RESIDUAL CURRENT WAS 0.019 MICROAMP
OXYGEN CONCENTRATION 3.02P O2 IN N2

NUMBER OF POINTS IN DOWNSTEP16

TTIME(SECS)	TIME(MM)	CURR(MICROA)
-0.000	0.000	4.101
0.960	2.000	3.777
5.760	12.000	0.731
8.159	17.000	0.391
10.559	22.000	0.256
12.959	27.000	0.176
15.360	32.000	0.138
17.760	37.000	0.101
20.159	42.000	0.081
22.560	47.000	0.064
24.959	52.000	0.051
27.360	57.000	0.044
29.739	62.000	0.038
32.160	67.000	0.030
34.559	72.000	0.025
36.959	77.000	0.022

POLAROGRAPHIC PROBE CHARACTERIZATION -CHART SPEED 125 MM/MIN -APRIL 4 1973
RESPONSE NUMBER V-6
DURATION OF EXPOSURE 2 MIN
RESIDUAL CURRENT WAS 0.019 MICROAMP
OXYGEN CONCENTRATION 3.02P O2 IN N2
NUMBER OF POINTS IN DOWNSTEP16

TTIME(SECS)	TIME(MM)	CURR(MICROA)
-0.000	0.000	4.101
1.440	3.000	3.500
6.239	13.000	0.581
8.639	18.000	0.371
11.040	23.000	0.251
13.440	28.000	0.181
15.840	33.000	0.138
18.240	38.000	0.110
20.639	43.000	0.085
23.040	48.000	0.066
25.439	53.000	0.055
27.840	58.000	0.048
30.239	63.000	0.041
32.639	68.000	0.035
35.040	73.000	0.030
37.440	78.000	0.026

POLAROGRAPHIC PROBE CHARACTERIZATION -CHART SPEED 125 MM/MIN -APRIL 4 1973
RESPONSE NUMBER V-7
DURATION OF EXPOSURE 1 MIN
RESIDUAL CURRENT WAS 0.018 MICROAMP
OXYGEN CONCENTRATION 3.02P O2 IN N2
NUMBER OF POINTS IN DOWNSTEP16

TTIME(SECS)	TIME(MM)	CURR(MICROA)
-0.000	0.000	4.056
1.920	4.000	3.223
6.720	14.000	0.532
9.120	19.000	0.332
11.520	24.000	0.234
13.920	29.000	0.164
16.319	34.000	0.129
18.720	39.000	0.100
21.119	44.000	0.079
23.520	49.000	0.063
25.919	54.000	0.051
28.319	59.000	0.043
30.720	64.000	0.036
33.120	69.000	0.030
35.520	74.000	0.027
37.919	79.000	0.023

POLAROGRAPHIC PROBE CHARACTERIZATION -CHART SPEED 125 MM/MIN -APRIL 4 1973
RESPONSE NUMBER V-8
DURATION OF EXPOSURE 3 MIN
RESIDUAL CURRENT WAS 0.018 MICROAMP
OXYGEN CONCENTRATION 3.02P O2 IN N2
NUMBER OF POINTS IN DOWNSTEP16

TTIME(SECS)	TIME(MM)	CURR(MICROA)
-0.000	0.000	4.056
1.920	4.000	3.269
6.720	14.000	0.582
9.120	19.000	0.357
11.520	24.000	0.249
13.920	29.000	0.179
16.319	34.000	0.142
18.720	39.000	0.112
21.119	44.000	0.091
23.520	49.000	0.073
25.919	54.000	0.062
28.319	59.000	0.053
30.720	64.000	0.047
33.120	69.000	0.040
35.520	74.000	0.033
37.919	79.000	0.030

POLAROGRAPHIC PROBE CHARACTERIZATION -CHART SPEED 125 MM/MIN -APRIL 4 1973
RESPONSE NUMBER V-9
DURATION OF EXPOSURE 1 MIN
RESIDUAL CURRENT WAS 0.020 MICROAMP
OXYGEN CONCENTRATION 3.02P O2 IN N2
NUMBER OF POINTS IN DOWNSTEP16

TTIME(SECS)	TIME(MM)	CURR(MICROA)
-0.000	0.000	4.054
2.880	6.000	2.480
5.279	11.000	0.980
7.680	16.000	0.450
10.079	21.000	0.277
12.479	26.000	0.195
14.879	31.000	0.147
17.279	36.000	0.112
19.680	41.000	0.087
22.080	46.000	0.073
24.479	51.000	0.059
26.880	56.000	0.050
29.279	61.000	0.042
31.680	66.000	0.036
34.080	71.000	0.030
36.480	76.000	0.026

POLAROGRAPHIC PROBE CHARACTERIZATION -CHART SPEED 125 MM/MIN -APRIL 4 1973
RESPONSE NUMBER V-10
DURATION OF EXPOSURE 3 MIN
RESIDUAL CURRENT WAS 0.019 MICROAMP
OXYGEN CONCENTRATION 3.02P O2 IN N2
NUMBER OF POINTS IN DOWNSTEP15

TTIME(SECS)	TIME(MM)	CURR(MICROA)
-0.000	0.000	4.055
3.360	7.000	2.574
8.159	17.000	0.486
10.559	22.000	0.296
12.959	27.000	0.216
15.360	32.000	0.163
17.760	37.000	0.130
20.159	42.000	0.098
22.560	47.000	0.082
24.959	52.000	0.066
27.360	57.000	0.056
29.759	62.000	0.049
32.160	67.000	0.043
34.559	72.000	0.034
36.959	77.000	0.032

POLAROGRAPHIC PROBE CHARACTERIZATION -CHART SPEED 125 MM/MIN -APRIL 4 1973
RESPONSE NUMBER V-11
DURATION OF EXPOSURE 1 MIN
RESIDUAL CURRENT WAS 0.020 MICROAMP
OXYGEN CONCENTRATION 3.02P O2 IN N2
NUMBER OF POINTS IN DOWNSTEP15

TTIME(SECS)	TIME(MM)	CURR(MICROA)

-0.000	0.000	4.054
1.920	4.000	3.174
6.720	14.000	0.540
9.120	19.000	0.335
11.520	24.000	0.232
13.920	29.000	0.172
15.319	34.000	0.129
18.720	39.000	0.101
21.119	44.000	0.080
23.520	49.000	0.068
25.919	54.000	0.054
28.319	59.000	0.046
30.720	64.000	0.040
33.120	69.000	0.034
35.520	74.000	0.028

POLAROGRAPHIC PROBE CHARACTERIZATION -CHART SPEED 125 MM/MIN -APRIL 4 1973
RESPONSE NUMBER V-12
DURATION OF EXPOSURE 1 MIN
RESIDUAL CURRENT WAS 0.021 MICROAMP
OXYGEN CONCENTRATION 3.02P O2 IN N2
NUMBER OF POINTS IN DOWNSTEP15

TTIME(SECS)	TIME(MM)	CURR(MICROA)
-0.000	0.000	4.053
3.360	7.030	2.525
8.159	17.000	0.449
10.559	22.000	0.279
12.959	27.000	0.199
15.360	32.000	0.151
17.760	37.000	0.113
20.159	42.000	0.094
22.560	47.000	0.074
24.959	52.000	0.059
27.360	57.000	0.048
29.759	62.000	0.040
32.160	67.000	0.034
34.559	72.000	0.031
36.959	77.000	0.026

POLAROGRAPHIC PROBE CHARACTERIZATION -CHART SPEED 125 MM/MIN -APRIL 4 1973
RESPONSE NUMBER VI-1
DURATION OF EXPOSURE .1 MIN
RESIDUAL CURRENT WAS 0.019 MICROAMP
OXYGEN CONCENTRATION 9.96P O2 IN N2
NUMBER OF POINTS IN DOWNSTEP20

TTIME(SECS)	TIME(MM)	CURR(MICROA)
-0.000	0.000	13.106
3.360	7.000	8.856
5.760	12.000	4.425

10.559	22.000	1.031
12.959	27.000	0.671
15.360	32.000	0.471
17.760	37.000	0.333
20.159	42.000	0.253
22.560	47.000	0.188
24.959	52.000	0.141
27.360	57.000	0.115
29.759	62.000	0.093
32.160	67.000	0.082
34.559	72.000	0.071
36.959	77.000	0.063
39.360	82.000	0.057
41.760	87.000	0.052
44.160	92.000	0.047
46.559	97.000	0.042
48.959	102.000	0.039

POLAROGRAPHIC PROBE CHARACTERIZATION -CHART SPEED 125 MM/MIN -APRIL 4 1973
RESPONSE NUMBER VI-2
DURATION OF EXPOSURE 1 MIN
RESIDUAL CURRENT WAS 0.021 MICROAMP
OXYGEN CONCENTRATION 9.96P O2 IN N2
NUMBER OF POINTS IN DOWNSTEP20

TTIME(SECS)	TIME(MM)	CURR(MICROA)
-0.000	0.000	12.854
2.880	6.000	9.354
5.279	11.000	5.349
7.680	16.000	2.664
12.479	26.000	0.819
14.879	31.000	0.549
17.279	36.000	0.389
19.680	41.000	0.294
22.080	46.000	0.229
24.479	51.000	0.176
26.880	56.000	0.145
29.279	61.000	0.120
31.680	66.000	0.101
34.080	71.000	0.086
36.480	76.000	0.075
38.879	81.000	0.066
41.279	86.000	0.060
43.680	91.000	0.054
46.080	96.000	0.049
48.480	101.000	0.044

POLAROGRAPHIC PROBE CHARACTERIZATION -CHART SPEED 125 MM/MIN -APRIL 4 1973
RESPONSE NUMBER VI-3
DURATION OF EXPOSURE 1 MIN
RESIDUAL CURRENT WAS 0.021 MICROAMP
OXYGEN CONCENTRATION 9.96P O2 IN N2
NUMBER OF POINTS IN DOWNSTEP20

TTIME(SECS)	TIME(MM)	CURR(MICROA)
-0.000	0.000	12.729
1.920	4.000	10.854
4.319	9.000	7.201
6.720	14.000	3.775
11.520	24.000	1.054
13.920	29.000	0.679
16.319	34.000	0.469
18.720	39.000	0.344
21.119	44.000	0.264
23.520	49.000	0.209
25.919	54.000	0.166
28.319	59.000	0.135
30.720	64.000	0.114
33.120	69.000	0.094
35.520	74.000	0.080
37.919	79.000	0.071
40.319	84.000	0.064
42.720	89.000	0.055
45.120	94.000	0.051
47.519	99.000	0.046

POLAROGRAPHIC PROBE CHARACTERIZATION -CHART SPEED 125 MM/MIN -APRIL 4 1973
RESPONSE NUMBER VI-4
DURATION OF EXPOSURE 2 MIN
RESIDUAL CURRENT WAS 0.019 MICROAMP
OXYGEN CONCENTRATION 9.96P O2 IN N2
NUMBER OF POINTS IN DOWNSTEP19

TTIME(SECS)	TIME(MM)	CURR(MICROA)
-0.000	0.000	12.606
1.920	4.000	10.901
6.720	14.000	4.564
9.120	19.000	2.759
13.920	29.000	1.081
16.319	34.000	0.696
18.720	39.000	0.481
21.119	44.000	0.366
23.520	49.000	0.286
25.919	54.000	0.228
28.319	59.000	0.188
30.720	64.000	0.158
33.120	69.000	0.136
35.520	74.000	0.116
37.919	79.000	0.103
40.319	84.000	0.093
42.720	89.000	0.087
45.120	94.000	0.073
47.519	99.000	0.068

POLAROGRAPHIC PROBE CHARACTERIZATION -CHART SPEED 125 MM/MIN -APRIL 4 1973
RESPONSE NUMBER VI-5
DURATION OF EXPOSURE 3 MIN
RESIDUAL CURRENT WAS 0.019 MICROAMP
OXYGEN CONCENTRATION 9.96P O2 IN N2
NUMBER OF POINTS IN DOWNSTEP20

TTIME(SECS)	TIME(MM)	CURR(MICROA)
-0.000	0.000	12.606
2.830	6.000	9.856
5.279	11.000	6.462
7.690	16.000	4.425
10.079	21.000	3.037
14.479	31.000	1.406
17.279	36.000	0.981
19.680	41.000	0.666
22.080	46.000	0.481
24.479	51.000	0.361
26.880	56.000	0.288
29.279	61.000	0.238
31.680	66.000	0.201
34.080	71.000	0.175
36.480	76.000	0.152
38.879	81.000	0.137
41.279	86.000	0.123
43.680	91.000	0.111
46.080	96.000	0.101
48.480	101.000	0.093

POLAROGRAPHIC PROBE CHARACTERIZATION -CHART SPEED 125 MM/MIN -APRIL 4 1973
RESPONSE NUMBER VI-6
DURATION OF EXPOSURE 1 MIN
RESIDUAL CURRENT WAS 0.019 MICROAMP
OXYGEN CONCENTRATION 9.96P O2 IN N2
NUMBER OF POINTS IN DOWNSTEP20

TTIME(SECS)	TIME(MM)	CURR(MICROA)
-0.000	0.000	12.606
2.880	6.000	9.606
5.279	11.000	5.907
7.680	16.000	3.407
12.479	26.000	1.193
14.879	31.000	0.751
17.279	36.000	0.511
19.680	41.000	0.371
22.080	46.000	0.286
24.479	51.000	0.226
26.880	56.000	0.183
29.279	61.000	0.153
31.660	66.000	0.127
34.080	71.000	0.108
36.480	76.000	0.092
38.879	81.000	0.083
41.279	86.000	0.072

43.480	91.000	0.067
46.080	96.000	0.057
48.480	101.000	0.053

POLAROGRAPHIC PROBE CHARACTERIZATION -CHART SPEED 125 MM/MIN -APRIL 4 1973
RESPONSE NUMBER VII-1
DURATION OF EXPOSURE 1 MIN
RESIDUAL CURRENT WAS 0.019 MICROAMP
OXYGEN CONCENTRATION 21 P O2 IN N2
NUMBER OF POINTS IN DOWNSTEP25

TTIME(SECS)	TIME(MM)	CURR(MICROA)
-0.000	0.000	26.496
2.880	6.000	20.814
5.279	11.000	14.356
7.630	16.000	10.356
10.079	21.000	7.481
12.479	26.000	5.583
14.879	31.000	4.009
17.279	36.000	2.851
22.040	46.000	1.406
24.479	51.000	1.006
26.880	56.000	0.716
29.279	61.000	0.531
31.640	66.000	0.418
34.080	71.000	0.343
36.480	76.000	0.293
38.879	81.000	0.248
41.279	86.000	0.217
43.680	91.000	0.192
46.080	96.000	0.173
48.480	101.000	0.157
50.879	106.000	0.143
53.279	111.000	0.130
55.680	116.000	0.122
58.080	121.000	0.113
60.479	126.000	0.107

POLAROGRAPHIC PROBE CHARACTERIZATION -CHART SPEED 125 MM/MIN -APRIL 4 1973
RESPONSE NUMBER VII-2
DURATION OF EXPOSURE 1 MIN
RESIDUAL CURRENT WAS 0.018 MICROAMP
OXYGEN CONCENTRATION 21 P O2 IN N2
NUMBER OF POINTS IN DOWNSTEP25

TTIME(SECS)	TIME(MM)	CURR(MICROA)
-0.000	0.000	26.497
2.880	6.000	20.058
5.279	11.000	13.232
7.680	16.000	8.982
10.079	21.000	6.186

12.479	26.000	4.155
14.879	31.000	2.760
19.680	41.000	1.207
22.080	46.000	0.792
24.479	51.000	0.552
26.880	56.000	0.412
29.279	61.000	0.334
31.680	66.000	0.279
34.080	71.000	0.237
36.480	76.000	0.204
38.879	81.000	0.181
41.279	86.000	0.158
43.680	91.000	0.146
46.080	96.000	0.131
48.480	101.000	0.117
50.879	106.000	0.111
53.279	111.000	0.099
55.680	116.000	0.093
58.080	121.000	0.083
60.479	126.000	0.077

POLAROGRAPHIC PROBE CHARACTERIZATION -CHART SPEED 125 MM/MIN -APRIL 4 1973
RESPONSE NUMBER VII-3
DURATION OF EXPOSURE 1 MIN
RESIDUAL CURRENT WAS 0.017 MICROAMP
OXYGEN CONCENTRATION 21 P O2 IN N2
NUMBER OF POINTS IN DOWNSTEP25

TTIME(SECS)	TIME(MM)	CURR(MICROA)
-0.000	0.000	25.362
2.480	6.000	19.680
5.279	11.000	13.483
7.680	16.000	9.608
10.079	21.000	6.927
12.479	26.000	4.937
14.879	31.000	3.409
17.279	36.000	2.298
22.080	46.000	1.145
24.479	51.000	0.793
26.880	56.000	0.578
29.279	61.000	0.438
31.680	66.000	0.355
34.080	71.000	0.295
36.480	76.000	0.250
38.879	81.000	0.217
41.279	86.000	0.190
43.680	91.000	0.170
46.080	96.000	0.152
48.480	101.000	0.138
50.879	106.000	0.125
53.279	111.000	0.114
55.680	116.000	0.104
58.080	121.000	0.098
60.479	126.000	0.090

POLAROGRAPHIC PROBE CHARACTERIZATION -CHART SPEED 125 MM/MIN -APRIL 4 1973
RESPONSE NUMBER VII-4
DURATION OF EXPOSURE 2 MIN
RESIDUAL CURRENT WAS 0.016 MICROAMP
OXYGEN CONCENTRATION 21 P O2 IN N2
NUMBER OF POINTS IN DOWNSTEP26

TTIME(SECS)	TIME(MM)	CURR(MICROA)
-0.000	0.000	25.363
1.920	4.000	21.575
4.319	9.000	15.984
6.720	14.000	14.484
9.120	19.000	9.609
11.520	24.000	7.762
13.920	29.000	6.234
16.319	34.000	4.938
18.720	39.000	3.919
21.119	44.000	3.086
23.920	49.000	2.438
28.319	59.000	1.521
30.720	64.000	1.446
33.120	69.000	0.946
35.520	74.000	0.754
37.919	79.000	0.619
40.319	84.000	0.519
42.720	89.000	0.439
45.120	94.000	0.379
47.519	99.000	0.331
49.919	104.000	0.296
52.319	109.000	0.266
54.720	114.000	0.241
57.120	119.000	0.224
59.519	124.000	0.203
61.919	129.000	0.186

POLAROGRAPHIC PROBE CHARACTERIZATION -CHART SPEED 125 MM/MIN -APRIL 4 1973
RESPONSE NUMBER VII-5
DURATION OF EXPOSURE 1 MIN
RESIDUAL CURRENT WAS 0.019 MICROAMP
OXYGEN CONCENTRATION 21 P O2 IN N2
NUMBER OF POINTS IN DOWNSTEP26

TTIME(SECS)	TIME(MM)	CURR(MICROA)
-0.000	0.000	24.981
2.880	6.000	19.481
5.279	11.000	13.356
7.680	16.000	9.981
10.079	21.000	7.731
12.479	26.000	5.814
14.879	31.000	4.333
17.279	36.000	3.175
19.680	41.000	2.296
22.080	46.000	1.706

24.479	51.000	1.268
26.880	56.000	0.918
29.279	61.000	0.691
31.660	66.000	0.526
34.080	71.000	0.418
36.400	76.000	0.346
38.879	81.000	0.296
41.279	86.000	0.253
43.639	91.000	0.223
46.080	96.000	0.197
48.480	101.000	0.176
50.879	106.000	0.162
53.279	111.000	0.145
55.680	116.000	0.133
58.080	121.000	0.121
60.479	126.000	0.113

POLAROGRAPHIC PROBE CHARACTERIZATION -CHART SPEED 125 MM/MIN -APRIL 4 1973
RESPONSE NUMBER VII-6
DURATION OF EXPOSURE 3 MIN
RESIDUAL CURRENT WAS 0.018 MICROAMP
OXYGEN CONCENTRATION 21 P O2 IN N2
NUMBER OF POINTS IN CONSTEP25

TTIME(SECS)	TIME(MM)	CURR(MICROA)
-0.000	0.000	25.361
2.400	5.000	20.815
4.800	10.000	15.232
7.199	15.000	12.232
9.600	20.000	10.232
12.000	25.000	8.732
14.399	30.000	7.528
16.799	35.000	6.371
19.200	40.000	5.399
21.599	45.000	4.565
24.000	50.000	3.825
26.400	55.000	3.223
28.799	60.000	2.713
31.200	65.000	2.292
36.000	75.000	1.767
38.400	80.000	1.445
40.800	85.000	1.219
43.199	90.000	1.044
45.599	95.000	0.857
48.000	100.000	0.727
50.400	105.000	0.677
52.800	110.000	0.597
55.199	115.0[illegible]	0.532
57.599	120.[illegible]	0.472
60.000	125.000	0.424

POLAROGRAPHIC PROBE CHARACTERIZATION -CHART SPEED 125 MM/MIN -APRIL 4 1973
RESPONSE NUMBER VII-7

DURATION CF EXPOSURE 1 MIN
RESIDUAL CURRENT WAS 0.019 MICROAMP
CXYGEN CONCENTRATICN 21 P O2 IN N2
NUMBER OF PCINTS IN DOWNSTEP24

TTIME(SECS)	TIME(MM)	CURR(MICROA)
-0.0C0	0.000	24.981
2.880	6.C00	19.678
5.279	11.CC0	13.856
7.680	16.C30	10.356
12.479	26.CC0	6.370
14.879	31.C00	4.842
17.279	36.000	3.638
19.680	41.C30	2.712
22.080	46.CC0	2.C64
26.880	56.CC0	1.168
29.279	61.000	0.876
31.680	66.CC0	0.671
34.CH0	71.CC0	0.526
36.480	76.C00	0.416
38.879	81.000	0.353
41.279	86.CC0	0.3C3
43.680	91.000	0.263
46.080	96.000	0.228
48.480	101.000	0.2C8
50.879	106.CC0	0.183
53.279	111.000	0.167
55.680	116.000	0.153
58.080	121.000	0.141
60.479	126.C00	0.132

APPENDIX 2.7

PROGRAM KOK2

Program KOK2 and subroutine POLY were used to calculate the following:

- The fifth-order least-square polynomials through the downstep data
- The probe currents as calculated from the polynomials
- The probe currents as calculated from the polynomials expressed as percentages of the maximum average current observed during exposure.

```
PAGE   1

// JOB    1122

LOG DRIVE   CART SPEC   CART AVAIL   PHY DRIVE
  0000        1122        1122         0000

V2 M10   ACTUAL  8K   CONFIG  8K

// DUP

*DELETE              POLY
CART ID 1122   DB ADDR  4955   DB CNT   0012

// FOR
* LIST SOURCE PROGRAM
* ONE WORD INTEGERS
C      ROBERT KOK
      SUBROUTINE POLY(N1,N,X,Y,A)
C A LEAST SQUARES APPROXIMATION FOR A POLYNOMIAL OF DEGREE N WITH N1 PTS
C X IS VECTOR OF INDEPENDENT VARIABLE, Y OF DEPENDENT VARIABLE,A IS OUTP
C UT VECTOR OF DEGREE N+1 OF COEFFICIENTS
      DIMENSION X(1),Y(1),A(1),S(400)
      NP1 =N+1
      DO 2 I=1,400
    2 S(I)=0.0
      DO 6 I=1,20
    6 A(I)=0.0
      DO 4 K=1,N1
      P1 = 1.0
      DO 4 I=1,NP1
      P2 = 1.0
      DO 3 J=1,I
      K1=(J-1)*NP1+I
      S(K1)=S(K1)+P1*P2
    3 P2 = P2*X(K)
      A(I)=A(I)+P1*Y(K)
    4 P1 = P1*X(K)
      DO 5 I=1,NP1
      DO 5 J=1,I
      K2=(I-1)*NP1+J
      K3=(J-1)*NP1+I
    5 S(K2)=S(K3)
      CALL SIMQ (S,A,NP1,0)
      RETURN
      END

FEATURES SUPPORTED
 ONE WORD INTEGERS

CORE REQUIREMENTS FOR POLY
 COMMON      0  VARIABLES     814  PROGRAM     258

RELATIVE ENTRY POINT ADDRESS IS 0336 (HEX)

END OF COMPILATION

// DUP

*STORE      WS  UA   POLY
```

```
PAGE   2

CART ID 1122   DB ADDR  4998   DB CNT   0012

*DELETE              KOK2
CART ID 1122   DB ADDR  4955   DB CNT   0C46

// FOR
* IOCS (CARD,1403 PRINTER)
* ONE WORD INTEGERS
* LIST SOURCE PROGRAM
* NAME KOK2
C ROBERT KOK
C PROGRAM KOK2 TO DETERMINE THE CLOSEST FITTING POLYNOMIALS OF DEGREE N6
C FOR SETS OF 1,2 AND 3-MINUTE EXPOSURE DOWNSTEPS FOR THE YSI POLAROGRAPHIC
C PROBE.REQUIRES USER-SUPPLIED SUBROUTINE POLY AND IBM-SUPPLIED SUB
C ROUTINE SIMQ
C DETAILED OUTPUT CAN BE SUPPRESSED BY MEANS OF DATA SWITCH NO. 1
C N1-NO. OF CALIBRATION GASES USED---N2-NO. OF DIFFERENT EXPOSURE TIMES-
C -- N3-NO. OF DOWNSTEPS AT GIVEN GAS CONC'N AND EXPOSURE TIME---N4-NO.
C OF POINTS IN A GIVEN DOWNSTEP RESPONSE---N5-TOTAL NO. OF PTS FOR POLYNOMIAL
C CALCULATION---N6-DEGREE OF POLYNOMIAL TO BE CALCULATED
C I1,I2,I3,I4 ARE DO-LOOP COUNTERS---I,J,K ARE GENERAL COUNTERS
C A2-TITLE PRINTOUT VARIABLE---COEFF-POLYNOMIAL COEFFICIENT VECTOR
C TIME-TIME VECTOR IN MM AT CHART SPEED OF 125 MM/MIN
C CURR-CURRENT VECTOR IN MICROAMPS
C TTIME-TIME IN SECONDS---PCURR-CURRENT AS CALCULATED FROM REGRESSION
C POLYNOMIAL---DCURR-DUMMY VARIABLE VECTOR---PROD-EXPONENTIALS OF TIME
C FOR THE DETERMINATION OF PCURR---DIFF-VECTOR OF DIFFERENCE BETWEEN LOGS
C OF OBSERVED AND CALCULATED CURRENT
C
C ****************************************************************
C
      DIMENSION A2(10),TIME(200),CURR(200),COEFF(20), DIFF(2),ECURR(2)
      READ(2,100)N1,N2,N6
  100 FORMAT(3I5)
      CALL DATSW(1,I1)
      GO TO (1,2),I1
    2 WRITE(5,101)
  101 FORMAT(1H1)
      WRITE(5,102)N1,N2,N6
  102 FORMAT(33H NUMBER OF CALIBRATION GASES USEDI5,/35H NUMBER OF DIFFE
     1RENT EXPOSURE TIMESI5,/32H DEGREE OF POLYNOMIAL CALCULATEDI5,/)
    1 DO 10 I1=1,N1
      DO 20 I2=1,N2
      READ(2,100)N3
      WRITE(5,101)
      WRITE(5,103)N3,I2
  103 FORMAT(23H NUMBER OF DOWNSTEPS ISI5, 6H AFTERI5,17H MINUTES EXPOSU
     1RE//)
      N5=0
      I4=1
      DIFFA=0.0
      DO 30 I3=1,N3
      READ(2,104)(A2(I),I=1,10),N4
  104 FORMAT(5A2,10X,5A2,I2)
      WRITE(5,105)(A2(I),I=1,10),N4
  105 FORMAT(13H DOWNSTEP NO.5A2, 8HUSED GAS5A2,9H O2 IN N2/19H NUMBER O
     1F POINTS  I2,/)
      N5=N5+N4
      READ(2,106)(TIME(I),CURR(I),I=I4,N5)
```

```
      DIFFA=DIFFA+CURR(I4)
  106 FORMAT(HF10.3)
      CALL CATSW(1,II)
      GO TO (30,3),II
    3 WRITE(5,107)
  107 FORMAT(24H TIME(MM)  CURR(MICRO-A)/)
      WRITE(5,108)(TIME(I),CURR(I),I=I4,N5)
  108 FORMAT(2F10.3)
   30 I4=I4+N4
      DO 40 I=1,N5
   40 CURR(I)=ALOG(CURR(I))
      CALL POLY(N5,N6,TIME,CURR,COEFF)
      J=N6+1
      WRITE(5,109)
  109 FORMAT(/44H COEFFICIENTS OF LEAST SQUARE POLYNOMIAL ARE/)
      WRITE(5,110)(COEFF(I),I=1,J)
  110 FORMAT(E15.5)
      CALL CATSW(1,II)
      GO TO (5,4),II
    4 WRITE(5,111)
      DIFFA=0.0
  111 FORMAT(/105H       TIME(MM)       TIME(SEC)      LN OF CURR    LN POL
     1Y CURR         DIFFA  CURR(MICRO-A)  POLY(MICRO-A)/)
      DO 50 I=1,N5
      TTIME=TIME(I)*0.48
      PCURR=COEFF(1)
      PROD=TIME(I)
      DO 60 K=2,J
      PCURR=PCURR+COEFF(K)*PROD
   60 PROD=PROD*TIME(I)
      DIFF(1)=ABS(ABS(PCURR)-ABS(CURR(I)))
      IF(TIME(I)-0.1)61,61,62
   62 DIFFA=DIFFA+(DIFF(1)+DIFF(2))/2*(TIME(I)-TIME(I-1))
   61 DIFF(2)=DIFF(1)
      ECURR(1)=EXP(CURR(I))
      ECURR(2)=EXP(PCURR)
   90 WRITE(5,112)TIME(I),TTIME,CURR(I),PCURR,DIFFA,ECURR(1),ECURR(2)
  112 FORMAT(7F15.3)
      GO TO 20
    5 N5=N5/N3
      DIFFA=DIFFA/N3
      WRITE(5,115)DIFFA
  115 FORMAT(/24H MAXIMUM AVERAGE CURRENTF10.3,11H MICRO-AMPS/)
      WRITE(5,113)
  113 FORMAT(/105H         TIME IN MM          TIME IN SECS        CURRENT-M
     1ICRO-A      CALCULATED CURR        PERCENT OF MAX CURR/)
      DO 70 I=1,N5
      TTIME=TIME(I)*0.48
      PCURR=CCEFF(1)
      PROD=TIME(I)
      DO 80 K=2,J
      PCURR=PCURR+COEFF(K)*PROD
   80 PROD=PROD*TIME(I)
      CURR(I)=EXP(CURR(I))
      PCURR=EXP(PCURR)
      ECURR(1)=PCURR/DIFFA*100.
   70 WRITE(5,114)TIME(I),TTIME,CURR(I),PCURR,ECURR(1)
  114 FORMAT(5F20.3)
   20 CONTINUE
```

```
PAGE   4

   10 CONTINUE
      CALL EXIT
      END

FEATURES SUPPORTED
 ONE WORD INTEGERS
 IOCS

CORE REQUIREMENTS FOR KOK2
 COMMON      0  VARIABLES     898  PROGRAM    1662

END OF COMPILATION

// DUP

*STORE       WS  UA  KOK2
CART ID 1122    DB ADDR  4967    DB CNT    0046

// XEQ KOK2
```

APPENDIX 2.8

RESULTS FROM PROGRAM KOK2

The following were listed by Program KOK2:

- The number of downsteps used for the calculations
- The exposure duration - min
- The downstep identification numbers
- The oxygen tension the probe was exposed to
  - % O_2 in N_2 or ppm O_2 in N_2
- The number of data points recorded during each downstep
- The coefficients of the least-square fifth-order polynomial
- The maximum average observed current-microamp

The following are shown in tabular format:

- The time elapsed since the downstep - mm
- The time elapsed since the downstep - sec
- The current observed during the first downstep listed - microamp
- The current calculated from the polynomial - microamp
- The current calculated from the polynomial as a percentage of the maximum average observed current - %

NUMBER OF CONSTEPS IS 8 AFTER 1 MINUTES EXPOSURE

CONSTEP NO. 1-1 USED GAS 0.3P O2 IN N2
NUMBER OF POINTS 9

CONSTEP NO. 1-2 USED GAS 0.3P O2 IN N2
NUMBER OF POINTS 10

CONSTEP NO. 1-3 USED GAS 0.3P O2 IN N2
NUMBER OF POINTS 10

CONSTEP NO. 1-5 USED GAS 0.3P O2 IN N2
NUMBER OF POINTS 11

CONSTEP NO. 1-7 USED GAS 0.3P O2 IN N2
NUMBER OF POINTS 11

CONSTEP NO. 1-9 USED GAS 0.3P O2 IN N2
NUMBER OF POINTS 10

CONSTEP NO. 1-11 USED GAS 0.3P O2 IN N2
NUMBER OF POINTS 10

CONSTEP NO. 1-12 USED GAS 0.3P O2 IN N2
NUMBER OF POINTS 11

COEFFICIENTS OF LEAST SQUARE POLYNOMIAL ARE

-0.828997E 00
0.422888E-01
-0.201618E-01
0.922038E-03
-0.169038E-04
0.111092E-06

MAXIMUM AVERAGE CURRENT 0.437 MICRO-AMPS

TIME IN MM	TIME IN SECS	CURRENT-MICRO-A	CALCULATED CURR	PERCENT OF MAX CURR
0.000	0.000	0.454	0.436	99.799
6.000	2.880	0.314	0.325	74.381
11.000	5.279	0.184	0.164	37.579
16.000	7.680	0.064	0.079	18.244
21.000	10.079	0.046	0.043	10.028
26.000	12.479	0.024	0.028	6.519
31.000	14.879	0.020	0.021	4.841
36.000	17.279	0.015	0.016	3.821
41.000	19.680	0.012	0.013	2.999
0.000	0.000	0.443	0.436	99.799

NUMBER OF DOWNSTEPS IS 2 AFTER 2 MINUTES EXPOSURE

DOWNSTEP NO. 1-4 USED GAS 0.3P O2 IN N2
NUMBER OF POINTS 10

DOWNSTEP NO. 1-6 USED GAS 0.3P O2 IN N2
NUMBER OF POINTS 10

COEFFICIENTS OF LEAST SQUARE POLYNOMIAL ARE

-0.83342E 00
0.45641E-01
-0.21188E-01
0.97046E-03
-0.17681E-04
0.11507E-06

MAXIMUM AVERAGE CURRENT 0.437 MICRO-AMPS

TIME IN MM	TIME IN SECS	CURRENT-MICRO-A	CALCULATED CURR	PERCENT OF MAX CURR
0.000	0.000	0.437	0.434	99.441
6.000	2.880	0.302	0.321	73.570
11.000	5.279	0.184	0.158	36.204
16.000	7.680	0.062	0.074	17.159
21.000	10.079	0.041	0.040	9.324
26.000	12.479	0.028	0.026	6.092
31.000	14.879	0.019	0.020	4.612
36.000	17.279	0.016	0.016	3.744
41.000	19.680	0.013	0.013	3.024
46.000	22.080	0.010	0.010	2.358

NUMBER OF COWNSTEPS IS 2 AFTER 3 MINUTES EXPOSURE

DOWNSTEP NO. 1-8 USED GAS 0.3P O2 IN N2
NUMBER OF POINTS 11

DOWNSTEP NO. 1-10 USED GAS 0.3P O2 IN N2
NUMBER OF POINTS 11

COEFFICIENTS OF LEAST SQUARE POLYNOMIAL ARE

-0.843066E 00
0.521677E-01
-0.195886E-01
0.864996E-03
-0.155618E-04
0.101546E-06

MAXIMUM AVERAGE CURRENT 0.432 MICRO-AMPS

TIME IN PP	TIME IN SECS	CURRENT-MICRO-A	CALCULATED CURR	PERCENT OF MAX CURR
0.000	0.000	0.432	0.430	99.627
5.000	2.400	0.357	0.377	87.468
10.000	4.800	0.227	0.209	48.608
15.000	7.199	0.097	0.104	24.172
20.000	9.600	0.048	0.056	12.993
25.000	12.000	0.035	0.034	8.095
30.000	14.399	0.028	0.024	5.779
35.000	16.799	0.017	0.019	4.478
40.000	19.200	0.015	0.015	3.548
45.000	21.599	0.012	0.012	2.801
50.000	24.000	0.010	0.009	2.305

NUMBER OF DOWNSTEPS IS 8 AFTER 1 MINUTES EXPOSURE

DOWNSTEP NO. 11-1 USED GAS 1.01P O2 IN N2
NUMBER OF POINTS 12

DOWNSTEP NO. 11-2 USED GAS 1.01P O2 IN N2
NUMBER OF POINTS 12

DOWNSTEP NO. 11-3 USED GAS 1.01P O2 IN N2
NUMBER OF POINTS 12

DOWNSTEP NO. 11-5 USED GAS 1.01P O2 IN N2
NUMBER OF POINTS 12

DOWNSTEP NO. 11-7 USED GAS 1.01P O2 IN N2
NUMBER OF POINTS 12

DOWNSTEP NO. 11-9 USED GAS 1.01P O2 IN N2
NUMBER OF POINTS 12

DOWNSTEP NO. 11-11 USED GAS 1.01P O2 IN N2
NUMBER OF POINTS 12

DOWNSTEP NO. 11-12 USED GAS 1.01P O2 IN N2
NUMBER OF POINTS 12

COEFFICIENTS OF LEAST SQUARE POLYNOMIAL ARE

0.39606E 00
-0.32697E-01
-0.12964E-01
0.61719E-03
-0.10950E-04
0.67998E-07

MAXIMUM AVERAGE CURRENT 1.424 MICRO-AMPS

TIME IN MM	TIME IN SECS	CURRENT-MICRO-A	CALCULATED CURR	PERCENT OF MAX CURR
0.000	0.000	1.441	1.485	104.278
8.000	3.840	0.790	0.655	46.021
13.000	6.239	0.300	0.316	22.184
18.000	8.639	0.157	0.162	11.430
23.000	11.040	0.097	0.097	6.815
28.000	13.440	0.075	0.067	4.734
33.000	15.840	0.053	0.052	3.682
38.000	18.240	0.042	0.042	3.014
43.000	20.639	0.033	0.034	2.453
48.000	23.040	0.026	0.027	1.929
53.000	25.439	0.022	0.021	1.506
58.000	27.840	0.018	0.018	1.301

NUMBER OF DOWNSTEPS IS 2 AFTER 2 MINUTES EXPOSURE

DOWNSTEP NO. II-4 USED GAS 1.01P O2 IN N2
NUMBER OF POINTS 12

DOWNSTEP NO. II-6 USED GAS 1.01P O2 IN N2
NUMBER OF POINTS 12

COEFFICIENTS OF LEAST SQUARE POLYNOMIAL ARE

0.37095E 00
-0.20453E-01
-0.15442E-01
0.76045E-03
-0.14091E-04
0.91494E-07

MAXIMUM AVERAGE CURRENT 1.422 MICRO-AMPS

TIME IN MM	TIME IN SECS	CURRENT-MICRO-A	CALCULATED CURR	PERCENT OF MAX CURR
0.000	0.000	1.428	1.449	101.870
4.000	1.920	1.029	1.091	76.704
9.000	4.319	0.619	0.550	38.708
14.000	6.720	0.204	0.259	18.267
19.000	9.120	0.129	0.137	9.643
24.000	11.520	0.091	0.086	6.071
29.000	13.920	0.065	0.063	4.481
34.000	16.319	0.049	0.051	3.638
39.000	18.720	0.042	0.042	3.011
44.000	21.119	0.033	0.034	2.406
49.000	23.520	0.025	0.026	1.861
54.000	25.919	0.022	0.021	1.527

NUMBER OF DOWNSTEPS IS 2 AFTER 3 MINUTES EXPOSURE

DOWNSTEP NO. II-8 USED GAS 1.01P O2 IN N2
NUMBER OF POINTS 12

DOWNSTEP NO. II-10 USED GAS 1.01P O2 IN N2
NUMBER OF POINTS 12

COEFFICIENTS OF LEAST SQUARE POLYNOMIAL ARE

0.37291E 00
-0.22762E-01
-0.14746E-01
0.72399E-03
-0.13340E-04
0.84009E-07

MAXIMUM AVERAGE CURRENT 1.415 MICRO-AMPS

TIME IN MM	TIME IN SECS	CURRENT-MICRO-A	CALCULATED CURR	PERCENT OF MAX CURR
0.000	0.000	1.415	1.451	102.576
7.000	3.360	0.849	0.747	52.796
12.000	5.760	0.394	0.357	25.275
17.000	8.159	0.174	0.180	12.767
22.000	10.559	0.109	0.106	7.537
27.000	12.959	0.081	0.074	5.263
32.000	15.360	0.060	0.058	4.150
37.000	17.760	0.048	0.048	3.437
42.000	20.159	0.039	0.039	2.800
47.000	22.560	0.032	0.030	2.182
52.000	24.959	0.025	0.024	1.700
57.000	27.360	0.022	0.021	1.532

NUMBER OF DOWNSTEPS IS 8 AFTER 1 MINUTES EXPOSURE

DOWNSTEP NO. III-1 USED GAS 926 PPM O2 IN N2
NUMBER OF POINTS 7

DOWNSTEP NO. III-2 USED GAS 926 PPM O2 IN N2
NUMBER OF POINTS 7

DOWNSTEP NO. III-3 USED GAS 926 PPM O2 IN N2
NUMBER OF POINTS 7

DOWNSTEP NO. III-5 USED GAS 926 PPM O2 IN N2
NUMBER OF POINTS 7

DOWNSTEP NO. III-7 USED GAS 926 PPM O2 IN N2
NUMBER OF POINTS 7

DOWNSTEP NO. III-9 USED GAS 926PPM O2 IN N2
NUMBER OF POINTS 7

DOWNSTEP NO. III-11 USED GAS 926 PPM O2 IN N2
NUMBER OF POINTS 7

DOWNSTEP NO. III-12 USED GAS 926 PPM O2 IN N2
NUMBER OF POINTS 7

COEFFICIENTS OF LEAST SQUARE POLYNOMIAL ARE

-0.21062E 01
0.34496E-01
-0.13303E-01
0.10003E-03
0.18354E-04
-0.32788E-06

MAXIMUM AVERAGE CURRENT 0.121 MICRO-AMPS

TIME IN MM	TIME IN SECS	CURRENT-MICRO-A	CALCULATED CURR	PERCENT OF MAX CURR
0.000	0.000	0.119	0.121	99.744
7.000	3.360	0.094	0.087	72.115
12.000	5.760	0.055	0.043	36.030
17.000	8.159	0.022	0.021	17.573
22.000	10.559	0.015	0.013	10.851
27.000	12.959	0.012	0.010	8.947
32.000	15.360	0.010	0.008	7.337

NUMBER OF CCNASTEPS IS 2 AFTER 2 MINUTES EXPOSURE

CONASTEP NC. III-4 USED GAS 926 PPM O2 IN N2
NUMBER OF PCINTS 7

CONASTEP NC. III-6 USED GAS 926 PPM O2 IN N2
NUMBER OF PCINTS 7

COEFFICIENTS OF LEAST SQUARE POLYNOMIAL ARE

-0.21058E 01
0.39171E-02
-0.12269E-02
-0.10718E-02
0.62359E-04
-0.94444E-06

MAXIMUM AVERAGE CURRENT 0.122 MICRO-AMPS

TIME IN MM	TIME IN SECS	CURRENT-MICRO-A	CALCULATED CURR	PERCENT OF MAX CURR
0.000	0.000	0.121	0.121	99.787
7.000	3.360	0.090	0.093	76.444
12.000	5.760	0.053	0.048	39.619
17.000	8.159	0.021	0.022	18.475
22.000	10.559	0.014	0.013	11.280
27.000	12.959	0.012	0.012	10.032
32.000	15.360	0.010	0.009	7.751

NUMBER OF DOWNSTEPS IS   2 AFTER   3 MINUTES EXPOSURE

DOWNSTEP NO. III-8   USED GAS   926 PPM O2 IN N2
NUMBER OF POINTS   7

DOWNSTEP NO. III-10   USED GAS   926 PPM O2 IN N2
NUMBER OF POINTS   7

COEFFICIENTS OF LEAST SQUARE POLYNOMIAL ARE

-0.20967E 01
0.91924E-02
-0.53037E-02
-0.70127E-03
0.51725E-04
-0.85684E-06

MAXIMUM AVERAGE CURRENT   0.123 MICRO-AMPS

TIME IN MN	TIME IN SECS	CURRENT-MICRO-A	CALCULATED CURR	PERCENT OF MAX CURR
0.000	0.000	0.123	0.122	99.882
6.000	2.880	0.098	0.097	79.601
11.000	5.279	0.055	0.052	42.479
16.000	7.680	0.022	0.024	20.323
21.000	10.079	0.016	0.015	12.463
26.000	12.479	0.012	0.013	10.886
31.000	14.879	0.010	0.010	8.476

NUMBER OF DOWNSTEPS IS 8 AFTER 1 MINUTES EXPOSURE

DOWNSTEP NO. IV-1 USED GAS 176 PPM O2 IN N2
NUMBER OF POINTS 6

DOWNSTEP NO. IV-2 USED GAS 176 PPM O2 IN N2
NUMBER OF POINTS 6

DOWNSTEP NO. IV-3 USED GAS 176 PPM O2 IN N2
NUMBER OF POINTS 6

DOWNSTEP NO. IV-5 USED GAS 176 PPM O2 IN N2
NUMBER OF POINTS 6

DOWNSTEP NO. IV-7 USED GAS 176 PPM O2 IN N2
NUMBER OF POINTS 6

DOWNSTEP NO. IV-9 USED GAS 176 PPM O2 IN N2
NUMBER OF POINTS 6

DOWNSTEP NO. IV-11 USED GAS 176 PPM O2 IN N2
NUMBER OF POINTS 6

DOWNSTEP NO. IV-12 USED GAS 176 PPM O2 IN N2
NUMBER OF POINTS 6

COEFFICIENTS OF LEAST SQUARE POLYNOMIAL ARE

-0.37032E 01
-0.18719E 00
0.55342E-01
-0.665866E-02
0.307376-03
-0.485186E-05

MAXIMUM AVERAGE CURRENT 0.024 MICRO-AMPS

TIME IN MM	TIME IN SECS	CURRENT-MICRO-A	CALCULATED CURR	PERCENT OF MAX CURR
0.000	0.000	0.025	0.024	100.072
5.000	2.400	0.020	0.019	80.569
10.000	4.800	0.018	0.016	65.508
15.000	7.199	0.013	0.009	37.815
20.000	9.600	0.009	0.007	28.793
25.000	12.000	0.008	0.005	23.013

NUMBER OF DOWNSTEPS IS 2 AFTER 2 MINUTES EXPOSURE

DOWNSTEP NO. IV-4 USED GAS 176 PPM O2 IN N2
NUMBER OF POINTS 6

DOWNSTEP NO. IV-6 USED GAS 176 PPM O2 IN N2
NUMBER OF POINTS 6

COEFFICIENTS OF LEAST SQUARE POLYNOMIAL ARE

-0.37075E 01
-0.13814E 00
0.30987E-01
-0.33850E-02
0.14606E-03
-0.22001E-05

MAXIMUM AVERAGE CURRENT 0.024 MICRO-AMPS

TIME IN MM	TIME IN SECS	CURRENT-MICRO-A	CALCULATED CURR	PERCENT OF MAX CURR
0.000	0.000	0.025	0.024	99.955
5.000	2.400	0.018	0.018	77.467
10.000	4.800	0.015	0.015	65.195
15.000	7.199	0.011	0.010	44.869
20.000	9.600	0.008	0.008	32.464
25.000	12.000	0.006	0.005	24.488

NUMBER OF DOWNSTEPS 2 AFTER 3 MINUTES EXPOSURE

DOWNSTEP NO. IV-8 USED GAS 176 PPM O2 IN N2
NUMBER OF POINTS 6

DOWNSTEP NO. IV-10 USED GAS 176 PPM O2 IN N2
NUMBER OF POINTS 6

COEFFICIENTS OF LEAST SQUARE POLYNOMIAL ARE

-0.37289E 01
-0.14985E 00
0.36574E-01
-0.44790E-02
0.20395E-03
-0.32002E-05

MAXIMUM AVERAGE CURRENT 0.024 MICRO-AMPS

TIME IN MN	TIME IN SECS	CURRENT-MICRO-A	CALCULATED CURR	PERCENT OF MAX CURR
0.000	0.000	0.023	0.024	100.074
6.000	2.880	0.014	0.017	74.180
11.000	5.279	0.010	0.012	52.461
16.000	7.680	0.005	0.007	31.335
21.000	10.079	0.003	0.005	23.931
26.000	12.479	0.003	0.003	16.200

NUMBER OF CONSTEPS IS 8 AFTER 1 MINUTES EXPOSURE

DCONSTEP NO. V-1 USED GAS 3.02P O2 IN N2
NUMBER OF POINTS 17

DCONSTEP NO. V-2 USED GAS 3.02P O2 IN N2
NUMBER OF POINTS 16

DCONSTEP NO. V-3 USED GAS 3.02P O2 IN N2
NUMBER OF POINTS 16

DCONSTEP NO. V-5 USED GAS 3.02P O2 IN N2
NUMBER OF POINTS 16

DCONSTEP NO. V-7 USED GAS 3.02P O2 IN N2
NUMBER OF POINTS 16

DCONSTEP NO. V-9 USED GAS 3.02P O2 IN N2
NUMBER OF POINTS 16

DCONSTEP NO. V-11 USED GAS 3.02P O2 IN N2
NUMBER OF POINTS 15

DCONSTEP NO. V-12 USED GAS 3.02P O2 IN N2
NUMBER OF POINTS 15

COEFFICIENTS OF LEAST SQUARE POLYNOMIAL ARE

0.14352E 01
-0.82552E-01
-0.71093E-02
0.32788E-03
-0.50152E-05
0.25834E-07

MAXIMUM AVERAGE CURRENT 4.083 MICRO-AMPS

TIME IN MM	TIME IN SECS	CURRENT-MICRO-A	CALCULATED CURR	PERCENT OF MAX CURR
0.000	0.000	4.148	4.200	102.865
3.000	1.440	3.361	3.102	75.961
8.000	3.840	2.018	1.596	39.102
13.000	6.239	0.507	0.776	19.019
18.000	8.639	0.337	0.398	9.763
23.000	11.040	0.227	0.229	5.618
28.000	13.440	0.162	0.151	3.698
33.000	15.840	0.114	0.112	2.755
38.000	18.240	0.084	0.091	2.251
43.000	20.639	0.069	0.078	1.933
48.000	23.040	0.051	0.068	1.668
53.000	25.439	0.041	0.057	1.396
58.000	27.840	0.032	0.045	1.111
63.000	30.239	0.025	0.034	0.848
68.000	32.639	0.022	0.026	0.651

NUMBER OF CONSTEPS IS 2 AFTER 2 MINUTES EXPOSURE

CONSTEP NO. V-4 USED GAS 3.02P O2 IN N2
NUMBER OF POINTS 15

CONSTEP NO. V-6 USED GAS 3.02P O2 IN N2
NUMBER OF POINTS 16

COEFFICIENTS OF LEAST SQUARE POLYNOMIAL ARE

0.15444E 01
-0.16921E 00
0.12522E-02
0.45279E-04
-0.10396E-05
0.60431E-08

MAXIMUM AVERAGE CURRENT 4.102 MICRO-AMPS

TIME IN MM	TIME IN SECS	CURRENT-MICRO-A	CALCULATED CURR	PERCENT OF MAX CURR
0.000	0.000	4.102	4.687	114.268
5.000	2.400	2.852	2.085	50.846
15.000	7.199	0.483	0.545	13.287
20.000	9.600	0.298	0.325	7.927
25.000	12.000	0.218	0.213	5.213
30.000	14.399	0.160	0.152	3.729
35.000	16.799	0.125	0.117	2.853
40.000	19.200	0.095	0.093	2.290
45.000	21.599	0.078	0.077	1.891
50.000	24.000	0.062	0.064	1.582
55.000	26.400	0.050	0.054	1.324
60.000	28.799	0.046	0.045	1.104
65.000	31.200	0.039	0.037	0.921
70.000	33.599	0.033	0.032	0.782
75.000	36.000	0.030	0.028	0.696

NUMBER OF DOWNSTEPS IS 2 AFTER 3 MINUTES EXPOSURE

DOWNSTEP NO. V-8 USED GAS 3.02P O2 IN N2
NUMBER OF POINTS 16

DOWNSTEP NO. V-10 USED GAS 3.02P O2 IN N2
NUMBER OF POINTS 15

COEFFICIENTS OF LEAST SQUARE POLYNOMIAL ARE

0.15043E 01
-0.11273E 00
-0.32071E-02
0.18196E-03
-0.28321E-05
0.14457E-07

MAXIMUM AVERAGE CURRENT 4.055 MICRO-AMPS

TIME IN MM	TIME IN SECS	CURRENT-MICRO-A	CALCULATED CURR	PERCENT OF MAX CURR
0.000	0.000	4.055	4.501	110.989
4.000	1.920	3.268	2.753	67.906
14.000	6.720	0.582	0.737	18.190
19.000	9.120	0.357	0.414	10.222
24.000	11.520	0.249	0.257	6.344
29.000	13.920	0.179	0.177	4.368
34.000	16.319	0.142	0.133	3.298
39.000	18.720	0.112	0.108	2.668
44.000	21.119	0.091	0.091	2.248
49.000	23.520	0.073	0.077	1.917
54.000	25.919	0.062	0.065	1.616
59.000	28.319	0.053	0.053	1.329
64.000	30.720	0.047	0.043	1.071
69.000	33.120	0.040	0.035	0.866
74.000	35.520	0.033	0.030	0.740

NUMBER OF DOWNSTEPS IS 4 AFTER 1 MINUTES EXPOSURE

DOWNSTEP NO. VI-1 USED GAS 9.96P O2 IN N2
NUMBER OF POINTS 20

DOWNSTEP NO. VI-2 USED GAS 9.96P O2 IN N2
NUMBER OF POINTS 20

DOWNSTEP NO. VI-3 USED GAS 9.96P O2 IN N2
NUMBER OF POINTS 20

DOWNSTEP NO. VI-6 USED GAS 9.96P O2 IN N2
NUMBER OF POINTS 20

COEFFICIENTS OF LEAST SQUARE POLYNOMIAL ARE

0.26363E 01
-0.62340E-01
-0.38155E-02
0.11639E-03
-0.12347E-05
0.45168E-08

MAXIMUM AVERAGE CURRENT 12.823 MICRO-AMPS

TIME IN MM	TIME IN SECS	CURRENT-MICRO-A	CALCULATED CURR	PERCENT OF MAX CURR
0.000	0.000	13.105	13.962	108.877
7.000	3.360	8.855	7.769	60.589
12.000	5.760	4.426	4.556	35.530
22.000	10.559	1.030	1.488	11.609
27.000	12.959	0.671	0.889	6.937
32.000	15.360	0.471	0.562	4.387
37.000	17.760	0.333	0.379	2.960
42.000	20.159	0.253	0.273	2.133
47.000	22.560	0.188	0.209	1.631
52.000	24.959	0.141	0.168	1.311
57.000	27.360	0.115	0.140	1.094
62.000	29.759	0.093	0.120	0.936
67.000	32.160	0.082	0.103	0.810
72.000	34.559	0.071	0.090	0.702
77.000	36.959	0.063	0.077	0.606
82.000	39.360	0.057	0.066	0.521
87.000	41.760	0.052	0.057	0.450
92.000	44.160	0.047	0.050	0.396
97.000	46.559	0.042	0.047	0.366
102.000	48.959	0.039	0.047	0.370

NUMBER OF CONSTEPS IS 1 AFTER 2 MINUTES EXPOSURE

CONSTEP NO. VI-4 USED GAS 9.96P O2 IN N2
NUMBER OF POINTS 19

COEFFICIENTS OF LEAST SQUARE POLYNOMIAL ARE

0.25425E 01
-0.30479E-01
-0.44482E-02
0.11877E-03
-0.11813E-05
0.41682E-08

MAXIMUM AVERAGE CURRENT 12.606 MICRO-AMPS

TIME IN MM	TIME IN SECS	CURRENT-MICRO-A	CALCULATED CURR	PERCENT OF MAX CURR
0.000	0.000	12.605	12.788	101.450
4.000	1.920	10.980	10.620	84.249
14.000	6.720	4.563	4.630	36.735
19.000	9.120	2.758	2.814	22.323
29.000	13.920	1.081	1.072	8.510
34.000	16.319	0.696	0.703	5.584
39.000	18.720	0.481	0.487	3.871
44.000	21.119	0.366	0.357	2.839
49.000	23.520	0.266	0.276	2.195
54.000	25.919	0.228	0.223	1.774
59.000	28.319	0.188	0.187	1.484
64.000	30.720	0.158	0.160	1.270
69.000	33.120	0.136	0.138	1.102
74.000	35.520	0.116	0.121	0.959
79.000	37.919	0.103	0.105	0.836
84.000	40.319	0.093	0.091	0.729
89.000	42.720	0.087	0.080	0.642
94.000	45.120	0.073	0.073	0.580
99.000	47.519	0.068	0.069	0.553

NUMBER OF DOWNSTEPS IS 1 AFTER 3 MINUTES EXPOSURE

DOWNSTEP NO. VI-5 USED GAS 9.96P O2 IN N2
NUMBER OF POINTS 20

COEFFICIENTS OF LEAST SQUARE POLYNOMIAL ARE

0.25542E 01
-0.43501E-01
-0.19272E-02
0.40505E-04
-0.28190E-06
0.63847E-09

MAXIMUM AVERAGE CURRENT 12.606 MICRO-AMPS

TIME IN MM	TIME IN SECS	CURRENT-MICRO-A	CALCULATED CURR	PERCENT OF MAX CURR
0.000	0.000	12.605	12.861	102.028
5.000	2.880	9.855	9.320	73.939
11.000	5.279	6.461	6.635	52.637
16.000	7.680	4.424	4.540	36.016
21.000	10.079	3.036	3.045	24.160
31.000	14.879	1.405	1.374	10.906
36.000	17.279	0.961	0.947	7.512
41.000	19.680	0.666	0.670	5.318
46.000	22.080	0.481	0.490	3.889
51.000	24.479	0.361	0.371	2.946
56.000	26.880	0.288	0.291	2.313
61.000	29.279	0.238	0.236	1.879
66.000	31.680	0.201	0.198	1.577
71.000	34.080	0.175	0.171	1.361
76.000	36.480	0.152	0.151	1.201
81.000	38.879	0.137	0.136	1.079
86.000	41.279	0.123	0.123	0.979
91.000	43.680	0.111	0.112	0.892
96.000	46.080	0.101	0.102	0.810
101.000	48.480	0.093	0.091	0.728

NUMBER OF CONSTEPS IS 5 AFTER 1 MINUTES EXPOSURE

CONSTEP NO. VII-1 USED GAS 21 P O2 IN N2
NUMBER OF POINTS 25

CONSTEP NO. VII-2 USED GAS 21 P O2 IN N2
NUMBER OF POINTS 25

CONSTEP NO. VII-3 USED GAS 21 P O2 IN N2
NUMBER OF POINTS 25

CONSTEP NO. VII-5 USED GAS 21 P O2 IN N2
NUMBER OF POINTS 26

CONSTEP NO. VII-7 USED GAS 21 P O2 IN N2
NUMBER OF POINTS 24

COEFFICIENTS OF LEAST SQUARE POLYNOMIAL ARE

0.325128E 01
-0.457918E-01
-0.836638E-03
0.110378E-04
-0.207548E-07
-0.103238E-09

MAXIMUM AVERAGE CURRENT 25.663 MICRO-AMPS

TIME IN MN	TIME IN SECS	CURRENT-MICRO-A,	CALCULATED CURR	PERCENT OF MAX CURR
0.000	0.000	26.495	25.821	100.617
6.000	2.880	20.415	18.968	73.912
11.000	5.279	14.355	14.151	55.141
16.000	7.680	10.355	10.302	40.143
21.000	10.079	7.480	7.372	28.728
26.000	12.479	5.582	5.222	20.349
31.000	14.879	4.008	3.685	14.359
36.000	17.279	2.850	2.605	10.152
46.000	22.080	1.405	1.337	5.212
51.000	24.479	1.005	0.980	3.819
56.000	26.880	0.716	0.732	2.854
61.000	29.279	0.531	0.559	2.180
66.000	31.680	0.418	0.438	1.707
71.000	34.080	0.343	0.352	1.371
76.000	36.480	0.293	0.290	1.131
81.000	38.879	0.248	0.245	0.956
86.000	41.279	0.217	0.212	0.828
91.000	43.680	0.192	0.188	0.734
96.000	46.080	0.173	0.169	0.662
101.000	48.480	0.157	0.155	0.606
106.000	50.879	0.143	0.143	0.559
111.000	53.279	0.130	0.132	0.518
116.000	55.680	0.122	0.122	0.477
121.000	58.080	0.113	0.111	0.433
126.000	60.479	0.107	0.098	0.384

NUMBER OF CONSTEPS IS 1 AFTER 2 MINUTES EXPOSURE

CONSTEP NO. VII-4 USED GAS 21 P - O2 IN N2
NUMBER OF POINTS 26

COEFFICIENTS OF LEAST SQUARE POLYNOMIAL ARE

0.32653E 01
-0.56279E-01
0.51426E-03
-0.12061E-04
0.11781E-06
-0.36297E-09

MAXIMUM AVERAGE CURRENT 25.363 MICRO-AMPS

TIME IN MM	TIME IN SECS	CURRENT-MICRO-A	CALCULATED CURR	PERCENT OF MAX CURR
0.000	0.000	25.362	26.190	103.261
4.000	1.920	21.574	21.068	83.065
9.000	4.319	15.983	16.321	64.351
14.000	6.720	14.483	12.800	50.470
19.000	9.120	9.608	10.109	39.858
24.000	11.520	7.761	8.007	31.570
29.000	13.920	6.233	6.343	25.012
34.000	16.319	4.937	5.019	19.788
39.000	18.720	3.918	3.962	15.624
44.000	21.119	3.085	3.123	12.315
49.000	23.520	2.437	2.459	9.697
59.000	28.319	1.520	1.530	6.036
64.000	30.720	1.445	1.215	4.790
69.000	33.120	0.946	0.971	3.829
74.000	35.520	0.754	0.783	3.090
79.000	37.919	0.619	0.640	2.523
84.000	40.319	0.519	0.529	2.089
89.000	42.720	0.439	0.445	1.756
94.000	45.120	0.379	0.381	1.502
99.000	47.519	0.331	0.331	1.306
104.000	49.919	0.296	0.293	1.155
109.000	52.319	0.266	0.263	1.038
114.000	54.720	0.241	0.239	0.945
119.000	57.120	0.224	0.220	0.869
124.000	59.519	0.203	0.203	0.803
129.000	61.919	0.186	0.187	0.741

NUMBER OF COMNSTEPS IS 1 AFTER 3 MINUTES EXPOSURE

COMNSTEP NO. VII-6 USED GAS 21 P O2 IN N2
NUMBER OF POINTS 25

COEFFICIENTS OF LEAST SQUARE POLYNOMIAL ARE

0.32497E 01
-0.57558E-01
0.67470E-03
-0.13904E-04
0.10026E-06
-0.25731E-09

MAXIMUM AVERAGE CURRENT 25.361 MICRO-AMPS

TIME IN MM	TIME IN SECS	CURRENT-MICRO-A	CALCULATED CURR	PERCENT OF MAX CURR
0.000	0.000	25.360	25.784	101.669
5.000	2.400	20.814	19.691	77.643
10.000	4.800	15.231	15.560	61.355
15.000	7.199	12.231	12.618	49.755
20.000	9.600	10.231	10.427	41.117
25.000	12.000	8.731	8.731	34.427
30.000	14.399	7.527	7.372	29.071
35.000	16.799	6.370	6.255	24.667
40.000	19.200	5.398	5.319	20.975
45.000	21.599	4.564	4.524	17.840
50.000	24.000	3.824	3.845	15.161
55.000	26.400	3.222	3.262	12.866
60.000	28.799	2.712	2.765	10.903
65.000	31.200	2.296	2.341	9.232
75.000	36.000	1.706	1.680	6.625
80.000	38.400	1.444	1.427	5.627
85.000	40.800	1.218	1.216	4.796
90.000	43.199	1.043	1.041	4.108
95.000	45.599	0.897	0.897	3.539
100.000	48.000	0.777	0.778	3.069
105.000	50.400	0.677	0.680	2.681
110.000	52.800	0.597	0.598	2.359
115.000	55.199	0.532	0.530	2.091
120.000	57.599	0.472	0.472	1.864
125.000	60.000	0.424	0.423	1.669

APPENDIX 2.9

SAMPLE CALCULATION OF THE CONFIDENCE INTERVAL FOR c_p IN TABLE 2.3

Factors contributing to the uncertainty of the value of c_p can be divided into two classes:

- randomly fluctuating variables
- constants whose values remained constant but which were known only with a limited accuracy

The extent of uncertainty caused by the former was appraised by a statistical analysis of the values of the maximum current obtained. The total confidence interval was then found by summing the statistically-obtained confidence interval and the bias error obtained by an error analysis of the calculations.

The data of downstep set I are used below to illustrate the method.

i) Statistical Analysis [62]

The values obtained for the maximum current were: 0.454, 0.443, 0.437, 0.437, 0.432, 0.432, 0.432, 0.432, 0.437, 0.437, 0.432 and 0.432 microamps. The arithmetic mean was 0.436

microamp. The standard deviation was 0.006 microamps. Since the sample size was smaller than 30, the t-distribution was used to estimate the confidence interval. At a confidence level of 0.95 the true mean of the distribution was found to lie within 0.003 microamps of the arithmetic mean.

ii) Bias Error

Factors contributing to this error were: the chain resistance (± 1%), the accuracy of the amplifiers (± 2%, estimated) and the accuracy of the calibration gas composition (± 2%, estimated).

Then from the statistical analysis:

$$C_p = 145 \pm 1$$

and from the bias error calculation:

$$C_p = 145 \pm 7$$

Therefore overall:

$$C_p = 145 \pm 8$$

APPENDIX 2.10

THE DERIVATION OF EQUATION 2.9

Boelter *et al.* [11] has presented Equation A.2.1 to describe the activity profile through a slab of thickness 'L' in response to a step input at the face at $x = 0$ while the other face at $x = L$ is kept at zero activity.

$$P_{0_2}(x,t) = P_1 - P_1\left(\frac{x}{L}\right) + \sum_{n=1}^{\infty}\left\{(-1)^n \frac{2P_1}{\pi}\frac{1}{n}\left[-\left(\frac{n\pi}{L}\right)^2 Dt\right]\right.$$

$$\left. \times \sin\left[\frac{n\pi x}{L}\right]\right\} \qquad \text{(A.2.1)}$$

By a redefinition of variables this becomes:

$$\frac{P_{0_2}(x^*,t^*)}{P_1} = x^* + \sum_{n=1}^{n=\infty}\left\{(-1)^n \frac{2}{\pi n}\exp[-(n\pi)^2 t^*]\right.$$

$$\left. \times \sin[n\pi x^*]\right\} \qquad \text{(A.2.2)}$$

where:

$x^* = 1 - x/L$

$t^* = t/B^2$

$B = L/D^{\frac{1}{2}}$

Probe output current as a fraction of steady-state output current is directly proportional to the oxygen activity gradient at $x = 0$:

$$\frac{\partial}{\partial x^*} \left\{ \frac{P_{O_2}(x^*,t^*)}{P_1} \right|_{x^*=0} = 1 + 2 \sum_{n=1}^{\infty} (-1)^n \exp[-(n\pi)^2 t^*]$$

(A.2.3)

Changing back to real time, Equation A.2.4 results:

$$i/i_\infty = 1 + 2 \sum_{n=1}^{\infty} (-1)^n \exp[-\left(\frac{n\pi}{B}\right)^2 t] \qquad \text{(A.2.4)}$$

This is equivalent to Equation 2.9.

APPENDIX 2.11

THE DERIVATION OF EQUATION 2.10

Churchill [16] has presented Equation A.2.5 as an alternate solution to Equation A.2.2:

$$\frac{P_{O_2}(x^*, t^*)}{P_1} = 1 - \sum_{n=0}^{\infty} \left[\operatorname{erf}\left(\frac{2n+1+x^*}{2\sqrt{t^*}} \right) - \operatorname{erf}\left(\frac{2n+1-x^*}{2\sqrt{t^*}} \right) \right] \qquad (A.2.5)$$

By the same reasoning as applied in Appendix 2.10, Equation A.2.6 results:

$$\frac{\partial}{\partial x^*} \left\{ \frac{P_{O_2}(x^*, t^*)}{P_1} \right|_{x^*=0} = 1 - \frac{2}{\sqrt{\pi t^*}} \sum_{n=0}^{\infty} \exp \left[\frac{-1}{4t^*} (2n+1)^2 \right] \qquad (A.2.6)$$

By changing back to real time Equation A.2.7 results:

$$i/i_\infty = 1 - \frac{2B}{\sqrt{\pi t}} \sum_{n=0}^{\infty} \exp \left[\frac{-B^2}{4t} (2n+1)^2 \right] \qquad (A.2.7)$$

This is equivalent to Equation 2.10.

APPENDIX 2.12

THE DERIVATION OF EQUATION 2.12 FROM EQUATION 2.11

Equation 2.11 states:

$$P_{o_2}(x,s) = s^{-1}\, k_1\, P_1 \sinh\left\{ \frac{x+a}{D_e^{1/2}}\, s^{1/2} \right\}$$

$$/ \left\{ \left(\frac{D_e}{D_m} \right)^{1/2} + k_2 \right\} \sinh\left\{ \left(\frac{b}{D_m^{1/2}} + \frac{a}{D_e^{1/2}} \right) s^{1/2} \right\}$$

$$+ \left\{ \left(\frac{D_e}{D_m} \right)^{1/2} - k_2 \right\} \sinh\left\{ \left(\frac{b}{D_m^{1/2}} - \frac{a}{D_e^{1/2}} \right) s^{1/2} \right\} \qquad \text{(A.2.8)}$$

Redefining:

$$B_e = a/D_e^{1/2}$$

$$B_m = b/D_m^{1/2}$$

$$C = a/b$$

Then:

$$P_{0_2}(x,s) = s^{-1} k_1 P_1 \sinh\{ \frac{x+a}{D_e^{\frac{1}{2}}} s^{\frac{1}{2}} \}$$

$$/ \{ \frac{B_m}{B_e} C + k_2 \} \sinh \{(B_m + B_e) s^{\frac{1}{2}} \}$$

$$+ \{ \frac{B_m}{B_e} C - k_2 \} \sinh \{(B_m - B_e) s^{\frac{1}{2}} \} \qquad (A.2.9)$$

Differentiating with respect to x at $x = -a$:

$$\left.\frac{\partial P_{0_2}(x,s)}{\partial x}\right|_{x=-a} = s^{-1} k_1 P_1 s^{\frac{1}{2}} D_e^{-\frac{1}{2}}$$

$$/ \{ \frac{B_m}{B_e} C + k_2 \} \sinh \{(B_m + B_e) s^{\frac{1}{2}} \}$$

$$+ \{ \frac{B_m}{B_e} C - k_2 \} \sinh \{(B_m - B_e) s^{\frac{1}{2}} \}$$

(A.2.10)

The desired final solution of the inversion is:

$$i/i_\infty = 1 - \frac{\left.\frac{\partial P_{0_2}(x,t)}{\partial x}\right|_{x=-a}}{\left.\frac{\partial P_{0_2}(x,t)}{\partial x}\right|_{\substack{t=\infty \\ x=-a}}} \qquad (A.2.11)$$

The Final Value Theorem states that:

$$\lim_{t \to \infty} [f(t)] = \lim_{s \to 0} [s F(s)] \qquad (A.2.12)$$

Therefore:

$$\lim_{t \to \infty} \left. \frac{\partial P_{02}(x,t)}{\partial x} \right|_{x=-a} = \lim_{s \to 0} \left. \frac{S \partial P_{02}(x,s)}{\partial x} \right|_{x=-a} \quad \text{(A.2.13)}$$

But:

$$\lim_{s \to 0} [\ k_1\ P_1\ s^{1/2}\ D_e^{-1/2}$$

$$/ \{ \frac{B_m}{B_e} C + k_2 \} \sinh \{ (B_m + B_e) s^{1/2} \}$$

$$+ \{ \frac{B_m}{B_e} C - k_2 \} \sinh \{ (B_m - B_e) s^{1/2} \}] = 0/0 \quad \text{(A.2.14)}$$

and is therefore indeterminate.

l'Hospital's rule states that:

$$\lim_{\tau \to a} [\ \frac{f(\tau)}{g(\tau)}\ ] = \lim_{\tau \to a} [\ \frac{f'(\tau)}{g'(\tau)}\ ] \quad \text{(A.2.15)}$$

Therefore:

$$\lim_{s \to 0} [\ \left. \frac{s \partial P_{02}(x,s)}{\partial x} \right|_{x=-a}$$

$$= k_1\ P_1\ D_e^{-1/2} / \{ \frac{B_m}{B_e} C + k_2 \} \{ B_m + B_e \} + \{ \frac{B_m}{B_e} C - k_2 \} \{ B_m - B_e \}$$

$$= k_1\ B_e\ P_1\ D_e^{-1/2} / \ 2 \{ B_m^2\ C + B_e^2\ k_2 \} \quad \text{(A.2.16)}$$

Therefore:

$$\left.\frac{\partial P_{O_2}(x,s)}{\partial x}\right|_{x=-a} \Big/ \lim_{s \to 0} \left[s \left.\frac{\partial P_{O_2}(x,s)}{\partial x}\right|_{x=-a} \right.$$

$$= 2\{B_m^2\ C + B_e^2\ k_2\}/s^{\frac{1}{2}}[\{B_m\ C + B_e\ k_2\}\sinh\{(B_m + B_e)s^{\frac{1}{2}}\}$$

$$+ \{B_m\ C - B_e\ k_2\}\sinh\{B_m - B_e)s^{\frac{1}{2}}\}\ ] \qquad \text{(A.2.17)}$$

By letting $C^* = C/k_2$, Equation A.2.18 results:

$$\left.\frac{\partial P_{O_2}(x,s)}{\partial x}\right|_{x=-a} \Big/ \lim_{s \to 0} \left[s \left.\frac{\partial P_{O_2}(x,s)}{\partial x}\right|_{x=-a} \right.$$

$$= 2\{B_m^2\ C^* + B_e^2\}/s^{\frac{1}{2}}[\{B_m\ C^* + B_e\}\sinh\{(B_m + B_e)s^{\frac{1}{2}}\}$$

$$+ \{B_m\ C^* - B_e\}\ \sinh\ \{(B_m - B_e)s^{\frac{1}{2}}\}] \qquad \text{(A.2.18)}$$

Equation A.2.18 is the Laplace transform of the response to an upstep.

APPENDIX 2.13

PROGRAM KOK3 - NUMERICAL INVERSION OF THE LAPLACE TRANSFORM BY BELLMAN'S *et al.* [9] METHOD

Presented below are:

i) Program KOK3 which is the inversion program

ii) Subroutine F(S,DATAV,DUMMY) which calculates the value of:

$$\left[\frac{\partial P_{O_2}(x,s)}{\partial x}\right|_{x=-a} \Big/ \lim_{s \to 0} \left[s \frac{\partial P_{O_2}(x,s)}{\partial x}\right|_{x=-a}$$

for any value of 's' and transmits this value to the main program KOK3 by means of the variable DUMMY.

iii) Results of the numerical inversion of Equation 2.12 describing the response of a two-layer system to a step input in oxygen tension. The values used were: $B_e = 2.0$, $B_m = 3.0$, $C^* = 1.0$.

iv) A comparison of the analytical and numerical solutions of the Laplace transform describing the response of a single-layer system to a step input. The layer response characteristic was 5.0 sec$^{\frac{1}{2}}$. This is shown in Figure A.2.1.

```
PAGE   1

// JOB

LOG DRIVE   CART SPEC   CART AVAIL  PHY DRIVE
  0000        1122        1122        0000

V2 M10   ACTUAL  8K  CONFIG  8K

// DUP

*DELETE              KOK3
D 26 NAME NOT FOUND IN LET/FLET


// FOR
* IOCS (CARD,1403 PRINTER)
* LIST SOURCE PROGRAM
* ONE WORD INTEGERS
* EXTENDED PRECISION
* NAME KOK3
C
C ********************************************************************
C
C ROBERT KOK
C KOK3 NUMERICALLY INVERTS THE GIVEN FUNCTION F(S) BY BELLMAN'S METHOD
C OVER THE TIME INTERVAL ZERO TO TMAX.DETAILED OUTPUT CAN BE SUPPRESSED BY
C MEANS OF DATA SWITCH NO. 1
C MAXIMUM PERMITTED NUMBER OF TIME SHIFTS IS 19
C KOK3 USES THE SUBROUTINE FUNCTION F(S,DATAV) TO SUPPLY VALUES OF F(S)
C
C VARIABLES USED
C VECTORS---CICWI=GIVEN INVERTED MATRIX---POLY=VECTOR OF SHIFTED
C LEGENDRE POLYNOMIAL ROOTS-ALSO A STORAGE VECTOR---SOL=SOLUTION VECTOR
C F(T) FROM F(S)---TIME= STORAGE AND SORTING VECTOR FOR TIME VARIABLE---
C ANS=STORAGE AND SORTING VECTOR FOR SOLUTION VARIABLE---DATAV=CONSTANT
C VECTOR FOR DEFINITION OF F(S)
C REAL VARIABLES---TMAX=MAXIMUM TIME IN SECONDS FOR WHICH SOLUTION IS
C DESIRED---TMULT=TIME BASE MULTIPLIER---DUMM=DUMMY VARIABLE---S=LAPLACE
C TRANSFORM VARIABLE
C INTEGER VARIABLES---N1= ORDER OF POLYNOMIALS AND MATRIX USED---N2=NUMBER
C OF TIME SHIFTS USED---N3=NO. OF CONSTANTS REQUIRED FOR F(S) CALCULATION
C ---II=COMPUTED GO TO INDEX---I1,I2=DO-LOOP COUNTERS---I,J,N= GENERAL
C COUNTERS
C
C ********************************************************************
C
      DIMENSION OIGWI(15,15),POLY(15),SOL(15),TIME(300),ANS(300),DATAV(1
     10)
      CALL DATSW(1,II)
      READ(2,100)N1,N2,N3,TMAX
  100 FORMAT(3I5,F10.0)
      READ(2,101)(DATAV(I),I=1,N3)
  101 FORMAT(4E20.5)
      WRITE(5,102)
  102 FORMAT(1H1)
      WRITE(5,103)N1,N2,TMAX
  103 FORMAT(27H ORDER OF OPERATIONS15,/22H NUMBER OF TIME SHIFTS15,/22H
     1 MAXIMUM SOLUTION TIMEF10.0,8H SECONDS)
      WRITE(5,104)N3
  104 FORMAT(34H NUMBER OF CONSTANTS USED FOR F(S)I5,//19H CONSTANTS USE
```

```
      1C ANF/1
      WRITE(5,105)(CATAV(I),I=1,N3)
  105 FORMAT(E20.5)
      DO 80 I=1,N1
   80 READ(2,105)(QIOW(I,J),J=1,N1)
      READ(2,106)(POLY(I),I=1,N1)
  106 FORMAT(4 20.13)
      GO TO (3,4),II
    3 WRITE(5,106)((QIOW(J,I),I=1,N1),J=1,N1)
      WRITE(5,106)(POLY(I),I=1,N1)
C CALCULATION OF TIME MULTIPLIER
    4 TMULT=(TMAX/(-ALOG(POLY(1))))**(1./N2)
      GO TO (6,5),II
    5 WRITE (5,107)TMULT
  107 FORMAT(/19H TIME MULTIPLIER 1SE20.5,/)
    6 N2=N2+1
      DO 10 I2=1,N2
      I=(I2-1)*N1+1
      J=I+N1-1
      DO 20 I1=I,J
      IF(I2-1)7,7,8
    7 TIME(I1)=-ALOG(POLY(I1))
      GO TO 20
    8 N=I1-N1
      TIME(I1)=TIME(N)*TMULT
   20 CONTINUE
      IF(I2-1)9,9,11
    9 DUMM=1.0
      GO TO 12
   11 DUMM=DUMM*TMULT
   12 DO 40 I1=1,N1
      S=I1/DUMM
C POLY IS NOW USED AS A STORAGE VECTOR
      CALL [illegible] CATAV,DUMMY)
   40 POLY(I1)=[illegible]/DUMM
      DO 50 I1=1,N1
      SOL(I1)=0.0
      DO 50 N=1,N1
   50 SOL(I1)=SOL(I1)+QIOW(I1,N)*POLY(N)
      GO TO (14,13),II
   13 DO 30 I1=1,N1
      I=(I2-1)*N1+I1
   30 WRITE(5,108)TIME(I),SOL(I1)
  108 FORMAT(2E20.5)
C TRANSFERRING OF SOLUTION TO STORAGE VECTOR
   14 DO 60 I1=1,N1
      I=(I2-1)*N1+I1
   60 ANS(I)=SOL(I1)
   10 CONTINUE
      GO TO (16,15),II
   15 I=N1*N2
      WRITE(5,108)(TIME(J),ANS(J),J=1,I)
C ORDERING SOLUTION INTO TIME-ASCENDING SEQUENCE
   16 N1=N1*N2
C N1 NOW REPRESENTS THE TOTAL NUMBER OF ANSWERS
      I=N1-1
      DO 70 I1=1,I
      J=I1+1
      DO 70 I2=J,N1
```

```
PAGE    3

      IF(TIME(I1)-TIME(I2))70,70,17
   17 DUMM=TIME(I1)
      TIME(I1)=TIME(I2)
      TIME(I2)=DUMM
      DUMM=ANS(I1)
      ANS(I1)=ANS(I2)
      ANS(I2)=DUMM
   70 CONTINUE
      WRITE(5,109)
  109 FORMAT(//43H         TIME(SECS)      INVERSE OF F(S)//)
      DO 90 I=1,N)
   90 ANS(I)=1.-ANS(I)
      WRITE(5,110)(TIME(I),ANS(I),I=1,N))
  110 FORMAT(2F20.5)
      CALL EXIT
      END

FEATURES SUPPORTED
 ONE WORD INTEGERS
 EXTENDED PRECISION
 IOCS

CORE REQUIREMENTS FOR KCK3
 COMMON       0  VARIABLES    2628  PROGRAM    938

END OF COMPILATION

// DUP

*STORE       WS  UA  KCK3
CART ID 1122    DB ADDR  49AC    DB CNT    003E

*DELETE              F
D 26 NAME NOT FOUND IN LET/FLET


// FOR
* LIST SOURCE PROGRAM
* ONE WORD INTEGERS
* EXTENDED PRECISION
      SUBROUTINE F(S,DATAV,DUMMY)
      DIMENSION DATAV(3)
      SINH(Y)=(EXP(Y)-EXP(-Y))/2.
      S=SQRT(S)
      A=DATAV(1)
      B=DATAV(2)
      D=DATAV(3)
      DUMMY=(D*B/A+1)*SINH((A+B)*S)+(D*B/A-1)*SINH((B-A)*S)
      DUMMY=2.*(D/A*B**2+A)/S/DUMMY
      RETURN
      END

FEATURES SUPPORTED
 ONE WORD INTEGERS
 EXTENDED PRECISION

CORE REQUIREMENTS FOR F
 COMMON       0  VARIABLES     36  PROGRAM    156
```

ORDER OF OPERATIONS 8
NUMBER OF TIME SHIFTS 10.
MAXIMUM SOLUTION TIME 15. SECONDS
NUMBER OF CONSTANTS USED FOR F(S) 3

CONSTANTS USED ARE

0.20000E 01
0.30000E 01
0.10000E 01

TIME(SECS)	INVERSE OF F(S)
0.02005	1.00076
0.02241	1.00060
0.02622	1.00042
0.02777	1.00023
0.03430	1.00008
0.03923	0.99999
0.04486	1.00001
0.05131	1.00013
0.05868	1.00030
0.06711	1.00042
0.07675	1.00037
0.10721	0.99877
0.12261	0.99904
0.14022	0.99933
0.16036	0.99963
0.18340	0.99986
0.20974	0.99998
0.23987	0.99997
0.27040	1.00169
0.27432	0.99970
0.39979	1.00131
0.41373	0.99946
0.35418	1.00089
0.35379	0.99937
0.40506	1.00049
0.41033	0.99964
0.46324	1.00020
0.52472	0.99763
0.52778	1.00006
0.60009	0.99890
0.60587	0.99999
0.68629	0.99800
0.69290	0.99761
0.78487	0.99697
0.79243	0.99808
0.86579	0.99747
0.89760	0.99371
0.90625	0.99408
1.02446	0.98950
1.02653	0.98656
1.03642	0.98579
1.17161	0.97560
1.17398	0.97325
1.33990	0.95334
1.34261	0.95143

1.43870	0.93150
1.53216	0.97042
1.53546	0.91890
1.64516	0.89368
1.75246	0.87519
1.75601	0.87409
1.88169	0.84286
2.00418	0.81705
2.00824	0.81643
2.15197	0.77714
2.28605	0.75689
2.29206	0.74675
2.44104	0.70401
2.61441	0.67482
2.62129	0.66618
2.31434	0.62028
2.79394	0.58606
[illegible]	0.57717
3.21846	0.53168
3.41941	0.49465
3.42840	0.48310
3.60121	0.44233
3.71056	0.40490
3.91429	0.38034
4.20397	0.35631
4.47227	0.32031
4.68775	0.30207
4.81468	0.27709
5.11465	0.24426
5.12607	0.23158
5.50675	0.20730
5.64931	0.17878
5.86236	0.17071
6.60349	0.12494
6.70442	0.12044
7.65035	0.08282
7.66742	0.08085
8.74923	0.05166
0.76875	0.05127
10.02827	0.03046
11.46871	0.01679
13.11604	0.00853
15.00000	0.00399

FIGURE A.2.1

Comparison of the Theoretical Downstep Responses
Of the Single Diffusion Layer Probe Model
Obtained By the Analytical (——) and the Numerical
(▲) Methods. Eight Quadrature Points and Two Time
Shifts Were Used For the Numerical Method [9]

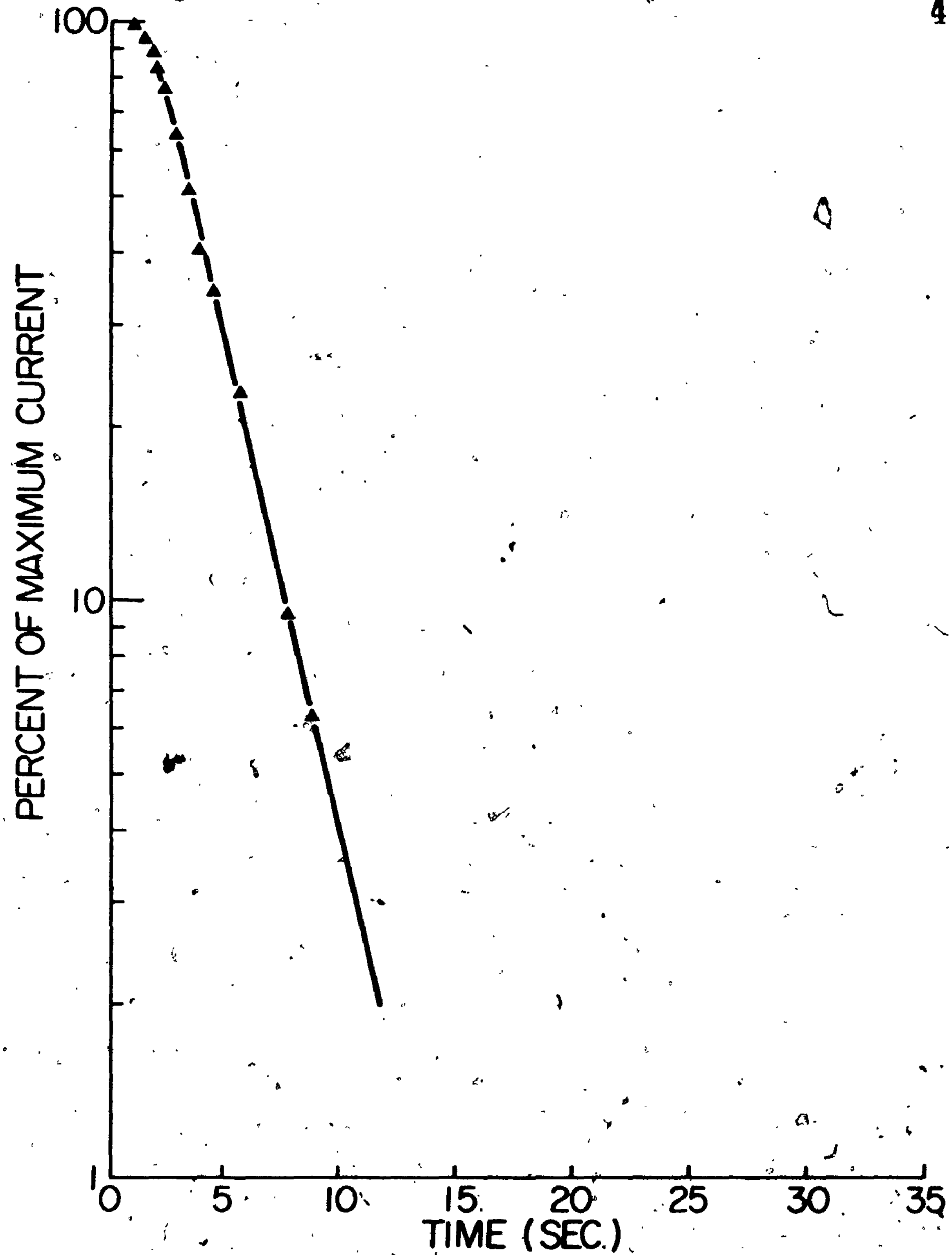
100
10
1
PERCENT OF MAXIMUM CURRENT
0
5
10
15
20
25
30
35
TIME (SEC.)

APPENDIX 2.14

THE DERIVATION OF EQUATION 2.13

Churchill [16] has presented Equation A.2.19 as representing the activity profile in a semi-infinite solid after a step increase of P_1 in activity at the solid's surface.

$$P_{O_2}(x,t) = P_1 \operatorname{erfc}\left(\frac{x}{2\sqrt{Dt}}\right) \quad (A.2.19)$$

By analogy, the activity at a distance 'a^*' from the face after an upstep P_1 at $t = -A$ and a downstep of P_1 at $t = 0$ is described by Equation A.2.20.

$$P_{O_2}(a^*,t) = P_1 \operatorname{erfc}\left(\frac{B_r}{\sqrt{t+A}}\right) - P_1 \operatorname{erfc}\left(\frac{B_r}{\sqrt{t}}\right) \quad (A.2.20)$$

where $B_r = \frac{a^*}{2\sqrt{D}}$

The oxygen activity at $x = a^*$ as a fraction of the oxygen activity at $t = 0$ is then:

$$\frac{P_{O_2}(a^*,t)}{P_{O_2}(a^*,o)} = \frac{\operatorname{erfc}\left(\frac{B_r}{\sqrt{t+A}}\right) - \operatorname{erfc}\left(\frac{B_r}{\sqrt{t}}\right)}{\operatorname{erfc}\left(\frac{B_r}{\sqrt{A}}\right)} \quad (A.2.21)$$

The current due to oxygen transfer through the membrane-electrolyte system as a fraction of this current at $t = 0$ is described by the following expression:

$$i_L / i_{L_{t=0}} = 1 - \frac{2B}{\sqrt{\pi t}} \sum_{n=0}^{\infty} \exp \left[\frac{-B^2}{4t} (2n+1)^2 \right] \quad (A.2.22)$$

If C_i is the fraction of the total current at $t = 0$ contributed by the oxygen flux from the reservoir, then the probe current can be described as a fraction of the total current observed at $t = 0$ by Equation A.2.23:

$$i/i_A = (1-C_i) \left\{ 1 - \frac{2B}{\sqrt{\pi t}} \sum_{n=0}^{\infty} \exp \left[\frac{-B^2}{4t} (2n+1)^2 \right] \right\} + C_i \left\{ \frac{\operatorname{erfc}\left(\frac{B_r}{\sqrt{t+A}} \right) - \operatorname{erfc}\left(\frac{B_r}{\sqrt{t}} \right)}{\operatorname{erfc}\left(\frac{B_r}{\sqrt{A}} \right)} \right\} \quad (A.2.23)$$

APPENDIX 2.15

METHODS AND EQUATIONS USED FOR PROGRAM KOK5.

THE CALCULATION OF E AND THE PARTIAL DERIVATIVES OF $\ln(i/i_A)$ WITH RESPECT TO B, C_i, AND B_r

Equation 2.13 states that:

$$i/i_A = (1-C_i)\ \{1 - \frac{2B}{\sqrt{\pi t}} \sum_{n=0}^{\infty} \exp[\frac{-B^2}{4t}(2n+1)^2]\}$$

$$+ C_i \{ \frac{\mathrm{erfc}(\frac{B_r}{\sqrt{t+A}}) - \mathrm{erfc}(\frac{B_r}{\sqrt{t}})}{\mathrm{erfc}(\frac{B_r}{\sqrt{A}})} \} \qquad (A.2.24)$$

The error E as defined below in Equation A.2.25 is the average percentage of deviation of the model from the experimental points

$$E = 100\ \frac{1}{n_1} \sum_{i=1}^{i=n_1} [\ln(\frac{i}{i_A})_{MODEL} - \ln(\frac{i}{i_A})_{EXPTL}]^2 \qquad (A.2.25)$$

Initial estimates of the parameters C_i, B and B_r were refined by Program KOK5 according to the partial derivative of i/i_A with respect to the parameters. The equations for the partial derivatives are presented below:

$$\frac{\partial}{\partial B}\{\ln(i/i_A)\} = \frac{2(C_i-1)}{(i/i_A)\sqrt{\pi t}}\left[\frac{-B^2}{2t}\sum_{n=0}^{\infty}(2n+1)^2\exp\{\frac{-B^2}{4t}(2n+1)^2\}\right.$$

$$\left. + \sum_{n=0}^{\infty}\exp\{\frac{-B^2}{4t}(2n+1)^2\}\right] \qquad (A.2.26)$$

$$\frac{\partial}{\partial C_i}\{\ln(i/i_A)\} = \frac{1}{(i/i_A)}\left[\frac{2B}{\sqrt{\pi t}}\sum_{n=0}^{\infty}\exp\{\frac{-B^2}{4t}(2n+1)^2\}\right.$$

$$\left. + \frac{\operatorname{erfc}(\frac{B_r}{\sqrt{t+A}}) - \operatorname{erfc}(\frac{B_r}{\sqrt{t}})}{\operatorname{erfc}(\frac{B_r}{\sqrt{A}})} - 1\right] \qquad (A.2.27)$$

$$\frac{\partial}{\partial B_r}\{\ln(i/i_A)\} = \frac{2C_i}{(i/i_A)\sqrt{\pi}}\left[\operatorname{erfc}(\frac{B_r}{\sqrt{A}})\right]^{-2}$$

$$\times\left[\operatorname{erfc}(\frac{B_r}{\sqrt{A}})\{\frac{1}{\sqrt{t}}\exp(\frac{-B_r^2}{t}) - \frac{1}{\sqrt{t+A}}\exp(\frac{-B_r^2}{t+A})\}\right.$$

$$\left. - \{\operatorname{erfc}(\frac{B_r}{\sqrt{t+A}}) - \operatorname{erfc}(\frac{B_r}{\sqrt{t}})\}\{\frac{1}{\sqrt{A}}\exp(\frac{-B_r^2}{A})\}\right]$$

$$(A.2.28)$$

APPENDIX 2.16

PROGRAM KOK5 WITH SUBROUTINES KOK5A, KOK5B, KOK5C and ERFC

Program KOK5 and its subroutines calculated values of the non-linear fitting parameters B, C_i, and B_r which yielded a smaller value of E than the original estimates of the parameters did.

The program stopped when the six values of E for two successive iterations of B, C_i and B_r were all within 0.2% of each other.

```
PAGE   1

// JOB

LOG DRIVE   CART SPEC   CART AVAIL  PHY DRIVE
  0000        1122        1122        0000

V2 M10   ACTUAL  8K  CONFIG  8K

// DUP

*DELETE              ERFC
D 26 NAME NOT FOUND IN LET/FLET

// FOR
* LIST SOURCE PROGRAM
* ONE WORD INTEGERS
* EXTENDED PRECISION
      FUNCTION ERFC(X)
      T = 1./(1.+0.3275911*X)
      A = 0.254829592*T-0.284496736*T*T+1.421413741*T*T*T-1.453152027*T*
     1T*T*T+1.061405429*T*T*T*T*T
      ERFC  = A*EXP(-X*X)
      RETURN
      END

FEATURES SUPPORTED
 ONE WORD INTEGERS
 EXTENDED PRECISION

CORE REQUIREMENTS FOR ERFC
 COMMON      0  VARIABLES      22  PROGRAM    114

RELATIVE ENTRY POINT ADDRESS IS 002B (HEX)

END OF COMPILATION

// DUP

*STORE      WS  UA  ERFC
CART ID 1122   DB ADDR  49F8   DB CNT   000A

*DELETE              KOKSA
D 26 NAME NOT FOUND IN LET/FLET

// FOR
* LIST SOURCE PROGRAM
* ONE WORD INTEGERS
* EXTENDED PRECISION
C
C ***********************************************************************
C
C PROGRAM CALCULATES VALUES OF THE PARTIAL DERIVATIVES---REQUIRES SUBROU
C TINES KOKSB,KOKSC,ERFC
C
C ***********************************************************************
C
      SUBROUTINE KOKSA(I2,TIME,I1,C,DFOCK,ATIME,DUMMY)
```

PAGE; 2

```
      DIMENSION TIME(1)
      DIMENSION C(3),DFDCK(3)
      DATA PI/1*3.1415927/
      CALL KCK5M(I2,TIME,C,DUMMY,ATIME,DUMM1)
      DUMMY=EXP(DUMMY)
      GO TO (1,2,3),II
C CALCULATION OF DFDCK(1)
    1 CALL KCK5C(I2,TIME,C,2,DUMM2)
      DFDCK(1)=-DUMM2*C(1)*C(1)/2./TIME(I2)+DUMM1
      DFDCK(1)=DFDCK(1)*2.*(C(2)-1.)/DUMMY/SQRT(PI*TIME(I2))
      GO TO 4
C CALCULATION OF DFDCK(2)
    2 DFDCK(2)=DUMM1*2.*C(1)/SQRT(PI*TIME(I2))-1.
      DFDCK(2)=DFDCK(2)+(ERFC(C(3)/SQRT(TIME(I2)+ATIME))-ERFC(C(3)/SQRT(
     1TIME(I2))))/ERFC(C(3)/SQRT(ATIME))
      DFDCK(2)=DFDCK(2)/DUMMY
      GO TO 4
C CALCULATION OF DFDCK(3)
    3 DFDCK(3)=EXP(-C(3)*C(3)/TIME(I2))/SQRT(TIME(I2))
      DFDCK(3)=DFDCK(3)-EXP(-C(3)*C(3)/(TIME(I2)+ATIME))/SQRT(TIME(I2)+A
     1TIME)
      DFDCK(3)=DFDCK(3)*ERFC(C(3)/SQRT(ATIME))
      DFDCK(3)=DFDCK(3)-(ERFC(C(3)/SQRT(TIME(I2)+ATIME))-ERFC(C(3)/SQRT(
     1TIME(I2))))*(EXP(-C(3)*C(3)/ATIME)/SQRT(ATIME))
      DFDCK(3)=DFDCK(3)/(ERFC(C(3)/SQRT(ATIME))**2)
      DFDCK(3)=DFDCK(3)*2.*C(2)/SQRT(PI)/DUMMY
    4 DUMMY=ALOG(DUMMY)
      RETURN
      END

FEATURES SUPPORTED
 ONE WORD INTEGERS
 EXTENDED PRECISION

CORE REQUIREMENTS FOR KCK5A
 COMMON      0  VARIABLES      46  PROGRAM     554

RELATIVE ENTRY POINT ADDRESS IS 0035 (HEX)

END OF COMPILATION

// DUP

*STORE      WS  UA  KCK5A
CART ID 1122   DB ADDR  4A02   DB CNT   0028

*DELETE             KCK5M
D 26 NAME NOT FOUND IN LET/FLET


// FOR
* LIST SOURCE PROGRAM
* ONE WORD INTEGERS
* EXTENDED PRECISION
C
C ******************************************************************
C
C PROGRAM CALCULATES THE VALUE OF THE FUNCTION AT GIVEN C AND TIME(I2)
```

```
PAGE    3

C IT REQUIRES KOK5C AND ERFC
C
C ****************************************************************
C
      SUBROUTINE KOK5B(I2,TIME,C,DUMMY,ATIME,DUMMI)
      DIMENSION TIME(1)
      DIMENSION C(3)
      DATA PI/1=3.1415927/
      CALL KOK5C(I2,TIME,C,1,DUMMI)
      DUMMY (1.-DUMMI*2.*C(1)/SQRT(PI*TIME(I2)))*(1.-C(2))
      DUMMY=DUMMY*C(2)*(ERFC(C(3)/SQRT(TIME(I2)+ATIME))-ERFC(C(3)/SQRT(T
     1IME(I2))))/ERFC(C(3)/SQRT(ATIME))
      DUMMY=ALOG(DUMMY)
      RETURN
      END

FEATURES SUPPORTED
 ONE WORD INTEGERS
 EXTENDED PRECISION

CORE REQUIREMENTS FOR KOK5B
 COMMON       0  VARIABLES       30  PROGRAM     168

RELATIVE ENTRY POINT ADDRESS IS 0025 (HEX)

END OF COMPILATION

// DUP

*STORE       WS  UA  KOK5B
CART ID 1122   DB ADDR  4A2A   DB CNT   000D

*DELETE              KOK5C
D 26 NAME NOT FOUND IN LET/FLET

// FOR
* LIST SOURCE PROGRAM
* ONE WORD INTEGERS
* EXTENDED PRECISION
C
C ****************************************************************
C
C PROGRAM CALCULATES SUM OF TERMS IN FUNCTIONAL EQ'N---FORM OF SUM IS
C DETERMINED BY II
C
C ****************************************************************
C
      SUBROUTINE KOK5C(I2,TIME,C,II,SUM)
      DIMENSION TIME (1)
      DIMENSION C(3)
      SUM=0.0
      N=0
    4 TERM=EXP(-C(1)*C(1)/4./TIME(I2)*(2*N+1)**2)
      GO TO (1,2),II
    2 TERM=TERM*(2*N+1)**2
    1 SUM=SUM+TERM
      N=N+1
      IF(TERM/SUM-1.0E-06*SUM)3,3,4
```

```
PAGE   4

   3 RETURN
     END

FEATURES SUPPORTED
 ONE WORD INTEGERS
 EXTENDED PRECISION

CORE REQUIREMENTS FOR KOKSC
 COMMON       0  VARIABLES       14  PROGRAM     126

RELATIVE ENTRY POINT ADDRESS IS 001A (HEX)

END OF COMPILATION

// DUP

*STORE      WS  UA  KOKSC
CART ID 1122   DB ADDR  4A37   DB CNT    000A

*DELETE              KOKS
D 26 NAME NOT FOUND IN LET/FLET


// FOR
* IOCS (CARD,1403 PRINTER)
* LIST SOURCE PROGRAM
* ONE WORD INTEGERS
* EXTENDED PRECISION
*NAME KOKS
C
C **********************************************************************
C
C KOKS FINDS VALUES OF THE NON-LINEAR FITTING PARAMETERS WHICH YIELD A
C SMALLER REMAINDER THAN THE ORIGINAL ESTIMATES---IT DOES SO BY SEQUENTI
C ALLY ALTERING VALUES OF C IN THE DIRECTION OPPOSITE TO THOSE OF THEIR
C PARTIAL DERIVATIVES BY THE AMOUNTS SPECIFIED IN DELC OR A FRACTION
C THEREOF AS NECESSARY
C IT REQUIRES USER-SUPPLIED SUBROUTINES KOKSA TO CALCULATE THE PARTIAL
C DERIVATIVES AND FUNCTION VALUE,KOKSB TO CALCULATE THE FUNCTION VALUE
C AND SUM OF TERMS,KOKSC TO CALCULATE THE SUM OF EXPONENTIAL TERMS
C INTERMEDIATE AND FINAL FITTED VALUES CAN BE OBTAINED BY MEANS OF DATA
C SWITCHES NOS. 1 AND 2
C FUNCTION SUBROUTINE FREC IS REQUIRED
C ALL FITTING IS DONE TO THE LOGARITHM OF THE DATA VALUES
C
C VECTORS---TIME=TIMES OF OBSERVATIONS---XIOIM=VALUES OF CURRENTS AS FRA
C CTIONS OF THE MAXIMAL CURRENT AT TIME=ZERO---C=NON-LINEAR PARAMETERS--
C -DELC=ADJUSTMENTS IN FITTING PARAMETERS---DELCX=DUMMY VECTOR FOR DELC-
C --DFDCK=VALUES OF PARTIAL DERIVATIVES
C REAL VARIABLES---ATIME=DURATION OF PROBE EXPOSURE---DUMMY,DUMM1,DUMM2=
C DUMMY VARIABLES---ROLD,RNEW=VALUES OF THE REMAINDER---DRDCI=SUM OF PAR
C TIAL DERIVATIVES OF REMAINDER WRT C(I)
C INTEGER VARIABLES---N1=NO. OF FITTING PARAMETERS---N2=NO. OF DATA PTS.
C ---I,I1,I2=COUNTERS---II=COMPUTED GO TO INDEX
C
C **********************************************************************
C
*     DIMENSION TIME(100),XIOIM(100)
```

```
      DIMENSION C(3),DELC(3),DELCX(3),DFDCK(3)
  100 FORMAT(1H1)
      READ(2,101)N1,N2,ATIME
  101 FORMAT(2I5,F10.0)
      READ(2,102)C,DELC
  102 FORMAT(3F20.5)
      READ(2,103)(TIME(I),XIOIM(I),I=1,N2)
  103 FORMAT(8F10.5)
      WRITE(5,100)
      WRITE(5,104)N1,N2,ATIME
  104 FORMAT(24H NUMBER OF PARAMETERS IS15,/25H NUMBER OF DATA POINTS IS
     1I5,/24H PROBE EXPOSURE TIME WASF10.0,8H SECONDS///)
      WRITE(5,105)C,DELC
  105 FORMAT(32H ORIGINAL PARAMETER ESTIMATE WAS/3F20.5,/36H VALUES FOR
     1PARAMETER ADJUSTMENT ARE/3F20.5,///)
      WRITE(5,106)
  106 FORMAT(16H INPUT DATA WERE/60H         TIME (SECS)            X
     1IOIM              LOG XIOIM/)
      DO 10 I=1,N2
      DUMMY=XIOIM(I)
      XIOIM(I)=ALOG(XIOIM(I))
   10 WRITE(5,107)TIME(I),DUMMY,XIOIM(I)
  107 FORMAT(3F20.5)
      WRITE(5,100)
C XIOIM IS NOW STORED IN LOGARITHMIC FORM
C FINDING THE INITIAL REMAINDER=ROLD
      ROLD=0.0
      DO 20 I2=1,N2
      CALL KOK5B(I2,TIME,C,DUMMY,ATIME,DUMM1)
   20 ROLD=ROLD+(DUMMY-XIOIM(I2))**2
      ROLD=SQRT(ROLD/N2)*100.
      I1=1
C I1 FROM NOW WILL REPRESENT THE PARAMETER BEING TESTED
C START OF ITERATION
C RESETTING OF DELCX
    1 DO 30 I=1,N1
   30 DELCX(I)=DELC(I)
C FINDING OF DRDCI
      DRDCI=0.0
      DO 40 I2=1,N2
      CALL KOK5A(I2,TIME,I1,C,DFDCK,ATIME,DUMMY)
   40 DRDCI=DRDCI+DFDCK(I1)*(DUMMY-XIOIM(I2))
      DRDCI=2*DRDCI
      WRITE(5,108)I1,DRDCI
  108 FORMAT(17H PARAMETER NUMBERI5,23H  PARTIAL DERIVATIVE ISE20.5)
C ADJUSTMENT OF C(I1)
   13 C(I1)=C(I1)-DELCX(I1)*DRDCI/ABS(DRDCI)
      WRITE(5,109)C
  109 FORMAT(24H NEW PARAMETER VECTOR IS3F20.5)
C FINDING THE NEW VALUE OF THE REMAINDER
      RNEW=0.0
      DO 50 I2=1,N2
      CALL KOK5B(I2,TIME,C,DUMMY,ATIME,DUMM1)
   50 RNEW=RNEW+(DUMMY-XIOIM(I2))**2
      RNEW=SQRT(RNEW/N2)*100.
      WRITE(5,110)ROLD,RNEW
  110 FORMAT(6H ROLD=E20.5,6H RNEW=E20.5)
C TESTING FOR VALIDITY OF PARAMETER CHANGE
```

```
      IF(ROLD-RNEW)11,12,12
C PARAMETER CHANGE WAS TOO LARGE---CHANGE IS NEGATED,DELCX(II) IS ADJUS-
C TED AND A NEW RNEW CALCULATED
   11 WRITE(5,111)II
  111 FORMAT(13H CHANGE IN C(I1,24H)WAS TOO LARGE,TRY AGAIN)
      C(II)=C(II)+DELCX(II)*DRDC(I/ABS(DRDC(I)
      DELCX(II)=DELCX(II)/2.
      GO TO 13
C PARAMETER CHANGE REDUCED REMAINDER
C TESTING FOR SIGNIFICANCE OF REMAINDER REDUCTION
   12 DUMMY=ROLD
      ROLD=RNEW
      IF(DUMMY-RNEW-0.01000*DUMMY)14,14,15
   14 WRITE(5,112)
  112 FORMAT(40H CHANGE IN REMAINDER WAS NOT SIGNIFICANT)
C CHANGING OF PARAMETERS
   15 II=II+1
      IF(II-N)16,16,17
   16 WRITE(5,113)II
  113 FORMAT(17H ********II IS NOW I5,7H ******)
      GO TO 1
   17 II=1
C CHOOSING BETWEEN CONTINUATION,PARTIAL PRINTOUT OR FINAL PRINTOUT
      CALL DATSW(1,II)
      GO TO (2,16),II
    2 WRITE(5,100)
      WRITE(5,114)C
  114 FORMAT(25H VALUES OF PARAMETERS ARE/3E20.5,///)
      WRITE(5,115)
  115 FORMAT(60H          TIME (SECS)                XIOIN     CALCULATED X
     1(OIP/)
      DO 60 I2=1,N2
      CALL KOKSH(I2,TIME,C,DUMMY,ATIME,DUMM1)
      DUMMY=EXP(DUMMY)
      DUMM1=EXP(XIOIN(I2))
   60 WRITE(5,107)TIME(I2),DUMM1,DUMMY
      WRITE(5,100)
      CALL DATSW(2,II)
      GO TO (3,16),II
    3 CALL EXIT
      END

FEATURES SUPPORTED
 ONE WORD INTEGERS
 EXTENDED PRECISION
 IOCS

CORE REQUIREMENTS FOR KOKS
 COMMON        0  VARIABLES     666  PROGRAM     916

END OF COMPILATION

// DUP

*STORE       WS  UA  KOKS
CART ID 1122   DB ADDR  4A41   DB CNT   0030
```

APPENDIX 2.17

DEVELOPMENT OF A MATHEMATICAL MODEL WITH CORRECTIONS FOR BOTH A CENTRAL WELL AND THE ELECTROLYTE RESISTANCE

Boelter *et al.* [11] has presented Equation A.2.29 describing the oxygen activity profile through a slab of thickness L having an initial oxygen activity profile $f(x)$ with the functions $F_1(\lambda)$ and $F_2(\lambda)$ applied at $x = 0$ (cathode) and $x = L$ (probe face) respectively.

$$P_{O_2}(x,t) = \sum_{n=1}^{\infty} \left[\frac{2}{L} \exp\left[\frac{-n^2\pi^2}{L^2} Dt \right] \sin\left(\frac{n\pi x}{L} \right) \left\{ \int_0^L f(x) \sin\left(\frac{n\pi x}{L} \right) dx \right.\right.$$

$$\left.\left. + \frac{n\pi D}{L} \int_0^t \exp\left[\frac{n^2\pi^2}{L^2} D\lambda \right] [F_1(\lambda) - (-1)^n F_2(\lambda)] d\lambda \right\} \right] \quad \text{(A.2.29)}$$

For this purpose $f(x) = 0$.

By redefining the constants as done previously:

$$P_{O_2}(x,t) = \sum_{n=0}^{\infty} n \left[\exp\left\{ \frac{-n^2\pi^2}{B^2} t \right\} \sin\left(\frac{n\pi x}{L} \right) \right.$$

$$\left. \times \int_0^t \exp\left\{ \frac{n^2\pi^2}{B^2} \lambda \right\} \{ F_1(\lambda) - (-1)^n F_2(\lambda) \} d\lambda \right] \quad \text{(A.2.30)}$$

The current arising from oxygen diffusion through the membrane-electrolyte system is directly proportional to the oxygen activity gradient at the cathode. Finding the derivative:

$$\left.\frac{\partial P_{O_2}(x,t)}{\partial x}\right|_{x=0} = \frac{2\pi^2}{B^2 L} \sum_{n=1}^{\infty} [n^2 \exp\left\{\frac{-n^2\pi^2}{B^2} t\right\}$$

$$\times \int_0^t \exp\left\{\frac{n^2\pi^2}{B^2}\lambda\right\}\{F_1(\lambda) - (-1)^n F_2(\lambda)\}d\lambda\ ] \qquad (A.2.31)$$

By integration by parts of each of the functions $F_1(\lambda)$ and $F_2(\lambda)$, Equation A.2.32 is obtained:

$$\left.\frac{\partial P_{O_2}(x,t)}{\partial x}\right|_{x=0} = \frac{F_2(t)}{L} - \frac{F_1(t)}{L} - \frac{2}{L}\sum_{n=1}^{\infty}[\int_0^t \exp\{\frac{n^2\pi^2}{B^2}(\lambda - t)\}dF_1(\lambda)$$

$$- (-1)^n \int_0^t \exp\left\{\frac{n^2\pi^2}{B^2}(\lambda - t)\right\}dF_2(\lambda)\ ] \qquad (A.2.32)$$

$F_2(t)$ was a step input:

$$F_2(t) = P_1 \qquad (A.2.33)$$

As a result, Equation A.2.34 is obtained:

$$\left.\frac{\partial P_{O_2}(x,t)}{\partial x}\right|_{x=0} = \frac{P_1}{L} - \frac{F_1(t)}{L} + \frac{2P_1}{L}\sum_{n=1}^{\infty}(-1)^n \exp\left\{\frac{-n^2\pi^2}{B^2}t\right\}$$

$$- \frac{2}{L}\sum_{n=1}^{\infty}\int_0^t \exp\left\{\frac{n^2\pi^2}{B^2}(\lambda - t)\right\}dF_1(\lambda) \qquad (A.2.34)$$

To allow numerical evaluation of the integral,

let $t = m\,\Delta\,\lambda$

$\lambda = i\,\Delta\,\lambda$

Then, by reversing the order of summing, Equation A.2.35 results:

$$\left.\frac{\partial P_{02}(x,t)}{\partial x}\right|_{x=0} = \frac{P_1}{L} - \frac{F_1(t)}{L} + \frac{2P_1}{L} \sum_{n=1}^{\infty} (-1)^n \exp\{ \frac{-n^2\pi^2}{B^2}\, t\}$$

$$- \frac{2}{L} \sum_{i=1}^{\infty} \sum_{n=1}^{\infty} \exp\{ \frac{n^2\pi^2}{B^2}(i-m-0.5)\Delta\lambda\}\{F_1(i\Delta\lambda)-F_1(i\Delta\lambda-\Delta\lambda)\}$$

(A.2.35)

But from the system developed for Program KOK5:

$$i_L = (1 - C_i)\, i_A \qquad \text{(A.2.36)}$$

$$\frac{\partial P_{02}(0,A)}{\partial x} = \frac{P_1}{L} \qquad \text{(A.2.37)}$$

$$i_A = C_p P_1 \qquad \text{(A.2.38)}$$

Therefore:

$$i_L = (1 - C_i)\, C_p\, L \left.\frac{\partial P_{02}(x,t)}{\partial x}\right|_{x=0} \qquad \text{(A.2.39)}$$

Thus Equation A.2.40 results:

$$i_L = (1-C_i)C_p[P_1 - F_1(t) + 2P_1 \sum_{n=1}^{\infty} (-1)^n \exp\{ \frac{-n^2\pi^2}{B^2} t\}$$

$$- 2 \sum_{i=1}^{\infty} \sum_{n=1}^{\infty} \exp\{ \frac{n^2\pi^2}{B^2} (i-m-0.5)\Delta\lambda\}\{F_1(i\Delta\lambda) - F_1(i\Delta\lambda - \Delta\lambda)\}] \qquad (A.2.40)$$

For the step input P_1 the oxygen activity profile in the central well can be modelled as before so that:

$$i_R = C_r \{ P_1 \text{ erfc } (\frac{B_r}{\sqrt{t}}) - F_1 \} \qquad (A.2.41)$$

where:

$$C_r^{\circ} = \frac{i_A C_i}{P_1^{\circ}} \text{ erfc}^{-1} (\frac{B_r}{\sqrt{A}}) \qquad (A.2.42)$$

C_r can be calculated from the data obtained from Program KOK5.

But

$$i = i_R + i_L \qquad (A.2.43)$$

and

$$F_1(t) = \alpha \exp [Pi] - \alpha \qquad (A.2.44)$$

The first term in Equation A.2.44 is a Nernst-type relationship and the second term is a correction for the irreversibility of the oxygen electrode.

6 OF/DE 6

Equations A.2.40, A.2.41, A.2.43 and A.2.44 form an implicit system which can be solved for $F_1(t)$ by an iterative scheme as performed by Program KOK6. The above equations represent the solution to an upstep P_1. The response to the downstep following the upstep after 'A' seconds can be similarly obtained.

APPENDIX 2.18

PROGRAM KOK6

Program KOK6 calculated the probe response to an upstep in oxygen tension followed by a downstep of the same magnitude as modelled by the single diffusion layer model with central well and electrolyte resistance corrections incorporated.

```
PAGE   1

// JOB

LOG DRIVE   CART SPEC   CART AVAIL   PHY DRIVE
  0000        1122        1122         0000

V2 M10   ACTUAL  8K   CONFIG  8K

// DUP

*DELETE              KOK6A
D 26 NAME NOT FOUND IN LET/FLET

// FOR
* LIST SOURCE PROGRAM
* ONE WORD INTEGERS
* EXTENDED PRECISION
C
C ******************************************************************************
C
C KOK6A CALCULATES THE SUM OF TERMS OF AN INFINITE SERIES
C IF I1=1 THEN DUMMY=SIGMA(FROM N=1 TO N=INFINITY) OF EXP((2*Y*(N*PI/X)
C **2))*Z
C IF I1=2,THEN DUMMY=SIGMA(FROM N=1 TO N=INFINITY) OF EXP((2*Y*(N*PI/X)
C **2))*Z*(-1)**N
C
C ******************************************************************************
C
      SUBROUTINE KOK6A(I1,I2,X,Y,Z,DUMMY)
      DATA PI/3.1415927/
      N=0
      I3=1
      DUMMY=0.0
    3 N=N+1
      GO TO (1,2),I1
    2 I3=-I*I3
    1 TERM=I3*EXP((N*PI/X)**2*I2*Y)*Z
      DUMMY=DUMMY+TERM
      IF(ABS(TERM)-1.0E-10)10,10,5
    5 IF (ABS(TERM/DUMMY)-1.0E-5*ABS(DUMMY))10,10,3
   10 RETURN
      END

FEATURES SUPPORTED
 ONE WORD INTEGERS
 EXTENDED PRECISION

CORE REQUIREMENTS FOR KOK6A
 COMMON       0  VARIABLES     18  PROGRAM    134

RELATIVE ENTRY POINT ADDRESS IS 001E (HEX)

END OF COMPILATION

// DUP

*STORE       WS  UA  KOK6A
CART ID 1122   DB ADDR  4A7E   DB CNT   000B
```

```
*DELETE              KOK6
D 26 NAME NOT FOUND IN LET/FLET

// FOR
* IOCS (CARD,1403 PRINTER)
* LIST SOURCE PROGRAM
* ONE WORD INTEGERS
* EXTENDED PRECISION
*NAME KOK6
C
C ******************************************************************
C
C PROGRAM KOK6 MODELS THE BEHAVIOR OF THE YSI POLAROGRAPHIC DISSOLVED
C OXYGEN PROBE FOR A STEP INCREASE FOLLOWED BY A STEP DECREASE IN
C OXYGEN TENSION
C IT IS A COMPOSITE MODEL ALLOWING FOR NONIDEALITIES ARISING FROM
C OXYGEN STORAGE IN THE ANODIC WELL AND A NERNST-EQUATION CORRECTION
C FOR OHMIC RESISTANCE OF THE PROBE
C SUBROUTINES REQUIRED ARE ERFC AND KOK6A
C DETAILED PRINTOUT MAY BE SUPPRESSED BY DATA SWITCH NO. 1
C EXECUTION MAY BE STOPPED BY DATA SWITCH NO. 2
C VECTORS---F=OXYGEN TENSION AT THE CATHODE FACE IN ATM---CURR=CURRENT
C VALUES OBTAINED AT MULTIPLES OF THE PRINTOUT INTERVAL
C REAL VARIABLES---STEP=STEP SIZE OF INPUT IN ATM O2---B=LAYER DIFFUSION
C FACTOR SEC**0.5---C=FRACTION OF CURRENT DUE TO RESERVOIR CONTRIBUTION
C FROM KOK5---CP=CALIBRATION CONSTANT OF PROBE IN MICROAMPS/ATM O2---
C CSTAR=PROPORTIONALITY CONSTANT FOR OXYGEN PRESSURE IN RESERVOIR AND RESUL
C TANT CURRENT IN MICROAMPS/ATM O2---D=RESERVOIR DIFFUSION FACTOR SEC**0.5
C ---ALPHA=O2 PRESSURE AT CATHODE AT V=0.8,I=0 IN ATM.---R=ELECTROLYTE
C RESISTANCE FACTOR IN 1/MICROAMPS---GAIN=GAIN FOR IMPLICIT FUNCTION SOLUTION
C ---DTIME=INTEGRATION INTERVAL IN SECS---TTIME=MAX TIME FOR INTEGRATION
C IN SECS---PTIME=PRINTOUT AND CURRENT MEMORY TIME INTERVAL IN SECS
C---ATIME=DURATION OF PROBE EXPOSURE IN SECS---TIME=TIME UNDER CONSIDE
C RATION IN SECS---DCDX=DERIVATIVE OF OXYGEN PRESSURE WRT X AT CATHODE
C IN ATM---IR=CURRENT CONTRIBUTION FROM RESERVOIR IN MICROAMPS---IL=CUR
C RENT DUE TO DIFFUSION THROUGH MEMBRANE AND ELECTROLYTE LAYER IN MICRO
C AMPS---IT=TOTAL CURRENT IN MICROAMPS
C    DUMMY VARIABLES---DUMM1,DUMM2,DUMM3,DUMMY,DCDX1,FOLD
C INTEGER VARIABLES---M=ITERATION VARIABLE---I3=COUNTER FOR CURR---
C DUMMY VARIABLES---I1,IJ,I1,I2
C
C ******************************************************************
C
      REAL IR,IL,IT
      DIMENSION F(400),CURR(200)
C DATA INPUT AND OUTPUT SECTION
      DATA PI/1=3.1415927/,F/ 400*0.0/,CURR/200*0.0/,M,I3/2*0/
      READ(2,101)B,C,CP,CSTAR,D,ALPHA,R,GAIN,DTIME,TTIME,PTIME,ATIME,STE
     1P
  101 FORMAT(4E20.5)
      WRITE(5,100)
  100 FORMAT(1H1)
      WRITE(5,102)STEP,B,C,CP
  102 FORMAT(15H INPUT DATA ARE//6H STEP=E15.5,/3H B=E15.5,/3H C=E15.5,/,
     14H CP=E15.5)
      WRITE(5,103)CSTAR,D,ALPHA,R,GAIN
  103 FORMAT(7H CSTAR=E15.5,/3H D=E15.5,/7H ALPHA=E15.5,/3H R=E15.5,/6H
```

```
      1GAIN=E15.5)
       WRITE(5,104)DTIME,TTIME,PTIME,ATIME
  104 FORMAT(7H DTIME=E15.5,/7H TTIME=E15.5,/7H PTIME=E15.5,/7H ATIME=E1
     15.5,/1H1)
C START OF ITERATION PROCEDURE
  400 M=M+1
      TIME=M*DTIME
      CALL DATSW(1,II)
      IF(TIME-TTIME)1,1,500
    1 GO TO (3,2),II
    2 WRITE(5,105)M,TIME
  105 FORMAT(3H M=I4,5X,6H TIME=F7.1)
C CALCN OF CONSTANT PART OF DCDX
C FIRST PART OF THE DERIVATIVE
    3 DCDX=STEP
      IF(TIME-ATIME-0.0001)302,302,301
  301 DCDX=0.0
  302 GO TO (5,4),II
    4 WRITE(5,106)STEP,DCDX
  106 FORMAT(20H FIRST PART OF DCDX=E15.5,13H DCDX IS NOW=E15.5)
C SECOND PART OF DERIVATIVE
    5 CALL KCK6A(2,-1,8,TIME,1.,DUMMY)
      DUMMY=2.*STEP*DUMMY
      DCDX=DCDX+DUMMY
      IF(TIME-ATIME-0.0001)304,304,303
  303 DUMM1=TIME-ATIME
      CALL KCK6A(2,-1,8,DUMM1,1.,DUMM2)
      DUMM2=2.*STEP*DUMM2
      DCDX=DCDX-DUMM2
  304 GO TO (7,6),II
    6 WRITE(5,107)DUMMY,DCDX
  107 FORMAT(21H SECOND PART OF DCDX=E15.5,13H DCDX IS NOW=E15.5)
C THIRD PART OF DCDX
    7 IF(M-1)8,8,9
    8 DUMM1=0.
      GO TO 13
    9 I1=M+0.5-10./DTIME*B*B/PI/PI
      IF(I1-1)11,11,12
   11 I1=1
   12 I2=M-1
      DUMM1=0.
      DO 10 I=I1,I2
      DUMM2=(I-M-0.5)*DTIME
      IF(I-1)201,201,202
  201 DUMM3=F(I)
      GO TO 203
  202 DUMM3=F(I)-F(I-1)
  203 CALL KCK6A(1,1,M,DUMM2,DUMM3,DUMMY)
   10 DUMM1=DUMM1+DUMMY
   13 DUMM1=-2*DUMM1
      DCDX=DCDX+DUMM1
      GO TO (15,14),II
   14 WRITE(5,108)DUMM1,DCDX
  108 FORMAT(20H THIRD PART OF DCDX=E15.5,13H DCDX IS NOW=E15.5)
C CALCULATION OF ITERATION CONSTANTS
   15 DUMMY=DTIME/2.
      CALL KCK6A(1,-1,8,DUMMY,1.,DUMM1)
      DUMM2=CSTAR*STEP*ERFC(D/SQRT(TIME))
```

470

```
      IF(TIME-ATIME-0.0001)306,306,305
  305 DUMM2=DUMM2-CSTAR*STEP*ERFC(D/SQRT(TIME-ATIME))
C SETTING UP OF ITERATIVE PROCEDURE FOR F(M)
  306 IF(M-1)16,16,17
   17 F(M)=F(M-1)
   16 GO TO (19,18),II
   18 WRITE(5,109)M,F(M)
  109 FORMAT(23H INITIAL ESTIMATE OF F(I4,2H)=E15.5)
C START OF ITERATION
   19 IF (M-1)21,21,22
   21 DCDX1=DCDX-F(M)-2*F(M)*DUMM1
      GO TO 23
   22 DCDX1=DCDX-F(M)-2.*(F(M)-F(M-1))*DUMM1
   23 GO TO (25,24),II
   24 WRITE(5,110)DCDX1
  110 FORMAT(34H VALUE OF DERIVATIVE AT THIS F(M)=E15.5)
C CALCULATION OF CURRENTS
   25 IR=CUMM2-CSTAR*F(M)
      IL=(1.-C)*CP*DCDX1
      IT=IR+IL
      GO TO (27,26),II
   26 WRITE(5,111)IR,IL,IT
  111 FORMAT(4H IR=E15.5,4H IL=E15.5,4H IT=E15.5)
   27 FOLD=F(M)
      F(M)=ALPHA*EXP(R*IT)-ALPHA
      GO TO (29,28),II
   28 WRITE(5,112)F(M)
  112 FORMAT(23H NEW VALUE FOR F(M)=E15.5)
C DETERMINATION OF IMPORTANCE OF CHANGE IN F(M)
   29 IF(ABS(F(M))-1.0E-10)35,35,31
   31 IF(ABS(F(M)-FOLD)-1.0E-03*ABS(F(M)))35,35,32
C FOR DIFFERENCE BETWEEN F(M) AND FOLD TOO LARGE
   32 F(M)=FOLD+GAIN*(F(M)-FOLD)
      GO TO (34,33),II
   33 WRITE(5,113)F(M)
  113 FORMAT(37H VALUE OF F(M) FOR NEXT ITERATION IS=E15.5)
   34 GO TO 19
C FOR DIFFERENCE BETWEEN F(M) AND FOLD ACCEPTABLE
   35 GO TO (37,36),II
   36 WRITE(5,114)TIME,IT,M,F(M)
  114 FORMAT(26H ITERATION WAS SUCCESSFULL/6H TIME=F7.1,4H IT=E15.5,19H
     1 FINAL VALUE OF F(I4,2H)=E15.5)
C TESTING FOR PRINTOUT AND CURRENT MEMORY
   37 IF(TIME-(I3+1.)*PTIME+0.0001)400,400,38
   38 I3=I3+1
      CURR(I3)=IT
      WRITE(5,115)TIME,CURR(I3)
  115 FORMAT(6H TIME=F7.1,12H    CURRENT=E15.5)
      CALL DATSW(2,IJ)
      GO TO (500,400),IJ
  500 WRITE(5,100)
      WRITE(5,116)
  116 FORMAT(40H       TIME         CURRENT       PERCENT OF/40H      (SECS)
     1  (MICROAMPS)    MAX CURRENT//)
      I1=ATIME/PTIME+0.001
      DO 20 I=1,I3
      TIME=I*PTIME
      DUMM1=CURR(I)/CURR(I1)*100.
   20 WRITE(5,117)TIME,CURR(I),DUMM1
```

```
PAGE   5

  117 FORMAT(F10.1,F15.4,F15.2)
      CALL EXIT
      END

FEATURES SUPPORTED
 ONE WORD INTEGERS
 EXTENDED PRECISION
 IOCS

CORE REQUIREMENTS FOR KOK6
 COMMON     0  VARIABLES    1894  PROGRAM   1314

END OF COMPILATION

// DUP

*STORE      WS  UA  KOK6
CART ID 1122   DB ADDR  4A89   DB CNT   00C2
```

APPENDIX 2.19

DEVELOPMENT OF THE EQUATIONS FOR PROGRAM KOK7

If a Michaelis-Menten relationship is assumed to exist between the rate of oxygen consumption and the oxygen tension, Equation A.2.45 results:

$$\frac{\partial P_{O_2}(t)}{\partial t} = \left(\frac{\partial P_{O_2}}{\partial t}\right)_{max} \frac{P_{O_2}(t)}{K_m + P_{O_2}(t)} \qquad \text{(A.2.45)}$$

Upon integration, Equation A.2.46 is obtained:

$$\ln P_{O_2} + P_{O_2} = \ln P_0 + P_0 + \left(\frac{\partial P_{O_2}}{\partial t}\right)_{max} \times t \qquad \text{(A.2.46)}$$

This implicit Equation is solved for P_{O_2} by Subroutine F_2 listed in Appendix 2.20.

Boelter *et al.* [11] has presented Equation A.2.47 as describing the oxygen activity profile through the membrane-electrolyte layer:

$$P_{O_2}(x,t) = -\frac{2\pi}{B^2}\sum_{n=1}^{\infty}\left[n \exp\left\{\frac{-n^2\pi^2}{B^2}t\right\}\sin\left(\frac{n\pi x}{L}\right)\right.$$

$$\left.\times \int_0^t \exp\left\{\frac{n^2\pi^2}{B^2}\lambda\right\}\{(-1)^n F_2(\lambda)\}d\lambda\right] \qquad \text{(A.2.47)}$$

To find the oxygen activity gradient at the cathode, Equation A.2.47 is differentiated with respect to x at $x = 0$:

$$\left.\frac{\partial P_{O_2}(x,t)}{\partial x}\right|_{x=0} = \frac{-2\pi^2}{B^2 L} \sum_{n=1}^{\infty} [n^2(-1)^n \exp\{\frac{-n^2\pi^2}{B^2} t\}$$

$$\times \int_0^t \exp\{\frac{n^2\pi^2}{B^2} \lambda\} F_2(\lambda) d\lambda] \qquad (A.2.48)$$

Upon integration by parts, Equation A.2.49 results:

$$\left.\frac{\partial P_{O_2}(x,t)}{\partial x}\right|_{x=0} = \frac{F_2(t)}{L} + \frac{2F_2(o)}{L} \sum_{n=1}^{\infty} (-1)^n \exp\{\frac{-n^2\pi^2}{B^2} t\}$$

$$+ \frac{2}{L} \sum_{n=1}^{\infty} (-1)^n \int_0^t \exp\{\frac{n^2\pi^2}{B^2} (\lambda - t)\} dF_2(\lambda) \qquad (A.2.49)$$

But:

$$i_L = (1 - C_i) C_p L \left.\frac{\partial P_{O_2}(x,t)}{\partial x}\right|_{x=0} \qquad (A.2.50)$$

Letting:

$$\lambda = i \Delta \lambda$$

$$t = m \Delta \lambda$$

Equation A.2.51 results:

$$i_L = (1-C_i)C_p \; [F_2(t) + 2F_2(o) \sum_{n=1}^{\infty} (-1)^n \exp\{\frac{-n^2\pi^2}{B^2} t\}$$

$$+ 2 \sum_{i=1}^{i=m} \sum_{n=1}^{\infty} (-1)^n \exp\{\frac{n^2\pi^2}{B^2}(i-m-0.5)\Delta\lambda\}\{F_2(i\Delta\lambda)$$

$$- F_2(i\Delta\lambda-\Delta\lambda)\}] \qquad (A.2.51)$$

Churchill [16] has presented Equation A.2.52 describing the oxygen activity profile in the central well in response to the function $F_2(t)$ being applied at the probe's face:

$$P_{O_2}(x,t) = \frac{x}{2\sqrt{\pi D}} \int_0^t \frac{F_2(t-\lambda)}{\lambda^{3/2}} \exp\{\frac{-x^2}{4D\lambda}\}d\lambda \qquad (A.2.52)$$

Redefining the variables as before:

$$P_{O_2}(a^*,t) = \frac{B_r}{\sqrt{\pi}} \int_0^t \frac{F_2(t-\lambda)}{\lambda^{3/2}} \exp\{\frac{-B_r^2}{\lambda}\}d\lambda \qquad (A.2.53)$$

But:

$$i_R = C_r P_{O_2}(a^*,t) \qquad (A.2.54)$$

By letting:

$$\lambda = i\,\Delta\,\lambda$$

$$t = m\,\Delta\,\lambda$$

Equation A.2.55 then results:

$$i_R = \frac{C_r B_r}{\sqrt{\pi}} \sum_{i=1}^{i=m} \frac{F_2\{(m-i+1)\Delta\lambda\}+F_2\{(m-i)\Delta\lambda\}}{2\{(i-0.5)\Delta\lambda\}^{3/2}} \exp\left[\frac{-B_r^2}{\{(i-0.5)\Delta\lambda\}}\right]\Delta\lambda \tag{A.2.55}$$

and

$$i = i_R + i_L \tag{A.2.56}$$

APPENDIX 2.20

PROGRAM KOK7

Program KOK7 and its subroutines calculated the probe response to the function $F_2(t)$ applied at the probe face. The single diffusion layer with central well correction model was used.

```
PAGE   1

// JOB

LOG DRIVE   CART SPEC   CART AVAIL  PHY DRIVE
  0000        1122        1122        0000

V2 M10   ACTUAL  8K  CONFIG  8K

// DUP

*DELETE              F2
D 26 NAME NOT FOUND IN LET/FLET

// FOR
* LIST SOURCE PROGRAM
* ONE WORD INTEGERS
C
C ******************************************************************
C
C PROGRAM F2 CALCULATES THE OXYGEN TENSION FUNCTION APPLIED TO THE FACE
C OF THE PROBE
C
C VARIABLES--- KM=MICHAELIS-MENTEN CONSTANT IN ATM.OXYGEN---PO=INITIAL
C OXYGEN PRESSURE IN ATM. OXYGEN---DFDTM=MAXIMUM SLOPE OF F2 IN ATM. OXY
C GEN/SEC---TIMEX=TIME IN SECONDS---F2OLD=STORAGE VARIABLE FOR F2 FOR
C ITERATIVE SCHEME---GAIN=GAIN FOR ITERATIVE SYSTEM---DUMMY=DUMMY VARIABLE
C
C ******************************************************************
C
      FUNCTION F2(KM,PO,DFDTM,TIMEX)
      REAL KM
      GAIN=0.05
C CHECKING FOR TIMEX=0
      IF(TIMEX-0.001)1,1,2
    1 F2=PO
      GO TO 10
    2 DUMMY=KM*ALOG(PO)+PO+DFDTM*TIMEX
C CHECKING FOR THE RATIO OF DUMMY VS KM
      IF(5.*KM-DUMMY)3,3,6
C INITIAL ESTIMATE OF F2OLD
    3 F2OLD=DUMMY
    5 F2=DUMMY-KM*ALOG(F2OLD)
      IF(ABS(F2-F2OLD)-1.00E-05*ABS(F2))10,10,4
    4 F2OLD=F2OLD+GAIN*(F2-F2OLD)
      GO TO 5
C INITIAL ESTIMATE FOR F2OLD
    6 F2OLD=1.0E-25
    8 F2=DUMMY-KM*ALOG(F2OLD)
      IF(ABS(F2/F2OLD)-1.00000)10,10,7
    7 F2OLD=F2OLD*EXP(GAIN*ALOG(F2/F2OLD))
      GO TO 8
   10 RETURN
      END

FEATURES SUPPORTED
 ONE WORD INTEGERS

CORE REQUIREMENTS FOR F2
 COMMON      0  VARIABLES     12  PROGRAM     172
```

```
PAGE   2
RELATIVE ENTRY POINT ADDRESS IS 0018 (HEX)

END OF COMPILATION

// DUP

*STORE       WS  UA  F2
CART ID 1122    DB ADDR  484B    DB CNT    000E

*DELETE              KOK7A
D 26 NAME NOT FOUND IN LET/FLET


// FOR
* LIST SOURCE PROGRAM
* ONE WORD INTEGERS
C
C ******************************************************************
C
C KOK7A CALCULATES THE SUM OF TERMS OF AN INFINITE SERIES
C DUMMY=SIGMA(FROM N=1 TO N=INFINITY) OF EXP(-N*N*PI*PI/B/B*TIMEX)*(-1)**N
C
C ******************************************************************
C
      SUBROUTINE KOK7A(B,TIMEX,DUMMY)
      DATA PI/3.1415927/
      N=0
      I3=1
      DUMMY=0.0
    1 N=N+1
      I3=-I3
      TERM=I3*EXP(-N*N*PI*PI/B/B*TIMEX)
      DUMMY=DUMMY+TERM
      IF(ABS(TERM/DUMMY)-1.0E-5*ABS(DUMMY))2,2,1
    2 RETURN
      END
FEATURES SUPPORTED
 ONE WORD INTEGERS

CORE REQUIREMENTS FOR KOK7A
 COMMON       0  VARIABLES      12  PROGRAM     106

RELATIVE ENTRY POINT ADDRESS IS 0012 (HEX)

END OF COMPILATION

// DUP

*STORE       WS  UA  KOK7A
CART ID 1122    DB ADDR  4859    DB CNT    0009

*DELETE              KOK7
D 26 NAME NOT FOUND IN LET/FLET


// FOR
* IOCS (CARD,1403 PRINTER)
```

```
* LIST SOURCE PROGRAM
* ONE WORD INTEGERS
*NAME                 KOK7
C
C ******************************************************************
C
C PROGRAM KOK7 CALCULATES THE RESPONSE OF THE YSI PROBE TO THE FUNCTION F2
C APPLIED AT THE PROBE FACE ACCORDING TO THE SINGLE DIFFUSION LAYER WITH
C CENTRAL-WELL CORRECTION MODEL---THE APPLIED FUNCTION USED IS THE OXYGEN
C PRESSURE VS TIME CURVE OBTAINED BY INTEGRATION OF A MICHAELIS-MENTEN
C TYPE RELATIONSHIP BETWEEN THE RATE OF OXYGEN TENSION DECREASE AND THE
C OXYGEN TENSION---DATA SWITCH NO. 1 CAN BE USED TO SUPPRESS A DETAILED
C CALCULATION PRINTOUT.
C
C $UBROUTINES REQUIRED ARE KOK7A AND F2
C REAL VARIABLES---DFDTM=MAXIMUM RATE OF OXYGEN TENSION DECREASE-ATM/SEC
C ---KM=MICHAELIS-MENTEN CONSTANT FOR F2-ATM---PO=INITIAL OXYGEN TENSION
C -ATM---CI=FRACTION OF TOTAL CURRENT DUE TO OXYGEN DIFFUSION FROM THE
C CENTRAL WELL AFTER A*SECONDS EXPOSURE---CP=PROBE CONSTANT-MICROAMP/ATM
C ---B=DIFFUSION CONSTANT FOR LAYER-SEC**0.5---BR=DIFFUSION CONSTANT FOR
C THE CENTRAL WELL-SEC**0.5---CR=PROPORTIONALITY CONSTANT BETWEEN OXYGEN
C PRESSURE AT A* AND RESULTANT CURRENT-MICROAMPS/ATM---CI,CP,B,BR,CR ARE
C DERIVED FROM KOK5 RUNS
C ---TTIME=TOTAL TIME MODELLED-SEC---DTIME=MODELLING INTERVAL AND INTEGRA-
C TION INTERVAL-SEC---F=VECTOR OF VALUES OF THE APPLIED OXYGEN TENSION-
C ATM---TIME=VECTOR OF TIME VALUES-SEC
C INTEGER VARIABLES---NI=NO. OF VALUES OF F CALCULATED
C DUMMY AND COUNTER VARIABLES---DUMMY,DUMM1,DUMM2,DUMM3,I,I1,I2,II
C
C ******************************************************************
C
      REAL IR,IL,IT,KM
      DIMENSION F(985),TIME(985)
      DATA PI/3.1415927/,I1,I2/2*0/
C VARIABLE INPUT AND OUTPUT SECTION
      READ(2,101)DFDTM,KM,PO,CI,CP,B,CR,BR,TTIME,DTIME
  101 FORMAT(4E20.5)
      READ(2,102)NI
  102 FORMAT(I5)
      WRITE(5,103)DFDTM,KM,PO,CI
  103 FORMAT(1H1,7H DFDTM=E20.5,/4H KM=E20.5,/4H PO=E20.5,/4H CI=E20.5)
      WRITE(5,104)CP,B,CR,BR
  104 FORMAT(4H CP=E20.5,/3H B=E20.5,/4H CR=E20.5,/4H BR=E20.5)
      WRITE(5,105)TTIME,DTIME
  105 FORMAT(7H TTIME=E20.5,/7H DTIME=E20.5,/1H1,40H          TIME (SECS)
     1          F2 (ATM)//)
C CALCULATION OF TIME AND APPLIED OXYGEN TENSION FUNCTION
      DO 10 I=1,NI
      TIME(I)=I*DTIME
      DUMMY=TIME(I)
      IF(I-1)2,2,1
    1 IF(F(I-1)-1.0E-06)3,3,2
    3 F(I)=1.0E-06
      I1=I1+1
      GO TO 4
    2 F(I)=F2(KM,PO,DFDTM,DUMMY)
    4 IF(I1-3)5,5,10
    5 WRITE(5,106)TIME(I),F(I)
  106 FORMAT(2E20.5)
```

```
   10 CONTINUE
      WRITE(5,107)
  107 FORMAT(1H1,80H        TIME (SECS)           F2 (ATM)    CURRENT(
     1MICRO-A)    MEASURED F2(ATM)//)
C CALCULATION OF CURRENTS
      DO 20 II=1,NI
      CALL DATSW(1,II)
      GO TO (7,6),II
    6 WRITE(5,108)II,TIME(II),F(II)
  108 FORMAT(4H II=I5,9H TIME(II)F15.1,7H F(II)=E20.5)
C CALCULATION OF IL
C CALCULATION OF FIRST PART OF LAYER DERIVATIVE
    7 DUMM1=F(II)
      GO TO (9,8),II
    8 WRITE(5,109)DUMM1
  109 FORMAT(32H FIRST PART OF LAYER DERIVATIVE=E20.5)
C CALCULATION OF SECOND PART OF DERIVATE
    9 DUMMY=TIME(II)
      CALL KCK7A(B,DUMMY,DUMM2)
      DUMM2=DUMM2*2.*PO
      DUMM1=DUMM1+DUMM2
      GO TO (12,11),II
   11 WRITE(5,110)DUMM2,DUMM1
  110 FORMAT(13H SECOND PART=E20.5,19H DERIVATIVE IS NOW=E20.5)
C CALCULATION OF THIRD PART OF LAYER DERIVATIVE
   12 DUMM2=0.
      DO 30 I=1,II
      DUMMY=(II+0.5-I)*DTIME
      CALL KCK7A(B,DUMMY,DUMM3)
      IF(I-1)13,13,14
   13 DUMM3=DUMM3*(F(I)-PO)
      GO TO 15
   14 DUMM3=DUMM3*(F(I)-F(I-1))
   15 DUMM2=DUMM2+DUMM3
   30 CONTINUE
      DUMM2= 2.*DUMM2
      DUMM1=DUMM1+DUMM2
      GO TO (17,16),II
   16 WRITE(5,111)DUMM2,DUMM1
  111 FORMAT(12H THIRD PART=E20.5,19H DERIVATIVE IS NOW=E20.5)
   17 IL=(1.-C1)*CP*DUMM1
      GO TO (19,18),II
   18 WRITE(5,112)IL
  112 FORMAT(4H IL=E20.5)
C CALCULATION OF IR
C CALCULATION OF OXYGEN TENSION AT AR
   19 DUMM1=0.
      DO 40 I=1,II
      DUMMY=(I-0.5)*DTIME
      IF(II-1)21,21,22
   21 DUMM2=(F(I)+PO)/2.
      GO TO 23
   22 I2=II-I+1
      DUMM2=(F(I2-1)+F(I2))/2.
   23 DUMM2=DUMM2/DUMMY**1.5*DTIME*EXP(-BR*BR/DUMMY)
      DUMM1=DUMM1+DUMM2
   40 CONTINUE
      DUMM1=DUMM1*BR/SQRT(PI)
C CALCULATION OF RESERVOIR CURRENT
```

```
PAGE  5

      IR=CR*DUMM1
      GO TO (25,24),II
   24 WRITE(5,113)DUMM1,IL
  113 FORMAT(23H OXYGEN PRESSURE AT A*=E20.5,19H RESERVOIR CURRENT=E20.5
     1)
   25 IT=IR+IL
      DUMM1=IT/CP
      WRITE(5,114)TIME(I1),F(I1),IT,DUMM1
  114 FORMAT(F20.1,3F20.5)
   20 CONTINUE
      CALL EXIT
      END

FEATURES SUPPORTED
 ONE WORD INTEGERS
 IOCS

CORE REQUIREMENTS FOR KCKT
 COMMON      0  VARIABLES    3990  PROGRAM    864

END OF COMPILATION

// DUP

*STORE      WS  UA  KCK7
CART ID 1J22   DB ADDR  4862   DB CNT   003D
```

APPENDIX 3.1

EXPERIMENTAL RESULTS FOR THE CALIBRATION OF THE DROPPING MERCURY POLAROGRAPH WITH DISTILLED WATER

Dosing solution was added at a concentration of 1 cc per 200 cc of sample (distilled water).

Temperature: 23°C

Pressure: 751 mm Hg.

Calibration Gas #	Oxygen tension (atm.)
0	0.0*
1	1.76×10^{-4}
2	9.26×10^{-4}
3	3.0×10^{-3}
4	1.01×10^{-2}
5	3.02×10^{-2}
6	9.96×10^{-2}
7	2.1×10^{-1}

Calibration gases were obtained from Liquid Carbonic Company. During all tests the liquid sample was sparged with the calibration gas, the DME lowered into the sample and

*pure nitrogen gas

the sample blanketed with the same gas during the current measurement.

TEST #	GAS #	POLAROGRAPH SENSITIVITY (μA/mm)	READING AT END OF DROP LIFE (mm)	CURRENT AT END OF DROP LIFE (μA)
I	0	0.0001	6	0.0006
	1	0.0001	42	0.0042
II	0	0.0001	5	0.0005
	0	0.0002	4	0.0008
	0	0.0003	3	0.0009
	0	0.0004	3	0.0012
	2	0.0001	180	0.0180
	2	0.0002	95	0.0190
	2	0.0003	64	0.0192
	2	0.0004	48	0.0192
	2	0.0006	32	0.0192
	2	0.0008	24	0.0192
	2	0.0010	20	0.0200
III	3	0.0004	170	0.0680
	3	0.0006	113	0.0678
	3	0.0008	85	0.0680
	3	0.001	68	0.0680
	3	0.002	35	0.0700
	3	0.004	18	0.0720
IV	4	0.002	116	0.232
	4	0.004	58	0.232
	4	0.006	38.5	0.231
	4	0.008	29	0.232

TEST #	GAS #	POLAROGRAPH SENSITIVITY (μA/mm)	READING AT END OF DROP LIFE (mm)	CURRENT AT END OF DROP LIFE (μA)
V	5	0.004	158	0.632
	5	0.006	105.5	0.633
	5	0.008	79	0.632
	5	0.010	63	0.630
	5	0.015	42	0.630
	5	0.020	32	0.640
VI	6	0.015	135	2.025
	6	0.020	102	2.040
	6	0.030	68	2.040
	6	0.040	51	2.040
	6	0.060	34	2.040
VII	7	0.030	142	4.26
	7	0.040	107	4.28
	7	0.060	71	4.26
	7	0.080	53	4.24
	7	0.100	42.5	4.25

CALCULATION OF SIGNAL CURRENTS

POLAROGRAPH SENSITIVITY (μA/mm)	COMPENSATION FOR RESIDUAL CURRENT (mm)	TEST NUMBER AND SIGNAL CURRENTS (μA)						
		I	II	III	IV	V	VI	VII
0.0001	5	0.0037	0.0175					
0.0002	4		0.0182					
0.0003	3		0.0183					
0.0004	3		0.0180	0.0668				
0.0006	1.5		0.0183	0.0669				
0.0008	1.5		0.0180	0.0668				
0.0010	1		0.0190	0.0670				
0.0020	0			0.070	0.232			
0.0040	0			0.072	0.232	0.632		
0.0060	0				0.231	0.633		
0.0080	0				0.232	0.632		
0.010	0					0.630		
0.015	0					0.630	2.025	
0.020	0					0.640	2.040	
0.030	0						2.040	4.26
0.040	0						2.040	4.28
0.060	0						2.040	4.27
0.080	0							4.24
0.100	0							4.25

APPENDIX 3.2

EXPERIMENTAL RESULTS FOR THE CALIBRATION OF THE DROPPING MERCURY POLAROGRAPH WITH FERMENTATION SUPERNATANT

The supernatant was obtained by centrifuging and filtering (0.8 micron, Millipore) broth from Fermentation 1. The temperature was 23°C; the ambient pressure was 751 mm Hg. The calibration gases used were the same as described in Appendix 3.1. The procedure was also identical to the one described in Appendix 3.1. No dosing solution was added. A special feature of the Polarograph was employed during these experiments to improve the accuracy of the measurements. The baseline of the polarogram was shifted by varying amounts to allow the use of higher sensitivities than would otherwise have been possible. The maximum 'baseline compensation' was 200 mm. This technique was used since the residual current observed with the fermentation liquid was much higher than with the distilled water.

TEST #	GAS #	POLAROGRAPH SENSITIVITY (μA/mm)	% BASELINE COMPENSATION (of 200 mm)	READING AT END OF DROP LIFE (mm)	CURRENT AT END OF DROP LIFE (μA)
I	0	0.0008	0	167	0.1336
	0	0.0008	50	67	0.1336
	0	0.0006	50	123	0.1338
	0	0.0006	100	23	0.1338
	0	0.0004	100	135	0.1340
	0	0.001	0	134	0.1340
	0	0.002	0	67	0.1340
	0	0.004	0	33.5	0.1340
	0	0.006	0	22	0.1320
	1	0.0008	0	171	0.1368
	1	0.0008	50	71	0.1368
	1	0.0006	50	129	0.1374
	1	0.0006	100	29	0.1374
	1	0.0004	100	144	0.1376
	1	0.001	0	136	0.1360
	1	0.002	0	68	0.1360
	1	0.004	0	34	0.1360
	1	0.006	0	23.5	0.1410

TEST #	GAS #	POLAROGRAPH SENSITIVITY (μA/mm)	% BASELINE COMPENSATION (of 200 mm)	READING AT END OF DROP LIFE (mm)	CURRENT AT END OF DROP LIFE (μA)
II	0	0.0008	0	166	0.1328
	0	0.0008	50	66	0.1328
	0	0.0006	50	120	0.1320
	0	0.0006	100	20	0.1320
	0	0.0004	100	132	0.1328
	0	0.001	0	132	0.1320
	0	0.002	0	65	0.1300
	0	0.004	0	33	0.1320
	0	0.006	0	22	0.1320
	2	0.0008	0	192	0.1536
	2	0.0008	50	92	0.1536
	2	0.0006	50	156	0.1536
	2	0.0006	100	56	0.1536
	2	0.0004	100	188	0.1552
	2	0.001	0	154	0.1540
	2	0.002	0	76	0.1520
	2	0.004	0	38.5	0.1540
	2	0.006	0	26	0.1560

TEST #	GAS #	POLAROGRAPH SENSITIVITY (μA/mm)	% BASELINE COMPENSATION (of 200 mm)	READING AT END OF DROP LIFE (mm)	CURRENT AT END OF DROP LIFE (μA)
III	0	0.0008	0	169	0.1352
	0	0.0008	50	69	0.1352
	0	0.0006	50	125	0.1350
	0	0.0006	100	25	0.1350
	0	0.0004	100	138	0.1352
	0	0.001	0	134	0.1340
	0	0.002	0	67	0.1340
	0	0.004	0	34	0.1360
	0	0.006	0	23	0.1380
	3	0.001	0	200	0.2000
	3	0.001	50	100	0.2000
	3	0.0008	50	152	0.2016
	3	0.0008	100	52	0.2016
	3	0.0006	100	133	0.1998
	3	0.002	0	99	0.1980
	3	0.004	0	51	0.2040
	3	0.006	0	34	0.2040

TEST #	GAS #	POLAROGRAPH SENSITIVITY (μA/mm)	% BASELINE COMPENSATION (of 200 mm)	READING AT END OF DROP LIFE (mm)	CURRENT AT END OF DROP LIFE (μA)
IV	4	0.002	0	171	0.3420
	4	0.002	50	71	0.3420
	4	0.002	100	-29	0.3420
	4	0.001	100	142	0.3420
	4	0.004	0	86.5	0.3460
	4	0.006	0	58	0.3480
	4	0.008	0	43	0.3440
	5	0.008	0	98	0.7840
	5	0.008	50	-2	0.7840
	5	0.006	50	30	0.7800
	5	0.004	50	95	0.7800
	5	0.004	100	-5	0.7800
	5	0.002	100	191	0.7820
	5	0.010	0	78	0.7800
	5	0.015	0	52	0.7800
	5	0.020	0	40	0.8000

TEST #	GAS #	POLAROGRAPH SENSITIVITY (μA/mm)	% BASELINE COMPENSATION (of 200 mm)	READING AT END OF DROP LIFE (mm)	CURRENT AT END OF DROP LIFE (μA)
VI	6	0.020	0	114	2.280
	6	0.015	0	152	2.280
	6	0.030	0	75.5	2.265
	6	0.040	0	56	2.240
	6	0.060	0	37	2.220
	6	0.080	0	28	2.240
VII	7	0.030	0	151	4.530
	7	0.040	0	113	4.520
	7	0.060	0	76	4.560
	7	0.080	0	57	4.560
	7	0.100	0	44	4.400
	7	0.150	0	30.5	4.575

	POLAROGRAPH SENSITIVITY (μA/mm)	READING TEST I (mm)	READING TEST II	READING TEST III	AVERAGE COMPENSATION FOR RESIDUAL CURRENT (mm)
	0.0008	167	166	169	167
	0.0006	223	220	225	223
	0.0004	335	332	338	335
	0.001	134	132	134	133
	0.002	67	65	67	66
	0.004	33.5	33	34	33.5
	0.006	22	22	23	22.5
AVERAGE RESIDUAL CURRENT (μA)		0.1336	0.1319	0.1353	0.1336
STANDARD DEVIATION OF RESIDUAL CURRENT (% OF AVERAGE RESIDUAL CURRENT)		0.5	0.7	0.9	1.3

CALCULATION OF AVERAGE BASELINE COMPENSATION FOR THE RESIDUAL CURRENT

CALCULATION OF SIGNAL CURRENTS

POLAROGRAPH SENSITIVITY (μA/mm)	COMPENSATION FOR RESIDUAL CURRENT (mm)	TEST NUMBER AND SIGNAL CURRENTS (μA) I	II	III	IV	V	VI	VII
0.0004	335	0.0036	0.0212					
0.0006	223	0.0036	0.0198	0.0660				
0.0008	167	0.0032	0.0200	0.0680				
0.001	133	0.0030**	0.0210	0.0670	0.2090			
0.002	66	0.0040**	0.0200	0.0660	0.2100	0.6500		
0.004	33.5	0.0020**	0.0200	0.0700	0.2120	0.6460		
0.006	22.5	0.0060**	0.0210	0.0690	0.2130	0.6450		
0.008	17*				0.2080	0.6480		
0.010	13*					0.6500		
0.015	9*					0.6450	2.145	
0.020	7*					0.6600	2.140	
0.030	4.5*						2.130	4.395
0.040	3.5*						2.100	4.380
0.060	2*						2.100	4.440
0.080	2*						2.080	4.400
0.100	1.5*							4.250
0.150	1*							4.425

* Calculated from overall average residual current

**Not used for further calculations

APPENDIX 4.1

PROGRAM KOK8

Program KOK8 and its subroutines calculated the dynamic response of a fermentor dissolved oxygen control system to a disturbance or a change in an operating parameter after operation at steady state for *A* seconds.

```
PAGE   1

// JOB

LOG DRIVE   CART SPEC   CART AVAIL  PHY DRIVE
  0000        1122        1122        0000

V2 M10   ACTUAL  8K  CONFIG  8K

// DUP

*DELETE              KCK8
D 26 NAME NOT FOUND IN LET/FLET

// FOR
* IOCS (CARD,1403 PRINTER)
* LIST SOURCE PROGRAM
* ONE WORD INTEGERS
*NAME KCK8
C
C ****************************************************************
C
C PROGRAM KCK8 CALCULATES THE DYNAMIC RESPONSE OF A FERMENTOR DISSOLVED
C OXYGEN CONTROL SYSTEM TO A DISTURBANCE OR A CHANGE IN OPERATING PARAMETER
C AFTER OPERATION AT STEADY STATE FOR ATIME SECONDS
C ASSUMPTIONS MADE WERE
C BOTH THE LIQUID CONTENTS AND THE HEAD SPACE ARE PERFECTLY MIXED
C GAS BUBBLES WHICH ENTER BY SPARGING HAVE A MEAN RESIDENCE TIME OF TOU
C SECONDS IRREGARDLESS OF THE SPARGING RATE
C THE RESIDENCE TIME DISTRIBUTION FUNCTION OF HOLDUP GAS BUBBLES IS A
C DECAYING EXPONENTIAL
C MASS TRANSFER FROM THE HEAD SPACE TO THE LIQUID OCCURS AT THE INTERFACE
C BETWEEN THE TWO PHASES ONLY - NO GAS BUBBLES ARE FORMED
C THE VOLUMETRIC MASS TRANSFER COEFFICIENT CAN BE RELATED TO THE SPARGING
C AIR FLOW BY A SIMPLE RELATIONSHIP
C BOTH MASS TRANSFER COEFFICIENTS ARE AFFECTED IN THE SAME WAY BY ADDITION
C OF A SURFACE ACTIVE MATERIAL
C DISSOLVED OXYGEN PROBE BEHAVIOR IS DESCRIBED AS IN PROGRAMS KOK5 AND
C KOK7
C OXYGEN CONSUMPTION RATE BY MICROORGANISMS IS RELATED TO OXYGEN TENSION IN A
C MICHAELIS-MENTEN MANNER
C
C SUBROUTINES USED WERE KOK8A TO READ ALL PARAMETERS AND TABULATE THEM,
C KCK8B TO CALCULATE THE INITIAL STEADY STATE,KOK8C TO CALCULATE THE PROBE
C RESPONSE,KCK8D TO DETERMINE THE MICROORGANISM OXYGEN CONSUMPTION,KOK8E
C IS REQUIRED BY KCK8C,KOK8F DETERMINES THE EFFECT OF THE CHANGE IN OPE-
C RATING CONDITIONS,KOK8G MODELS THE CONTROLLER,KOK8H CALCULATES THE DYNA-
C MIC RESPONSE OF THE SYSTEM
C
C VECTORS USED---A=TITLE STORAGE VECTOR---KV=MASS TRANSFER COEFFICIENT
C FROM BUBBLES TO LIQUID-KGMOLE O2/HR/M**3/ATM.O2---Q=AIR FLOW RATE M**3/HR
C --- PC2HL=HOLD-UP GAS OXYGEN PRESSURE-ATM O2---PO2=OXYGEN PRESSURE IN
C LIQUID PHASE-ATM O2---CONC=DATA VECTOR FOR KOK8C
C
C REAL VARIABLES---POW=POWER INPUT PER UNIT VOLUME-HP/M**3---CON1=EMPIRI-
C CAL CONSTANT FOR KV,Q RELATION---VL=LIQUID VOLUME IN FERMENTOR-L---VH=
C HEAD SPACE VOLUME-L---KG=MASS TRANSFER COEFFICIENT FROM HEAD SPACE TO LIQUID-
C CM/SEC---DIA=TANK DIAMETER-CM---PO2G=OXYGEN PRESSURE IN INCOMING GAS-
C ATM O2---DTIME=ITERATION INTERVAL-SEC---MHU=ORGANISM GROWTH RATE-HR**-1
```

```
C ---MHUMX=MAX ORGANISM GROWTH RATE-HR**-1---KM=ORGANISM MICHEALIS-MENTEN
C GROWTH CONSTANT-ATM O2---CELL=CELL CONCENTRATION-GM/L---YO2=OXYGEN UTILIZA-
C TION PER CELLS PRODUCED-GM O2/GM CELLS---DO2=OXYGEN CONSUMPTION RATE-
C GM O2/L/SEC---CONTG=CONTROLLER GAIN-M**3/HR/ATM O2---CONTI=CONTROLLER
C INTEGRATION GAIN-M**3/HR/ATM O2/SEC---ERINT=INTEGRAL OF THE CONTROLLER
C ERROR---AIRMX=MAXIMUM AIR FLOW THROUGH CONTROL VALVE-M**3/HR---PO2S=
C SET PT FOR OXYGEN CONTROL-ATM---TTIME=TOTAL CALCULATION TIME-SEC---
C ATIME=INITIAL STEADY-STATE PERIOD-SEC---TIME=TIME VARIABLE-SEC---QO2A=
C SUPPLY RATE TO FERM'N FROM HEAD GAS-GM O2/L/SEC---PO2P=OXYGEN PRESSURE
C INDICATION RECEIVED FROM PROBE-ATM O2---SO2=SOLUBILITY OF OXYGEN-GM O2
C /L/ATM O2---PO2E=HEAD SPACE OXYGEN PRESSURE-ATM O2---TOU=MEAN RESIDENCE
C TIME FOR BUBBLES IN HOLDUP-SEC---R=GAS CONSTANT-L-ATM/DEG-MOLE---T=
C TEMPERATURE-DEG K---GAIN1=GAIN FOR ITERATIVE SYSTEM CALCULATING THE
C   INITIAL CONDITIONS---GAIN2=MULTIPLIER FROM STEP CHANGE FROM STEADY
C STATE
C
C INTEGER VARIABLES---N1=TOTAL NO. OF TIME INTERVALS USED---N2=NO. OF TIME
C INTERVALS USED FOR INITIAL STEADY-STATE---N3=NO. OF TIME INTERVALS USED
C FOR INTEGRATIONS AND RESIDENCE TIME DISTRIBUTIONS
C
C ****************************************************************
C
      REAL KV(100),KG,MMU,MMUMX,KM
      COMMON KV,O(100),PO2MU(200),PO2(500),A(10),CONC(5)
      COMMON POW,CON1,VL,VH,KG,DIA,PO2G,DTIME,MMU,MMUMX,KM,CELL,YO2,DO2
      COMMON CONTC,CONTI,ERINT,AIRMX,PO2S,TTIME,ATIME,TIME,QO2A,QO2B,SO2
      COMMON PO2E,TOU,R,T,GAIN1,DUMMX
      COMMON N1,N2,N3,I1
C PARAMETER INPUT AND LISTING PERFORMED BY KOK8A
      CALL KOK8A
C CALCULATION OF INITIAL CONDITIONS
      CALL KOK8B
C CHANGE OF OPERATING PARAMETERS
      CALL KOK8F
C CALCULATION OF THE DYNAMIC RESPONSE
      CALL KOK8H
      CALL EXIT
      END

FEATURES SUPPORTED
 ONE WORD INTEGERS
 IOCS

CORE REQUIREMENTS FOR KOK8
 COMMON   1896  VARIABLES       0  PROGRAM     32

END OF COMPILATION

// DUP

*STORE      WS  UA  KOK8
CART ID 1122   DB ADDR  489F   DB CNT   0003

*DELETE             KOK8A
D 26 NAME NOT FOUND IN LET/FLET

// FOR
```

```
* LIST SOURCE PROGRAM
* ONE WORD INTEGERS
      SUBROUTINE KOKBA
      REAL K/(100),KG,MMU,MMUMX,KM
      COMMON KV,U(100),PU2MU(200),PO2(500),A(10),CONC(5)
      COMMON PCW,CONI,VL,VH,KG,DIA,PO2G,DTIME,MMU,MMUMX,KM,CELL,YO2,DO2
      COMMON CONTG,CONTI,ENTNT,AIRMX,PO2S,TTIME,ATIME,TIME,OO2A,OO2B,SO2
      COMMON PO2E,TOU,R,T,GAIN1,DUMMX
      COMMON N1,N2,N3,I1
      WRITE(5,100)
  100 FORMAT(1H1,22H LIST OF SPECIFIED PARAMETERS//)
      READ(2,101)PCW,CONI,VL,VH,KG,DIA,PO2G,DTIME,MMUMX,KM,CELL
      READ(2,101)YO2,CONTG,CONTI,PO2S,TTIME,ATIME,SO2,TOU,R,T,GAIN1
      READ(2,101)(CONC(I),I=1,5)
  101 FORMAT(4E20.5)
      WRITE(5,102)PCW,CONI,VL,VH,KG
  102 FORMAT(24H POWER INPUT PER UNIT VOLUMEE20.5, 8H HP/M**3/37H EMPIRI
     1CAL CONSTANT FOR Q-KV RELATIONE20.5,/14H LIQUID VOLUMEE20.5,6H LIT
     2ER/18H HEAD SPACE VOLUMEE20.5,6H LITER/32H MASS TRANSFER COEFF HEA
     3D TC LIQ E20.5,7H CM/SEC)
      WRITE(5,103)DIA,PO2G,DTIME,MMUMX
  103 FORMAT(15H VESSEL DIAMETERE20.5,3H CM/25H SPARGING GAS O2 PRESSURE
     1E20.5,7H ATM O2/24H ITERATION TIME INTERVALE20.5,4H SEC/29H MAXIMU
     2M ORGANISM GROWTH RATEE20.5,7H HR**-1)
      WRITE(5,104)KM,CELL,YO2,CONTG,CONTI
  104 FORMAT(24H M.M. CONSTANT FOR ORGANISMSE20.5,7H ATM O2/19H CELL CON
     1CENTRATIONE20.5,5H GM/L/32H OXYGEN CONSUMED PER CELLS GROWNE20.5,1
     25H GM O2/GM CELLS/16H CONTROLLER GAINE20.5,15H M**3/HR/ATM O2/28H
     3CONTROLLER INTEGRATION GAINE20.5,19H M**3/HR/ATM O2/SEC)
      WRITE(5,105)PO2S,TTIME,ATIME,SO2,TOU,R,T,GAIN1
  105 FORMAT(26H SET PT FOR OXYGEN CONTROLE20.5,7H ATM O2/21H TOTAL ITER
     1ATION TIMEE20.5,4H SEC/28H INITIAL STEADY-STATE PERIODE20.5,4H SEC
     2/21H SOLUBILITY OF OXYGENE20.5,12H GM O2/L/ATM/41H MEAN RESIDENCE
     3TIME OF BUBBLES IN HOLDUPE20.5,4H SEC/13H GAS CONSTANTE20.5,15H L-
     4ATM/MOLE-DEG/12H TEMPERATUREE20.5,6H DEG K/6H GAINIE20.5)
      WRITE(5,106)(CONC(I),I=1,5)
  106 FORMAT(3H CIE20.5,/3H CPE20.5,16H MICROAMP/ATM O2/2H BE20.5,9H SEC
     1**0.5/3H CRE20.5,16H MICROAMP/ATM O2/3H BRE20.5,9H SEC**0.5)
      N1=TTIME/DTIME+0.00001
      N2=ATIME/DTIME+0.00001
      N3=3.*TOU/DTIME+0.0001
      WRITE(5,107)N1,N2,N3
  107 FORMAT(31H TOTAL NUMBER OF TIME INTERVALSI5,/45H NUMBER OF TIME IN
     1TERVALS DURING STEADY-STATEI5,/32H NUMBER OF INTEGRATION INTERVALS
     2I5,///19H INITIAL CONDITIONS//)
      RETURN
      END

FEATURES SUPPORTED
 ONE WORD INTEGERS

CORE REQUIREMENTS FOR KOKBA
 COMMON   1896  VARIABLES      2  PROGRAM    802

RELATIVE ENTRY POINT ADDRESS IS 025A (HEX)

END OF COMPILATION

// DUP
```

```
*STCRE      WS  UA  KOKRA
CART ID 1122   DB ACDR  40A2   DB CNT   0033

*CELETE              KOK8B
D 26 NAME ACT FOUNC IN LET/FLET

// FOR
* LIST SOURCE PROGRAM
* ONE WCRC INTEGERS
      SUBROUTINE KCK8B
      REAL KV(100),KG,MMU,MMUMX,KM
      COMMON KV,Q(100),PO2MU(200),PO2(500),A(10),CONC(5)
      COMMON PCW,CON1,VL,VH,KG,DIA,PO2G,DTIME,MMU,MMUMX,KM,CELL,YO2,DO2
      COMMON CONTG,CCNTI,ERINT,AIRMX,PO2S,TTIME,ATIME,TIME,QO2A,QO2B,SO2
      COMMON PO2E,TOU,R,T,GAIN1,DUMMX
      COMMON N1,N2,N3,I1
      DATA PI/3.1415927/
      ERINT=0.0
      DO 1C I=1,N2
   10 PO2(I)=PO2S
      DUMMX=0.
      DC 30 I=1,N3
   30 DUMMX=DUMMX+EXP((1-I)*DTIME/TOU)
      I1=N2
      CALL KCK3D
      WRITE(5,100)CO2
  100 FORMAT(19H OXYGEN CONSUMPTIONE20.5,12H GM O2/L/SEC)
C STEADY-STATE IS DETERMINED BY PERFORMING A MASS BALANCE OVER DTIME
C INITIALLY ASSUME A  FLOWRATE OF 0.05 M**3/HR
      Q(1)=0.05
C CALCULATION OF FLOWRATES
    1 DO 20 I=2,N3
   20 Q(I)=Q(1)
C CALCULATION OF MASS TRANSFER COEFFICIENTS
      KV(1)=CON1/DUMMX*(4.E+4/DIA/DIA/PI)**0.67*POW**0.95*Q(1)**0.67
      DC 40 I=2,N3
   40 KV(I)=KV(1)*EXP((1-I)*DTIME/TOU)
C CALCULATION OF HOLDUP GAS OXYGEN PRESSURES
      DUMMY=1000.*Q(1)/R/T/VL
      PO2MU(1)=PO2G
      DC 50 I=1,N3
   50 PO2MU(I+1)=(DUMMY*PO2MU(I)-KV(I)/2.*(PO2MU(I)-2.*PO2S))/(DUMMY+KV(
     1I)/2.)
C CALCULATION OF QO2A
      QO2A=0.0
      DC 60 I=1,N3
   60 QO2A=QO2A+KV(I)/112.5*(PO2MU(I)/2.+PO2MU(I+1)/2.-PO2S)
C CALCULATION OF EXHAUST GAS PRESSURES
      DUMM1=0.
      DUMM2=0.
      DC 70 I=1,N3
      DUMMY=EXP((1-I)*DTIME/TOU)-EXP(-I*DTIME/TOU)
      DUMM1=DUMM1+DUMMY
   70 DUMM2=DUMM2+DUMMY*PO2MU(I+1)
      PO2E=DUMM2/DUMM1
C CALCULATION OF MASS TRANSFER FROM HEAD SPACE
      QO2B=KG*PI*DIA*DIA*(PO2E-PO2S)*32./4./1000./R/T/VL
```

```
PAGE   5

C IF SUM OF OC2A AND CO2B IS LARGER THAN CO2,O WAS TOO LARGE
      IF(ABS(CC2A+CO2B-DO2)-1.0E-4*DO2)3,3,2
    2 Q(1)=C(1)+GAIN1*(DO2-CO2A-CO2B)/DO2*Q(1)
      GC TC 1
C ASSUME MAXIMUM AIR FLOW IS TWICE AIR FLOW AT STEADY STATE
    3 AIRMX=2.*C(1)
      WRITE(5,101)C(1),KV(1),OO2A,PO2E,OO2B,AIRMX
  101 FORMAT (13H AIR FLOWRATEE20.5,8H M**3/HR/32H INITIAL VOL MASS TRAN
     1SFER COEFFE20.5,23H KG MOLE O2/M**3/HR/ATM/26H OXYGEN TRANSFER FRO
     2M BULKE20.5,12H GM O2/L/SEC/28H EXHAUST GAS OXYGEN PRESSUREE20.5,4
     3H ATM/26H OXYGEN TRANSFER FROM HEADE20.5,12H GM O2/L/SEC/17H MAXIM
     4UM AIR FLOWE20.5,8H M**3/HR)
      RETURN
      END

FEATURES SUPPORTED
 ONE WORD INTEGERS

CORE REQUIREMENTS FOR KOK8B
 COMMON   1896  VARIABLES      18  PROGRAM    680

RELATIVE ENTRY POINT ACCRESS IS 00C1 (HEX)

END OF COMPILATION

// DUP

*STORE      WS  UA  KOK8B
CART ID 1122   DB ADDR  4BC5   DB CNT   0031

*DELETE             KOK8C
D 26 NAME NOT FOUND IN LET/FLET

// FOR
* LIST SOURCE PROGRAM
* ONE WORD INTEGERS
C
C ******************************************************************
C
C SUBROUTINE KOK8C CALCULATES THE PROBE OUTPUT FROM THE SINGLE DIFFUSION
C LAYER WITH CENTRAL WELL CORRECTION MODEL AND THE DISSOLVED OXYGEN TENSION
C FUNCTION PO2.THE METHOD USED IS THE SAME AS IN KOK7---SUBROUTINE KOK8E
C IS REQUIRED
C
C VARIABLES---II,DTIME,TIME HAVE THE SAME MEANING AS IN KOK8
C --- CONC(1),CI=FRACTION OF TOTAL CURRENT DUE TO OXYGEN DIFFUSION FROM
C THE CENTRAL WELL AFTER ATIME SECONDS---CONC(2),CP=PROBE CONSTANT-MICRO
C AMP/ATM---CONC(3),B=DIFFUSION CONSTANT FOR LAYER-SEC**0.5---CONC(4),CR
C =PROPORTIONALITY CONSTANT BETWEEN OXYGEN PRESSURE AT A* AND RESULTANT
C CURRENT-MICROAMPS/ATM---CONC(5),BR=DIFFUSION CONSTANT FOR THE CENTRAL
C WELL-SEC**0.5---XL=CURRENT DUE TO OXYGEN DIFFUSION THROUGH LAYER-MICRO
C AMP---DUMMY,DUMM1,DUMM2,DUMM3=DUMMY VARIABLES
C
C ******************************************************************
C
      SUBROUTINE KOK8C(DUMM1)
      REAL KV(100),KG,MMU,MMUMX,KM
      COMMON KV,Q(100),PO2MU(200),PO2(900),A(10),CONC(5)
```

```
PAGE   6

      COMMON POW,CON1,VL,VM,KG,DIA,PO2G,DTIME,MMU,MMUMX,KM,CELL,YO2,DO2
      COMMON CONTG,CONTI,ERINT,AIRMX,PO2S,TTIME,ATIME,TIME,QO2A,QO2B,SO2
      COMMON PO2E,TCU,R,T,GAIN1,DUMMX
      COMMON N1,N2,N3,I1
      DATA PI/3.1415927/
      C1=CCNC(1)
      CP=CCNC(2)
      B=CCNC(3)
      CR=CCNC(4)
      BR=CCNC(5)
C CALCULATION OF FIRST PART OF THE LAYER DERIVATIVE
      DUMM1=PO2(I1)
C CALCULATION OF SECOND PART OF THE LAYER DERIVATIVE
      CALL KOKAE(B,TIME,DUMM2)
      DUMM2=DUMM2*2.*PO2(1)
      DUMM1=DUMM1+DUMM2
C CALCULATION OF THE THIRD PART OF THE LAYER DERIVATIVE
      DUMM2=0.
      I2=I1-20.*B*B/PI/PI/CTIME
      IF (I2) 1,1,2
    1 I2=2
    2 DO 10 I=I2,I1
      DUMMY=(I1+0.5-I)*DTIME
      CALL KOKAF(B,DUMMY,DUMM3)
   10 DUMM2=DUMM2+DUMM3*(PO2(I)-PO2(I-1))
      XL=(1.-C1)*CP*(DUMM1+2.*DUMM2)
C CALCULATION OF THE OXYGEN TENSION AT A*
      DUMMY=(I1-0.5)*CTIME
      DUMM1=(PO2S+PO2(1))/2./DUMMY**1.5*DTIME*EXP(-BR*BR/DUMMY)
      I2=I1-1
      IF (I1-1)4,4,3
    3 DO 20 I=1,I2
      DUMMY=(I-0.5)*CTIME
      I2=I1-I+1
      I3=I1-I
      DUMM2=(PO2(I3)+PO2(I2))/2.
   20 DUMM1=DUMM1+DUMM2/DUMMY**1.5*DTIME*EXP(-BR*BR/DUMMY)
    4 DUMM1=DUMM1*BR/SQRT(PI)
      DUMM1=(XL+CR*DUMM1)/CP
      RETURN
      END

FEATURES SUPPORTED
 ONE WORD INTEGERS

CORE REQUIREMENTS FOR KOK8C
 COMMON   1896  VARIABLES     38  PROGRAM    370

RELATIVE ENTRY POINT ADDRESS IS 0034 (HEX)

END OF COMPILATION

// DUP

*STORE      WS  UA  KOK8C
CART ID 1122   DB ADDR  4C06   DB CNT   001C

*DELETE             KOK80
```

```
PAGE   7

D 26 NAME NCT FOUND IN LET/FLET

// FOR
* LIST SOURCE PROGRAM
* ONE WORD INTEGERS
      SUBROUTINE KOK8D
      REAL MV(100),KS,MMU,MMUMX,KM
      COMMON MV,C(100),PO2MU(200),PO2(500),A(10),CONC(5)
      COMMON PCW,CON1,VL,VH,KG,DIA,PO2G,DTIME,MMU,MMUMX,KM,CELL,YO2,DO2
      COMMON CONTG,CONT1,ERINT,AIAMX,PO2S,TTIME,ATIME,TIME,OO2A,OO2B,SO2
      COMMON PO2E,IOU,R,T,GAIN1,DUMMX
      COMMON N1,N2,N3,I1
      MMU=MMUMX*(PO2(I1)+PO2(I1-1))/2./((PO2(I1)+PO2(I1-1))/2.+KM)
      DO2=MMU*CELL*YO2/3600.
      RETURN
      END

FEATURES SUPPORTED
 ONE WORD INTEGERS

CORE REQUIREMENTS FOR KOK8D
 COMMON   1876  VARIABLES       4  PROGRAM      58

RELATIVE ENTRY POINT ADDRESS IS 0008 (HEX)

END OF COMPILATION

// DUP

*STORE       WS  UA  KOK8D
CART ID 1122   DB ADDR  4C22    DB CNT    0006

*DELETE              KOK8E
D 26 NAME NCT FOUND IN LET/FLET


// FOR
* LIST SOURCE PROGRAM
* ONE WORD INTEGERS
C
C ******************************************************************
C
C SUBROUTINE KOK8E CALCULATES THE SUM OF TERMS OF AN INFINITE SERIES
C DUMMY=SIGMA(FROM N=1 TO N=INFINITY) OF EXP(-N*N*PI*PI/B/B*TIMEX)*(-1)**N
C
C ******************************************************************
C
      SUBROUTINE KOK8E(B,TIMEX,DUMMY)
      DATA PI/3.1415927/
      N=0
      I3=1
      DUMMY=0.0
    1 N=N+1
      I3=-1*I3
      TERM=I3*EXP(-N*N*PI*PI/B/B*TIMEX)
      DUMMY=DUMMY+TERM
      IF(ABS(TERM/DUMMY)-1.0E-5*ABS(DUMMY))2,2,1
```

```
PAGE   8

    2 RETURN
      END

FEATURES SUPPORTED
 ONE WORD INTEGERS

CORE REQUIREMENTS FOR KOKBE
 COMMON       0  VARIABLES      12  PROGRAM    106

RELATIVE ENTRY POINT ADDRESS IS 0012 (HEX)

END OF COMPILATION

// DUP

*STORE       WS  UA  KOKBE
CART ID 1122   DB ADDR  4C28   DB CNT   0C09

*DELETE              KOKBF
D 26 NAME NOT FOUND IN LET/FLET

// FOR
* LIST SOURCE PROGRAM
* ONE WORD INTEGERS
      SUBROUTINE KOKBF
      REAL KV(100),KG,MHU,MHUMX,KM
      COMMON KV,Q(100),PO2MU(200),PO2(500),A(10),CONC(5)
      COMMON P2W,CON1,VL,VF,KG,DIA,PO2G,DTIME,MHU,MHUMX,KM,CELL,YO2,DO2
      COMMON CONTG,CONTI,ERINT,AIRMX,PO2S,TTIME,ATIME,TIME,QO2A,QO2B,SO2
      COMMON PO2E,TGU,R,T,GAIN1,DUMMX
      COMMON N1,N2,N3,I1
      READ(2,100)(A(I),I=1,10),GAIN2
  100 FORMAT (10A4,E20.5)
      KG=KG*GAIN2
      CON1=CON1*GAIN2
      WRITE(5,101)(A(I),I=1,10),GAIN2,KG,CON1
  101 FORMAT(//721H CHANGE IN CONDITIONS//10A4,/14H MULTIPLIER 1SE20.5,/
     116H NEW VALUE OF KGE20.5,7H CM/SEC/54H NEW VALUE OF EMPIRICAL CONS
     2TANT FOR KV-G RELATIONSHIPE20.5,/1H1/40H         TIME (SECS)
     3     PO2 (ATM)//)
      DO 10 I=1,N3
   10 KV(I)=KV(I)*GAIN2
      RETURN
      END

FEATURES SUPPORTED
 ONE WORD INTEGERS

CORE REQUIREMENTS FOR KOKBF
 COMMON    1896  VARIABLES        PROGRAM    204

RELATIVE ENTRY POINT ADDRESS IS 0073 (HEX)

END OF COMPILATION

// DUP

*STORE       WS  UA  KOKBF
```

```
PAGE   9

CART ID 1122   DB ADDR  4C31   DB CNT   000E

*DELETE              KOK8G
D 26 NAME ACT FOUND IN LET/FLET


// FOR
* LIST SOURCE PROGRAM
* ONE WORD INTEGERS
      SUBROUTINE KOK8G(PO2P,DUMMY)
      REAL K/(100),KG,MMU,MMUMX,KM
      COMMON KV,Q(100),PO2MU(200),PO2(500),A(10),CONC(5)
      COMMON POW,CCN1,VL,VM,KG,DIA,PO2G,DTIME,MMU,MMUMX,KM,CELL,YO2,DO2
      COMMON CONTG,CONTI,ERINT,AIRMX,PO2S,TTIME,ATIME,TIME,QO2A,QO2B,SO2
      ERINT=ERINT+(PO2S-PO2P)*DTIME
      DUMMY=AIRMX/2.+(PO2S-PO2P)*CONTG+CONTI*ERINT
      IF (DUMMY) 1,1,2
    1 DUMMY=0.
    2 IF(DUMMY-AIRMX)4,4,3
    3 DUMMY=AIRMX
    4 RETURN
      END

FEATURES SUPPORTED
 ONE WORD INTEGERS

CORE REQUIREMENTS FOR KOK8G
 COMMON   1880  VARIABLES       4  PROGRAM      72

RELATIVE ENTRY POINT ADDRESS IS 0008 (HEX)

END OF COMPILATION

// DUP

*STORE       WS  UA  KOK8G
CART ID 1122   DB ADDR  4C3F   DB CNT   0007

*DELETE              KOK8H
D 26 NAME ACT FOUND IN LET/FLET


// FOR
* LIST SOURCE PROGRAM
* ONE WORD INTEGERS
      SUBROUTINE KOK8H
      REAL K/(100),KG,MMU,MMUMX,KM
      COMMON KV,Q(100),PO2MU(200),PO2(500),A(10),CONC(5)
      COMMON POW,CCN1,VL,VM,KG,DIA,PO2G,DTIME,MMU,MMUMX,KM,CELL,YO2,DO2
      COMMON CONTG,CONTI,ERINT,AIRMX,PO2S,TTIME,ATIME,TIME,QO2A,QO2B,SO2
      COMMON PO2E,TOU,R,T,GAIN1,DUMMX
      COMMON N1,N2,N3,I1
      DATA PI/3.1415927/
      N2=N2+1
      DUMMY=Q(1)
      DO 10 I1=N2,N1
      TIME=I1*DTIME
C CALCULATION OF Q AND KV
      NDUM1=N3-1
```

PAGE 10

```
      DO 20 I=1,NDUM1
      NDUMM=N+1-I
      C(NDUMM)=C(NDUMM-1)
   20 KV(NDUMM)=KV(NDUMM-1)*EXP(-DTIME/TOU)
C DUMMY=OUTPUT FROM CONTROLLER FROM LAST DTIME
      C(1)=DUMMY
      KV(1)=CCN1/DUMMX*(4.E+4/DIA/DIA/PI)**0.67*POW**0.95*Q(1)**0.67
C INITIAL ASSUMPTION FOR PO2(II)=PO2(II-1)
      PO2(II)=PO2(II-1)
C CALCULATION OF HOLDUP GAS OXYGEN PRESSURES
C PO2HU(1-100) CONTAIN STARTING PTS,PO2HU(101-200) CONTAIN END PTS
    1 DO 30 I=1,N3
      DUMMY=C(I)*1000./R/T/VL*EXP((I-1)*DTIME/TOU)
      PO2HU(I+100)=DUMMY*PO2HU(I)+KV(I)/2.*(PO2(II-1)+PO2(II)-PO2HU(I))
   30 PO2HU(I+100)=PO2HU(I+100)/(KV(I)/2.+DUMMY)
C CALCULATION OF OXYGEN TRANSFER RATE - QO2A
      QO2A=0.0
      DO 40 I=1,N3
   40 QO2A=QO2A+1000./112.5*Q(I)*EXP((I-1)*DTIME/TOU)/R/T/VL*(PO2HU(I)-P
     1O2HU(I+100))
C CALCULATION OF OXYGEN TRANSFER RATE FROM HEAD - QO2B
      QO2B=KG*PI/4.*DIA*DIA*32./1000./R/T/VL*(PO2E-PO2(II)/2.-PO2(II-1)/
     12.)
C CALCULATION OF OXYGEN CONSUMPTION RATE - QO2
      CALL KOKRO
C CALCULATION OF NEW VALUE OF PO2(II)
      DUMMY=PO2(II-1)+(QO2A+QO2B-QO2)*DTIME/SO2
C ADJUST ESTIMATE OF PO2(II) ACCORDING TO DIFF BETWEEN DUMMY AND PO2(II)
      IF(ABS(PO2(II)-DUMMY)-1.0E-02*PO2(II))3,3,2
    2 PO2(II)=PO2(II)+GAIN1*(DUMMY-PO2(II))
      GO TO 1
    3 PO2(II)=DUMMY
      IF(PO2(II))4,5,5
    4 PO2(II)=0.0
    5 IF(PO2(II)-PO2G)7,7,6
    6 PO2(II)=PO2G
C CALCULATION OF PROBE OUTPUT
    7 CALL KOKBC(PO2P)
C CALCULATION OF FLOWRATE DUMMY FOR NEXT TIME PERIOD
      CALL KOKBG(PO2P,DUMMY)
C CALCULATION OF HEAD GAS O2 PRESSURE FOR NEXT DTIME
      DUMM1=0.0
      DUMM2=0.0
      DO 50 I=1,N3
      DUMM3=C(I)*DTIME*TOU*(EXP((I-1)*DTIME/TOU)-EXP(-I*DTIME/TOU))
      DUMM1=DUMM1+DUMM3
   50 DUMM2=DUMM2+DUMM3*PO2HU(I+100)
      PO2E=(VH*PO2E+DUMM2)/(VH+DUMM1)
C SETTING END POINTS TO STARTING POINTS FOR PO2HU
      DO 60 I=2,N3
   60 PO2HU(I)=PO2HU(I+99)
      WRITE(5,100)TIME,PO2(II)
  100 FORMAT(2E20.5)
   10 CONTINUE
      RETURN
      END

FEATURES SUPPORTED
 ONE WORD INTEGERS
```

LIST OF SPECIFIED PARAMETERS

```
POWER INPUT PER UNIT VOLUME          0.10000E 02 HP/M**3
EMPIRICAL CONSTANT FOR Q-KV RELATION          0.63500E-01
LIQUID VOLUME          0.10000E 02 LITER
HEAD SPACE VOLUME          0.10000E 02 LITER
MASS TRANSFER COEFF HEAD TO LIQ          0.40000E-01 CM/SEC
VESSEL DIAMETER          0.25000E 02 CM
SPARGING GAS O2 PRESSURE          0.21000E 00 ATM O2
ITERATION TIME INTERVAL          0.10000E 01 SEC
MAXIMUM ORGANISM GROWTH RATE          0.10000E 00 HR**-1
M.M. CONSTANT FOR ORGANISMS          0.10000E-02 ATM O2
CELL CONCENTRATION          0.50000E 01 GM/L
OXYGEN CONSUMED PER CELLS GROWN          0.10000E 01 GM O2/GM CELLS
CONTROLLER GAIN          0.50000E 00 M**3/HR/ATM O2
CONTROLLER INTEGRATION GAIN          0.50000E-02 M**3/HR/ATM O2/SEC
SET PT FOR OXYGEN CONTROL          0.10000E 00 ATM O2
TOTAL ITERATION TIME          0.50000E 03 SEC
INITIAL STEADY-STATE PERIOD          0.10000E 03 SEC
SOLUBILITY OF OXYGEN          0.40000E-01 GM O2/L/ATM
MEAN RESIDENCE TIME OF BUBBLES IN HOLDUP          0.20000E 02 SEC
GAS CONSTANT          0.82055E-01 L-ATM/MOLE-DEG
TEMPERATURE          0.30000E 03 DEG K
GAIN1          0.10000E 00
CI          0.10000E 00
CP          0.14400E 03 MICROAMP/ATM O2
B          0.50000E 01 SEC**0.5
CR          0.15500E 02 MICROAMP/ATM O2
BR          0.12000E 01 SEC**0.5
TOTAL NUMBER OF TIME INTERVALS   500
NUMBER OF TIME INTERVALS DURING STEADY-STATE   100
NUMBER OF INTEGRATION INTERVALS   60
```

INITIAL CONDITIONS

```
OXYGEN CONSUMPTION          0.13751E-03 GM O2/L/SEC
AIR FLOWRATE          0.24945E-01 M**3/HR
INITIAL VOL MASS TRANSFER COEFF          0.18456E-01 KG MOLE O2/M**3/HR/ATM
OXYGEN TRANSFER FROM BULK          0.79687E-04 GM O2/L/SEC
EXHAUST GAS OXYGEN PRESSURE          0.12266E 00 ATM
OXYGEN TRANSFER FROM HEAD          0.57839E-04 GM O2/L/SEC
MAXIMUM AIR FLOW          0.49490E-01 M**3/HR
```

CHANGE IN CONDITIONS

```
ANTIFOAM INJECTION CAUSES DROP IN KV,KG
MULTIPLIER IS          0.80000E 00
NEW VALUE OF KG          0.31999E-01 CM/SEC
NEW VALUE OF EMPIRICAL CONSTANT FOR KV-Q RELATIONSHIP          0.50799E-01
```

TIME (SECS)	PO2 (ATM)
0.10100E 03	0.99339E-01
0.10200E 03	0.98802E-01
0.10300E 03	0.98360E-01
0.10400E 03	0.97994E-01
0.10500E 03	0.97689E-01
0.10600E 03	0.97433E-01
0.10700E 03	0.97218E-01
0.10800E 03	0.97037E-01
0.10900E 03	0.96885E-01
0.11000E 03	0.96757E-01
0.11100E 03	0.96650E-01
0.11200E 03	0.96561E-01
0.11300E 03	0.96488E-01
0.11400E 03	0.96428E-01
0.11500E 03	0.96380E-01
0.11600E 03	0.96342E-01
0.11700E 03	0.96312E-01
0.11800E 03	0.96290E-01
0.11900E 03	0.96275E-01
0.12000E 03	0.96265E-01
0.12100E 03	0.96260E-01
0.12200E 03	0.96259E-01
0.12300E 03	0.96261E-01
0.12400E 03	0.96267E-01
0.12500E 03	0.96275E-01
0.12600E 03	0.96285E-01
0.12700E 03	0.96297E-01
0.12800E 03	0.96310E-01
0.12900E 03	0.96324E-01
0.13000E 03	0.96340E-01
0.13100E 03	0.96356E-01
0.13200E 03	0.96372E-01
0.13300E 03	0.96389E-01
0.13400E 03	0.96406E-01
0.13500E 03	0.96423E-01
0.13600E 03	0.96441E-01
0.13700E 03	0.96458E-01
0.13800E 03	0.96475E-01
0.13900E 03	0.96492E-01
0.14000E 03	0.96509E-01
0.14100E 03	0.96526E-01
0.14200E 03	0.96542E-01
0.14300E 03	0.96558E-01
0.14400E 03	0.96574E-01
0.14500E 03	0.96590E-01
0.14600E 03	0.96606E-01
0.14700E 03	0.96621E-01
0.14800E 03	0.96636E-01
0.14900E 03	0.96651E-01
0.15000E 03	0.96665E-01
0.15100E 03	0.96679E-01
0.15200E 03	0.96693E-01
0.15300E 03	0.96707E-01
0.15400E 03	0.96720E-01
0.15500E 03	0.96734E-01
0.15600E 03	0.96747E-01
0.15700E 03	0.96760E-01

APPENDIX 5.1

PROGRAM KOK9

Program KOK9 calculated the oxygen tension at which the oxygen consumption rate equalled one-half the maximum consumption rate and the theoretical oxygen tension-time curve.

```
PAGE   1

// JOB

LOG DRIVE   CART SPEC   CART AVAIL   PHY DRIVE
  0000        1122        1122         0000

V2 M10   ACTUAL  8K   CONFIG  8K

// DUP

*DELETE             KOK9
D 26 NAME NOT FOUND IN LET/FLET

// FOR
* IOCS (CARD,1403 PRINTER)
* LIST SOURCE PROGRAM
* EXTENDED PRECISION
* ONE WORD INTEGERS
*NAME KOK9
C
C ****************************************************************
C
C KOK9 CALCULATES THE OXYGEN TENSION AT WHICH THE OXYGEN CONSUMPTION RATE
C EQUALS ONE-HALF THE INITIAL OXYGEN CONSUMPTION RATE.IT THEN CALCULATES
C THE OXYGEN TENSION AFTER TIME SECONDS AT INTERVALS OF DT SECONDS
C
C REAL VARIABLES---K1=M.M. CONSTANT WRT GLUCOSE-GM/L---K2=M.M. CONSTANT
C WRT OXYGEN -ATM---DT=TIME INTERVAL-SEC---PMIN=MINIMUM TENSION FOR CALCU
C LATION-ATM---PO=INITIAL OXYGEN TENSION-ATM---SO=INITIAL GLUCOSE CON'N
C -GM/L---C=SOLUBILITY OF OXYGEN-GM/L/ATM---Y=RATIO OF GLUCOSE/OXYGEN
C CONSUMPTION-GM/GM---DPDTM=MAXIMUM RATE OF OXYGEN TENSION DECREASE-ATM/
C SEC---P=OXYGEN TENSION-ATM---TIME=TIME VARIABLE-SEC---S=GLUCOSE CONCEN
C TRATION---DUMMY VARIABLES---A,B,C,D,DUMM1,DUMM2,DIFF1,DIFF2,DP,DUMMY
C
C ****************************************************************
C
      REAL K1,K2
      DO 10 II=1,4
C INITIAL DATA INPUT AND OUTPUT
      READ(2,100)DT,PMIN,PO,SO,K1,K2,Q,Y,DPDTM
  100 FORMAT(4E20.5)
      WRITE(5,101)DT,PMIN,PO,SO
  101 FORMAT(1H1,/15H TIME INCREMENTE20.5,4H SEC/12H MINIMUM PO2E20.5,4H
     1 ATM/13H STARTING PO2E20.5,4H ATM/31H STARTING GLUCOSE CONCENTRATI
     2ONE20.5,5H GM/L)
      WRITE(5,102)K1,K2,Q,Y,DPDTM
  102 FORMAT(26H M.M. CONSTANT FOR GLUCOSEE20.5,5H GM/L/25H M.M. CONSTAN
     1T FOR OXYGENE20.5,4H ATM/17H SOLUBILITY OF O2E20.5, 9H GM/L/ATM/21
     2H GLUCOSE/OXYGEN RATIOE20.5,14H GM GLUC/GM O2/14H MAXIMUM SLOPEE20
     3.5,11H ATM O2/SEC)
C CALCULATION OF INITIAL SLOPE
      DUMMY=DPDTM*SO*PO/(K1+SO)/(K2+PO)
      WRITE(5,103)DUMMY
  103 FORMAT(////14H INITIAL SLOPEE20.5,11H ATM O2/SEC)
C CALCULATION OF P AT HALF-INITIAL SLOPE
      A=SO*PO/(K1+SO)/(K2+PO)
      B=SO-Q*Y*PO
      C=Q*Y
      D=K1+B
```

PAGE 2

```
      DUMMY=SQRT((A*D+A*C*K2-2.*B)**2-4.*(A*C-2*C)*(A*D*K2))
      DUMMY=(2.*D-A*C*K2-A*D-DUMMY)/2./(A*C-2.*C)
      S=SO-C*Y*(PO-DUMMY)
      DUMM1=DPDIM*DUMMY*S/(K1+S)/(K2+DUMMY)
      WRITE(5,104)DUMMY,S,DUMM1
  104 FORMAT(24H P AT HALF-INITIAL SLOPE E20.5,4H ATM/15H GLUCOSE CONC'NE
     1E20.5,9H GM/L/ 9H SLOPE (SE20.5,8H ATM/SEC////49H     TIME (SEC)
     2   PO2 (ATM)    GLUC (GM/L)/)
C CALCULATION OF OXYGEN TENSION DECREASE
      P=PO
      TIME=0.0
      WRITE(5,105)TIME,PO,SO
      A=SO-C*Y*PO
      B=C*Y
      C=K1*Y/K2*SO-Q*Y*PC*K2
      D=Q*Y*K2*K1*SO-C*Y*PO
      DUMM1=D/B-A/B-C/A
      DUMM2=PO*C/A*ALOG(PO)+DUMM1*ALOG(A+B*PO)
    1 TIME=TIME+DT
C ASSUME PRESSURE=PREVIOUS PRESSURE
      DIFF1=P*C/A*ALOG(B)+DUMM1*ALOG(A+B*P)-DPDTM*TIME-DUMM2
      DP=-0.01*P
    2 P=P+DP
      DIFF2=P*C/A*ALOG(P) +DUMM1*ALOG(A+B*P)-DPDTM*TIME-DUMM2
C CHECKING DIFF1 AND DIFF2 FOR DIFFERENT SIGNS
      IF(ABS(ABS(DIFF1)/DIFF1+ABS(DIFF2)/DIFF2)-0.001)3,3,4
    3 P=P-DP
      DP=DP/2.
      GO TO 2
    4 TIMEX=(P*C/A*ALOG(P)+DUMM1*ALOG(A+B*P)-DUMM2)/DPDTM
      IF(ABS(TIMEX-TIME)-0.01)6,6,5
    5 DIFF1=DIFF2
      GO TO 2
    6 S=SO-C*Y*(PO-P)
      WRITE(5,105)TIME,P,S
  105 FORMAT(3F15.5)
      IF(P-PMIN)10,10,1
   10 CONTINUE
      CALL EXIT
      END

FEATURES SUPPORTED
 ONE WORD INTEGERS
 EXTENDED PRECISION
 IOCS

CORE REQUIREMENTS FOR KOK9
 COMMON       0  VARIABLES      88  PROGRAM     960

END OF COMPILATION

// DUP

*STORE        WS  UA  KOK9
CART ID 1122   DB ADDR  4C79    DB CNT   0049
```

APPENDIX 5.2

ANALYTICAL METHODS USED TO MONITOR THE CONTINUOUS CULTURE

i) The Anthrone Method For Carbohydrate Determination

The anthrone method as described by Neish [50] was used. Composition of the anthrone reagent was as follows:

Anthrone		2 gm
Distilled H_2O		50 cc
H_2SO_4	to	1000 cc

10 cc of the anthrone reagent was added to 5 cc of aqueous sample. After shaking together they were allowed to stand for 15 minutes. Transmittance in a 1 cm Pyrex cell was measured at 5400 Å (slit width 0.25 mm) in a Beckman (DB-G) spectrophotometer. The reference cell was filled with 10 cc anthrone solution with 5 cc distilled water added.

ii) Calibration and Interference With the Anthrone Method

Plots of $\log_{10}$ of the percent transmittance vs the glucose concentration in distilled water were always found to yield straight lines within experimental error for glucose concentrations in the range 0.0 to 0.20 gm/l. These plots were found not to be affected either by the addition of KH_2PO_4, NH_4Cl or any combination of the two substances up to 1/5 the concentration present of glucose for KH_2PO_4 and up to 2/5 the glucose concentration for NH_4Cl. Experiments with higher concentrations of the two substances were not performed.

Since Abe and Tabuchi [1] have reported the production of significant quantities of citric acid by *C. lipolytica* and since the pH of batch cultures was found to decrease substantially when no pH control was used, the anthrone method was checked for interference by citric acid. No change in the relationship between the transmittance and the glucose concentration could be detected at citric acid concentrations up to twice the glucose concentration over a range of 0 to 0.16 gm/l glucose.

When known amounts of glucose were added to centrifuged supernatant from a preliminary fermentation, the changes in transmittance of the supernatant were exactly in accordance with those predicted from the calibration curves.

iii) Carbohydrate Determination in Samples From the Continuous Fermentation

A 20 cc sample was obtained through the sampling port on the fermentor vessel. It was centrifuged for 10 minutes at 10,000 rpm (Sorvall Centrifuge, Model RC2-B). The supernatant was diluted with distilled water until the glucose concentration was below 0.16 gm/l. Anthrone reagent was then added to the sample, a standard of 0.0128 gm/l and distilled water to be used in the reference cell.

iv) Dry Weight Determination in Samples From the Continuous Fermentation

10 cc of fermentation broth was filtered through a preweighed 0.8 micron Millipore filter. The residue was washed with 10 cc of distilled water. The filter and residue were placed in an aluminum weighing dish and dried in an oven at 75°C for 24 hours.

v) Checks on the Dry Weight Determination Method

Millipore filters when wetted with distilled water and dried for 24 hours at 75°C showed a loss in weight approximately equal to the accuracy of the balance used (0.5 mg). Duplicate samples always yielded dry weights within 3% of each other.

vi) pH Measurement

The pH of the fermentor contents was measured by obtaining a 25 cc sample and immediately measuring its pH (Fisher Accumet, Model 220).

APPENDIX 5.3

RESULTS FROM THE DRY WEIGHT, CARBOHYDRATE AND pH ANALYSES FOR FERMENTATION 1

TIME (HOURS AFTER INOCULATION)	SAMPLE #	CARBOHYDRATE CONCENTRATION (AS mg/l Glucose)	DRY WEIGHT CONCENTRATION (gm/l)	pH
94.5	1	44.5	0.96	5.2
96.5	2	40.1	0.97	5.3
98.5	3	34.8	1.00	5.2
100.5	4	38.8	1.01	5.3
118.5	5	38.6	0.98	5.3
120.5	6	38.6	0.95	5.3
122.5	7	35.8	0.94	5.4
124.5	8	37.3	0.81	5.4
142.5	9	39.5	0.78	5.4
144.5	10	38.6	0.83	5.3
146.5	11	37.3	0.81	5.4
148.5	12	38.6	0.81	5.3
166.5	13	40.1	0.81	5.3
168.5	14	40.1	0.89	5.3
170.5	15	40.3	0.84	5.3
172.5	16	40.1	0.68	5.4
190.5	17	N.A.*	N.A.	5.5
192.5	18	N.A.	1.10	5.3
194.5	19	38.9	1.10	5.3
196.5	20	40.3	1.06	5.3
214.5	21	44.5	1.22	5.4
216.5	22	43.1	1.26	5.4
218.5	23	41.2	1.29	5.4
220.5	24	38.8	1.30	5.3

TIME (HOURS AFTER INOCULATION)	SAMPLE #	CARBOHYDRATE CONCENTRATION (As mg/l glucose)	DRY WEIGHT CONCENTRATION (gm/l)	pH
238.5	25	35.0	1.39	5.4
240.5	26	37.6	1.39	5.5
242.5	27	36.3	1.22	5.4
244.5	28	41.7	1.21	5.3
262.5	29	41.3	1.26	5.3
264.5	30	40.1	1.32	5.3
266.5	31	40.3	1.25	5.2
268.5	32	38.8	1.38	5.3
286.5	33	43.1	1.44	5.4
288.5	34	40.1	1.50	5.3
290.5	35	40.3	1.54	5.3
292.5	36	40.3	1.51	5.3
310.5	37	38.8	1.56	5.3
312.5	38	37.5	1.46	5.4
314.5	39	40.3	1.51	5.4
316.5	40	38.9	1.53	5.3
334.5	41	37.6	1.62	5.4
336.5	42	36.3	1.52	5.5
338.5	43	37.6	1.55	5.5
340.5	44	40.3	1.62	5.4
358.5	45	34.8	1.30	5.5
360.5	46	36.3	1.36	5.5
362.5	47	36.3	1.36	N.A.
364.5	48	37.6	1.32	N.A.
382.5	49	41.6	1.14	N.A.
384.5	50	38.8	1.14	N.A.
386.5	51	34.9	1.18	N.A.
388.5	52	37.5	1.14	N.A.
406.5	53	37.6	1.08	N.A.
408.5	54	33.8	1.29	N.A.
410.5	55	33.7	1.20	N.A.

TIME (HOURS AFTER INOCULATION)	SAMPLE #	CARBOHYDRATE CONCENTRATION (As mg/l glucose)	DRY WEIGHT CONCENTRATION (gm/l)	pH
412.5	56	32.6	1.40	N.A.
430.5	57	38.8	1.51	N.A.
432.5	58	40.1	1.61	N.A.
434.5	59	37.3	1.54	N.A.
436.5	60	38.8	1.60	N.A.
454.5	61	38.8	1.42	5.4
456.5	62	38.9	1.28	5.4
458.5	63	37.6	1.29	5.4
460.5	64	40.3	1.37	5.4
478.5	65	39.0	1.17	5.4
480.5	66	43.1	1.18	5.3
482.5	67	41.7	1.25	5.4
484.5	68	40.3	1.25	5.4
502.5	69	41.7	1.18	5.4
504.5	70	43.1	1.15	5.2
506.5	71	40.3	1.11	5.4
508.5	72	41.7	1.14	5.3
526.5	73	43.1	1.19	5.5
528.5	74	46.0	1.24	5.4
530.5	75	43.1	1.21	5.4
532.5	76	44.5	1.15	5.4
550.5	77	49.0	1.13	5.4
552.5	78	44.6	1.20	5.4
554.5	79	41.7	1.26	5.4
556.5	80	43.1	1.21	5.3
574.5	81	46.0	1.19	5.3
576.5	82	44.6	1.14	5.1
578.5	83	44.6	1.17	5.2
580.5	84	40.3	1.21	5.2
598.5	85	41.7	1.23	5.4
600.5	86	43.1	1.28	5.4

TIME (HOURS AFTER INOCULATION)	SAMPLE #	CARBOHYDRATE CONCENTRATION (As mg/l glucose)	DRY WEIGHT CONCENTRATION (gm/l)	pH
602.5	87	43.1	1.26	5.5
604.5	88	43.1	1.30	5.3
622.5	89	38.9	1.24	5.4
624.5	90	40.3	1.29	5.4
626.5	91	40.1	1.26	5.4
628.5	92	40.3	1.26	5.3
646.5	93	37.6	1.21	5.3
648.5	94	37.6	1.22	5.2
650.5	95	40.3	1.17	5.1
652.5	96	40.3	1.23	5.1
670.5	97	38.8	1.30	5.2
672.5	98	36.3	1.30	5.2
674.5	99	37.6	1.34	5.1
676.5	100	37.6	1.40	5.2
694.5	101	44.5	1.75	5.4
696.5	102	46.1	1.79	5.4
698.5	103	43.1	1.80	5.3
700.5	104	43.1	1.87	5.3
718.5	105	40.3	1.80	5.4
720.5	106	41.7	1.78	5.4
722.5	107	49.0	1.73	5.3
724.5	108	41.7	1.76	5.4
742.5	109	54.0	1.93	5.4
744.5	110	43.1	1.78	5.3
746.5	111	41.7	1.89	5.4
748.5	112	41.7	1.87	5.1
766.5	113	38.8	1.86	5.2
768.5	114	38.9	1.88	5.3
770.5	115	40.3	1.89	5.3
772.5	116	41.6	1.92	5.3
790.5	117	43.1	1.90	5.3
792.5	118	37.6	1.87	5.3

TIME (HOURS AFTER INOCULATION)	SAMPLE #	CARBOHYDRATE CONCENTRATION (As mg/l glucose)	DRY WEIGHT CONCENTRATION (gm/l)	pH
794.5	119	40.3	1.89	5.2
796.5	120	39.0	1.98	5.2
814.5	121	38.9	1.74	5.2
816.5	122	38.8	1.81	5.1
818.5	123	36.1	1.76	5.2
820.5	124	38.8	1.81	5.2
838.5	125	36.9	1.65	5.3
840.5	126	33.7	1.71	5.3
842.5	127	34.8	1.71	5.2
844.5	128	N.A.	N.A.	N.A.
862.5	129	34.6	1.62	5.3
864.5	130	36.0	1.69	5.3
866.5	131	33.7	1.64	5.2

* N.A. - Not Available

APPENDIX 5.4

PROGRAM KOK10

Program KOK10 and its subroutines performed the following functions:

- Tabulation and checking of probe current-time data
- Calculation of the sixth-order least-square polynomials through the probe current-time data (for probe currents below 1 microamp).
- Calculation of the probe current at which the slope of the fitting polynomials was one-half the maximum slope of the observed probe current-time curve
- Calculation of the numerical derivatives of the probe current-time data below probe currents of 1 microamp
- The least-square hyperbolas and least-square sixth-order polynomials through the numerical derivatives
- Calculation of the probe current at which the numerical derivative was one-half the maximum slope of the observed probe current-time curve from the least-square hyperbola and fitting polynomial of the numerical derivatives.

```
PAGE   1

// JOB

LOG DRIVE   CART SPEC   CART AVAIL  PHY DRIVE
  0000        1122        1122        0000

V2 M10.  ACTUAL  8K  CONFIG  8K

// DUP

*DELETE              POLY
CART ID 1122   DB ADDR  4955   DB CNT   0012

// FOR
* LIST SOURCE PROGRAM
* ONE WORD INTEGERS
C       ROBERT KCK
        SUBROUTINE POLY(N1,N,X,Y,A)
C A LEAST SQUARES APPROXIMATION FOR A POLYNOMIAL OF DEGREE N WITH N1 PTS
C X IS VECTOR OF INDEPENDENT VARIABLE, Y OF DEPENDENT VARIABLE,A IS OUTP
C UT VECTOR OF DEGREE N+1 OF COEFFICIENTS
        DIMENSION X(1),Y(1),A(1),S(400)
        NP1 =N+1
        DO 2 I=1,400
      2 S(I)=0.0
        DO 6 I=1,20
      6 A(I)=0.0
        DO 4 K=1,N1
        P1 = 1.0
        DO 4 I=1,NP1
        P2 = 1.0
        DO 3 J=1,I
        K1=(J-1)*NP1+I
        S(K1)=S(K1)+P1*P2
      3 P2 = P2*X(K)
        A(I)=A(I)+P1*Y(K)
      4 P1 = P1*X(K)
        DO 5 I=1,NP1
        DO 5 J=1,I
        K2=(I-1)*NP1+J
        K3=(J-1)*NP1+I
      5 S(K2)=S(K3)
        CALL SIMQ (S,A,NP1,0)
        RETURN
        END

FEATURES SUPPORTED
 ONE WORD INTEGERS

CORE REQUIREMENTS FOR POLY
 COMMON     0  VARIABLES    814  PROGRAM    258

RELATIVE ENTRY POINT ADDRESS IS 0336 (HEX)

END OF COMPILATION

// DUP

*STORE      WS  UA  POLY
```

```
CART ID 1122   DB ADDR  4CB0   DB CNT  '0012

*DELETE            KO10A
D 26 NAME NOT FOUND IN LET/FLET

// FOR
* LIST SOURCE PROGRAM
*ONE WORD INTEGERS
C
C ******************************************************************
C
C SUBROUTINE KO10A CALCULATES THE LEAST-SQUARE HYPERBOLA OF Y VS X BY
C HOHMANN'S (1972) METHOD FOR II POINTS---HYPERBOLA HAS FORM Y=(A+BX)/(1
C .0+CX)
C
C VARIABLES---S1,S2 ETC CONTAIN SUMS---SA,SB,SC,SD HAVE MEANING AS SHOWN
C BELOW---A,B,C ARE IN COEFF
C
C ******************************************************************
C
      SUBROUTINE KO10A(II,X,Y,COEFF)
      DIMENSION X(1),Y(1),COEFF(3)
      S1=0.0
      S2=0.0
      S3=0.0
      S4=0.0
      S5=0.0
      S6=0.0
      S7=0.0
      DO 10 I=1,II
      S1=S1+X(I)*X(I)
      S2=S2+X(I)
      S3=S3+X(I)*X(I)*Y(I)
      S4=S4+X(I)*X(I)*Y(I)*Y(I)
      S5=S5+X(I)*Y(I)
      S6=S6+X(I)*Y(I)*Y(I)
   10 S7=S7+Y(I)
      SA=II*(S1*S3-S1*S4)+S2*(S2*S4-S5*S3)+S5*(S1*S5-S2*S3)
      SB=S1*(S5*S6-S7*S4)+S5*(S2*S4-S5*S3)+S3*(S7*S3-S2*S6)
      SC=II*(S3*S6-S5*S4)+S2*(S7*S4-S5*S6)+S5*(S5*S5-S7*S3)
      SD=II*(S1*S6-S5*S3)+S2*(S7*S3-S2*S6)+S5*(S2*S5-S1*S7)
      COEFF(1)=SB/SA
      COEFF(2)=SC/SA
      COEFF(3)=SD/SA
      RETURN
      END

FEATURES SUPPORTED
 ONE WORD INTEGERS

CORE REQUIREMENTS FOR KO10A
 COMMON      0  VARIABLES     38  PROGRAM    400

RELATIVE ENTRY POINT ADDRESS IS 0029 (HEX)

END OF COMPILATION

// DUP
```

```
PAGE   3

*STORE      WS  UA  K010A
CART ID 1122   DB ADDR  4CC2   DB CNT   0021

*DELETE              K010B
D 26 NAME NOT FOUND IN LET/FLET


// FOR
* LIST SOURCE PROGRAM
* ONE WORD INTEGERS
C
C ********************************************************************
C
C SUBROUTINE K010B FINDS THE VALUE OF A POLYNOMIAL OF ORDER NO HAVING THE
C COEFFICIENT VECTOR COEFF FOR THE ARGUMENT X
C
C ********************************************************************
C
      SUBROUTINE K010B(X,COEFF,NO)
      DIMENSION COEFF(1)
      DUMMY=COEFF(1)
      DUMM1=1.0
      DO 10 I=1,NO
      DUMM1=DUMM1*X
   10 DUMMY=DUMMY+DUMM1*COEFF(I+1)
      X=DUMMY
      RETURN
      END

FEATURES SUPPORTED
 ONE WORD INTEGERS

CORE REQUIREMENTS FOR K010B
 COMMON       0  VARIABLES       6  PROGRAM      62

RELATIVE ENTRY POINT ADDRESS IS 0009 (HEX)

END OF COMPILATION

// DUP

*STORE      WS  UA  K010B
CART ID 1122   DB ADDR  4CE3   DB CNT   0006

*DELETE              K010C
D 26 NAME NOT FOUND IN LET/FLET


// FOR
* LIST SOURCE PROGRAM
* ONE WORD INTEGERS
C
C ********************************************************************
C
C SUBROUTINE K010C FINDS THE ARGUMENT FOR THE VALUE Y OF A POLYNOMIAL
C OF ORDER NO WITH COEFFICIENT VECTOR COEFF BY HALVING OF THE INTERVAL--
C INITIAL TRIAL ARGUMENT IS XI---INITIAL INTERVAL IS DX
C
C ********************************************************************
```

```
PAGE   4
C
      SUBROUTINE KO10C(Y,NO,COEFF,XI,DX)
      DIMENSION COEFF(1)
      II=1
      DUMMY=XI
      CALL KO10B(DUMMY,COEFF,NO)
      DIFF1=Y-DUMMY
    1 XI=XI+DX
      II=II+1
      IF(II-1000)6,6,7
    7 WRITE(5,100)Y,DIFF1
  100 FORMAT(//21H II GREATER THAN 1000/15H DESIRED SLOPE=E20.5,/10H DIF
     1F1 WAS=E20.5,//)
      GC TC 5
    6 CUMMY=XI
      CALL KC10B(DUMMY,COEFF,NO)
      CIFF2=Y-DUMMY
C DETERMINE SIZE OF DIFF2 WRT Y
      IF(ABS(CIFF2)-1.0E-04*ABS(Y))5,5,2
C DETERMINE IF DIFF1,CIFF2 ARE SAME SIGN
    2 IF(ABS(ABS(DIFF1)/DIFF1+ABS(DIFF2)/DIFF2)-0.001)3,3,4
    3 XI=XI-DX
      CX=CX/2.
      GO TO 1
    4 DIFF1=DIFF2
      GC TO 1
    5 Y=XI
      RETURN
      END

FEATURES SUPPORTED
 ONE WORD INTEGERS

CORE REQUIREMENTS FOR KO10C
 COMMCN       0  VARIABLES      12  PROGRAM     20C

RELATIVE ENTRY POINT ADDRESS IS 0C39 (HEX)

END OF COMPILATION

// DUP

*STCRE      WS  UA  KO10C
CART ID 1122   DB ADDR  4CE9  DB CNT   000F

*DELETE                KOK10
D 26 NAME NCT FOUND IN LET/FLET

// FCR
* IOCS (CARD,1403 PRINTER)
* LIST SOURCE PROGRAM
* CNE WCRC INTEGERS
*NAME KOK10
C
C ***************************************************************
C
C KOK10 ANC SUBS PERFORM THE FOLLOWING FUNCTIONS
```

PAGE 5

```
C 1-TABULATE AND CHECK DATA FOR ERRORS
C 2-CALCULATES POLYNOMIAL OF ORDER NO THROUGH DATA LESS THAN 1 MICROAMP
C 3-CALCULATES CURRENT AT WHICH SLOPE OF POLYNOMIAL=SLOMX/2
C CALCULATES NUMERICAL DERIVATIVES OF DATA BELOW 1 MICROAMP
C 5-FITS LEAST-SQUARE HYPERBOLA AND FIND CURRENT AT SLOMX/2
C 6-FITS POLYNOMIAL OF ORDER NO AND FINDS CURRENT AT SLOMX/2
C
C SUBROUTINES REQUIRED---POLY TO FIND POLYNOMIAL COEFFICIENTS---K010A TO
C FIND HYPERBOLA FITTING COEFFICIENTS---K010B TO FIND VALUE OF POLYNOMIAL
C FOR A GIVEN ARGUMENT---K010C FINDS ARGUMENT FOR A VALUE OF A POLYNOMIAL
C
C VECTORS---DIST=DISTANCE ON CHART-MM-TIME EQUIVALENT---CURR=CURRENT-OXY
C GEN TENSION EQUIVALENT-MICROAMPS---AA=ERROR VECTOR---CURRH=CURRENTS AT
C MIDPOINTS OF DATA-MICROAMPS---SLOPE=DERIVATIVES-MICROAMPS/MM---COEFA=
C COEFFICIENTS FOR HYPERBOLA---COEFB=COEFFICIENTS FOR POLYNOMIAL---COEFC=
C COEFFICIENT FOR DERIVATIVE OF POLYNOMIAL---A=SYMBOL STORAGE VECTOR
C
C REAL VARIABLES---SLOMX=MAXIMUM SLOPE OF CURVE-MICROAMPS/MM---N4=CURVE
C IDENTIFIER
C
C INTEGER VARIABLES---N1=NO. OF DATA SETS TO BE TREATED---NO=ORDER OF
C FITTING POLYNOMIALS---N2=NO. OF POINTS IN A SET
C
C DUMMY VARIABLES---DUMMY,DUMM1,I1,N3,I,I2
C
C ******************************************************************
C
      REAL N4
      DIMENSION DIST(100),CURR(100),AA(100),CURRH(100),SLOPE(100)
      DIMENSION COEFB(20),COEFC(20),A(3),COEFA(3)
C READ IN OVERALL RUN DATA
      READ(2,100)N1,A,NO
  100 FORMAT(I5,3A4,I5)
      WRITE(5,101)N1,A,NO
  101 FORMAT(1H1,12H NO. OF SETSI5,/17H SYMBOLS USED ARE3A4,/29H ORDER O
     1F FITTING POLYNOMIALSI5,/)
      DO 10 I1=1,N1
C READ IN DATA FOR THIS SET
      READ(2,102)N2,N3,N4,SLOMX
  102 FORMAT(2I5,6X,A4,E20.5)
      WRITE(5,103)N3,N4,N2,SLOMX
  103 FORMAT(1H1,10H CURVE NO.I5,A4,/19H NUMBER OF DATA PTSI5,/14H MAXIM
     1UM SLOPEF16.5,12H MICROAMP/MM///38H   DIST-MM CUR MIC-A  ERROR    P
     2OLY CUR//)
      READ(2,104)(DIST(I),CURR(I),I=1,N2)
  104 FORMAT(4(F10.0,F10.3))
C CHECKING FOR PUNCHING ERRORS
      DO 20 I=1,N2
   20 AA(I)=A(2)
      DO 30 I=2,N2
      IF(DIST(I)-DIST(I-1))1,1,2
    1 AA(I)=A(1)
    2 IF(CURR(I)-CURR(I-1))30,30,3
    3 AA(I)=A(1)
   30 CONTINUE
C ELIMINATING D-CURVES FROM FITTING PROCEDURE
      IF(N4-A(3))5,4,5
    4 N5=N2+1
      GO TO 6
```

```
C FINDING CURR(I) SMALLER THAN 1 MICROAMP
    5 DC 40 I=1,N2
      IF(CURR(I)-1.0)6,6,40
    6 N5=I
      GC TC 7
   40 CONTINUE
C CURRH,SLOPE ARE USED FOR TEMPORARY STORAGE
    7 DC 50 I=N5,N2
      N3=I-N5+1
      CURRH(N3)=CURR(I)
   50 SLOPE(N3)=DIST(I)
C FINDING COEFFICIENTS OF LEAST SQUARE POLYNOMIAL
      CALL POLYIN(N3,NO,SLOPE,CURRH,COEFB)
C WRITING OUT DATA,ERRORS AND POLYNOMIAL FIT
    8 N3=N5-1
      WRITE(5,105)(DIST(I),CURR(I),AA(I),I=1,N3)
  105 FORMAT(F10.1,F10.4,2X,A4)
      IF(A4-A(2))9,10,9
C CALCULATION OF POLYNOMIAL FIT
    9 DO 60 I=N5,N2
      DUMMY=DIST(I)
      CALL KOIOR(DUMMY,COEFB,NO)
   60 WRITE(5,106)DIST(I),CURR(I),AA(I),DUMMY
  106 FORMAT(F10.1,F10.4,2X,A4,2X,F10.4)
C PRINTING OF POLYNOMIAL COEFFICIENTS
      WRITE(5,107)
  107 FORMAT(///39H COEFFICIENTS OF FITTING POLYNOMIAL ARE/)
      N3=NO+1
      DC 70 I=1,N3
   70 WRITE(5,108)I,COEFB(I)
  108 FORMAT(7H COEFB(I2,2H)=E20.5)
C CALCULATION OF DERIVATIVE OF POLYNOMIAL
      DC 80 I=1,NO
   80 COEFC(I)=I*COEFB(I+1)
C PRINTING OF DERIVATIVE POLYNOMIAL COEFFICIENTS
      WRITE(5,109)
  109 FORMAT(///42H COEFFICIENTS OF DERIVATIVE POLYNOMIAL ARE/)
      DC 90 I=1,NO
   90 WRITE(5,208)I,COEFC(I)
  208 FORMAT(7H COEFC(I2,2H)=E20.5)
C FINDING CURR AT WHICH DCURR/DDIST=SLOMX/2.
      DUMMY=-SLOMX/2.
      N3=NO-1
      DUMM1=DIST(N2)
      DX=-5.0
      CALL KOIGC(DUMMY,N3,COEFC,DUMM1,DX)
      DUMM1=DUMMY
      CALL KOIOR(DUMMY,COEFB,NO)
      WRITE(5,111)DUMM1,DUMMY
  111 FORMAT(///28H POINT OF HALF-MAXIMAL SLOPE/ 9H DISTANCEF10.2,3H MM/
     18H CURRENTF10.4,9H MICROAMP///45H          CURRH          SLOPE
     2  POLY SLOPE/)
C FINDING DERIVATIVES AND MIDPOINTS
      N2=N2-1
      I2=NO-1
      DC 110 I=N5,N2
      N3=I-N5+1
      CURRH(N3)=(CURR(I)+CURR(I+1))/2.
```

```
      SLOPE(N3)=(CURR(I)-CURR(I+1))/(DIST(I+1)-DIST(I))
      DUMMY=(DIST(I)+DIST(I+1))/2.
      CALL KOIOB(DUMMY,COEFC,I2)
      DUMMY=-DUMMY
  110 WRITE(5,112)CURRH(N3),SLOPE(N3),DUMMY
  112 FORMAT(3F15.5)
C FINDING LEAST-SQUARES HYPERBOLA
      CALL KOIOA(N3,CURRH,SLOPE,COEFA)
C FINDING HALF-MAXIMAL SLOPE CURRENT
      DUMMY=(COEFA(1)-SLOMX/2.)/(SLOMX/2.*COEFA(3)-COEFA(2))
      WRITE(5,113)COEFA,DUMMY
  113 FORMAT(///30H COEFFICIENTS OF THE HYPERBOLA/3(/E15.5),//30H CURREN
     1T AT HALF-MAXIMAL SLOPE/F15.5,///40H      CURRH             SLOPE     C
     2ALCC SLOPE/)
C CALCULATION OF HYPERBOLIC FIT
      DO 120 I=1,N3
      DUMMY=(COEFA(1)+COEFA(2)*CURRH(I))/(1.0+COEFA(3)*CURRH(I))
  120 WRITE(5,114)CURRH(I),SLOPE(I),DUMMY
  114 FORMAT(F10.4,2E15.5)
C CALCULATION OF POLYNOMIAL FIT
      CALL POLY(N3,NO,CURRH,SLOPE,COEFB)
C WRITING OF POLYNOMIAL COEFFICIENTS
      WRITE(5,115)
  115 FORMAT(///43H COEFFICIENTS OF THE FITTING POLYNOMIAL ARE/)
      N5=NO+1
      DO 130 I=1,N5
  130 WRITE(5,108)I,COEFB(I)
C FINDING CURR AT HALF-MAXIMAL SLOPE
      DUMMY=SLOPX/2.
      DUMM1=CURRH(N3)
      DX=0.01
      CALL KOIOC(DUMMY,NO,COEFB,DUMM1,DX)
      WRITE(5,116)DUMMY
  116 FORMAT(///30H CURRENT AT HALF-MAXIMAL SLOPE/E20.5,///40H      CURRH
     1              SLOPE      POLY SLOPE//)
      DO 140 I=1,N3
      DUMMY=CURRH(I)
      CALL KOIOB(DUMMY,COEFB,NO)
  140 WRITE(5,114)CURRH(I),SLOPE(I),DUMMY
   10 CONTINUE
      CALL EXIT
      END

FEATURES SUPPORTED
 ONE WORD INTEGERS
 IOCS

CORE REQUIREMENTS FOR KOK10
 COMMON      0  VARIABLES    1116  PROGRAM    1320

END OF COMPILATION

// DUP

*STORE      WS  UA  KOK10
CART ID 1122   DB ADDR  4CF8   DB CNT   0058
```

APPENDIX 5.5

RESULTS FROM THE DRY WEIGHT, CARBOHYDRATE AND pH ANALYSES FOR FERMENTATION 2

TIME (HOURS AFTER INOCULATION)	SAMPLE #	CARBOHYDRATE CONCENTRATION (As mg/l glucose)	DRY WEIGHT CONCENTRATION (gm/l)	pH
21.3	1	N.A.*	0.51	5.2
23.0	2	N.A.	0.52	5.3
25.0	3	N.A.	0.58	5.1
27.0	4	N.A.	0.68	5.0
45.0	5	38.3	1.29	5.2
47.0	6	32.5	1.27	5.2
49.0	7	33.6	1.33	5.2
51.0	8	35.0	1.36	5.2
69.0	9	42.6	1.44	5.3
71.0	10	39.8	1.43	5.3
73.0	11	40.1	1.38	5.3
75.0	12	41.0	1.37	5.3
93.1	13	39.5	0.98	5.3
95.0	14	N.A.	0.99	5.3
97.0	15	37.2	1.03	5.3
99.0	16	N.A.	0.96	5.3
117.0	17	38.6	0.97	5.2
119.0	18	37.5	0.99	5.3
121.0	19	37.5	1.00	5.2
123.0	20	36.9	1.02	5.2
141.0	21	37.6	1.25	5.2
143.0	22	33.5	1.23	5.2
145.0	23	33.7	1.27	5.2
147.0	24	33.7	1.27	5.1
165.0	25	36.0	1.29	5.3

TIME (HOURS AFTER INOCULATION)	SAMPLE #	CARBOHYDRATE CONCENTRATION (As mg/l glucose)	DRY WEIGHT CONCENTRATION (gm/l)	pH
167.0	26	36.9	1.31	5.3
169.0	27	34.8	1.28	5.2
171.0	28	35.4	1.32	5.2
189.0	29	38.2	1.27	5.2
191.0	30	37.5	1.32	5.1
193.0	31	37.5	1.32	5.2
195.0	32	38.8	1.35	5.2
213.0	33	38.2	1.46	5.2
215.0	34	36.9	1.57	5.2
217.0	35	38.9	1.51	5.2
219.0	36	37.6	1.40	5.3
237.0	37	N.A.	1.20	5.3
239.0	38	N.A.	1.24	5.2
241.0	39	37.6	1.21	5.2
242.5	40	47.1	1.41	5.1
261.0	41	41.6	1.43	5.2
263.0	42	48.1	1.49	5.2
265.0	43	43.7	1.48	5.2
267.0	44	41.3	1.49	5.0
285.0	45	N.A.	1.32	5.2
287.0	46	42.7	1.35	5.1
289.0	47	43.8	1.35	5.1
291.0	48	43.1	1.41	5.1
309.0	49	42.3	1.47	5.1
311.0	50	43.0	1.45	5.0
313.0	51	44.1	1.51	5.1
315.0	52	39.9	1.56	5.1
333.0	53	43.0	1.50	5.2
335.0	54	44.1	1.52	5.2
337.0	55	44.1	1.49	5.1
339.0	56	43.8	1.61	5.1
357.0	57	44.4	1.49	5.1
359.0	58	41.7	1.49	5.1

TIME (HOURS AFTER INOCULATION)	SAMPLE #	CARBOHYDRATE CONCENTRATION (As mg/l glucose)	DRY WEIGHT CONCENTRATION (gm/l)	pH
361.0	59	42.3	1.49	5.1
363.0	60	42.3	1.51	5.1
381.0	61	42.4	1.30	5.0
383.0	62	42.4	N.A.	5.0
385.0	63	40.9	1.29	5.0
387.0	64	41.6	1.31	5.0
405.0	65	43.0	1.21	5.2
407.0	66	37.9	1.24	5.1
409.0	67	N.A.	1.24	5.2
411.0	68	38.8	1.34	5.1
429.0	69	40.9	1.21	5.2
431.0	70	38.0	1.20	5.2
433.0	71	40.2	1.20	5.2
434.5	72	37.5	1.12	5.1
453.0	73	37.0	1.13	5.1
455.0	74	36.3	1.08	5.1
457.0	75	38.0	1.12	5.1
459.0	76	36.2	1.06	5.1
477.0	77	33.2	1.09	5.1
479.0	78	34.4	1.01	5.0
481.0	79	34.4	1.14	5.0
483.0	80	34.0	1.11	5.1
501.0	81	35.1	1.14	5.1
503.0	82	38.9	1.14	5.0
506.0	83	37.5	1.22	5.1
508.0	84	N.A.	N.A.	N.A.
525.0	85	36.7	1.24	5.0
527.0	86	35.6	1.18	5.0
529.0	87	36.8	1.27	5.0
531.0	88	33.7	1.23	5.0
549.0	89	34.5	1.22	5.0

TIME (HOURS AFTER INOCULATION)	SAMPLE #	CARBOHYDRATE CONCENTRATION (As mg/l glucose)	DRY WEIGHT CONCENTRATION (gm/l)	pH
551.0	90	36.3	1.24	5.0
553.0	91	37.3	1.31	5.0
554.3	92	37.5	1.37	5.0
573.0	93	47.4	1.72	5.0
575.0	94	45.2	1.58	5.1
577.0	95	41.6	1.52	5.0
579.0	96	45.9	1.56	5.0
597.0	97	47.1	1.59	5.1
599.0	98	45.9	1.38	5.1
601.0	99	45.2	1.55	5.0
603.0	100	46.0	1.59	5.0
621.0	101	46.1	1.44	5.0
623.0	102	42.3	1.53	5.0
625.0	103	43.0	1.51	5.0
627.0	104	45.8	N.A.	5.0
645.0	105	55.8	1.50	5.0
647.0	106	45.0	1.48	5.0
648.3	107	45.0	1.43	5.0
657.0	108	43.0	1.54	5.1
669.0	109	59.4	1.40	5.1
671.0	110	42.9	1.44	5.0
673.0	111	40.1	1.37	5.0
674.4	112	40.7	1.36	5.1
693.0	113	38.3	1.38	5.1
695.0	114	36.3	1.39	5.1
697.0	115	38.9	1.38	5.1
699.0	116	36.3	1.36	5.1
717.0	117	32.0	1.22	5.1
719.0	118	35.0	1.25	5.0
721.0	119	36.9	1.23	5.0
723.0	120	38.9	1.30	5.0

TIME (HOURS AFTER INOCULATION)	SAMPLE #	CARBOHYDRATE CONCENTRATION (As mg/l glucose)	DRY WEIGHT CONCENTRATION (gm/l)	pH
741.0	121	32.2	1.07	5.1
743.0	122	35.8	1.18	5.2
745.0	123	34.1	1.11	5.1
747.0	124	40.1	1.23	5.1
765.0	125	39.5	1.31	5.1
767.0	126	39.2	1.28	5.1
769.0	127	47.4	1.38	5.1
771.0	128	35.9	1.37	5.1
784.0	129	42.3	1.37	5.1
786.0	130	38.3	1.31	5.0
788.0	131	38.3	1.44	5.1
789.0	132	37.0	1.37	5.1
808.0	133	37.6	1.35	5.1
810.0	134	38.9	1.40	5.1
812.0	135	36.3	1.44	5.1

REFERENCES

1. Abe, M., T. Tabuchi. Occurrence of Biologically Active Isocitric Acid in Cultures of Yeast. *Agricultural and Biological Chemistry*, 32(3), pp. 392-3 (1968).

2. Aiba, S., S.Y. Huang. Membrane-Covered Electrode. *J. Ferment. Tech.*, 47(6), pp. 372-81 (1969).

3. Aiba, S., A.E. Humphrey, H.F. Millis. *Biochemical Engineering*. Academic Press (1965), N.Y.

4. Aiba, S., M. Ohashi, S.Y. Huang. Rapid Determination of Oxygen Permeability of Polymer Membranes. *Ind. Eng. Chem.; Fund.*, 7(3), pp. 497-502 (1968).

5. Anonymous. *Journal of Teflon*. (Jan-Feb. 1970) pp. 3-4. (E.I. Du Pont de Nemours & Co.).

6. Arnold, B.H., R. Steel. Oxygen Supply and Demand in Aerobic Fermentations. *Biochemical Engineering* (R. Steel ed.). London and Heywood & Co. Ltd. (1958).

7. Babij, T., F.J. Moss, B.J. Ralph. Effects of Oxygen and Glucose Levels on Lipid Composition of Yeast *Candida utilis* Grown in Continuous Culture. *Biotech. Bioeng.*, 11, pp. 593-603 (1969).

8. Baumberger, J.P. The Relationship Between Oxidation-Reduction Potential and the Oxygen Consumption Rate of Yeast Cell Suspensions. *Cold Springs Harbour Symp. Quant. Biol.*, 7, pp. 195-215 (1939).

9. Bellman, R.E., R.E. Kalaba, J. Lockett. *Numerical Inversion of the Laplace Transform*. Elsevier, N.Y. (1966).

10. Benedek, A.A., W.J. Heideger. Polarographic Oxygen Analyzer Response; The Effect of Instrument Lag in the Nonsteady-State Reaeration Test. *Water Res.*, 4(9), pp. 627-40 (1970).

11. Boelter, L.M.K., V.H. Cherry, H.A. Johnson, R.C. Martinelli. *Heat Transfer Notes.* McGraw-Hill, N.Y. (1965).

12. Borkowski, J.D., M.J. Johnson. Long-Lived Steam-Sterilizable Membrane Probes For Dissolved Oxygen Measurement. *Biotechnol. Bioeng.*, 9(4), pp. 635-9 (1967).

13. Brookes, R. Dissolved Oxygen Control. *Process Biochem.*, 4, pp. 27-32 (1969).

14. Carter, B.L.A., A.T. Bull. Studies of Fungal Growth and Intermediary Carbon Metabolism Under Steady and Nonsteady-State Conditions. *Biotechnol. Bioeng.*, 11(5), pp. 785-804 (1969).

15. Chance, B. Cellular Oxygen Requirement. *Fedn. Proc. Am. Soc. Exp. Biol.*, 16, pp. 671-80 (1957).

16. Churchill, R.V. *Operational Mathematics.* 3rd ed. McGraw-Hill, N.Y. (1972).

17. Cooper, C.M., G.A. Fernstrom, S.A. Miller. Performance of Agitated Gas-Liquid Contactors. *Ind. Engg. Chem.*, 36(6), pp. 504-9 (1944).

18. Deindorfer, F.H. Fermentation Kinetics and Model Processes. *Advances in Applied Microbiology* (Umbreit, W.W. ed.), 2, pp. 321-34 (1960). Academic Press, N.Y.

19. Dostalek, M. Cultivation of *Candida lipolytica* on Hydrocarbons I - Degradation of n-alkanes in Batch Fermentation of Gas Oil. *Biotech. Bioeng.*, 10, pp. 33-43 (1968).

20. Ecker, R.E., W.R. Lockhart. Specific Effect of Limiting Nutrient on Physiological Events During Continuous Culture. *J. Bact.*, 82, pp. 511-16 (1961).

21. Enoch, H., V. Falkenflug. Improved Membrane For Oxygen Probes. *Soil Sci. Soc. Amer. Proc.*, 32(3), pp. 445-6 (1968).

22. Estabrook, R.W. Mitochondrial Respiratory Control and the Polarographic Measurement of ADP:O Ratios. *Methods in Enzymology* (Estabrook and Pullman eds.), 10, pp. 41-7 (1967). Academic Press, N.Y.

23. Feren, J., R.W. Squires. The Relationship Between Critical Oxygen Level and Antibiotic Synthesis of Capreomycin and Cephalosporin C. *Biotechnol. Bioeng.*, 11, pp. 583-92 (1969).

24. Finn, R.K. Agitation-Aeration in the Laboratory and in Industry. *Bact. Rev.*, 18, pp. 254-74 (1954).

25. Flynn, D.S., M.D. Lilly. A Method For the Control of the Dissolved Oxygen Tension in Microbial Cultures. *Biotechnol. Bioeng.*, 9, pp. 515-31 (1967).

26. Fredrickson, A.G., R.D. Megee, H.M. Tsuchiya. Mathematical Models For Fermentation Processes. *Advances In Applied Microbiology*, 13, pp. 41-65 (1970).

27. Fuller, E.C., R.H. Crist. The Rate of Oxidation of Sulfite Ions by Oxygen. *J. Am. Chem. Soc.*, 63, pp. 1644-1650 (1941).

28. Hanhart, J., H. Kramers, K.R. Westerterp. The Residence-Time Distribution of the Gas in an Agitated Gas-Liquid Contactor. *Chem. Eng. Sci.*, 18, pp. 503-9 (1963).

29. Harrison, D.E.F., S.J. Pirt. The Influence of Dissolved Oxygen Concentration on the Respiration and Glucose Metabolism of *Klebsiella aerogenes* During Growth. *J. Gen. Microbiol.*, 46, pp. 193-211 (1967).

30. Harrison, D.E.F., S.J. Pirt. Oxygen Tension and Glucose Metabolism of *Klebsiella aerogenes*. *J. Gen. Microbiol.*, 41(1), pp. ix-x (1965).

31. Harrison, D.E.F., A.H. Stouthamer. Growth, Oxygen and Respiration. *CRC Critical Reviews in Microbiology*, pp. 185-228 (Jan. 1973).

32. Herbert, D. Microbial Respiration and Oxygen Tension. *J. Gen. Microbiol.*, 41(1), pp. viii-ix (1965).

33. Herbert, D., P.J. Phipps, D.W. Tempest, Chemostat Design and Instrumentation. *Laboratory Practice*, 14(10), pp. 1150-61 (1965).

34. Heyrovsky, J., J. Kuta, *Principles of Polarography*. Academic Press, N.Y. (1966).

35. Hohmann, E.C., F.J. Lockhart. Remember the Hyperbola. *Chemtech*, pp. 614-19 (Oct. 1972).

36. Ingram, M. *An Introduction To the Biology of Yeast.* Pitman and Sons, London (1955).

37. Johnson, M.H. Aerobic Microbial Growth at Low Oxygen Concentrations. *J. Bact.*, 94(1), pp. 101-108 1967).

38. Johnson, M.J., J. Borkowski. Steam Sterilizable Probes For Dissolved Oxygen Measurement. *Biotechnol. Bioeng.*, 6, pp. 457-68 (1964).

39. Kirk-Othmer. Electroanalytical Methods. *Encyclopia of Chemical Technology.* 2nd. ed., 7, pp. 726-84 (1963).

40. Lodder, J. (ed.) *The Yeasts.* North Holland Publishing Co., Amsterdam (1971).

41. Longmuir, I.S. Respiration Rate of Bacteria as a Function of Oxygen Concentration. *Biochem. J.*, 57, pp. 81-87 (1954).

42. MacLennan, D.G., S.J. Pirt. Automatic Control of Dissolved Oxygen Concentration in Stirred Microbial Cultures. *J. Gen. Microbiol.*, 45, pp. 289-302 (1966).

43. Mackereth, F.J.H. An Improved Galvanic Cell For Determination of Oxygen Concentrations in Fluids. *J. Sci. Instr.*, 41, pp. 38-41 (1964).

44. Maxon, W.D. Aeration Studies on Propagation of Baker's Yeast. *Ind. Eng. Chem.*, 45, pp. 2554-60 (1953).

45. Molloy, E.W. *Polarographic Sensor.* U.S. Patent 3,406,109 (Oct. 15, 1968).

46. Moss, F. The Influence of Oxygen Tension on Respiration and Cytochrome a_2 Formation of *E. coli*. *Aust. J. Exp. Biol. Med. Sci.*, 30, pp. 531-40 (1952).

47. Moss, F.J., P.A.D. Rickard, G.A. Beech, F.E. Bush. The Response By Microorganisms To Steady-State Growth In Controlled Concentrations of Oxygen and Glucose I - *Candida utilis. Biotechnol. Bioeng.*, 11, pp. 561-80 (1969).

48. Moss, F.J., P.A.D. Rickard, F.E. Bush. Response By Microorganisms to Steady-State Growth in Controlled Concentrations of Oxygen and Glucose II - *Saccharomyces carlsbergensis*. *Biotechnol. Bioeng.*, 13, pp. 63-75 (1971).

49. Nagai, S., S. Aiba. Kinetics of the Growth Yield as Affected By Dissolved Oxygen in a Chemostat Culture of *Azotobacter vinelandii*. *Proc. Fourth International Fermentation Symposium*, pp. 143-45 (1972).

50. Neish, A.C. Analytical Methods For Bacterial Fermentations. *National Research Council Report 46-8-3* (1952).

51. Petering, H.G., F. Daniels. The Determination of Dissolved Oxygen by Means of the Dropping Mercury Electrode With Applications in Biology. *J. Am. Chem. Soc.*, 60, pp. 2796-802 (1938).

52. Phillips, D.H., M.J. Johnson. Measurement of Dissolved Oxygen in Fermentations. *J. Biochem. Microbiol. Technol. Eng.*, 3, pp. 261-75 (1961).

53. Pijanowski, B.S. Salinity Correction For Dissolved Oxygen Measurement. *Environmental Science and Technology*, 7(10), p. 957 (Oct. 1973).

54. Pirt, J. Oxygen Requirement of Growing Cultures of an Aerobic Species Determined By Means of the Continuous Culture Technique. *J. Gen. Microbiol.*, 16, pp. 59-75 (1957).

55. Prokop, A., L.E. Erickson, O. Paredes-Lopez. Growth Models of Cultures With Two Liquid Phases V - Substrate Dissolved in Dispersed Phase-Experimental Observations. *Biotechnol. Bioeng.*, 13(2), pp. 241-56 (1971).

56. Rickard, P.A.D., F.J. Moss, M. Ganez. Effects of Glucose and Oxygen on the Cytochromes and Metabolic Activity of Yeast Batch Cultures I - *Saccharomyces spp.* *Biotechnol. Bioeng.*, 13(1), pp. 1-16 (1971).

57. Rickard, P.A.D., F.J. Moss, D. Phillips, T.C.K. Mok. Effects of Glucose and Oxygen on the Cytochromes and Metabolic Activity of Yeast Batch Culture II - *Candida utilis*. *Biotechnol. Bioeng.*, 13(2), pp. 169-84 (1971).

58. Robinson, J., J.M. Cooper. Methods of Determining Oxygen Concentrations in Biological Media, Suitable For Calibration of the Oxygen Electrode. *Anal. Biochem.*, 33(2), pp. 390-9 (1970).

59. Saito, Y. A Sputtered Platinum Film Electrode For Polarographic Oxygen Measurement. *J. Appl. Physiol.*, 23(6), pp. 979-83 (1967).

60. Shu, P. Control of Oxygen Uptake in Deep-Tank Fermentations. *Ind. Eng. Chem.*, 48, pp. 2204-8 (1956).

61. Smith, C.G., M.J. Johnson. Aeration Requirements For the Growth of Aerobic Microorganisms. *J. Bact.*, 68, pp. 346-50 (1954).

62. Spiegel, M.R. *Theory and Problems of Statistics-Schaum's Outline Series.* McGraw-Hill (1961).

63. Tempest, D.W., D. Herbert. Effect of Dilution Rate and Growth-Limiting Substrate on the Metabolic Activity of *Torula utilis* Cultures. *J. Gen. Microbiology*, 41, pp. 143-50 (1965).

64. Terui, G., M. Sugimoto. Analysis of the Behaviors of Industrial Microbes Toward Oxygen IV - Non Michaelis-Menten Type Response of Respiration Rate of Yeast To Dissolved Oxygen. *J. Ferment. Tech.*, 47(6), pp. 382-88 (1969).

65. Terui, G., N. Konno, M. Sase. Analysis of the Behaviors of Some Industrial Microbes Toward Oxygen I - Effect of Oxygen Concentration Upon the Rates of Oxygen Adaptation and Metabolisms of Yeasts. *Technol. Rept. Osaka Univ.*, 10(413), pp. 527-44 (1960).

66. Terui, G., N. Konno. Analysis of the Behavior of Industrial Microbes Toward Oxygen II - Respiration of Gaseous and Dissolved Oxygen by *Aspergillus oryzae* Grown in Surface and Submerged Cultures. *Technol. Rept. Osaka Univ.*, 10(445), pp. 889-903 (1960).

67. Terui, G., N. Konno. Analysis of the Behaviors of Some Industrial Microbes Toward Oxygen III - Effect of Oxygen Concentration Upon the Growth and Hydrolase-Producing Activity of *Bacillus amylosolvens*. *Technol. Rept. Osaka Univ.*, 11 (487), pp. 447-458 (1961).

68. Van Hemert, P., D.G. Kilburn, R.C. Righelato, A.L. Van Wezel. A Steam-Sterilizable Electrode of the Galvanic Type For Dissolved Oxygen Measurement. *Biotechnol. Bioeng.*, 11(4), pp. 549-60 (1969).

69. Van Stekelenburg, G.J. Oxygen Pressure or Oxygen Concentration. *J. Electroanalytical Chem.*, 28(1), pp. 222-8 (1970).

70. Wimpenny, J.W.T. Oxygen and Carbon Dioxide As Regulators of Microbial Growth and Metabolism. *Symp. Soc. Gen. Microbiol.*, 19, pp. 161-97 (1969).

71. Winzler, R.J. The Respiration of Baker's Yeast At Low Oxygen Tension. *J. Cell Comp. Physiol.*, 17, pp. 263-76 (1941).